

PHENOTYPIC FACTORS INFLUENCING
***MYCOBACTERIUM TUBERCULOSIS* PHENOTYPE**



Lorraine Moses

Thesis presented for the approval for the Masters degree of Science in Medical Science at the
Faculty of Health Sciences, University of Stellenbosch

Promoters: Dr Robin M. Warren and Dr Gael Fenhalls

December 2002

DECLARATION

I, the undersigned, hereby declare that the work contained in this thesis is my own original work and has not previously in its entirety or in part been submitted at any university for a degree.

Signature

Date

SUMMARY

Tuberculosis accounts for 7% of global deaths annually, and more than one in four preventable deaths in developing countries. According to the World Health Organisation (WHO), South Africa remains one of the twenty-three countries most affected by the tuberculosis epidemic. In countries of high prevalence, tuberculosis occurs frequently in children and young adults, contrasting with the current epidemiology in much of the developed world. During the initial infection with *Mycobacterium tuberculosis*, bacilli disseminate to different organs and tissues, often resulting in tuberculosis lymphadenitis particularly in paediatric patients. Granuloma formation, in response to infection, is an essential component of the anti-mycobacterial defence as it is within these structures that T-cell-macrophage co-operation can take place, which allows macrophages to display effective bactericidal activities.

In this study, we employed the immunohistochemistry technique to analyse the immune response in granulomatous lymph nodes from paediatric patients ($n = 6$) with tuberculosis by analysing the expression pattern of the type 1 cytokines (IL-12, IFN- γ , TNF- α) and type 2 cytokines (IL-4 and IL-10). One of these patients had received 2 days anti-tuberculosis therapy prior the biopsy. Comparing the cytokine profiles from the different patients demonstrated a predominant Th0 response in the lymph node granulomas. This implies a balance in the expression of type 1 and type 2 cytokines. This balance was not altered during the initial phase of treatment. Significant co-ordinated expression correlations were identified between IL-4 and IL-10 ($p = 0.0000006$), IL-10 and IL-12 ($p = 0.021$) and between IL-10 and TNF- α ($p = 0.0054$). The expression of IL-10 and TNF- α was also significantly associated with the presence of caseous necrosis in granulomas ($p = 0.000046$ and $p = 0.0041$, respectively).

M. tuberculosis bacilli in the granulomas were detected using the DNA:DNA *in situ* hybridisation technique. Mycobacterial DNA was detected in six patients, in contrast to the ZN staining where only 5 of the patients were positive for acid-fast bacilli. This suggests that the hybridisation technique is more sensitive than the standard ZN staining, and could be possibly used for the diagnosis of tuberculosis infection.

RNA:RNA *in situ* hybridisation was done in order to identify transcription state of the bacilli at the site of disease. A series of riboprobes were used to analyse the expression of specific genes either involved in mycobacterial metabolism that are key targets for anti-tuberculosis drugs (*rpoB*, *katG*), as well as genes thought to contribute to the survival of bacilli in host cells under conditions of

stress (*narX*, *icl*, *mbtB*, *rel_{Mtb}*). The mycobacterial genes analysed in this study also included two potential immunodominant antigens (*esat-6*, *PPE Rv3018c*). A rapid bacillary response to the anti-tuberculosis drugs was observed in the granulomas of the treated patient, where the drug targets for rifampin and isoniazid (*rpoB* and *katG*, respectively) were significantly downregulated. The presence of RNA transcripts of certain genes within the necrosis confirms that the mycobacteria detected in the necrotic region represent transcriptionally active cells.

The absence of *rpoB* and *mbtB* in these restrictive granuloma regions suggests that the development of caseous necrosis inhibited active bacterial growth. Statistical assessment of the mycobacterial gene expression data identified co-ordinated expression correlations between *katG* and *icl* ($p = 0.008$), *katG* and *rel_{Mtb}* ($p = 0.0106$), *icl* and *rel_{Mtb}* ($p = 0.00003$), *katG* and *PPE Rv3018c* ($p = 0.008$) and *icl* and *narX* ($p = 0.00003$). An inverse expression pattern was observed between *esat-6* and *icl* ($p = 0.043$) and between *esat-6* and *mbtB* ($p = 0.026$). We identified subpopulations of bacilli that occurred in different phases of growth in the individual granulomas. We hypothesise that the different environments in the granulomas determines the expression profiles of these subpopulations. A significant association was observed between the expression of *narX* and the presence of caseous necrosis ($p = 0.0062$).

The stratification of the combined host cytokine and mycobacterial gene expression data also identified significant associations between the host response and *M. tuberculosis* gene expression. A co-ordinated expression pattern was identified between IL-4 and *mbtB* ($p = 0.005$) and IL-12 and *esat-6* ($p = 0.043$). An inverse expression correlation was observed between IL-12 and *rel_{Mtb}* ($p = 0.005$). Stratifying the data according to mode of transcription (passive vs. active) identified significant correlations between IL-4 and *mbtB* ($p = 0.020$) in the *rpoB* negative (passive) subgroup. An inverse expression pattern was identified between IL-12 and *rel_{Mtb}* in both the passive and active transcribing granuloma subgroups ($p = 0.05$ and $p = 0.021$, respectively). Significant correlations were observed between IL-4 and *katG* ($p = 0.049$) and between IL-10 and *narX* ($p = 0.026$) in the active transcribing subgroup, and an inverse expression pattern was identified between IL-12 and *mbtB* ($p = 0.035$). The techniques used in this study thus allowed us to demonstrate the interaction between host factors, *M. tuberculosis* survival mechanisms, as well as the interaction between the host and pathogen within the tuberculosis granulomas.

OPSOMMING

Tuberkulose is die oorsaak van 7% wêreldwye sterftes jaarliks en 25% voorkombare sterftes in ontwikkelde lande. Suid-Afrika is volgens die Wêreld Gesondheids Organisasie (WGO) een van 23 lande wat die meeste geaffekteer word deur die tuberkulose epidemie. In teenstelling met ontwikkelde lande, is die insidens van tuberkulose hoog onder kinders en jong volwassenes in onderontwikkelde lande met 'n hoë tuberkulose voorkoms. In jong kinders veral, lei infeksie met *Mikobakterium tuberkulose* tot disseminasie van die bakterium na verskillende organe en weefsel. Dit word tuberkulose limfadenitis genoem. Granuloom vorming is 'n noodsaaklike komponent van die immuunsisteem in 'n poging om die infeksie te bekamp. T sel en makrofaag interaksie binne granulome help makrofage om meer effektiewe bakterie-dodende aktiwiteite uit te voer.

In die studie is immunohistochemie aangewend om die immuunrespons in granuloom bevattende limfnodes van kinders (n=6) met tuberkulose te analiseer. Daar is gekyk na tipe I sitokiene (IL-12, IFN- γ en TNF- α) en tipe II sitokiene (IL-4 en IL-10). Een van die pasiënte het vir twee dae anti-tuberkulose behandeling ontvang voor die limfnode biopsie. Die resultate van die studie het aangetoon dat 'n T-helper 0 immuunrespons die dominante respons in limfnode granulome van kinders is. Dit is aanduidend van 'n balans tussen die uitdrukking van tipe I en tipe II sitokiene. 'n Beduidende korrelasie is geïdentifiseer tussen die uitdrukking van IL-4 en IL-10 ($p=0.0000006$), IL-10 en IL-12 ($p=0.021$) en TNF- α en IL-10 ($p=0.0054$). Die uitdrukking van TNF- α en IL-10 is ook beduidend geassosieer met verkasende nekrose in granulome ($p=0.000046$ en $p=0.0041$, onderskeidelik).

DNS:DNS *in situ* hibridisasie is gebruik om *M. tuberkulose* bakterie in granulome te identifiseer. Mikobakterieële DNS is gevind in al 6 pasiënte terwyl Ziehl-Neelsen (ZN) kleuring suurvaste bakterie aangedui het in 5 pasiënte. Die resultate stel voor dat die hibridisasie tegniek meer sensitief is as die ZN kleuring en moontlik gebruik kan word vir diagnose van tuberkulose infeksie.

RNS:RNS *in situ* hibridisasie is uitgevoer om die transkripsie status van die mikobakterie in die geïnfekteerde weefsel te bepaal. 'n Reeks ribo-oligonukleotied peilers is gebruik om die uitdrukking van spesifieke gene te analiseer. Van die gene is betrokke by mikobakterieële metabolisme wat teikens is van anti-tuberkulose middels (*ropB*, *katG*), ander is gene wat belangrik is vir oorlewing van die basilli in die gasheerselle tydens stres toestande (*narX*, *icl*, *mbtB*, *rel_{Mtb}*). Ander mikobakterieële gene wat geanaliseer is, sluit twee potensieel immunodominante antigene, *esat-6* en *PPE* (Rv3018c), in. Die uitdrukking van *katG* en *rpoB*, teikens van rifampin en isoniasied, is

betekenisvol onderdruk in die granulome van die behandelde pasiënt wat aanduidend is van 'n vinnige anti-mikobakteriele respons na slegs twee dae van behandeling. Die teenwoordigheid van RNS transkripte van sekere gene binne in die nekrose van nekrotiserende granulome is aanduidend van transkripsioneel aktiewe mikobakterie.

Die afwesigheid van *rpoB* en *mbtB* in die nekrose stel voor dat verkasende nekrose bakteriele groei inhibeer. Statistiese analises van die mikobakteriele geen uitdrukking dui op gekoördineerde uitdrukking tussen *katG* en *icl* ($p=0.008$), *katG* en *rel_{Mtb}* ($p=0.0106$), *icl* en *rel_{Mtb}* ($p=0.00003$), *katG* en *PPE Rv3018c* ($p=0.008$) en *icl* en *narX* ($p=0.00003$). 'n Omgekeerde uitdrukking patroon is waargeneem tussen *esat-6* en *icl* ($p=0.043$) en tussen *esat-6* en *mbtB* ($p=0.026$). Subpopulasies van basilli in verskillende groeifases is geïdentifiseer in die verskillende granulome. Ons hipotiseer dat die verskillende omgewings in granulome die uitdrukkingprofile van die subpopulasies bepaal. 'n Betekenisvolle assosiasie is gemaak tussen die uitdrukking van *narX* en die teenwoordigheid van verkasende nekrose ($p=0.0062$).

Stratifikasie van die gekombineerde gasheer sitokien en mikobakteriele geen uitdrukking data het assosiasies geïdentifiseer tussen die gasheer immuunrespons en *M. tuberkulose* geen uitdrukking. 'n Gekoördineerde uitdrukkingpatroon is geïdentifiseer tussen IL-4 en *mbtB* ($p=0.005$) en IL-12 en *esat-6* ($p=0.043$). 'n Omgekeerde uitdrukking korrelasie is waargeneem tussen IL-12 en *rel_{Mtb}* ($p=0.005$). Stratifikasie van die data ten opsigte van aktiewe en passiewe transkripsie het betekenisvolle korrelasies geïdentifiseer tussen IL-4 en *mbtB* ($p=0.020$) in die *rpoB* negatiewe (passiewe) populasie. 'n Omgekeerde uitdrukking patroon is geïdentifiseer tussen IL-12 en *rel_{Mtb}* in beide passiewe en aktiewe transkripsie granuloom subpopulasies ($p=0.05$ en $p=0.021$, onderskeidelik). Betekenisvolle korrelasies tussen IL-4 en *katG* ($p=0.049$) en tussen IL-10 en *narX* ($p=0.026$), sowel as 'n omgekeerde uitdrukkingpatroon tussen IL-12 en *mbtB* ($p=0.035$), is waargeneem in die aktiewe transkripsie populasie. Die tegnieke wat in die studie gebruik is het ons toegelaat om die interaksie tussen die gasheer faktore, *M. tuberkulose* oorlewings meganismes, sowel as die interaksie tussen die gasheer en patogeen in tuberkulose granulome te bestudeer.

TABLE OF CONTENTS

INDEX	PAGE
Acknowledgments	i
List of Abbreviations	ii
List of Figures	iv
List of Tables	vi
Chapter 1: Introduction	1
Chapter 2: Materials and Methods	39
Chapter 3: Results	63
Chapter 4: Discussion	106
Appendix I: Buffers and Solutions	128
Appendix II: Consent Form	135
Appendix III: Diagnostic Tools	139
Appendix IV: Individual Patient Assessment	147
Appendix V: Overall Stratification of Granulomas	175
Appendix VI: List of Suppliers	184
Appendix VII: WHO Country Grouping	187
References	188

ACKNOWLEDGEMENTS

I would like to thank the following people who contributed to this thesis in many different ways:

Firstly, to Dr Gael Fenhalls, whose help and support went above and beyond “the call of duty”. Without your help, this project would not have been at all possible. You have my deepest gratitude.

To Dr Rob Warren, thank you for all your help and fantastic scientific input, and for putting in that extra effort when desperately needed.

To Liesel Muller and Madalene Richardson, thank you for taking time out of your very busy schedules to teach and help me with my work. Your sincerity and patience is genuinely appreciated. Great debt is also owed to sister Priscilla Samaai, whose warmth and friendliness has made working together an absolute pleasure. I would also like to extend my gratitude to the research nurses who filled in for Priscilla, putting their work aside to help me.

To Dr Juanita Bezuidenhout, Juliana Pathaaysen, Annalene Huishaman and Willie Pietersen, firstly, my humblest apologies for “bugging” you so much, and secondly, thank you for never complaining. I cannot thank you enough for all your help which contributed so much to this thesis.

I would also like to acknowledge both Prof. Nulde Beyers and Prof. Sam Moore for all their help and contributions.

To the staff of Tygerberg Hospital Day Surgery and Ward J6, thank you for your help with the patient recruitment.

To my friends and colleagues in the Department of Medical Biochemistry, especially Sian and Craig(s), who made this an interesting learning environment, thank you so much for all your support (and shoulder...).

To my family, thank you for your magnificent support throughout my academic endeavours. Your encouragement has helped me achieve not only this goal, but also much more in life. Mere words cannot express my gratitude.

Finally, to the most important person in my life - my mother: Your love and faith in me is what kept me going at times when everything looked bleak. I can never thank you enough for all the sacrifices you made that allowed me to achieve this goal. You are my driving force and I dedicate this thesis to you.

This project would never been possible without the financial assistance of GlaxoSmithKline and the South African Medical Research Council.

LIST OF ABBREVIATIONS

Ab	Antibody
1° Ab	Primary Antibody
2° Ab	Secondary Antibody
AFB	Acid-fast bacilli
AIDS	Acquired Immune Deficiency Syndrome
AM	Alveolar Macrophages
AP	Alkaline Phosphatase
APC	Antigen Presenting Cell
ATP	Adenosine triphosphate
BAL	Bronchoalveolar lavage
BCG	Bacille-Calmette-Guerin
BCIP	5-Bromo-4-chloro-3-indolyl-phosphate
CMI	Cell Mediated Immunity
CTP	Cytosine triphosphate
DEPC	Diethyl-pyrocabonate
dH ₂ O	distilled Water
DNA	Deoxyribonucleic acid
DR	Direct Repeat
DTH	Delayed-type hypersensitivity
DTT	1,4-Dithiothreitol
<i>esat-6</i>	6 kDa early secreted antigenic target
EtOH	Ethonal
GTP	Guanisine triphosphate
HIV	Human Immunodeficiency Virus
HRP	Horse-radish peroxidase
<i>icl</i>	Isocitrate lyase
IFN- γ	Interferon gamma
IL	Interleukin
INH	Isoniazid
ISH	In situ hybridisation
LB	Luria-Bertani
LJ	Lowenstein-Jensen
M ϕ	Macrophage

MHC	Major Histocompatibility Complex
MPTR	Major polymorphic tandem repeat
<i>M.tb</i> / MTB	<i>Mycobacterium tuberculosis</i>
NBT	4-Nitro blue tetrazolium
PBS	Phosphate buffered Saline
PCR	Polymerase chain reaction
PPD	Purified protein derivative
(p)ppGpp	Hyperphosphorylated guanine
RFLP	Restriction Fragment Length Polymorphism
RIF	Rifampin
RNA	Ribonucleic acid
TB	Tuberculosis
Tc	Cytotoxic T cells
Th	Helper T cells
TNF- α	Tumor necrosis factor alpha
TTP	Thymidine triphosphate
UTP	Uracil triphosphate
WHO	World Health Organisation
ZN	Ziehl-Neelsen

LIST OF FIGURES

FIGURES	PAGE
Figure 1.1. Proportions of all notified cases, and smear-positive cases, by WHO, 1999.	4
Figure 1.2. Estimated numbers of TB cases	7
Figure 1.3. Detection rates of smear-positive and all TB cases	7
Figure 1.4. Reported Incidence of Tuberculosis in South Africa 1995 – 1998	10
Figure 1.5. Age distribution of TB patients in South Africa in 1999	10
Figure 1.6. History of Tuberculosis Infection	13
Figure 1.7. Schematic Representation of a Necrotic Granuloma	19
Figure 1.8. The Mitchison Hypothesis	30
Figure 2.1. Schematic representation of the pGEM-T easy vector containing <i>Mtb</i> gene fragments cloned between the T7 and SP6 promoters	42
Figure 2.2. Synthesis of Antisense and Sense Oligonucleotide Probes	48
Figure 2.3. <i>In Situ</i> Hybridisation	49
Figure 2.4. Immunohistochemistry	53
Figure 2.5. IS6110 Profile Typing using the Standard Methodology	58
Figure 3.1. Amplification of the various <i>M. tuberculosis</i> gene fragments	67
Figure 3.2. Reproducibility of <i>In Situ</i> Hybridisation	69
Figure 3.3. Immunohistochemical Staining for IL-4 in a non-necrotic and necrotic granuloma	71
Figure 3.4. Immunohistochemical Staining for IL-10 in a non-necrotic and necrotic granuloma	72
Figure 3.5. Immunohistochemical Staining for IL-12 in a non-necrotic and necrotic granuloma	73
Figure 3.6. Immunohistochemical Staining for IFN- γ in a non-necrotic and necrotic granuloma	74

Figure 3.7. Immunohistochemical Staining for TNF- α in a non-necrotic and necrotic granuloma	75
Figure 3.8. Negative control for Immunohistochemical staining	76
Figure 3.9. Analysis of the Individual Host Cytokine Pattern in each of the Patients	78
Figure 3.10. Th Phenotypes Detected for the Individual Patients	78
Figure 3.11. <i>In situ</i> hybridisation of sections through necrotic granuloma 18 of patient L6	82
Figure 3.12. <i>In situ</i> hybridisation of sections through non-necrotic granuloma 16 from patient L5	83
Figure 3.13. Co-localisation of <i>M. tuberculosis</i> DNA to CD68 positive cells	85
Figure 3.14. High Magnification Illustrating the Co-localisation of <i>M. tuberculosis</i> DNA to CD68 positive (a) Macrophages and (b) Giant Cell	86
Figure 3.15. Percentage Granulomas Positive for Mycobacterial DNA Detected for Individual Patients	87
Figure 3.16. <i>In situ</i> hybridisation of necrotic granuloma number 15 from patient L5 at x100 Magnification Analysis using Immunohistochemistry	90
Figure 3.17. <i>In situ</i> hybridisation of non-necrotic granuloma number 15 from patient L6 at x100 Magnification	92
Figure 3.18. <i>In situ</i> hybridisation of sections through granuloma 15 from patient L6 at x200 Magnification	94
Figure 3.19. Co-localisation of <i>rpoB</i> mRNA to CD68 positive cells	96
Figure 3.20. Expression Analysis of the Individual <i>M. tuberculosis</i> Genes	97
Figure 3.21. Strain Typing <i>M. tuberculosis</i> Clinical Isolates	104
Figure 4.1. Schematic Diagram Illustrating Spatial Arrangements of <i>M. tuberculosis</i> Gene Expression	124

LIST OF TABLES

TABLE CONTENT	PAGE
Table 1.1. Summary of Notifications by WHO region, 1999	4
Table 1.2. Estimated Incidence of TB: 23 high-burden countries, 1999	6
Table 1.3. Reporting Completeness for South Africa (1995 – 1999)	10
Table 1.4. TB Hotspots in South Africa for 1996	11
Table 1.5. Estimated Tuberculosis Caseloads per Province and Proportion Expected to be HIV Co-infected in 2000	12
Table 1.6. Putative Virulence Genes of <i>M. tuberculosis</i>	31
Table 2.1. Size of <i>M. tuberculosis</i> gene inserts cloned into pGEM-T easy vector systems	50
Table 2.2. Primer sequences for the amplification of the various genes from <i>M. tuberculosis</i> H37Rv genome	50
Table 2.3. T7 and SP6 Primers	53
Table 2.4. Primary Antibodies and Dilution Factors	61
Table 3.1 Clinical Data of Patients who Donated Biopsy Tissue	65
Table 3.2 Treatment History, ZN and Culture Results of Patients Included In Study	65
Table 3.3 Summary of Cytokine Data Stratification	80
Table 3.4 Summary of <i>M. tuberculosis</i> Gene Expression Stratification	99
Table 3.5. Summary of Host Cytokine and <i>M. tuberculosis</i> Gene Expression Stratification	101
Table 3.6 Stratification of Granuloma into Passive and Active Transcribing Subgroups	103
Table 3.7 Strain Typing of Isolated Clinical Strains	105

CHAPTER ONE

INTRODUCTION

INDEX	PAGE
1.1 GLOBAL BURDEN OF TUBERCULOSIS	3
1.2 TUBERCULOSIS IN SOUTH AFRICA	
1.2.1 Development of Tuberculosis in South Africa	8
1.2.2 Present Tuberculosis Epidemic in South Africa	8
1.2.3 TB “Hotspots” in South Africa	11
1.3 CLINICAL TUBERCULOSIS	12
1.3.1 Childhood Tuberculosis	14
1.4 EPIDEMIOLOGICAL TYPING OF <i>M. TUBERCULOSIS</i>	15
1.4.1 Strain Typing of <i>M. tuberculosis</i>	16
1.5 THE PATHOLOGY OF TUBERCULOSIS	17
1.6 HOST IMMUNE RESPONSE TO TUBERCULOSIS	18
1.6.1 Tuberculous Granulomas	18
1.6.1.1 Granuloma Function	19
1.6.1.2 Granuloma Formation	20
1.6.2 The Role of Macrophages in Host Defence	21
1.6.3 Antigen Presenting Cells (APCs)	21
1.6.4 T Lymphocytes	22
1.6.4.1 CD4+ T lymphocytes	22
1.6.4.2 CD8+ T lymphocytes	24
1.6.4.3 γ/δ T lymphocytes	24
1.6.5 Cytokines	25
1.7 BIOLOGY OF <i>M. TUBERCULOSIS</i>	27
1.7.1 Metabolic Factors / Drug Targets	
1.7.1.1 <i>rpoB</i>	28
1.7.1.2 <i>katG</i>	29
1.7.2 Potential Persistent Factors	30
1.7.2.1 <i>icl</i>	32
1.7.2.1 <i>narX</i>	32
1.7.2.3 <i>mbtB</i>	33

1.7.2.4	rel _{Mtb}	34
1.7.3	Immunological Significant Antigenic Proteins	35
1.7.3.1	esat-6	36
1.7.3.2	PPE	37
1.8	AIMS OF STUDY	37

1.1 GLOBAL BURDEN OF TUBERCULOSIS

“If the number of victims which a disease claims is the measure of its significance, then all diseases, particularly the most dreaded infectious disease, must rank far behind tuberculosis. Statistics teach that one-seventh of all human beings die of tuberculosis, and that if one considers only productive middle-age groups, tuberculosis carried away one-third and often more of these...”

Robert Koch, 1880

Tuberculosis is an ancient disease with the earliest definitive evidence in Egypt dating back as far as the Dynastic period, which started about 3 400 BC. An example of this is the mummy of a five-year-old child with evidence of pulmonary and vertebral tuberculosis (Zimmerman, 1979). The burden of ill health and death caused by tuberculosis makes it one of the most important diseases in the history of human society. There has been no other single disease which has been so prevalent and widespread over such an extensive period in time.

Tuberculosis remains a major global problem today. The causative agent, *Mycobacterium tuberculosis*, was recognised over 100 years ago, and effective treatment has now been available for over 50 years (Dolin *et al*, 1994). However, TB programmes are still struggling to control one of the world’s most important infectious diseases. The breakdown in health services, the spread of HIV/AIDS and the emergence of multidrug-resistant TB are contributing to the worsening impact of this disease. In 1993, the World Health Organisation (WHO) took an unprecedented step and declared tuberculosis a global emergency, so great was the concern about the modern TB epidemic. This disease accounts for 7% of global deaths annually and more than one in four preventable deaths in developing countries (Murray *et al*, 1990).

In 1999, 171 countries reported to the WHO a total of 3 689 822 cases (62 per 100 000 population), of which 1 485 783 (40%) were sputum-smear positive (Table 1.1) (WHO report 2001). The African (17%), South-East Asia (41%) and Western Pacific Regions (22%) together accounted for 80% of all notified cases and similar proportions of sputum-smear positive cases (Figure 1.1). Tuberculosis notification data reflect health services coverage and the efficiency of case finding and reporting activities of national tuberculosis control programs. Often poor performance of these programs results in considerable under-detection and under-reporting of cases. In addition, case definitions vary among countries and case notification data often include all cases, both new and retreatment cases. Nevertheless, case notifications under stable program conditions in any country may provide useful data on the trend of incidence and for obtaining rates by age, sex and risk group.

Table 1.1. Summary of Notifications by WHO region, 1999

Regions	Number of Notifications	New Sputum-Smear Positives
Africa	644 972	321 260
America	233 823	133 363
Eastern Medditeranean Region	156 637	67 135
Europe	362 532	86 271
S.E. Asian Region	1 469 672	485 7901
Western Pacific Region	822 177	391 964
Global	3 689 813	1 485 783

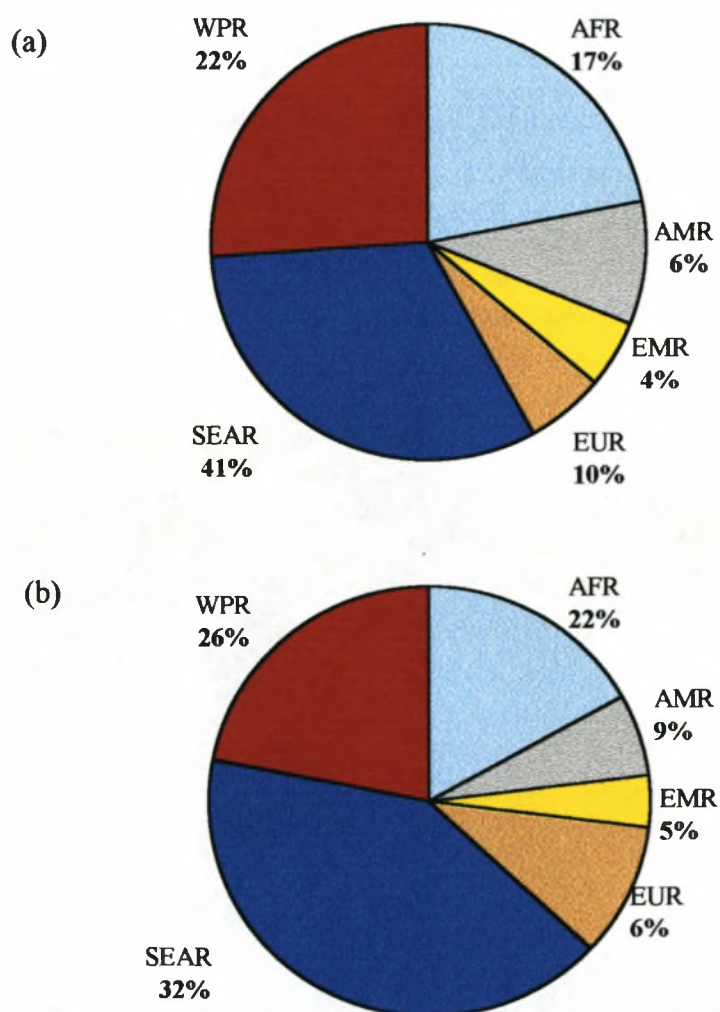


Figure 1.1. Proportions of all (a) notified cases, and (b) smear-positive cases, by WHO, 1999. AFR: African region; EMR: Eastern Mediterranean Region; EUR: European Region; SEAR: South-East Asian Region; WPR: Western Pacific Region

Because of the limitations of case notification data, alternatives to case notification are necessary for estimating incidence and size of the tuberculosis disease burden. The estimated number of new tuberculosis cases globally (Table 1.2) was 8.42 million for 1999 (WHO Report 2001), with twenty-three countries accounting for 80% of all the new cases. The global total rose from 7.96 million in 1997 to an 8.42 million in 1999. Of the 8.42 million cases in 1999, an estimated 3.67 million were smear positive. These totals are larger than previously forecast by mathematical modelling (Dye *et al*, 1998). The four African countries, Nigeria, Ethiopia, DR Congo and Kenya, as well as Russia, are now ranked higher than in 1997, with Mozambique now included in the league of high-burden countries, and Peru dropping off the list in the year 2000.

The total numbers of cases are predicted to increase in all regions up to 2005 (Figure 1.2), except in those with established market economies, with an expected decline of 2 – 3% per year (Appendix 7 lists the groups of countries where incidence was estimated using regional trends). The rate of increase is 3% per year globally, but much higher in the African countries that are most affected by HIV/AIDS (10%), and in Eastern Europe (8%). If present trends continue, a total of 10.2 million cases are expected in 2005. Africa will have more cases (3.4 million) than any other WHO region by 2005, followed by South East Asia with an expected total of 3.2 million cases.

Case notification is the cornerstone for any effective TB programme. However, the 3 689 813 cases of tuberculosis notified in 1999 represent 44% of the 8.42 million estimated cases. The total of 1 485 783 new smear positives is 40% of the 3.72 million estimated smear positive cases. Case detection rates in 1999 (Figure 1.3) were grossly underscored and were lowest in the Eastern Mediterranean Region.

Statistics show that tuberculosis remains an enormous health and economic problem in the developing world. In these countries of high prevalence, tuberculosis occurs frequently in children and young adults, contrasting with the current epidemiology in much of the developed world. In 1990, Murray and colleagues reported that 15% of the total numbers of cases in the developing countries were children younger than 15 years of age. Of the deaths from tuberculosis in the developed and developing countries, 10% - 20% were also among children under 15 years of age.

Table 1.2. Estimated Incidence of TB: 23 high-burden countries, 1999

Country (ranked by burden)	Population (1000s)	Number Estimated					Change in Rank 97 – 99*
		All cases		Smear Positive cases		Cumulative Incidence (%)	
		Thousands	Rate per 100 000 pop	Thousands	Rate per 100 000 pop		
1 India	998 056	1 847	185	827	83	22	0
2 China	1 266 838	1 300	103	584	46	37	0
3 Indonesia	209 255	590	282	265	127	44	0
4 Nigeria	108 945	327	301	142	130	48	2
5 Bangladesh	126 947	306	241	138	108	52	-1
6 Pakistan	152 331	269	177	121	79	55	-1
7 Phillipines	74 454	234	314	105	141	58	0
8 Ethiopia	61 095	228	373	96	157	61	1
9 South Africa	39 900	197	495	80	201	63	-1
10 Russian Fed.	147 196	181	123	81	55	65	1
11 DR Congo	50 335	151	301	65	130	67	1
12 Viet Nam	78 705	149	189	67	85	69	-2
13 Kenya	29 549	123	417	51	173	70	2
14 Brazil	167 988	118	70	53	31	72	-1
15 UR Tanzania	32 793	112	340	47	145	73	-1
16 Thailand	60 856	86	141	38	62	74	0
17 Mozambique	19 286	79	407	33	169	75	9
18 Myanmar	45 059	76	169	34	76	76	-1
19 Uganda	21 143	72	343	31	146	77	0
20 Afghanistan	21 923	71	325	32	146	77	-2
21 Zimbabwe	11 529	65	562	26	226	78	0
22 Cambodia	10 945	61	560	27	251	79	0
23 Peru	25 230	58	228	26	102	80	-3
Total, 23 high-burden countries	3 760 358	6 700	178	2 969	79	80	
Global Total	5 975 045	8 417	141	3724	62	100	

*change in rank resulting from re-estimation of incidence. A positive value indicates that a country has moved up the table

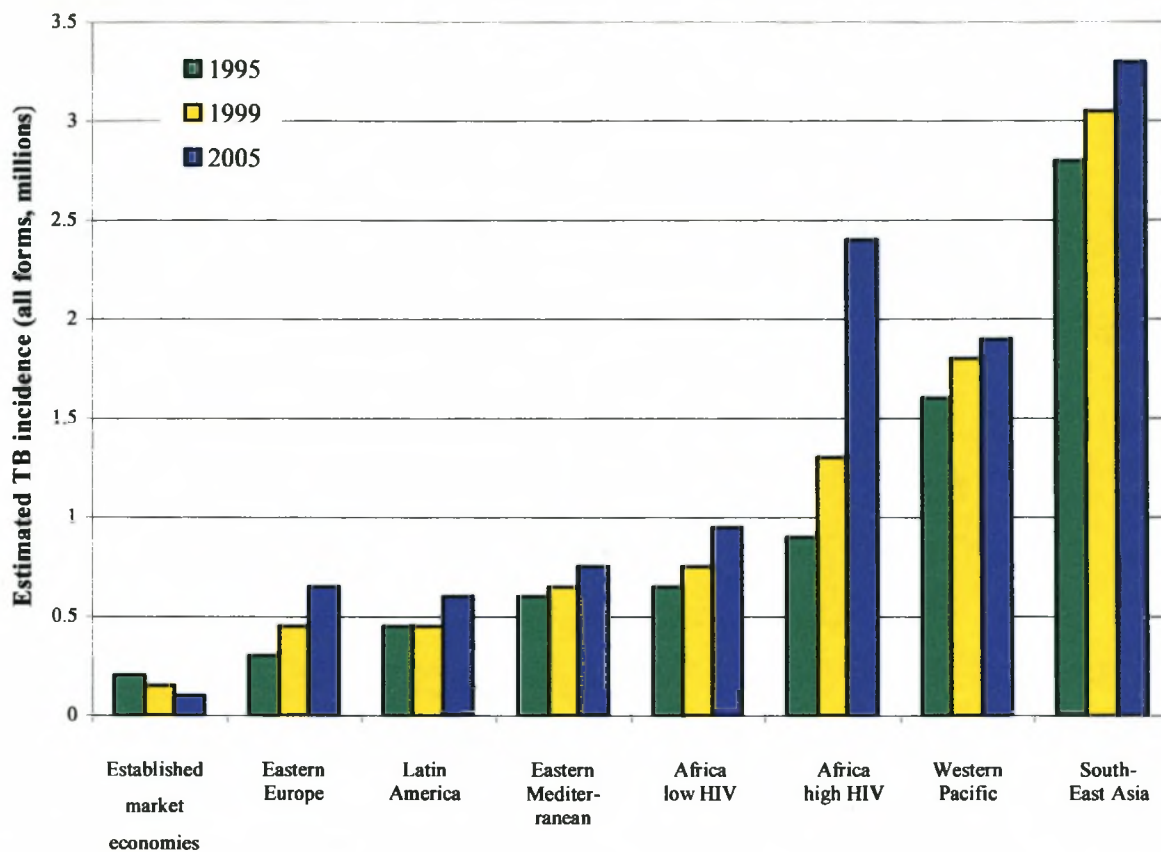


Figure 1.2. Estimated numbers of TB cases in 1995 (blue), 1999 (yellow) and 2005 (green), by region.

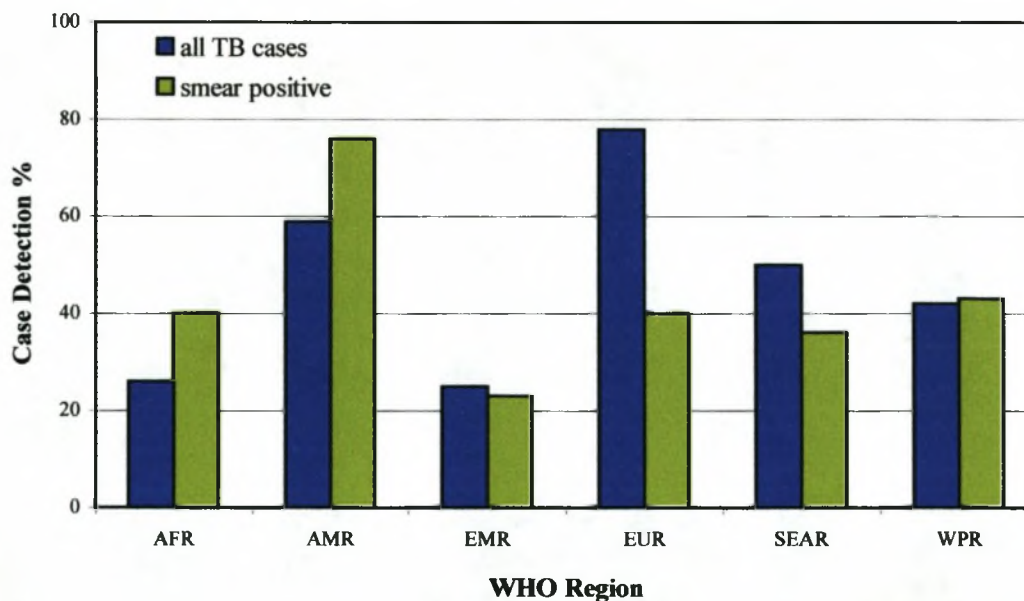


Figure 1.3. Detection rates of smear-positive (green bars) and all TB cases (blue bars) by WHO Region, 1999. Abbreviations as in Figure 1.1

1.2 TUBERCULOSIS IN SOUTH AFRICA

1.2.1 Development of Tuberculosis in South Africa

Tuberculosis is a relatively new disease in southern Africa, although it had been endemic in Europe and Asia for millennia. It is unlikely that it occurred to any great extent among races native to southern Africa prior to the era of European colonization, which began in the southwestern Cape in the mid-seventeenth century. Knowledge of the extent and prevalence of tuberculosis in South Africa prior to the 20th century is very limited as the compilation of health statistics is a relatively recent innovation. The introduction of compulsory registration of deaths in the Cape Colony in 1895 enabled tuberculosis mortality rates to be calculated for the first time (Metcalf, 1991).

Historically it appears that the initial spread of tuberculosis among the different people native to South Africa was closely related to their degree of European contact (McVicar N., 1932). In the early nineteenth century tuberculosis was reported to be a problem among Hottentots who lived in the southwestern parts of South Africa. The black people who remained geographically separate for a longer period were apparently relatively free of tuberculosis until later in the century.

It is unlikely that tuberculosis was ever absent from Europeans in South Africa. However, promoting South Africa as a health resort for “Consumptive Invalids” during the last quarter of the 19th century undoubtedly boosted the pool of infection (Metcalf, 1991). This resulted in an influx of consumptive people fleeing to South Africa, hoping to be cured by the climate. Its dry interior was recommended as being suitable for “limited non-progressive disease”. Towns in South Africa which were popular among diseased immigrants included Beaufort West, Kimberley, Bloemfontein, Harrismith, Cradock and Middelberg, with Cape Town being the main port of entry. However, many people arrived in such an advanced stage of tuberculosis that they were not able to travel into the interior. The 1912 Tuberculosis Commission found that tuberculosis was three times as prevalent in towns as in rural areas, and that it was most prevalent in the large coastal and industrial towns, on the mines and in those places previously favoured by the consumptives.

1.2.2 Present Tuberculosis Epidemic in South Africa

According to the WHO, South Africa remains one of 23 countries worst affected by the tuberculosis epidemic (Table 1.2). It is expected to contribute at least 15% of the total tuberculosis caseload for Africa (Fourie and Weyer, 2000) yet it accounts for only about 7% of the continents total population.

The incidence of tuberculosis, based on figures from national tuberculosis quarterly reports, has shown a steady increase over the four-year period between 1995 and 1998 (Figure 1.4). The incidence rates in South Africa averaged at 392 per 100 000 members of the population in 1997. The tuberculosis epidemic in South Africa, in contrast to the industrialised countries, mainly affects the economically active age group (The South African Tuberculosis Control Programme, 2000) where 86.6% of tuberculosis patients reported in 1999 were in the age group of 20 – 59 years (Figure 5). Interestingly, 80% of the notified tuberculosis cases in the industrialised countries are aged 50 years and older (Kochi, 1991). South Africa also has a fatality rate of 166 per 100 000, a rate which is five times higher than the global tuberculosis fatality average of 32 per 100 000, and is second to Zimbabwe's world wide (Dye *et al*, 1999).

Prompt identification, and therefore case finding, remains the cornerstone of effective tuberculosis programs (Diagnostic techniques summarised in Appendix 3). As with many other developing countries, case notifications in South Africa often represent only a fraction of the true incident cases where only a minority of the population has access to effective tuberculosis care. The low reporting rates continue to be a major impediment to accurate estimation of the tuberculosis epidemic in South Africa (Table 1.3). Complete case reporting for South Africa in 1999 (37%) declined to nearly half of that of the previous year (71.6%). The actual number of cases reported for 1999 (87 566) represented a mere 40% of the estimated new cases for that year (236 665), assuming 100% reporting rate.

The WHO and the International Union Against Tuberculosis and Lung Disease advocate use of the DOTS strategy to control tuberculosis. DOTS, which stands for Direct Observed Treatment, Short-course, is an internationally recognised health care management system, and was implemented in South Africa in 1996. The principle cornerstone of the DOTS strategy is a patient-centred approach which provides support to TB patients by observing them as they swallow their TB drugs and ensuring that they complete their treatment. DOTS also follow a passive case-finding method in South Africa. However, the low case-reporting rate for South Africa in 1999 indicates that this strategy of case finding is not very successful in this country.

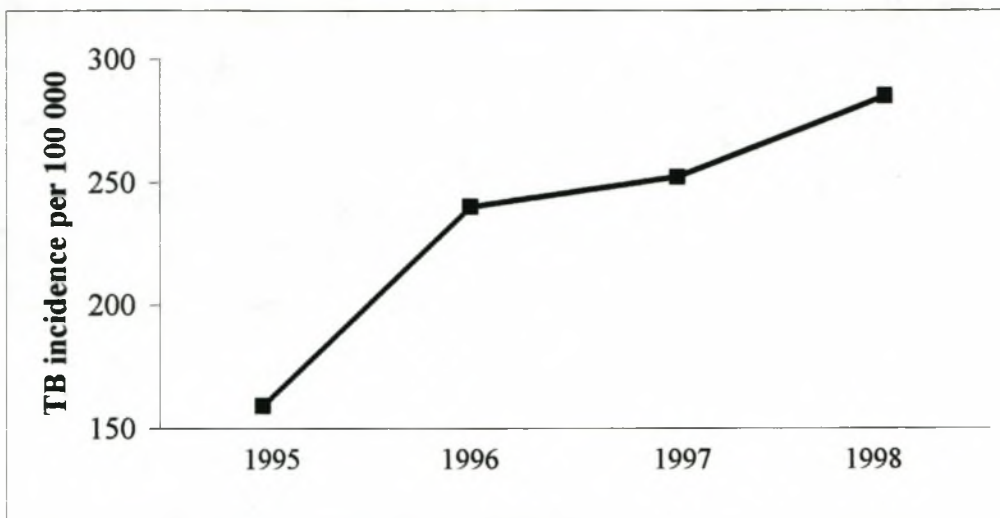


Figure 1.4. Reported Incidence of Tuberculosis in South Africa 1995 - 1998

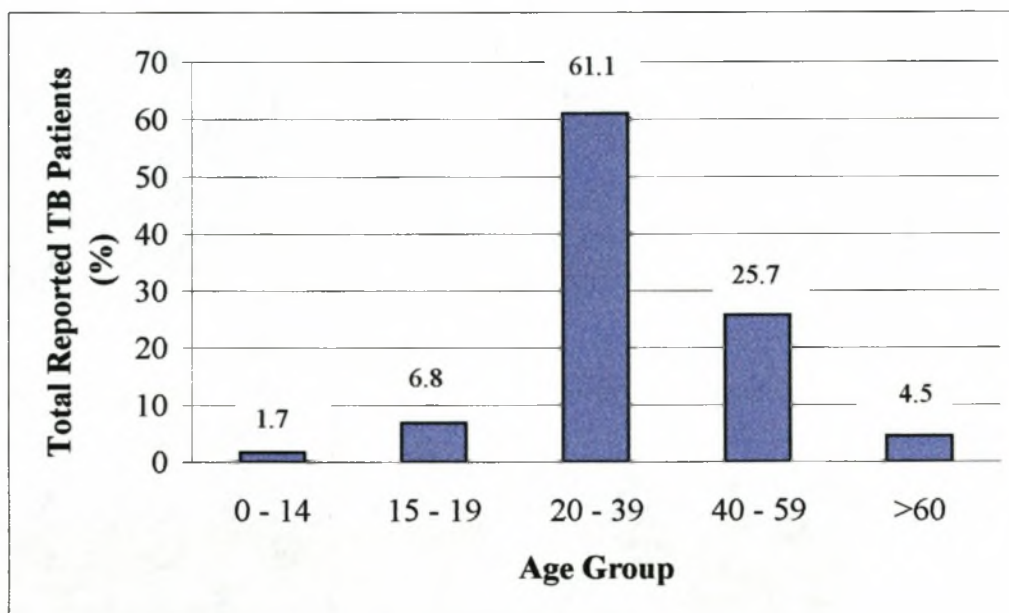


Figure 1.5. Age distribution of TB patients in South Africa in 1999

Table 1.3. Reporting Completeness for South Africa (1995 – 1999)

Year	% Reporting Facilities	TB Cases Reported	Estimated Cases (assuming 100% report rate)
1995	45.3	73 917	164 260
1996	68.0	109 328	160 776
1997	62.7	118 741	188 478
1998	71.6	135 904	188 756
1999	37.0	87 566	236 665

1.2.3 TB “Hotspots” in South Africa

Within South Africa, certain areas can be singled out as “TB hotspots”, or places where tuberculosis levels are the highest in the country. The tuberculosis epidemic in the Western Cape is one of the most alarming ever documented. The Western Cape had an estimated 559 tuberculosis cases per 100 000 in 1996 (Table 1.4) (MRC TB Report, 1998). In comparison, countries struggling with heavy tuberculosis burdens had an average number of tuberculosis cases in approximately 200 per 100 000. The problem is most severe in areas such as the Cape Flats, which were black and coloured townships during the apartheid era, as well as recently established informal settlements (squatter camps). In the Western Cape, tuberculosis has been an especially vicious killer among the coloured population, for a variety of reasons including urbanisation, population dynamics, and treatment programmes which while accessible, fail to cure tuberculosis. Tuberculosis is also very high in the wine lands of the Western Cape where this disease is extensive among the farm workers. South Africans in the Eastern Cape Province suffer the second highest reported tuberculosis rates in the country at 504 per 100 000 (Table 1.4).

Table 1.4. TB Hotspots in South Africa for 1996

Province	Estimated Cases in 1996 (per 100 000)
Western Cape	559
Eastern Cape	504
KwaZulu-Natal	381
Gauteng	375
Northern Cape	340
Mpumalanga	286
Free State	282
North West	271
Northern Province	260

In South Africa, as in many other countries in the Sub-Saharan Africa region, the epidemic is compounded by the effect of the rapidly growing spread of the HIV infection. It is currently estimated that South Africa has a TB/HIV co-infection rate of 2 540 per 100 000 (for established TB patients). The synergy between a disease of antiquity and a newer pathogen has resulted in up to 47% of tuberculosis patients in South Africa being co-infected with HIV (The South African

Tuberculosis Control Programme, 2000). The prevalence of HIV infection among TB patients varies according to province (Table 1.5), with KwaZulu-Natal (64.5%) and Mpumalanga (59.1%) provinces reporting the highest co-infection rates. Interestingly, the Western Cape that reported the highest incidence rates of tuberculosis has the lowest co-infection rates (31.1%). Poverty, rather than the HIV/AIDS epidemic, appears to be largely responsible for the heavy tuberculosis burden in this province. The Medical Research Council estimated that for the year 2000, HIV co-infection caused an excess of 123 616 new cases of tuberculosis in South Africa, which would otherwise not have occurred. The pandemic of HIV/AIDS has thus caused a marked increase in the tuberculosis notifications in South Africa.

Table 1.5. Estimated Tuberculosis Caseloads per Province and Proportion Expected to be HIV Co-infected in 2000

Province	Total TB Cases	Proportion HIV Positive (%)
KwaZulu-Natal	65 695	64.6
Mpumalanga	15 657	59.1
Free State	14 654	51.7
North West	15 549	45.5
Gauteng	45 598	44.8
Eastern Cape	56 495	40.0
Northern Province	23 338	36.3
Northern Cape	4 649	33.2
Western Cape	34 211	31.6
South Africa	273 365	47.6

1.3 CLINICAL TUBERCULOSIS

It was first thought that for tuberculosis patients to be infectious, they must have pulmonary tuberculosis with the sputum containing acid-fast bacilli visible on direct microscopy (Louden *et al*, 1958). However, Behr and colleagues (1999) reported that patients with established pulmonary tuberculosis, which did not stain positive for acid-fast bacilli in their sputum, were also highly infectious. The likelihood of developing disease is greatest immediately following infection and

declines exponentially from that point (Chiba and Kuriahar, 1979). The incidence of clinically significant disease within the first year after infection is approximately 1.5%. Within the first 5 years after infection the cumulative risk of disease is between 5% and 10%. The majority of people infected with *M. tuberculosis* do not develop disease, but have a lifetime risk of approximately 5% (Figure 1.6).

Usually, the first event to occur following infection (within 12 weeks after contact with the infectious case) is the conversion of the tuberculin skin test. In most individuals, systematic response to the infection includes a slight rise in temperature, possibly accompanied by flu-like symptoms. A minority of people who become infected with tuberculosis develop primary disease (Figure 1.6).

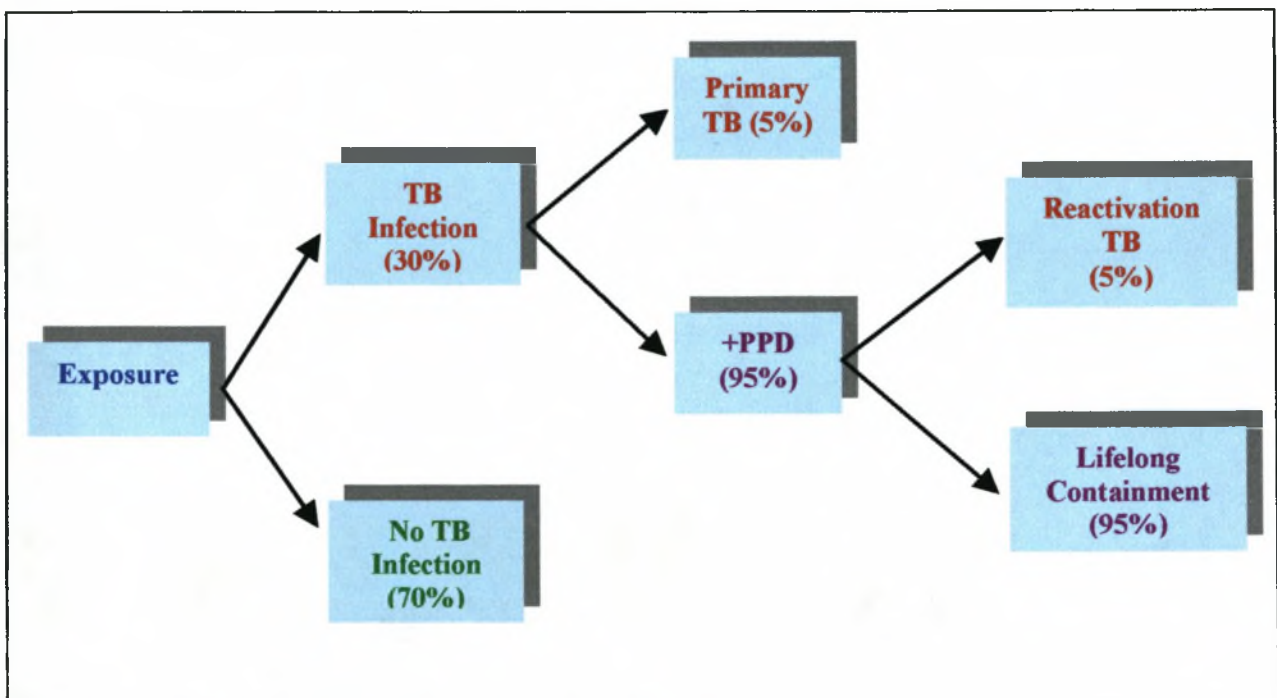


Figure 1.6. History of Tuberculosis Infection

For the twenty five percent of individuals infected with *M. tuberculosis*, that does not progress to disease development, the infection is localized in the lung and the regional lymph nodes within the chest and generally resolves without treatment. In a small proportion of patients with primary tuberculosis, complications may occur. These include local extensions and cavitations, the phase of infection referred to as progressive primary tuberculosis. Dissemination throughout the body may also occur, leading to miliary tuberculosis, which is often accompanied by tuberculosis meningitis. With miliary tuberculosis, in addition to general symptoms, headache from co-existent tuberculous

meningitis frequently occurs. Cough, dyspnoea (laboured respiration) and haemoptysis (expectoration of blood from the respiratory tract) are less common symptoms.

In high incidence areas, tuberculous lymphadenitis / scrofula (inflammation of the nodes) is the most common form of extrapulmonary disease (Humphries *et al*, 1994) and occurs quite early following infection. Although the most common presentation is pulmonary disease, extrapulmonary tuberculosis is also an important manifestation. Tuberculosis can obviously affect virtually any organ in the body and may present in a variety of ways.

1.3.1 Childhood Tuberculosis

Tuberculosis remains a disease resulting in significant morbidity and mortality in children of many developing countries. Tuberculous symptoms are often mild and non-specific and cannot be easily differentiated from many other childhood illnesses. Primary infection occurs when a child is exposed to tubercle bacilli by prolonged, close contact with an adult who has untreated open pulmonary tuberculosis.

During the initial infection, bacilli disseminate to different organs and tissues resulting in different clinical forms of tuberculosis at varying periods after the primary infection. This can result in miliary tuberculosis and / or tuberculous meningitis, which along with pulmonary tuberculosis and tuberculous lymphadenitis, are the most common clinical forms of childhood tuberculosis. Children younger than 4 years of age have a higher risk of mortality and morbidity since early dissemination occurs more commonly in this age group (Humphries *et al*, 1994).

In populations with high prevalence, tuberculous lymphadenitis has its greatest incidence in early childhood (Humphries *et al*, 1994), and occurs shortly after the primary infection. Lymphatic involvement is thought to be an integral part of tuberculous infection with generalised lymphatic and haematogenous spread rather than a localized disease process. Lymph node tuberculosis occurs predominantly in the cervical region. The lymph node swelling is usually of insidious onset and is painless, although it may be tender early in the infection when it is enlarging more rapidly. Initially the lymph nodes are discrete and firm, but later they become matted together and fluctuant. The overlying skin may break down with abscess formation and chronic sinuses (Sheffield, 1994).

In childhood pulmonary tuberculosis, the radiological hallmark is hilar or paratracheal lymphadenopathy. The infected patient may have an occasional cough or low-grade fever. In

younger children and infants, the hilar lymph nodes can be large enough to cause bronchial obstruction, resulting in localized hyperaeration and eventually atelectasis (collapse of expanded lung). Pleural effusion is also a common finding in children with pulmonary tuberculosis. Progressive primary tuberculosis and chronic pulmonary tuberculosis are, however, rare in the paediatric population.

1.4 EPIDEMIOLOGICAL TYPING OF *M. TUBERCULOSIS*

Understanding the tuberculosis epidemic in adults and children has been greatly advanced by the advent of epidemiological typing of *M. tuberculosis* clinical isolates. This provides essential data that improves the efficacy of efforts to control tuberculosis. Following primary infection with tubercle bacilli, a proportion of people develop tuberculosis quite soon, but in a substantial majority the initial challenge is overcome without symptoms and the bacilli then lie dormant. Post primary tuberculosis can then result either from endogenous reactivation of the original infection following a waning of immunity or from a further exogenous reinfection. The relative contribution of the two mechanisms is not known because the clinical result is identical and most isolates of *M. tuberculosis* could not be distinguished from each other. An increase in tuberculosis among children is considered a definite indication that transmission is occurring in the community. Social conditions in poor urban areas where tuberculosis remains prevalent, combined with high rates of HIV infection, may facilitate the development of tuberculosis disease after infection with *M. tuberculosis* (Nardell, 1993). However, not only has the virus affected the chance of disease development by causing an increase in both susceptibility to infection (Daley *et al*, 1992), it also increases the risk of reactivation (Selwyn *et al*, 1989).

Molecular techniques that are able to differentiate between isolates of *M. tuberculosis* can therefore help to answer not only fundamental questions about the pathogenesis of tuberculosis, but also more pragmatic ones about clusters of infection and likely routes of transmission. Molecular fingerprinting by restriction-fragment-length-polymorphism (RFLP) analysis yields a unique, strain-specific pattern of bands that is stable for at least two years. Strains isolated from patients who were infected from a common source would have matching band profiles (Takahashi *et al*, 1993). Molecular fingerprinting has revealed that *M. tuberculosis* can be transmitted during contact between persons who do not live or work together (Genevein *et al*, 1993). These studies suggest that patients with the same *M. tuberculosis* RFLP pattern constitute an epidemiologically linked cluster. Furthermore, because tuberculosis developed during a relatively short period in patients in a

cluster, the clustering is an indication of recent infection, and rapid progression to clinical illness (Chevrel-Dellagi *et al*, 1993). Small and colleagues (1994) reported that 40% of the patients studied ($n = 473$) appeared to have active tuberculosis as a result of recent infection. Similarly, Alland and colleagues (1994) found that in the inner city of New York, recently transmitted tuberculosis accounted for approximately 40% of the incident cases, and almost two thirds of the drug-resistant cases. In the communities of Ravensmead and Uitsig, Cape Town, South Africa, Warren and colleagues (1996) observed an unexpected and unexplained low rate of transmission (30%), but as in New York, also found clustering of drug-resistant strains. This suggests that transmission, rather than lack of compliance, drives the spread of antibiotic resistance in the study target communities.

Since clustering has been equated with recent transmission, considerable caution should be exercised in conducting and interpreting these studies. Groups of strains may be identical for reasons other than recent transmission, depending, for example, on the stability of the marker and the number of strains in the population over time. Cases actually due to recent transmission may not be seen as clustered if they are new immigrants to the population or if not all cases in the population are included in the study (Glynn, 1999).

1.4.1 Strain Typing of *M. tuberculosis*

The presence of repetitive genetic insertional elements in *M. tuberculosis* permits the identification of individual strains by DNA fingerprinting with RFLP analysis. The list of repetitive elements that have been applied for strain typing *M. tuberculosis* includes insertion sequences (IS6110 (Thierry *et al*, 1990)), the major polymorphic tandem repeat (MPTR (Hermans *et al*, 1992)), the direct repeat (DR (Hermans *et al*, 1991)) and the (GTG)₅ sequence (Wiid *et al*, 1994). The most widely used of the repetitive elements for typing strains of *M. tuberculosis* and *M. bovis* is IS6110. The number of copies and exact locus of insertion varies for different *M. tuberculosis* strains.

A standardised methodology for exploitation of IS6110 related polymorphisms have been published (van Embden *et al*, 1993). This IS6110 typing method by Southern blot is very reliable and highly reproducible. In fact, it has become the standard against which other systems are judged. IS6110 typing methods have been used to perform community based studies in which all available strains isolated within a given population and time frame are analysed (Alland *et al*, 1994; Small *et al*, 1994; Chevrel-Dellagi *et al*, 1993). Strains carrying five or more copies of the element that exhibit indistinguishable band profiles can usually be shown to have a close epidemiological association. The proportion of strains that cluster by IS6110 profiling can thus be used to estimate the extent to

which the transmission of tuberculosis is occurring within the target community. Non-clustered cases are assumed to result largely from reactivation of pre-existing disease.

A very small number of strains have been found that do not contain *IS6110* elements. Le and colleagues (2000) found that only 1.8% of the isolated strains ($n = 168$) contained no *IS6110* elements. Secondary typing methods, employed in conjunction with *IS6110*, are generally used in community-based studies. Oligonucleotide (GTG)₅ probes were used to genotype geographically linked strains of *M. tuberculosis* previously shown to have identical *IS6110* patterns. This allowed subclassification of *IS6110* defined clusters into composites of smaller clusters and unique strains. Fingerprinting of the polymorphic GC-rich repetitive sequence genes as secondary typing procedures for *M. tuberculosis* isolates having fewer than six copies of *IS6110* were found to enhance the accuracy of epidemiological studies (Yang *et al*, 2000).

1.5 THE PATHOLOGY OF TUBERCULOSIS

The pathology of tuberculosis takes into account the inherent virulence of the organism, the immunity of the person infected, the development of hypersensitivity and the formation of epithelioid granulomata. Primary tuberculosis is the first infection of an unsensitised host. Tubercle bacilli usually enter the lung via the airways, whereby droplet nuclei containing one to three bacilli (particle size $< 5 \mu\text{m}$) gain access to alveoli (Dannenbergh, 1980; Lurie, 1964; Riley, 1959). When inhaled, only these fine particles are capable of starting the infection because they remain suspended in the airstreams that enter the alveolar spaces. The heavier bacillary particles, containing more bacilli and / or bits of caseous material, impinge upon the mucosal surfaces of both the nasal passages and the bronchial tree, and do not cause disease. These bacilli are phagocytosed and the majority of the organisms are killed. However, a proportion of bacilli survives and replicate within macrophages and cause cell death. Additional monocytes are recruited from the circulation and transform into macrophages, but unless they are activated, they are inefficient at destroying the tubercle bacilli. Tubercle bacilli are transported via the lymphatics to regional lymph nodes (Sheffield, 1994).

Lymph nodes are a major site of interaction between antigen and the immune system, and are involved in a broad spectrum of disease processes, including tuberculosis infection (Byren, 1999). Cervical lymphadenopathy was found to be almost always secondary to tuberculosis infection in children. Afferent lymph from the circulation containing antigens, microorganisms and macrophages are processed in lymph nodes. The lymph node structure includes the paracortex,

cortex and medulla. The paracortex is the major site of T cell localisation, of which 80% are CD4+ T helper cells and 20% are CD8+ cytotoxic T cells. The cortex contains primary lymphoid follicles which, on exposure to afferent lymph, develop into secondary lymphoid follicles, containing germinal centres which are the major site of B cell proliferation. The medulla consists of macrophage rich sinuses. Lymphatic channels are distributed regionally, and this anatomical consistency results in predictable patterns of lymph node enlargement. The infectious causes of lymphadenopathy are characterised by the infiltration of inflammatory and phagocytic cells.

Once the tubercle bacilli are transported to lymph nodes, epitheloid cell granulomas develop. Granulomas develop typical central necrosis as delayed-type hypersensitivity (DTH) to the bacilli develops. The number of viable bacilli becomes stationary because their growth is inhibited by the immune response to antigens released from the bacilli (Dannenberg, 1991). The lesion then contains a solid caseous centre within which the (now extracellular) bacilli do not multiply (Dannenberg, 1994). Surrounding this centre are immature / nonactivated macrophages that permit intracellular bacillary multiplication, and partly activated macrophages (immature epitheloid cells) produced by cell-mediated immunity (CMI). The disease regresses if a strong CMI response develops, activating the macrophages to kill or inhibit the intracellular bacteria. However, an inefficient CMI results in the non-inhibition of bacillary growth in the macrophages, and as a result, the tissue damaging DTH response again kills the bacilli laden macrophages, causing an enlargement of the caseous centre.

1.6 HOST IMMUNE RESPONSE TO TUBERCULOSIS

The chances of an infected individual developing clinical tuberculosis are approximately 2 – 23% during their lifetime. Although the case notification of tuberculosis patients is staggering, if viewed in the opposite light, these figures indicate that for most exposed or infected individuals the immune system is capable of preventing the development of clinical disease. This observation raises a key question: what is the difference between the response of those who succumb to disease and those that remain infected but non-symptomatic? The key element(s) that determine the development of protective immunity in the absence of disease are as yet unknown.

1.6.1 Tuberculous Granulomas

Granuloma formation, a critical event in the immune response against *M. tuberculosis*, is an essential component of normal host defence (Kaufmann, 1993; Sheffield, 1994). The formation of granulomas can also contribute to the destruction of normal tissues and thereby participate in the

pathogenesis of the disease. Granulomas are dynamic structures composed of multiple cell types with different activities of cells in varying regions of the granuloma. The predominant cells in all granulomata are non-lymphoid mononuclear cells, including blood monocytes and tissue macrophages (Figure 1.7). Giant cells of the predominantly Langerhans type also occur. The nuclei of these giant cells are arranged in an arc around central granular cytoplasm. Lymphocytes, the majority of which are T cells, are also present in the tuberculous granuloma. These lymphocytes are seen in close association with the activated macrophage / monocyte cells. A higher proportion of CD4⁺ helper cells are present in the centre of tuberculous granulomata (Modlin *et al*, 1984), while CD8⁺ and B cells tend to be associated with epithelioid cells at the periphery (van den Oord *et al*, 1984).

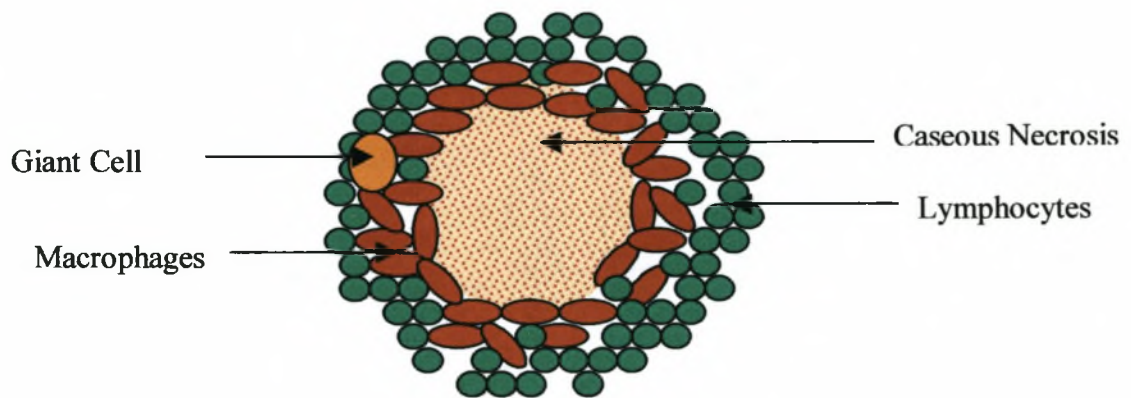


Figure 1.7. Schematic Representation of a Necrotic Granuloma

1.6.1.1 Granuloma Function

In tuberculosis granuloma, Th1 cytokines (including IFN- γ and TNF- α), are produced which activate the surrounding macrophages. In the classical theory of cell-mediated immunity to mycobacteria, antigens of the pathogens are specifically recognised by helper T cells (Th1), which then activate macrophages so that they are able to destroy the intracellular pathogen. However, it so happens that activated macrophages may be unable to inhibit / destroy the ingested tubercle bacilli. While the isolated macrophage may be of limited effectiveness against tubercle bacilli, collectively they may form a powerful defence in the form of the granuloma. Typical central necrosis may then result as the tissue damaging DTH develop which further inhibits the intracellular pathogen, by killing the bacilli laden macrophages (Sheffield, 1994). Mycobacteria are thought to proliferate poorly in the anoxic caseous material, and the appearance of caseous necrosis was shown to correlate temporally with the end of log phase growth of the bacilli in guinea pigs (Dannenbergh,

1991). Thus, the host locally destroys its own tissues to control the uninhibited growth of bacilli within non-activated macrophages. The initial focus of caseous necrosis together with the lymphadenopathy is known as the Ghon complex (Sheffield, 1994).

A wide spectrum of granulomatous reactions can be seen in patients with tuberculosis. At one extreme are individuals who develop a weak granulomatous response in which extensive tissue necrosis and large numbers of mycobacteria are present. At the other end of the spectrum are patients with indolent paucibacillary forms of tuberculosis characterised by the presence of florid noncaseating granulomatous reactions containing few detectable organisms. It is generally assumed that granuloma formations provide the framework whereby T cells (which produce the cytokines) and activated macrophages are able to maintain the close apposition necessary for effective macrophage activation. These cellular accumulations could also possibly serve to circumscribe the toxic environment. A third potentially crucial function of the granuloma is to limit dissemination of the infection from the lungs (Saunders *et al*, 1999). The initiation of the correct type of granuloma could be crucial to limiting bacterial growth, and also tissue damage and dissemination, two key components of mycobacterial disease.

Bergeron and colleagues (1997) analysed the cytokine profiles in tuberculous granulomas in adult lymph node tissue and showed that a number of cytokines were increased in these microenvironments. The tuberculous granulomas expressed either a Th1 or Th0 profile. A Th0 response, incidentally, is the simultaneous release of Th1 and Th2 cytokines. This can be attributed to the simultaneous activation of Th1 and Th2 cells, or to the activation of Th0 cells that are capable of releasing a spectrum of type 1 and type 2 cytokines. Similarly, Fenhalls and colleagues (2000) analysed the cytokine expression in adult granulomas in lung tissue of haemoptysis patients and observed a predominant Th1 response, although some patients also presented a few Th0 granulomas. These results are consistent with prior evidence for heterogeneity in the pattern of cytokines produced in response to *M. tuberculosis*.

1.6.1.2 Granuloma Formation

The factors controlling granuloma formation are only partially defined, but studies using a variety of animal models indicate that cytokines play a prominent role. In response to *M. tuberculosis* infection, the production of Th1 cytokines (IFN- γ and TNF- α) has been found to be dominant (Kindler *et al*, 1989; Chensue *et al*, 1995). The role of IFN- γ in granuloma formation is overshadowed by the importance of this molecule in limiting mycobacterial growth. In IFN- γ knockout mice, an increase in granulocytic cells with a high percentage of eosinophils entering the

lung was observed (Pearlman *et al*, 1999). IFN- γ may also therefore play a role in limiting early granulocyte accumulation to the inflammatory site. In TNF- α knockout mice, death 4 – 5 weeks after aerosol infection was associated with a massive bacterial load in the lungs and widespread dissemination to other tissues (Bean *et al*, 1999). The striking feature of this model is the failure of T cells and macrophages to form granulomas. T cells are recruited across the endothelium and accumulate in the perivascular regions of the lung, but fail to migrate into the infected tissue. TNF- α is thus crucial for the migration and aggregation of lymphocytes and mononuclear phagocytes to form granulomas. The absence of γ/δ T cells, while not affecting bacterial growth, also leads to disrupted granulomatous lesions with a marked increase in neutrophilic influx (De Souza, 1999), suggesting that the main function of these cells is controlling lesion formation.

1.6.2 The Role of Macrophages in Host Defence

Macrophages are the hosts' first line of defence when confronted with *M. tuberculosis*. This cell is capable of inhibiting growth of the bacillus through phagocytosis, which usually begins with the engulfing of the invading microbe in a membrane-bound tight vacuole (Riley, 1996). The creation of this vacuole, or phagosome, is accompanied by binding of the organism to the phagocyte through complement receptors CR1, CR3 and CR4, as well as mannose receptors (Schlesinger, 1994). Once inside the macrophages, the mycobacteria are killed by several different mechanisms. The macrophage is capable of producing reactive oxygen and nitrogen species that are crucial in growth inhibition (Flesch and Kaufmann, 1991).

A number of complicated interactions, mediated by cytokines can also cause growth inhibition or killing of these intracellular pathogens. Keane and colleagues (1997) reported that alveolar macrophages undergo apoptosis in response to intracellular infection by a TNF- α -dependent mechanism. Apoptosis of infected cells may benefit the host by eliminating a supportive environment for mycobacterial growth.

1.6.3 Antigen Presenting Cells (APCs)

Macrophages are also capable of participating in a broader context of cellular immunity through the process of antigen presentation and recruitment of T-lymphocytes, which further stimulate the APCs to inhibit growth or kill infecting mycobacteria.

Other APCs, such as dendritic cells are also present in large numbers in the airways. Dendritic cells are considered the most potent APC and play a crucial role in the initiation and development of the

acquired immune response. This initiation depends on the interaction of APCs and naïve T cells, which occurs in lymphoid organs, including lymph nodes. Dendritic cells are motile and therefore capable of homing from the peripheral tissues to the lymphoid organs after phagocytosing live *M. tuberculosis* bacteria (Austyn, 1996). Dendritic cells process antigens and migrate to the draining mediastinal lymph nodes where they activate T lymphocytes. Infected dendritic cells, as well as macrophages, are capable of producing interleukin (IL)-12 (Hsieh *et al*, 1993; Macatonia *et al*, 1995) that stimulates naïve and immune T cells to produce interferon (IFN)- γ (Gonzdez-Juarrera and Orme, 2001), which in response, stimulates the bactericidal activity of the APCs.

Bodnar and colleagues (2001) have shown that activation of dendritic cells and macrophages with IFN- γ inhibited the growth of intracellular mycobacteria. However, while this activation enabled macrophages to kill the intracellular bacteria, the *M. tuberculosis* bacilli within the activated dendritic cells were not killed. Thus, dendritic cells could restrict the growth of the intracellular bacteria, but were less efficient than macrophages at eliminating the infection.

1.6.4 T Lymphocytes

There is a role for many types of T lymphocytes in the host defence against *M. tuberculosis*. These include the T lymphocytes that express the γ/δ T cell receptor (γ/δ T cells) and more importantly the α/β T lymphocytes that comprise the T-helper cells, which express the surface protein CD4 (CD4+ T cells) and the T-cytotoxic cells which express the CD8 marker (CD8+ T cells). These lymphocytes have been shown to react to mycobacterial antigens and also expand in numbers within infected lungs (Orme, 1987; Boom, 1992; Feng and Britton, 2000).

1.6.4.1 CD4+ T lymphocytes

The major effector cell in cell-mediated immunity in tuberculosis is the CD4+ T lymphocytes (Boom, 1992; Boesan, 1995). CD4+ T cells are involved in recognition of antigens that have been processed in phagosomes and presented as small peptide fragments in the context of Major-Histocompatibility-Complex (MHC) class II molecules. These molecules occur on the surface of antigen presenting cells such as monocytes, macrophages or dendritic cells. In general, CD4+ cells help to amplify the host immune response by activating effector cells and recruiting additional immune cells to the site of disease.

It was in an effort to elucidate the role of T helper lymphocytes in the induction of the delayed-type hypersensitivity (DTH) reaction that Mosmann and colleagues (1986) first described the existence of subpopulations of CD4+ cells known as T helper type 1 (Th1) and T helper type 2 (Th2)

lymphocytes. This paradigm was initially developed in the murine model, but has now accumulated a substantial amount of support in a variety of human disease studies. By assaying cytokine production of CD4⁺ T helper cells from inbred mice, investigators were able to divide the T cell clones into two phenotypes. It was found that Th1 cells produced IL-12, IFN- γ and lymphotoxin (LT)- α , and conversely, Th2 cells produced IL-4 and other cytokines that had yet to be characterised. It has since been shown that cytokines secreted by mature Th2 cells include IL-5, IL-9, IL-10 and IL-13 (Seder and Paul, 1994; Del Prete, 1994). In humans, this division is not as stringent as in inbred mice. For example, some human Th1 cells secrete IL-10 (Yssel *et al*, 1992) and IL-13 (de Waal *et al*, 1995). In part because of such overlap of cytokine secretion, the conventional definition of a Th1 or Th2 cell depends strictly on the secretion of IFN γ or IL-4, respectively.

There is also a subset of T helper cells that have been described which produces cytokine patterns distinct from the canonical Th1 or Th2 sets, and are referred to as Th0 cells (Firestein *et al*, 1989). These T helper cells are capable of producing, among others, both IL-4 and IFN- γ . All T helper lymphocytes start out as naïve Th0 cells, which, after being activated, differentiate into either Th1 or Th2 effector cells (Sad and Mosmann, 1994). T cells in lymph nodes do not differentiate until they are exposed to specific cytokine milieus after travelling to peripheral effector sites, which occur two to three days following activation in the lymph nodes. Thus, Th1 or Th2 differentiation may not occur until an activated T cell arrives at the site of danger and samples the local cytokine milieu to determine if an inflammatory or antibody response is appropriate (Sad and Mosmann, 1994).

Both the CMI and DTH are immunological responses dependent on the Th1 type T cells. The CMI can be defined as a beneficial host response characterised by an expanded population of specific T lymphocytes, the Th1 T cell, that in the presence of microbial antigens, produce cytokines (IFN- γ , TNF- α) (Dannenberg, 1991). These cytokines attract monocytes / macrophages from the bloodstream into the lesion and activate them. Activated macrophages produce reactive nitrogen and oxygen intermediates, and other factors that kill and digest tubercle bacilli. DTH is immunologically the same process of CMI, involving Th-1 type T cells and their cytokines. DTH results in the death of local macrophages nearby tissues (caseous necrosis) and is often referred to as tissue damaging DTH or cytotoxic DTH. Such necrosis develops locally wherever the tuberculin-like antigens from the bacillus reach excessive concentrations (Dannenberg, 1991). The tissue damaging DTH inhibit bacilli growth (multiplication) by destroying bacilli-laden, non-

activated macrophages and nearby tissues, thereby eliminating the intracellular environment that is so favourable for bacillary growth.

1.6.4.2 CD8⁺ T lymphocytes

CD8⁺ cells recognize antigens that have been processed in the cytosol and that are presented in the context of MHC class I molecules on the cell surface of most nucleated cells. CD8⁺ T cytotoxic lymphocytes are known to mediate lysis of autologous cells infected by intracellular pathogens. The importance of CD8⁺ T cells in the control against tuberculosis is controversial. Contributing to the controversy has been the extreme difficulty in isolating and characterisation of mycobacteria-specific CD8⁺ T cells from infected mice and humans.

There are several studies that support the idea that stimulation of the CD8⁺ T cell population must be considered in vaccine design. Mice deficient in β -2-microglobulin (β -2m^{-/-}), a component of MHC class I molecules, exhibit increased susceptibility to tuberculosis, implying that MHC class I restricted cells are important in control of tuberculosis (Flynn *et al*, 1992). In another study, CD8⁺ T cells, from mice and humans, stimulated with *M. tuberculosis* candidate antigens (Ag85, 38K, 19K and ESAT-6) were found to be able to lyse target cells expressing the candidate antigens, as well as produce IFN- γ upon stimulation (Mohagheghpour *et al*, 1998; Zhu *et al*, 1997; Lalvani, 1998). Similarly, Lewinsohn and colleagues (1998) described human CD8⁺ T cells recognising *M. tuberculosis* infected dendritic cells that were isolated preferentially from *M. tuberculosis* infected subjects. These T cells too produced IFN- γ upon stimulation with infected cells, but lysis of infected targets was low.

Several other groups have attempted to characterise the role of CD8⁺ cells in the blood and lung in patients with pulmonary tuberculosis. Faith and colleagues (1992) and Nowakowski and colleagues (1992) each found a decreased CD4/CD8 ratio in bronchoalveolar lavage (BAL) cells from patients with pulmonary tuberculosis, whereas the ratio on peripheral blood cells was not nearly so depressed. In a similar study where lung lavage cells of tuberculosis patients were compared to that of normal control subjects, a normal CD4/CD8 ratio was observed in both study groups (Hoheisel *et al*, 1994). These data, although not consistent from study to study, support the hypothesis that MHC class I-restricted CD8⁺ T cells are required for control of tuberculosis.

1.6.4.3 γ/δ T lymphocytes

The γ/δ T cells are large granular lymphocytes that can develop a dendritic morphology in lymphoid tissues and comprise less than 10% of circulating T lymphocytes (Kaufmann, 1996). These γ/δ T

lymphocytes are prominent in organs directly exposed to antigens from the outside environment, such as the lung, intestine and skin (Boismenu and Havron, 1997). They seem to be a major type of lymphocyte involved in the early primary response to mycobacterial antigens (Bendelac and Fearon, 1997; Boismenu and Havron, 1997; Barnes *et al*, 1992; Boom *et al*, 1992). The γ/δ T lymphocytes, in general, are non-MHC-restricted. In other words, γ/δ T cells do not require antigen processing or the presentation of antigenic peptides in a class I or class II MHC restricted manner (Boismenu and Havron, 1997). Unlike the α/β T cells, antigen-specific γ/δ T-receptors are able to combine directly with peptides while they are still part of intact antigens (Chien *et al*, 1996). γ/δ T lymphocytes are activated by IL-12, secreted by infected macrophages, and produce IFN- γ and IL-12 (Boismenu and Havron, 1997). Therefore, these lymphocytes are important in host defence against the early stages of tuberculosis. *M. tuberculosis* reactive γ/δ T cells were found in the peripheral blood of tuberculin-positive healthy subjects, and those cells were found to be cytotoxic for monocytes pulsed with mycobacterial antigens (Munk *et al*, 1990). It is suggested that the γ/δ T lymphocytes, by means of their cytokines, influence and help regulate macrophages, the Th1 and Th2 responses of α/β T lymphocytes, and the production of the IgE and IgG production of B-lymphocytes. Their cytotoxic effects on nonactivated macrophages containing tubercle bacilli might play an important role in limiting the symbiotic stage of tuberculosis.

1.6.5 Cytokines

The most important factors in Th1 or Th2 phenotype development are the IL-12 and IL-4 cytokines, respectively (Constant and Bottomly, 1997). Th1 cells are the principal regulators of type-1 immunity that has been shown to be protective against mycobacteria, and other various intracellular pathogens. Development of Th1 responses depends on IL-12 produced by macrophages and dendritic cells during early stages of an infection (Hsieh *et al*, 1993; Macatonia *et al*, 1995), which as stated before, stimulates both naïve and immune T cells to produce IFN- γ (Gonzdez-Juarrera and Orme, 2001). Unlike Th1 cells and naïve T cells that absolutely require IL-12 for activation and proliferation (Kurt-Jones, 1987), Th2 cells are perfectly capable of proliferating without IL-12 if IL-4 (Kurt-Jones, 1987; Fernandez-Botran, 1986) and / or IL-1 (Chang *et al*, 1990; Litchman, 1988) are present. Therefore, in situations where IL-12 is in limited supply, only Th2 cells will be able to proliferate in response to antigenic exposure. Also, when the immune system is “in doubt” about whether Th1 or Th2 cells should be generated, Th2 outcomes are favoured. For instance, if both IL-12 and IL-4 are present at the time of T cell activation, IL-4 dominates, and the T lymphocytes differentiate to become Th2 effectors (Seder *et al*, 1993; Hsieh *et al*, 1993; Perez *et al*, 1995).

The cytokine chiefly responsible for the proinflammatory effect of the type 1 immunity is IFN- γ . Patients suffer from increased susceptibility to mycobacteria due to the lack of functional IL-12 (Frucht and Holland, 1996) or IL-12-receptor (IL-12R) (Altare *et al*, 1998) which results in an impaired IFN- γ production. IFN- γ stimulates phagocytosis (Livingston, 1989), the oxidative burst (Johnston and Kitagawa, 1985), and intracellular killing of *M. tuberculosis* bacilli. IFN- γ also upregulates expression of class I (Lapierre *et al*, 1988; Johnson *et al*, 1990), and class II MHC molecules (Volk *et al*, 1986; Male *et al*, 1987) on a variety of cells, thereby stimulating antigen presentation to T cells. Both IFN- γ and lymphotoxin- α induce other cell types, including non-leukocytes such as endothelial cells (Goebeler *et al*, 1997), keratinocytes (Teunissen *et al*, 1998), and fibroblasts (Rathanaswami *et al*, 1993; Teran *et al*, 1999), to secrete proinflammatory cytokines such as TNF- α and chemokines (Nickoloff *et al*, 1994). TNF- α is synthesised by a wide range of cell types, including macrophages and lymphocytes, and exhibits an extensive range of pro-inflammatory and macrophage-activating functions (Britton *et al*, 1998). Murine knockout models of the 55kD TNF receptor have revealed the importance of TNF- α for survival against *M. tuberculosis* infection, probably through induction of reactive nitrogen species (Flynn *et al*, 1995). Macrophages were also reported to undergo apoptosis in response to intracellular infection by a TNF- α -dependent mechanism (Keane *et al*, 1997). TNF- α was shown to be crucial to antimycobacterial immunity, with TNF knockout mice being as susceptible to an aerogenic infection with *M. tuberculosis* infection as IFN- γ knockout mice (Flynn *et al*, 1995). It is clear that IFN- γ participates in protective immunity in synergy with other factors such as TNF- α . Th2 cells, conversely, stimulate high titres of antibody production. In particular, IL-4, IL-10 and IL-13 activate B cell proliferation, antibody production, and class switching between antibodies (Lundgren *et al*, 1989; Punnomen and de Vries, 1994).

In addition to their stimulatory effects, Th1 and Th2 cells cross-regulate one another (Gajewski *et al*, 1988; D'Andrea *et al*, 1993). The IFN- γ secreted by Th1 cells directly suppresses IL-4 secretion and thus inhibits differentiation of naïve Th0 cell into Th2 cells (Gajewski *et al*, 1988). Conversely, IL-4 and IL-10 inhibit the secretion of IL-12 and IFN- γ , thereby blocking the ability of Th0 cells to differentiate into Th1 cells (D'Andrea *et al*, 1993). IL-10 is perhaps the most anti-inflammatory cytokine known (Rennick *et al*, 1995). It inhibits the secretion of proinflammatory cytokines (Fiorentino *et al*, 1991), suppresses phagocytosis (Laichalk *et al*, 1996), the oxidative burst (Romani *et al*, 1994), intracellular killing (Oswald *et al*, 1992), and inhibits antigen presentation to T cells (Enk *et al*, 1993). It is important to produce enough of a proinflammatory type 1 response to

keep the intracellular infection under control, while producing at the same time just enough of a type 2 response to prevent the type 1 response from causing damage to the host.

It is generally accepted that type 1 cytokines are expressed during the protective phase of an immune response. A switch is made to expression of type 2 cytokines during the resolution phase and to re-establish homeostasis once the infection is under control. Orme and colleagues (1993) studied the evolution of an immune response to tuberculosis in infected mice and obtained results that were in concordance with this theme. It was reported that during early infection in mice, and peaking with the time of maximum protective inflammation, IFN- γ dominated the cytokine response. When the infection had been contained (3 – 5 weeks later), IL-4 and IL-10 dominated the cytokine profile, and IFN- γ was markedly suppressed. However, there is a dichotomy between a high humoral response (induced by type 2 cytokines) and high DTH response (induced by type 1 cytokines) among patients infected with *M. tuberculosis* (Lenzini *et al*, 1977). Patients with active tuberculosis have been shown to have diminished DTH reactions, cell proliferation and IFN- γ production in response to PPD, as well as higher levels of antimycobacterial antibodies than normal PPD-positive, uninfected case control subjects (Sanchez *et al*, 1994). In addition, patients with active disease were found to produce higher levels of IL-4 (Seah *et al*, 2000). These data are consistent with the notion that active *M. tuberculosis* infection was related to dominant type-2 immunity, whereas protected patients mounted type 1 immune responses to the organism.

1.7 BIOLOGY OF *M. TUBERCULOSIS*

Mycobacteria are intracellular pathogens that survive and grow in host macrophages. Following phagocytosis, sustained intracellular bacterial growth depends on its ability to avoid destruction by macrophage-mediated host defences. The ability of *M. tuberculosis* to survive within macrophages and granulomas, as well as the onslaught of anti-tuberculosis drugs, is likely to depend upon its ability to mount an effective response to these hostile environments. However, all conventional anti-tuberculosis drugs have one thing in common: they target cellular processes involved in cell growth and division, such as cell wall biogenesis and DNA replication. The magnitude of the widening tuberculosis epidemic underscores the inadequate effectiveness of the current treatment. An improved understanding of the pathogenesis of this highly infectious disease is thus crucial if we are to develop new and improved strategies to prevent its further spread. Understanding the bacterial roles of the various *M. tuberculosis* genes identified is vital to achieve this aim.

1.7.1 Metabolic Factors / Drug Targets

1.7.1.1 *rpoB*

Rifampin (RIF) is one of the most potent drugs used in the treatment of tuberculosis and has proven to be an effective agent against susceptible strains. The molecular mechanism of RIF activity involves inhibition of the DNA-dependent RNA polymerase, by binding to the β subunit of this enzyme (Musser, 1995). This multifunctional enzyme carries out the principal biochemical steps of gene transcription, including specific promoter binding, melting of the DNA double helix, template-directed *de novo* initiation, processive elongation, and release of RNA at terminators. The purification of substantial amounts of RNA polymerase from *E. coli*, have made it possible to study the structure of this enzyme.

The active enzyme molecule is a complex oligomer containing four different subunits, termed α , β' , β and σ^{70} (Zubay, 1993). A complex with the subunit structure of $\alpha_2\beta\beta'\sigma^{70}$ can carry out the functions necessary for correct and efficient synthesis of RNA and is referred to as the holoenzyme. The σ^{70} subunit only transiently associates with the core ($\alpha_2\beta\beta'$) to catalyse transcription initiation at promoter sites, whereas the β subunit, which has a homolog in every living organism, has been implicated in each basic step of the RNA polymerase functional cycle (Kashlev *et al*, 1990). RIF binds to this subunit of the RNA polymerase holoenzyme and leads to abortive initiation of transcription (McClure and Cech, 1978).

The genes encoding subunits α , β , β' and σ^{70} have been designated *rpoA*, *rpoB*, *rpoC* and *rpoD*, respectively. The *rpoB* gene of *M. tuberculosis* was found to have 57% homology with *E. coli* β subunit. Dykxhoorn and colleagues (1996) examined the expression of the *rpoBC* genes in response to varied intracellular concentrations of the RNA polymerase subunits, and found that elevated concentrations of either β or β' repressed the expression of both *rpoB* and *rpoC* at the translational level. However, the elevated concentrations of all the subunits that comprise the holoenzyme also led to a reduction of *rpoB* and *rpoC* expression, but at the transcriptional level. It was also demonstrated that the assembly of the core enzyme ($\alpha_2\beta\beta'$) was limited by the concentrations of the β and β' subunits. The maximum transcriptional capacity of the cell therefore appears to be governed by the synthesis of β and β' . Mariani and colleagues (2000) also detected a change in the expression of *rpoB* between infected, non-activated macrophages and those macrophages activated with IFN- γ and LPS. Messenger RNA for *rpoB* was detected in the non-activated macrophages, but not in the activated host cells. This suggests that the bacilli responded to the host response by down

regulating the transcription of *rpoB*. Analysing the expression of the genes encoding the RNA polymerase enzyme subunits is thought to be a means of measuring the transcriptional activity of the bacilli, and could be an indication of the logarithmic growth phase.

1.7.1.2 *katG*

Isoniazid (INH), a widely used frontline anti-mycobacterial agent, requires oxidative activation before exerting a lethal effect (Barry, 1997). Catalase peroxidase, a heme protein encoded by the *katG* gene, is found in many microorganisms, including *M. tuberculosis*. This enzyme has high catalase and peroxidase activities that will allow it to oxidize a variety of electron donors (Johnsson *et al*, 1997). A broad range of studies has been directed at explaining the chemistry and biology of isoniazid action by establishing an association between the KatG enzyme and drug efficacy (Chouchane *et al*, 2000; Kiepiela *et al*, 2000, Heym *et al*, 1999).

Mycobacteria residing in macrophages are exposed to the reactive oxygen and nitrogen intermediates produced by phagolysosomal membranes. Little is known about the chemical processes that ensue in and around resident bacteria, but it has been shown that mycobacteria are relatively resistant to hydrogen peroxide and peroxyxynitrite (Yu *et al*, 1999). This resistance was believed to be mediated by the sole mycobacterial catalase peroxidase (KatG), a secreted protein (Sonnenberg and Belisle, 1997; Raynaud *et al*, 1998), and the alkyl hydroperoxide reductase protein (*ahpC*), respectively (Wengenack *et al*, 1999).

The effect of specific gene mutation associated with reduced susceptibility to INH on human virulence has not been thoroughly documented. The various investigations of the role of catalase peroxidase in the virulence of *M. tuberculosis* have produced conflicting results. Some investigators have observed no correlation between loss of KatG activity and virulence of *M. tuberculosis* in mice and guinea pigs (Jackett *et al*, 1978; O'Brien *et al*, 1991), and no correlation between KatG levels and susceptibility to killing by hydrogen peroxide (Jackett *et al*, 1978 (a)). However, others have found a strong correlation between KatG status and *M. tuberculosis* virulence (Manca *et al*, 1999; Li *et al*, 1998). These studies have shown that both catalase and peroxidase activity levels correlate significantly with resistance of mycobacteria to hydrogen peroxide-mediated killing. These results suggest that mycobacterial resistance to oxidative metabolites may be an important mechanism of bacillary survival within the host phagocyte.

1.7.2 Potential Persistent Factors

The current anti-tuberculosis drugs are highly effective against actively replicating cells, but they are less potent against cells in persistent phase. There is a long established observation that slow- and non-growing bacteria are phenotypically resistant or 'tolerant' to killing by antimicrobials. The Mitchison hypothesis (Figure 1.8), based on this observation, states that anti-tuberculosis drugs target distinct subpopulations of bacteria within tuberculous lesions (Mitchison, 1979). Rapidly growing bacteria are killed most effectively by INH, RIF and Streptomycin. Bacteria in the acidic environment of the phagolysosome are killed by Pyrazinamide, and the intermittently active bacteria are killed by RIF. Evidently, none of the conventional drugs are efficient killers of non-growing or persistent bacteria. Therefore, improved understanding of the physiology and metabolism of bacteria in a non-replicating dormant phase would be crucial to the identification of new and potentially more relevant drug targets. Everyday "new" genes of the tubercle bacillus are assigned different functions, some of which are summarised in Table 1.6. However, most of these studies have focussed on genes required for *in vitro* growth or in animal model systems. These have been termed virulence genes.

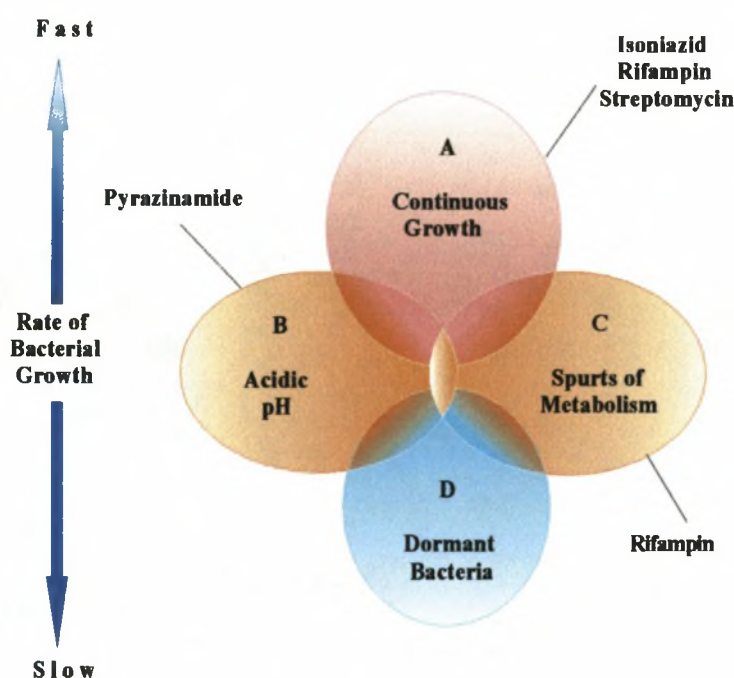


Figure 1.8. The Mitchison Hypothesis. **A.** RIF, INH and Streptomycin targets rapidly growing bacteria. **B.** PZA kills bacteria in the acidic phagolysosome, **C.** RIF also targets intermittently growing bacteria, **D.** but no conventional drugs target dormant bacteria

Table 1.6. Some Putative Virulence Genes of *M. tuberculosis*

Gene	Function	Expression System used for Analysis	References
<i>ahpC</i>	defence against oxidative stress and INH resistance	<i>M. bovis in vitro</i> culture	Wilson <i>et al</i> , 1998; Wilson <i>et al</i> , 1997
<i>eis</i>	enhanced intracellular survival protein	infection of macrophage-like cell line	Wei <i>et al</i> , 2000
<i>erp</i>	involved multiplication of <i>M.tb</i>	infection of murine macrophages	Berthet <i>et al</i> , 1998
<i>inhA</i>	INH resistance; role in mycolic acid synthesis	guinea pig model	Wilson <i>et al</i> , 1995
<i>mceD</i>	involved in cell invasion and persistence	invasion of HeLa cells	Arruda <i>et al</i> , 1993
<i>sigE</i>	sigma factor involved in gene transcription	infection of cultured macrophages	Graham and Clarke-Curtiss, 1999
<i>sigH</i>	sigma factor, involved in gene transcription	infection of cultured macrophages	Graham and Clarke-Curtiss, 1999
<i>drmC</i>	Involved in the synthesis of PDIM	Standard liquid medium	Camacho <i>et al</i> , 1999
<i>fadD26</i>	Lipid metabolism	Bone marrow macrophages from BALB/c mice	Camacho <i>et al</i> , 1999
<i>fad30</i>	biosynthesis and translocation of lipids	Bone marrow macrophages from BALB/c mice	Camacho <i>et al</i> , 1999
<i>glnA1</i>	cell wall synthesis	stationary phase broth cultures, THP-1 cells	Harth and Horwitz, 1999
<i>lipF</i>	lipid degradation; synthesis and transfer of diols in PDIM	standard liquid medium	Camacho <i>et al</i> , 1999
<i>mas</i>	synthesis of PDIM; required for growth in lungs	B57BL/6 mice spleen and liver	Cox <i>et al</i> , 1999
<i>mmpL1</i>	involved in transport and biosynthesis of PDIM	bone marrow macrophages from BALB/c mice	Camacho <i>et al</i> , 1999
<i>mmpL2</i>	transport and biosynthesis of PDIM	bone marrow macrophages from BALB/c mice	Camacho <i>et al</i> , 1999
<i>mmpL4</i>	involved in the transport of PDIM	B57BL/6 mice spleen and liver	Cox <i>et al</i> , 1999
<i>pksb</i>	polyketide synthase	bone marrow macrophages from BALB/c mice	Camacho <i>et al</i> , 1999
<i>ppsA-E</i>	synthesis of PDIM; required for growth in lung	B57BL/6 mice liver and spleen	Cox <i>et al</i> , 1999

PDIM – Phthiocerol dimycocerosate, a cell wall lipid

1.7.2.1 *icl*

The strategy for survival during chronic stages of infection entails a metabolic shift in the bacteria's carbon source to C2 substrates generated by oxidation of fatty acids. Most microorganisms growing on acetate or fatty acids as the sole carbon source employ the glyoxylate bypass for the biosynthesis of cellular material (Kornberg, 1966).

The glyoxylate cycle effectively circumvents the loss of two CO₂ of the tricarboxylic acid (TCA) cycle, thereby permitting net incorporation of carbon into cellular structures during growth on acetate and fatty acids (Umbarger and Zubay, 1993). It is an alternative pathway that, like the TCA, begins with citrate formation, but results in anabolism to the four-carbon level rather than catabolism to the one-carbon level. Isocitrate is split into two molecules, glyoxylate and succinate, rather than being oxidatively decarboxylated, as would occur in the TCA cycle. The reaction is catalysed by isocitrate lyase, an enzyme encoded by the *icl* gene. Even during the operation of the TCA cycle, many fatty acids are partially metabolised to acetyl-CoA, thus requiring the presence of ICL (Vanni *et al*, 1990).

Honer-Zu Bentrop and colleagues (1999) reported that in both *M. tuberculosis* and *M. avium*, the production and activity of ICL was enhanced under minimal growth conditions, but only when supplemented with acetate or palmitate. It was recently demonstrated that disruption of *icl* attenuates persistence of *M. tuberculosis* in mice and inflammatory macrophages (McKinney *et al*, 2000). While the deletion of *icl* did not affect bacterial growth in immunocompetent mice during the acute phase of infection (0 – 2 weeks), significant reduction in bacterial loads and macroscopic lesions were observed during the chronic phase (2 – 6 weeks).

The glyoxylate-pathway enzymes are present in most prokaryotes, lower eukaryotes and plants, but have not been observed in vertebrates, making it a potential new drug target. Current anti-tuberculosis drugs have traditionally been identified by their ability to suppress or kill replicating cultures of bacteria *in vitro*. Drug targeting ICL would have therefore been missed in traditional screens because this enzyme is non-essential under standard culture conditions. There is thus an urgent need for an improved understanding of the biology of bacteria growing *in vivo*.

1.7.2.2 *narX*

It is largely unknown how the bacteria survive during the persistent stage of infection. Disease progression is halted when an effective immune response is mounted and the bacilli become restricted to the characteristic tuberculous lesions. The bacillus can survive in the caseous necrotic

centre of these lesions, but it apparently cannot multiply because of oxygen deprivation and other adverse conditions (Cunningham and Spreadbury, 1998). It is within this anaerobic environment consisting of caseous necrotic material that bacterial dormancy probably occurs (Wayne, 1994). It was shown that *M. tuberculosis* and its close relative *M. bovis* BCG are obligate aerobes (require oxygen for growth) but have the ability to adapt to and survive anaerobiosis by shifting down to a state of synchronised, non-replicating persistence (Wayne and Hayes, 1996). This suggested that the bacteria switch from an aerobic metabolism supporting growth to an anaerobic metabolism supporting non-growing persistence.

The *M. tuberculosis* genome project revealed the presence of enzymes that might be involved in anaerobic respiration and fermentation (Cole *et al*, 1998). Based on the genome sequence, Hutter and Dick (1999) carried out a Northern blot screen and found that *narX*, a putative fused nitrate reductase, was strongly upregulated in the anaerobic non-growing state of *M. bovis* BCG. In aerobic growing bacilli, *narX* transcripts were not detectable. The induction of *narX* indicated that the corresponding gene product might play a role in the dormant state of the late cycle of the bacilli. Wayne and Hayes (1998) also reported a rapid increase of nitrate reduction in *M. tuberculosis* cultures grown with nitrate during the shift down to anaerobic persistence. In addition, the presence of several putative transmembrane domains at the C-terminus indicated that NarX could be an integral membrane protein and might be associated with the electron transport chain. The structural features of the NarX protein together with the observation that *narX* expression appears to depend on anaerobiosis (Hutter and Dick, 1999), suggested that NarX might function as a respiratory nitrate reductase. This response may help the bacilli survive in oxygen depleted regions of inflammatory tissue where nitrate can occur as a degradation product of nitric oxide.

1.7.2.3 *mbtB*

The various defensive mechanisms expressed by the eukaryotic host include a dramatic restriction of available iron to support microbial growth (Kontoghiorghes and Weinberg, 1995). The mechanism that allows pathogenic bacteria to grow in such iron-limited environment is dependent on its ability to scavenge this limited metal. Mycobacteria produce and secrete specialised iron chelators known as siderophores (Gobin *et al*, 1995), and then specifically take up those complexed with ferric ion. *M. tuberculosis* synthesise two forms of mycobactin siderophores that have been proposed to have different physical properties, particularly regarding aqueous solubility, leading to the proposition that they have discrete biological roles. This slow growing pathogen produces the lipophilic, membrane-associated mycobactin T (Snow, 1970) and the water-soluble / hydrophilic mycobactin T, also referred to as exochelins (Macham and Ratledge, 1975). The hydrophilic

mycobactin T has been proposed to be secreted into the aqueous growth medium for direct competition with iron-binding molecules of the environment. The membrane-associated mycobactin T has been proposed to operate as an ionophore to shuttle iron across the extremely hydrophobic cell wall after transfer of the iron from the extracellular siderophore (Gobin and Horwitz, 1996).

Mycobactins consists of a core hydroxyphenyloxazoline structure that is thought to be derived from salicylic acid after condensation with a serine residue. The virulence-conferring mycobactins of *M. tuberculosis* have sufficient structural homology to other siderophores (Chambers *et al*, 1996). It was therefore suggested that they probably arose through a common biosynthetic strategy using comparable non-ribosomal peptide synthetase catalytic logic. Quadri and colleagues (1998) identified the gene cluster in *M. tuberculosis* responsible for mycobactin synthesis, which they named *mbtA-J*. This was in concordance with the publication of the complete *M. tuberculosis* genome by Cole and colleagues (1998), in which they suggested that these genes could encode mycobactin biosynthetic proteins.

This cluster encodes a mixed polyketide synthase / non-ribosomal peptide synthetase system (Quadri *et al*, 1998). The *mbtB* gene encodes an enzyme proposed to catalyse the initial steps in the mycobactin T biosynthetic pathway, the condensation of salicylic acid with serine, and the formation of the hydroxyphenyloxazoline nucleus of these siderophores (De Voss *et al*, 1999). Analyses of siderophores by a $\Delta mbtB$ mutant revealed that biosynthesis of all salicylate-derived siderophores were interrupted (De Voss *et al*, 2000). This allowed investigators to establish that under conditions of iron limitation, siderophore production is essential for optimal growth of *M. tuberculosis*. In addition, the $\Delta mbtB$ mutant was also unable to replicate in cultured macrophages, suggesting that siderophore production enhances growth in these host cells.

1.7.2.4 rel_{Mtb}

Adaptation of bacilli to long-term survival with restricted access to nutrients or oxygen may be associated with coordinated alterations in patterns of gene expression in specific metabolic networks. In *E. coli*, the stringent response is a broad transcriptional program encompassing approximately 80 genes that mediates adaptation to survival under conditions of starvation. Induction of the stringent response stimulates polyphosphate synthesis (Rao and Kornberg, 1996), increases fatty acid cyclopropanation (Eichel *et al*, 1999), upregulates glycogen (Bridger *et al*, 1978), as well as stationary-phase sigma factor RpoS synthesis (Loewen *et al*, 1998). This response also inhibits fatty acid, phospholipid (Heath *et al*, 1994) and RNA synthesis (Liang *et al*, 2000).

Amino acid, carbon, nitrogen or phosphorous deficiency as well as fatty acid starvation (Seyfzadeh *et al*, 1993), were shown to induce the stringent response.

The stringent response is mediated by increased intracellular levels of hyperphosphorylated guanine nucleotides, specifically the 3'-pyrophosphate derivative of GDP (ppGpp), and the 3'-pyrophosphate derivative of GTP (pppGpp). Binding of (p)ppGpp (mixture of both derivatives) to RNA polymerase changes the structure of the polymerase so that it has a lowered affinity for rRNA, tRNA and ribosomal protein promoters, and at the same time, a greater affinity for some other promoters (Zubay, 1993; Kvint *et al*, 2000). The stringent response utilizes hyperphosphorylated guanine as a signalling molecule to control bacterial gene expression involved in long-term survival under starvation conditions.

In gram negative bacteria, (p)ppGpp is produced by the activity of the related RelA and SpoT proteins. RelA is ribosome associated and is activated by binding uncharged tRNAs to the ribosome upon depletion of amino acids (Mitchison, 1992; Liang *et al*, 2000). SpoT is not associated with ribosomes and has both (p)ppGpp synthetic and hydrolytic activities (Heinemeyer *et al*, 1978). *M. tuberculosis* only has a single RelA or SpoT homolog, designated Rel_{Mtb} (Cole *et al*, 1998) and responds to nutrient starvation by producing (p)ppGpp (Ojha *et al*, 2000). Primm and colleagues (2000) demonstrated that there was a very low basal level of (p)ppGpp in log-phase wild-type *M. tuberculosis* grown axenically on glucose, with accumulation starting in early stationary-phase cultures, and reaching a maximum in long-term stationary-phase cultures. It was consequently suggested that the Rel_{Mtb}-mediated production of (p)ppGpp induced proteins are involved in stationary-phase survival. This assumption was supported when late-log phase cultures of the *rel_{Mtb}* knockout *M. tuberculosis* H37Rv strain failed to reduce the amount of stable RNA and ribosomal proteins, and was, as anticipated, unable to adapt to the stationary phase (Primm *et al*, 2000). No (p)ppGpp was detected in these cultures. The Δ rel_{Mtb} mutant also displayed a significantly slower aerobic growth rate than the wild-type in synthetic liquid media, whether rich or minimal. The knockout model therefore shows that in the absence of the stringent response, *M. tuberculosis* fails to adapt to the stationary phase and long-term survival is severely compromised. The results also suggested that during aerobic growth under standard or enriched conditions, some level of (p)ppGpp is required for optimum growth.

1.7.3 Immunological Significant Antigenic Proteins

For the development of both new vaccines and diagnostic reagents to replace the tuberculin purified protein derivative (PPD), there is a need to identify and evaluate the human response against

defined *M. tuberculosis* antigens. Several studies suggested that surface proteins and proteins actively secreted by *M. tuberculosis* are important targets for the immune system during the early phase of infection (Andersen *et al*, 1992; Andersen Heron, 1993; Andersen, 1994; Pal and Horwitz, 1992). In recent years, research has been focussed on antigens released by live *M. tuberculosis* into the culture media, as these antigens are believed to be at least partially responsible for the efficacy of live vaccines. Pools of such extracellular antigens have been tested in several laboratories as subunit vaccines and demonstrated to induce substantial levels of protection in animal models (Andersen *et al*, 1994; Pal and Horwitz, 1992).

1.7.3.1 *esat-6*

A novel protein, designated the 6-kDa early-secreted antigenic target (ESAT-6), was identified in culture filtrates of virulent *M. tuberculosis* (Sorensen *et al*, 1995; Harboe *et al*, 1996). ESAT-6 expression was found to be restricted to the *M. tuberculosis* complex, whereas *M. bovis* BCG and the majority of environmental mycobacteria lack this antigen. The physiological role of ESAT-6 in *M. tuberculosis* remains to be established as well as how it is exported into the surrounding medium remains to be elucidated.

The ESAT-6 protein stimulates T cells from tuberculosis patients to proliferate and produce IFN- γ (Ulrichs *et al*, 1998; Lalvani *et al*, 2001; Arend *et al*, 2000; Ravn *et al*, 1999). ESAT-6 has been considered a possible candidate for use in the diagnosis of tuberculosis because of its high specificity and sensitivity. Ulrichs and colleagues (1998) demonstrated that *M. tuberculosis* ESAT-6 can stimulate T cells from tuberculosis patients, but not T cells from tuberculin-positive healthy donors. These healthy PPD+ donors were assumed to be positive due to previous BCG vaccination. In a later study, Ulrich and colleagues (2000) reported that the number of IFN- γ producing cells reactive to ESAT-6, were increased in tuberculosis patients, as well as recent converters to PPD positivity, but as in the previous study, no reactivity was observed in unvaccinated or vaccinated healthy donors. They proposed that ESAT-6 is a potential candidate for use in detection of active disease as well early tuberculosis. In addition, Lalvani and colleagues (1998) also demonstrated that the majority of the healthy, tuberculin positive adults, with normal chest radiographs, harbour IFN- γ secreting T cells specific for ESAT-6. These investigators also proposed that the ESAT-6 specific IFN- γ secreting T cells could also be used to identify latently infected, tuberculin positive, healthy household contacts of patients with sputum-smear positive tuberculosis.

1.7.3.2 PPE

The complete genome sequence of *M. tuberculosis* H37Rv (Cole *et al*, 1998) highlighted the existence of the large gene family, namely the PPE gene family that consists of 68 members. The PPE genes have a relatively conserved 180 amino acid (aa) N-terminal region in common (Cole *et al*, 1998) and range in size from 77 aa to 3 300 aa. The function of the glycine rich PPE proteins has not been established. It has been suggested that they may be of immunological significance, either by providing a source of antigenic variation in, what is considered, a genetically homogenous bacterium, or by antigen processing by host cells (Cole *et al*, 1998).

There is currently very limited knowledge of the PPE gene expression profiles. Rivera and colleagues (1998) provided the first proof of *in vitro* expression of PPE genes when they demonstrated the upregulation of the PPE gene Rv0755c in H37Ra relative to H37Rv. Similarly, the PPE gene Rv2770c was shown to be upregulated in *M. tuberculosis* H37Rv vs. H37Ra (Rindi *et al*, 1999). Rodriguez and colleagues (1999) recently reported the upregulation of the PPE gene Rv2123 under low iron conditions *in vitro*, and speculated that the gene product may be involved in iron uptake. Indirect evidence for *in vivo* expression of the PPE genes was provided by a study of a serine-rich antigen from *M. leprae* (Vega-Lopez *et al*, 1993), which was recognized by serum from both leprosy and tuberculosis patients. This protein is now known to be a member of the PPE gene family. It was recently shown that a mutant strain of *M. tuberculosis* with a transposon-generated knockout PPE gene Rv3018c is attenuated for growth in lungs of mice (Camacho *et al*, 1999). This implies a role for this gene in early infection, although *in vivo* expression in the human host of the gene was not confirmed.

1.8 AIMS OF STUDY

A major drawback of all the techniques utilised in the studies described above is that they do not allow for the detection of viable bacilli within its natural host environment, the granuloma. The aims of the study were to analyse *M. tuberculosis* gene expression and host cytokine expression in the human granulomas, from lymph node tissue from children. This was done in order to determine whether the bacterial gene expression profile responds to the host environment, or conversely, whether the host cytokine expression responds to the bacterial growth state. Lymph node child tissue was thought to be the ideal target material for analysis, in order to avoid the confounding effects of these drugs. The anti-tuberculosis drugs would influence bacterial gene expression, resulting in the killing of the bacilli, and would therefore also affect the host response. In this study we used *in situ* hybridisation to demonstrate that DNA from *M. tuberculosis* is present in a high

proportion of granulomas from TB patients. This technique allows for the localisation of the bacilli within the host tissue. This study also addressed the question of *M. tuberculosis* differential gene expression, specifically *rpoB*, *katG*, *narX*, *icl*, *mbtB*, *rel_{Mtb}*, *esat-6* and *PPE Rv3018c*, within the human granuloma in order to determine whether these genes were expressed within the granuloma microenvironment during host infection. Expression profiles of the infecting bacilli were investigated by RNA:RNA *in situ* hybridisation. We studied the host immune response induced by the infecting *M. tuberculosis* strains, by analysing the cytokine production in the human lymph node granuloma using immunohistochemistry. The cytokines analysed included type-1 cytokines IL-12, IFN- γ and TNF- α , as well as type-2 cytokines IL-4 and IL-10. The data was then stratified to identify any correlations between *M. tuberculosis* gene expression and state of disease. The co-localisation of mycobacterial DNA and mRNA with host cytokines was a case study to identify any correlations between the bacterial growth phase and host response. The findings of this study present new opportunities for investigating the interaction between the pathogen and its host.

CHAPTER TWO

MATERIALS AND METHODS

INDEX	PAGE
2.1 TISSUE SPECIMENS	
2.1.1 Lymph Node Biopsies	41
2.2 PREPARATION OF SLIDES FOR <i>IN SITU</i> HYBRIDISATION AND IMMUNOHISTOCHEMISTRY	41
2.3 PREPARATION OF PROBES FOR <i>IN SITU</i> HYBRIDISATION	
2.3.1 DNA MTB484 Probe	41
2.3.2 Riboprobes	42
2.3.2.1 Recombinant Vectors Containing <i>M. tuberculosis</i> Gene Inserts	42
2.3.2.1.1 Preparation and Transformation of Competent <i>E. coli</i> Cells	44
2.3.2.1.2 Large Scale Isolation of Plasmid DNA	44
2.3.2.2 Polymerase Chain Reaction (PCR)	
2.3.2.2.1 Oligonucleotide Primers	45
2.3.2.2.2 PCR Conditions	46
2.3.2.3 Agarose Gel Electrophoresis	46
2.3.2.4 Purification of Amplified PCR Products	47
2.3.2.5 Preparation of Biotinylated Riboprobes	47
2.4 <i>IN SITU</i> HYBRIDISATION	49
2.4.1 Brief Description	49
2.4.2 Pretreatment of Tissue for <i>In Situ</i> Hybridisation	49
2.4.3 Hybridisation of Biotinylated Probes	50
2.4.3.1 DNA:DNA Hybridisation	50
2.4.3.2 RNA:RNA Hybridisation	51
2.4.3.3 Hybridisation	51
2.4.4 Detection of Hybridised Probes	51
2.4.5 Counterstaining	52

2.5 IMMUNOHISTOCHEMISTRY	52
2.5.1 Brief Description	52
2.5.2 Pretreatment of Tissue for Immunohistochemistry	53
2.5.3 Binding of Primary and Secondary Antibodies	54
2.5.4 Detection of Bound Antibody Probes	54
2.5.5 Counterstaining	55
2.6 DUAL LABELING	55
2.6.1 Brief Description	55
2.6.2 Immunohistochemistry Staining of CD68 Receptors	
2.6.2.1 Pretreatment of Tissue	55
2.6.2.2 Binding of Primary and Secondary Antibody	55
2.6.2 <i>In Situ</i> Hybridisation	56
2.7 PHOTOGRAPHY	57
2.8 ASSESSMENT OF SLIDES	57
2.9 STATISTICAL EVALUATION OF DATA	57
2.10 DNA FINGERPRINTING OF ISOLATED CLINICAL STRAINS FROM LYMPH NODE TISSUE	57
2.10.5 Brief Description	57
2.10.6 Extraction of Mycobacterial DNA	58
2.10.7 Restriction Enzyme Digestion of the DNA	59
2.10.8 Altering Concentrations of the Restricted DNA	60
2.10.9 Gel Electrophoresis of Restricted DNA	60
2.10.10 Southern Transfer of the Fingerprinting Gel	60
2.10.11 Labeling of Probes and Hybridisation	61
2.10.12 Data Analysis	62

2.1 TISSUE SPECIMENS: LYMPH NODE BIOPSIES

Lymph node biopsy tissue was collected in a clean, sterile container. A portion of the lymph node of each patient was immersed in saline and was subsequently submitted for culture (BACTEC) for the isolation of the infecting strain (Department of Medical Microbiology, Tygerberg Hospital, Cape Town, South Africa). The remaining portion of the infected node for each patient was immediately fixed in formalin (Appendix 1), processed and embedded in wax (Department of Anatomical Pathology, Tygerberg Hospital, Cape Town, South Africa). Sections of the embedded tissue were used for histological analysis and ZN staining, while culture was requested for confirmation of tuberculosis lymphadenitis.

Informed consent was obtained from a parent / guardian of all the patients (Appendix 2), and the study was approved by the Stellenbosch University Ethical Review Committee.

2.2 PREPARATION OF SLIDES FOR *IN SITU* HYBRIDISATION AND IMMUNOHISTOCHEMISTRY

Retention of cells on the slides requires pretreating the slides with an appropriate agent for increasing cell adhesion, as samples would otherwise be lost from untreated slides. Precleaned slides (Sigma, USA) were incubated overnight in chromic acid (Appendix 1), which was carefully decanted, after which the slides were rinsed thoroughly in tap water to remove residual acid. The slides were then rinsed (x5) with distilled H₂O (dH₂O) and then incubated for 30 minutes in dH₂O. The water was poured off and the slides were immersed in acetone (Merck, UK) for 30 minutes. This was followed by incubating the slides in 2% 3-aminopropyltriethoxysilane (Sigma, USA) in acetone for a further 30 minutes. The slides were dried at 70°C for 1 hour, and then incubated in diethyl-pyrocabonate (Sigma, USA) treated water (DEPC-dH₂O) for 2 hours. The slides were baked at 70°C overnight and finally stored in a dust-free box at room temperature.

2.3 PREPARATION OF PROBES FOR *IN SITU* HYBRIDISATION

2.3.1 DNA MTB484 Probe

The plasmid pMTB484 containing PGRS repeat sequences (Warren *et al*, 1996) was digested with *Hinf*I and electrophoretically fractionated through a 0.8% agarose gel (1x TBE pH8). A 4.5 kb DNA

fragment was purified using the DNA purification system (Promega, USA) according to the manufacturers instructions. The purified fragment was biotinylated with Bio-11-dUTP according to the nick translation method (Sambrook et al, 1989). Briefly, the DNA fragments (1g), DNase I (1 U) and DNA polymerase (5 U) were added to a solution containing 1x BSA, 1x DNase I buffer and 10 mM dNTP mix (dATP, dCTP, dGTP and Bio-11-dUTP). The labeling reaction was incubated at 16C for 1 hour, after which 0.01 M EDTA pH8.0 was added. The biotinylated labeled DNA was then desalted over 950 M Sephradex equilibrated in STE pH8.0.

2.3.2 Riboprobes

2.3.2.1 Recombinant Vectors Containing *M. Tuberculosis* Gene Inserts

Regions complementary to the *M. tuberculosis* genes *rpoB*, *ICL*, *narX*, *relA*, *mbtB*, *ESAT-6*, *PPE* and *katG* (Table 2.1, 2.2) had been cloned into pGEM-T easy vector systems (Promega, UK) (Figure 2.1) in the Department of Medical Biochemistry, University of Stellenbosch, Tygerberg, South Africa. All the plasmids were sequenced to confirm the presence of the correct *M. tuberculosis* sequence as well as to determine the orientation of the cloned fragments. These recombinant plasmids were transformed into *E. coli* JM109 cells in order to generate more plasmids for the synthesis of riboprobes.

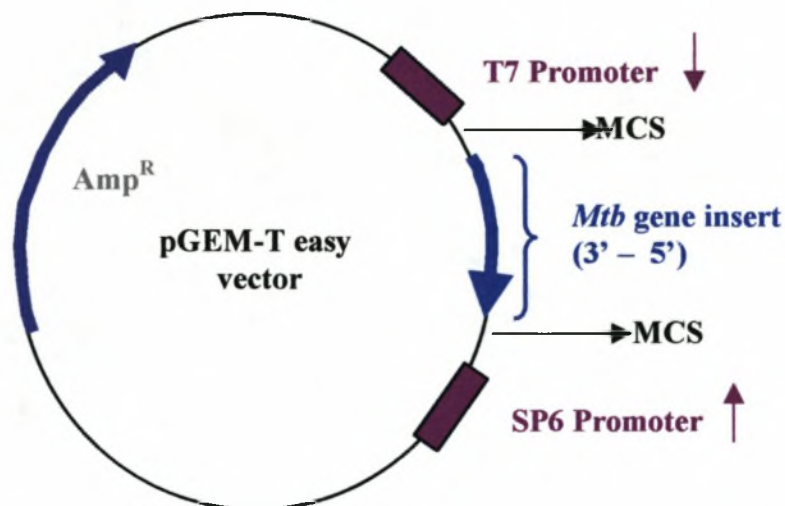


Figure 2.1. Schematic representation of the pGEM-T easy vector containing *Mtb* gene fragments cloned between the T7 and SP6 promoters

Table 2.1 Size of *M. tuberculosis* gene inserts cloned into pGEM-T easy vector systems

<i>M. tuberculosis</i> Gene	Gene Code	Size of Insert (bp)
<i>rpoB</i>	Rv0667	393
<i>narX</i>	Rv1763c	452
<i>icl</i>	Rv467	466
<i>rel_{Mtb}</i>	Rv2583c	442
<i>mbtB</i>	Rv2383c	429
<i>esat-6</i>	Rv0282	295
<i>PPE</i>	Rv3018c	403
<i>katG</i>	Rv1908c	412

Table 2.2 Primer sequences for the amplification of the *M. tuberculosis* genes from H37Rv genome

<i>M. tb</i> Genes	Forward Primer	Reverse Primer
<i>rpoB</i>	TGGTCCGCTTGCACGAGGGTCAGA	ATGTGCCCGATCGAAACCCCTGAG
<i>narX</i>	AGTTCGCCCATCATGTCACC	AACTCACGGCAACTCGGCAC
<i>icl</i>	AAGACGTAGCCGCCACTCAG	TGATAAACGGGCGGAAGTC
<i>rel_{Mtb}</i>	CCTGTCGATCTTGCAGCGAG	GGTGCAATGACTTCCAACGTC
<i>mbtB</i>	AGCAGGTCGACGTCTGGATG	ATGAGCTACCGCATCTTGCTG
<i>esat-6</i>	GAGCAGCAGTGGAAATTCGC	TCCAGTGACGTTGCCTTC
<i>PPE</i>	ATTCGGCGGTGCTAAGTGC	AACTCAGCACTGGGACCCTG
<i>katG</i>	ATGGCCGCGGCGGTCGACATT	GGGGTCGTTGACCTCCCACCCGAC

2.3.2.1.1 Preparation and Transformation of Competent *E. coli* Cells

The method of Draper *et al.* (1988) was used for the transformation of *E. coli* JM109 cells.

A 1 ml aliquot of an overnight culture was placed into 100 ml of Luria Bertani (LB) broth (Appendix 1), and was grown with shaking at 37°C until the optimal density (OD) of the cells measured at 600 nm (OD_{600}) reached 0.35. The OD was determined in a Milton Roy series 120i spectrophotometer (USA). The culture was transferred into a sterile GSA bottle and chilled on ice for 15 minutes. Cells were pelleted by centrifugation at 4°C for 5 minutes at 3000 rpm in a Sorvall RC-5B refrigerated super-speed centrifuge (rotor GSA). The supernatant was decanted and the cells were gently resuspended in ice-cold 21 ml TFB1 solution (Appendix 1), and incubated on ice for 90 minutes. The cells were again pelleted at 3000 rpm for 5 minutes at 4°C, and the supernatant removed. Cells were gently resuspended in 3.5 ml chilled TFB2 (Appendix 1) and the competent cells were either used immediately for transformation, or frozen in liquid nitrogen and stored at -80°C.

Plasmid DNA (10 ng) in TE buffer (Appendix 1) was added to 100 µl of competent cells in a sterile Eppendorf microfuge tubes, and incubated on ice for 15 minutes. The cells were heat shocked by placing the tubes in a 45°C water bath for 60 seconds, then returned immediately to the ice for a further 2 minutes. LB broth (800 µl) was added to each Eppendorf microfuge tube, which was then incubated at 37°C for 30 minutes. Cell aliquots of 100 µl were plated onto LB agar plates (Appendix 1) containing 50 µg/ml of ampicillin (Appendix 1).

2.3.2.1.2 Large Scale Isolation of Plasmid DNA (Nucleobond Kit)

The procedure as outlined by Machery-Nagel was followed for the preparation of plasmid DNA.

A single colony from a freshly streaked bacterial plate was inoculated into 5 ml LB broth, containing 50 µg/ml ampicillin, and grown at 37°C until the OD_{600} reached 0.35. One ml of the starter culture was then inoculated into 100 ml prewarmed LB broth (1/100 dilution) containing ampicillin (50 µg/ml) and incubated overnight at 37°C.

The cells were transferred to a sterile GSA bottle, and were harvested in a Sorvall RC-5B refrigerated super speed centrifuge (GSA rotor) at 5000 rpm for 5 minutes at 4°C. The supernatant was decanted and the pellet was resuspended in 4 ml of buffer S1. The cells were disrupted by adding 4 ml of buffer S2, mixing the contents by gently inverting the tube 6 – 8 times, then incubating for a maximum time of 5 minutes at room temperature. Buffer S3 (4 ml) was added; the contents were mixed again by inverting the tube 6 – 8 times and incubated on ice for 5 minutes.

Centrifugation at 15 000 rpm for 40 minutes at 4°C was done to pellet the cell and protein debris. The nucleobond cartridge was equilibrated with 2 ml of buffer N2, and the supernatant of the previous step was loaded onto the AX100 column. The supernatant was allowed to flow through the column, followed by two successive wash steps using 4 ml of N3 buffer per wash. The plasmid DNA was eluted from the column with 2 ml of buffer N5 and precipitated with 0.7 volume of isopropanol (Merck, UK). After incubating at room temperature for 60 minutes, the plasmid DNA was pelleted by centrifugation in a benchtop microcentrifuge at top speed (13 000 rpm) for 30 minutes at 4°C. The pellet was washed with 70% ethanol (Appendix 1) and centrifuged at 13 000 rpm for 10 minutes at 4°C. The ethanol was carefully decanted and the pellet was air dried for 15 to 20 minutes before being resuspended in 50 µl 1M Tris-EDTA (TE) buffer (Appendix 1).

The OD of the DNA was determined in a Milton Roy series 120i spectrophotometer (USA) at 260 nm (OD_{260}) with absorbance of TE buffer (standard) at 0. The concentration of the purified DNA was determined by diluting 10 µl of plasmid DNA in 490 µl of TE buffer, and the measured OD_{260} was multiplied by a factor of 2.5 ($1/20 \times OD_{260} \times 50$ (dilution factor)). This provided the DNA concentration in µg/µl. The purity of the DNA was determined by calculating the ratio of the OD_{260} and the OD_{280} , which should be approximately 1.8 for pure DNA.

2.3.2.2 Polymerase Chain Reaction (PCR)

2.3.2.2.1 Oligonucleotide Primers

Oligonucleotide primers are homologous to the unique sequence flanking the area being amplified, which makes the PCR very specific. *Taq* DNA polymerase is capable of locating the region to which the primers bind to the denatured single stranded DNA, and proceed from this point to synthesise a complementary DNA strand in the 5' to 3' direction (Figure 2.2). T7 and SP6 promoter regions flank the multiple cloning sites of the pGEM-T easy vectors. The T7 and SP6 primers (Table 2.3) were designed using the DNAMAN (Lynnon Biosoft Copyright[®]) computer program. These primers were complementary to the regions flanking the T7 and SP6 phage promoters, and were thus designed to amplify the various *M. tuberculosis* genes cloned (Table 2.1) in this region (Figure 2.1). The oligonucleotide primers were synthesized according to standard phosphoramidite methodology (GibcoBRL, Switzerland).

Table 2.3. T7 and SP6 Primer Sequences.

Primer	Length (bp)	Sequence (5' to 3')	T _m °C
SP6	20	CAC TTT ATG CTT CCG GCT CG	62
T7	21	GCG ATT AAG TTG GGT AAC GCC	65

2.3.2.2.2 PCR Conditions

PCR amplification was performed using 100 ng plasmid DNA, i.e. pGEM-T easy vectors containing various *M. tuberculosis* genes were aliquoted into sterile 0.5 ml Eppendorf microfuge tubes. One micromolar of each primer, 200 µM of dNTP mixture (Appendix 1), 1.5 mM MgCl₂, 5 µl of a 10x *Taq* DNA polymerase buffer (Roche, Germany), 0.5 U *Taq* DNA polymerase (Roche, Germany) and ddH₂O to a final volume of 50 µl was added to the plasmid DNA. The reaction mixture was subsequently overlaid with 30 µl mineral oil (Sigma, USA) to prevent evaporation during thermal cycling. Amplification was carried out in a Hybaid Touchdown Thermal Cycler (Hybaid Ltd, UK), with the PCR conditions for the amplification reactions summarised in Table 2.4.

Table 2.4. PCR conditions for the amplification of *M. tuberculosis* gene fragments

Temperature (°C)	Time	Cycles
94	4 minutes	1
94	30 seconds	
60	60 seconds	35
72	60 seconds	
72	5 minutes	1

2.3.2.3 Agarose Gel Electrophoresis

Agarose gels, made with high purity wide range agarose (Whitehead Scientific, RSA), were used for verification of success of the PCR amplification. Five microlitres of the PCR product were mixed with 1 µl of bromophenol blue loading dye (Appendix 1). The samples were subsequently loaded in 1% horizontal agarose gels (1 g agarose in 100 ml 1xTAE (Appendix 1)) containing 1 µg/µl Ethidium Bromide (Appendix 1), and electrophoresed at 70 V for approximately 2 hours in

1x TAE electrophoresis running buffer. The samples were co-electrophoresed with Marker X (Roche, Germany) (Appendix IV), which was used as a molecular size marker. All gels were visualised on a longwave ultraviolet transilluminator (3UV Transilluminator model LMS-26E) and a photograph was taken using an ITC camera (Berkenhoff and Drebes, Germany) and a Sony video graphic printer (UP-860 CE).

2.3.2.4 Purification of Amplified PCR Products (Concert Rapid PCR Purification System)

The procedure as outlined by Gibco BRL (Switzerland) was followed for the purification of amplified PCR products.

The amplification reaction mixture was mixed with 400 µl H1 Binding Solution, and subsequently loaded into a spin cartridge placed into a 2 ml wash tube. This mixture was centrifuged for 1 minute at 14 000 rpm at room temperature in a microcentrifuge. Seven hundred microlitres H2 Wash Buffer was added to the spin cartridge after the eluate was discarded, and centrifuged at 14 000 rpm for 1 minute at room temperature. The eluate was decanted and the residual wash buffer was removed by centrifuging at 14 000 rpm for 1 minute. To elute the DNA, the spin cartridge was placed in a new 1.5 ml recovery tube and 50 µl of preheated TE buffer (65 - 70°C) was added directly to the centre of the spin cartridge. After incubation of 1 minute at room temperature, the purified PCR product was eluted by centrifugation at 14 000 rpm for 2 minutes.

2.3.2.5 Preparation of Biotinylated Riboprobes

All the *M. tuberculosis* gene fragments were cloned in the 3' – 5' orientation, relative to the T7 promoter (Figure 2.2). The antisense probes, used for the detection of mRNA, are synthesised using T7 RNA polymerase (GibcoBRL, Switzerland), from the T7 promoter using the sense DNA strand of the amplified *M. tuberculosis* gene fragments as template (Figure 2.2c). For the synthesis of sense probes, as with mRNA synthesis, the antisense DNA strand was used as template (figure 2.3b) with SP6 RNA polymerase. The antisense probes thus had the complementary sequence to that of the target mRNA, and as a result hybridised to it, while the sense probe showed no homology to any RNA species and therefore served as a control. All procedures were done under RNase-free conditions. Briefly, biotinylated riboprobes were prepared in sterile 1.5 ml DEPC treated Eppendorf microfuge tubes using 1 µg DNA, 1x T7 or SP6 transcript buffer, 1 mM of each dATP, dGTP, UTP and Biotin-14-CTP, 0.5 mM dCTP, 5 mM DTT, 120 U RNase OUT Inhibitor, 100 U T7 polymerase or 52.5 U SP6 polymerase and DEPC dH₂O to a final volume of 50 µl. The

polymerase or 52.5 U SP6 polymerase and DEPC dH₂O to a final volume of 50 µl. The contents were briefly spun in a microcentrifuge, and incubated for 90 minutes at 37°C in a waterbath. One hundred and fifty microlitres of cold 100% ethanol (Merck, UK) was added to the reaction mixture and incubated for 16 – 18 hours at 20°C to allow for precipitation of the riboprobes. The following day the riboprobes were pelleted by centrifugation at 4°C for 30 minutes at 14 000 rpm in a microcentrifuge. The supernatant was discarded and the pellet was washed with cold 70% ethanol (Appendix 1). The riboprobes were again pelleted by centrifugation at 4°C for 5 minutes at 7 000 rpm, and after careful removal of most of the ethanol, the pellet was dried in a Speed Vac Concentrator (Savant, USA) for approximately 5 minutes. The riboprobes were then resuspended in 100 µl DEPC dH₂O (Appendix 1) and incubated at 37°C for 30 minutes, then stored at -20°C. Concentrations of the riboprobes were between 0.1 and 0.5 µg/ml.

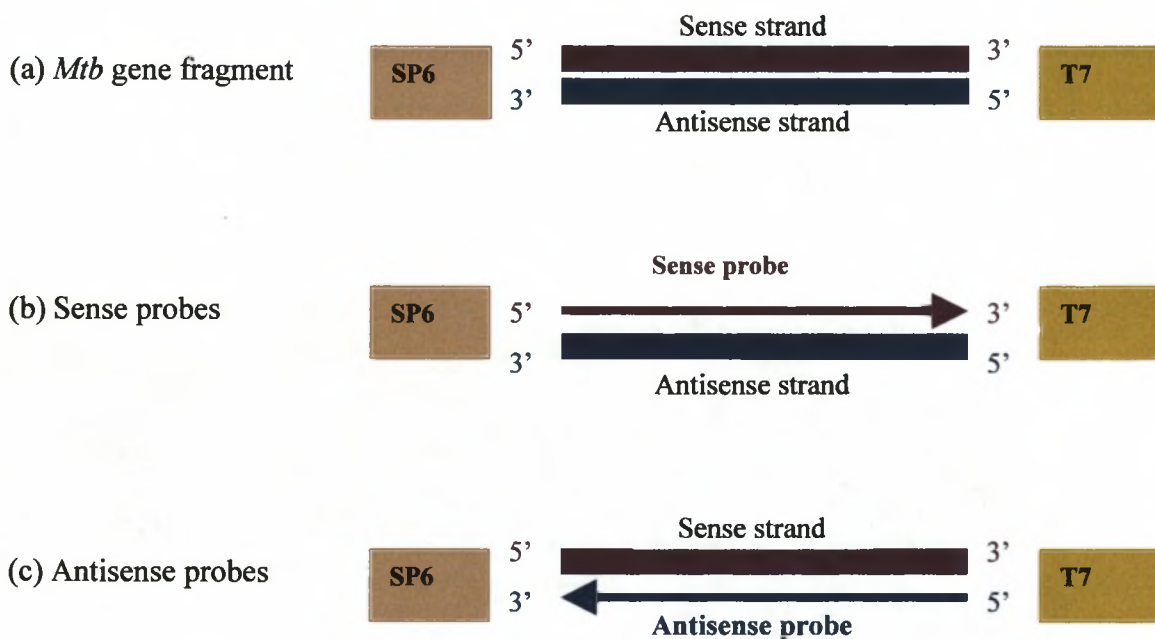


Figure 2.2. Synthesis of Antisense and Sense Oligonucleotide Probes. The (a) double stranded *M.tuberculosis* (*Mtb*) gene fragment cloned into the pGemT vectors serves as template for the synthesis of the (b) sense probes and the (c) antisense probes.

Biotinylation of the probes was confirmed by spotting 5 – 10 µl of the respective probes onto Hybond N+ membranes (Amersham, UK) followed by detection with streptavidin-conjugated alkaline phosphatase in conjunction with the NBT/BCIP substrate (GibcoBRL, Switzerland), as will be discussed in detail in section 2.3.3.

2.4 *IN SITU* HYBRIDISATION

2.4.1 Brief Description

The *in situ* hybridisation method was designed for non-radioactive detection of RNA and DNA in tissue preparations. This method provides a highly sensitive detection system for biotinylated probes that takes advantage of the very high affinity of biotin for streptavidin. These complexes are also extremely stable over a wide range of temperatures and pH. In brief, a biotin-labelled probe is hybridised to target DNA or mRNA in cells or tissues *in situ* on a microscope slide. A signalling group (i.e. alkaline phosphatase) covalently attached to streptavidin is then bound to the biotinylated probe. The hybridised probe is detected by incubating the samples with dye substrates for alkaline phosphatase. Formation of a blue signal indicates the location of the hybridised probe (Figure 2.3) which is then viewed under a light microscope.

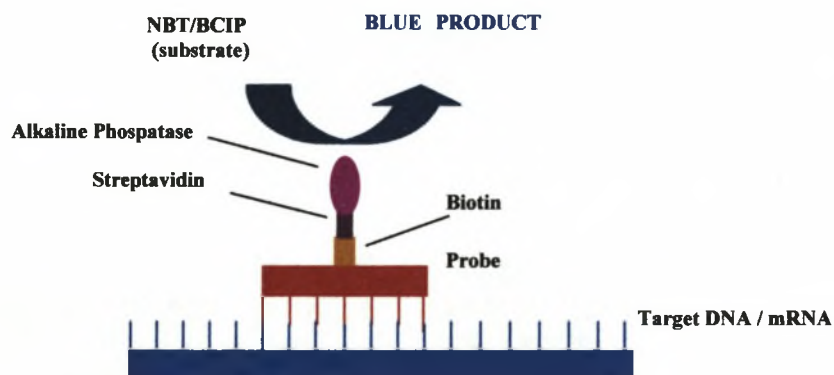


Figure 2.3. *In Situ* Hybridisation. The hybridisation and detection of a biotinylated probe on the target DNA / mRNA on a microscopic slide

2.4.2 Pretreatment of Tissue for *In Situ* Hybridisation

Paraffin embedded lymph node tissue was cut into 5 μm sections using a microtome (Department of Anatomical Pathology, Faculty of Health Sciences, University of Stellenbosch, Tygerberg, South Africa), and consecutive sections were applied to RNase-free slides (Section 2.2). The paraffin embedded sections were deparaffinised by incubation in two changes of xylene (MERCK, UK) for 10 minutes each. Sections were rehydrated through graded ethanols, i.e. in two changes of absolute ethanol (EtOH), 90% EtOH and finally in 70% EtOH for 2 minutes each. The slides were then

saline (DEPC 1xPBS) (Appendix 1) for 5 minutes each. The sections were incubated with 500 μ l prewarmed (37°C) Proteinase K (1 μ g/ml) in 10 mM Tris-HCl pH 7.5, 5 mM EDTA for 20 minutes at 37°C in a humidified chamber. The proteinase treatment breaks down some of the cross-links made by the fixative, thereby enabling access of probes to the target sequence. DNase I or RNase A were only added to those slides to be hybridised with the MTB484 DNA probe. DNase I (10 μ g/ml) was added together with the proteinase K and incubated as described before. This step was included to determine whether this probe would bind mycobacterial mRNA. Conversely, to ensure that the positive signals obtained when using the MTB484 probe was due to the presence of *M. tuberculosis* DNA rather than *M. tuberculosis* mRNA, the sections were incubated with RNase A (20 μ g/ml) for 20 minutes at 37°C prior to hybridisation.

After being washed with DEPC 1xPBS for 5 minutes, the sections were immersed in 0.4% paraformaldehyde (Appendix 1) in DEPC 1xPBS for 5 minutes to inhibit further Proteinase K digestion. The paraformaldehyde treatment was also imperative as it refixed the digested tissue. The sections were then washed with DEPC dH₂O for 2 minutes and acetylated (with stirring) for 10 minutes in a 1:400 (vol / vol) solution of triethanolamine (Merck, UK) in DEPC dH₂O and 750 μ l Acetic Anhydride (Merck, UK) which was added dropwise close to the sections. The acetylation procedure prevented non-specific binding of the nucleic acid probes. The slides were then rinsed in DEPC 1xPBS for 5 minutes and dehydrated through a graded ethanol series, i.e. 2 minutes each in 70% EtOH, 90% EtOH and in two changes of 100% EtOH. The sections were air dried at room temperature for 40 – 60 minutes before hybridisation.

2.4.3 Hybridisation of Biotinylated Probes

The *In Situ* Hybridisation and Detection System (Gibco BRL, Switzerland) was used, as instructed, for the hybridisation and detection of biotinylated probes (see below).

2.4.3.1 DNA:DNA Hybridisation

The hybridisation mixture, which consisted of 20 μ l of the 20% dextran sulphate solution and 20 μ l of the 2x hybridisation buffer, was mixed with 3 μ l of the biotinylated MTB484 probe (2 μ g/ml) and was added to the sections before being covered with a glass coverslip (Sigma, USA). The dextran sulphate, as with the acetylation, reduced the possibility of cellular electrostatic interactions and also locally concentrated the probe, thus enhancing the rate of hybridisation. These sections

were then heated at 95°C for 5 minutes in a Hybaid Omnislide Humidity Chamber (Hybaid Ltd, UK) to denature both the MTB484 probe and the target mycobacterial DNA.

2.4.3.2 RNA:RNA Hybridisation

Three µl of the antisense (5 µg/ml) or sense biotin-labelled riboprobes (5 µg/ml) were added to the hybridisation mixtures (20 µl of 20% dextran sulphate solution and 20 µl of 2x hybridisation buffer). The probe mixture was added to the sections and covered with a coverslip. No denaturation took place prior to hybridisation.

2.4.3.3 Hybridisation and Stringency Washing

The sections were incubated with the hybridisation mixture containing either the biotinylated MTB484 or the biotinylated riboprobes for 16 – 18 hours at 50°C in a humidified chamber. After hybridisation the sections were washed twice in 2x SSC (Appendix 1) for 15 minutes at room temperature to remove unhybridised probes.

2.4.4 Detection of Hybridised Probes

The tissue sections were covered with 100 µl Blocking Solution (Gibco ISH Kit) and incubated at room temperature for 20 minutes. Blocking agents are required to block endogenous enzyme activity when using enzyme-based detection methods. A working conjugate solution was prepared by mixing 10 µl of streptavidin-alkaline phosphatase conjugate (Gibco ISH Kit, Switzerland) with 90 µl of conjugate dilution buffer (Gibco ISH Kit, Switzerland) for each slide. The Blocking Solution was removed from each slide by touching absorbent paper to the edge of the slide. Each section was covered with 100 µl of working conjugate solution and incubated in the humid chamber at room temperature for 15 minutes. It is also important to measure any endogenous activity with a test slide without the streptavidin-alkaline phosphatase conjugate. Production of signal when leaving out the alkaline phosphatase is an indication of a false positive signal. The slides were washed twice in Buffer A (Appendix 1) for 15 minutes each at room temperature, then incubated in prewarmed alkaline-substrate buffer, Buffer B (Appendix 1), at 37°C for 5 minutes. Three hundred microlitres of NBT and 249 µl BCIP was added to 75 ml Buffer B prewarmed at 37°C. Levamisole (200 µg/ml) (Vector, USA) was added to the alkaline-substrate solution to further inhibit the endogenous phosphatase activity. At that concentration, levamisole is a potent inhibitor of many endogenous alkaline-phosphatases, but has no effect on the streptavidin-alkaline phosphatase conjugate. The slides were then incubated in the NBT/BCIP solution at 37°C until the desired level

of signal was achieved (10 min. to 1 hour), then rinsed briefly in distilled water to stop the development of further signal.

2.4.5 Counterstaining

Slides were counterstained with methyl green (DAKO, USA), which allowed negative cells to be visualised and aided in the identification of particular cell types. Methyl green, a basic dye, reacts with anionic groups of tissue, including phosphate groups of nucleic acids. Thus, the tissue components that were stained with this basic dye were heterochromatin and nucleoli of the nucleus. The slides were immersed in the methyl green solution for 5 minutes, rinsed with 95% EtOH to remove excess reagent then dehydrated through graded alcohols (2x 95% and 2x 100% EtOH for 30 seconds each), and finally incubated twice in xylene for 2 minutes. The slides were then mounted in a compatible permanent mounting medium (Entellen, Merck)

2.5 IMMUNOHISTOCHEMISTRY

2.5.1 Brief Description

The reaction between antigen and antibody is the underlying basis of immunohistochemistry. In brief, the tissue is first incubated with a primary antibody (1° Ab) that binds only with the specific protein under investigation. Tagged secondary antibody (2° Ab) can be used to identify the location of the various bound primary antibodies. Signalling molecules, such as horse-radish peroxidase (HRP) or alkaline phosphatase (AP) enzymes, conjugated to link molecules (avidin or streptavidin, respectively) are bound to the biotinylated secondary antibodies. The bound antibodies are detected by incubating the tissue with the appropriate substrates for the enzymes, such as DAB or Fuchsin-substrate-chromogen. Formation of a brown or red signal indicates the location of the bound antibodies (Figure 2.4).

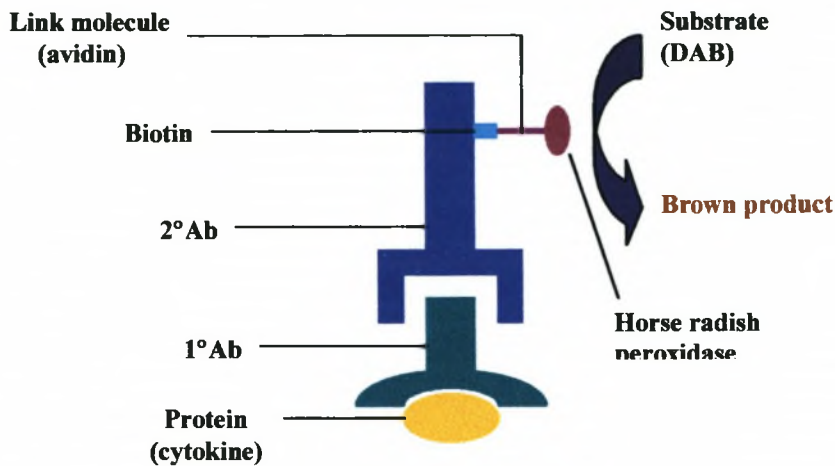


Figure 2.4. Immunohistochemistry. Recognition of target cytokines by 1°Ab with subsequent binding of labelled 2°Ab required for detection

2.5.2 Pretreatment of Tissue for Immunohistochemistry

Sections of paraffin embedded lymph node tissue, applied to pretreated slides (Section 2.2), were deparaffinised in two changes of xylene for 10 minutes each. The sections were dehydrated, as in section 2.4, through a graded ethanol series and washed in dH₂O for 5 minutes. The sections were then immersed in 3% H₂O₂ in methanol (Merck, UK) for 15 minutes to block endogenous peroxidase, then rinsed under running tap H₂O. For antigen retrieval, the sections were microwaved in 0.01 M citrate buffer pH 6.0 (Appendix 1) at high power for 20 minutes, topping up the buffer every 5 minutes. Fixation preserves tissues, but also alters the access of antibodies to antigenic sites in the tissue. Formaldehyde fixation forms complex aldehyde-linked protein aggregates in which primary and secondary protein structures might be preserved, while tertiary or quaternary protein structures, are altered by extensive cross-linking (Merz *et al*, 1995). To avoid this deleterious effect of fixation there are several retrieval systems, including heat-induced antigen retrieval such as microwaving (Cuevas *et al*, 1994). After microwaving, the slides were left in the heated citrate buffer for an additional 20 minutes, and then washed in 1x PBS for 5 minutes at room temperature. The sections were then incubated with 100 µl of 3% rabbit serum in 1x PBS for 10 minutes. This was intended to block non-specific binding of the primary antiserum with tissue structures. The type of serum used depends on the type of 2° Ab, i.e. serum of the host that produced the 2° Ab (Table 2.4).

2.5.3 Binding of Primary and Secondary Antibodies

One hundred μ l of the cytokine-specific primary antibody diluted in rabbit serum (dilutions listed in Table 2.5) was added to each lymph node section and incubated in a humidified chamber overnight at 4°C. Negative controls (absence of primary antibody) were included to confirm specificity of the immunoreactions, and were incubated overnight at 4°C with rabbit serum. Non-specific immunoreactivity would thus present deposition of reaction product via unspecific binding of the secondary antibody at a site other than the location of the desired antigen. Such false positivity can arise from non antibody-specific binding of the secondary antibody. The slides were then washed three times in 1x PBS for 5 minutes each to remove unbound primary antibodies. The sections were incubated with the secondary antibody (Table 2.4) diluted with 1x PBS (1:100 dilution) and placed in a humidified chamber for 1 hour at 4°C. The slides were again washed three times in 1x PBS for 5 minutes each to remove unbound antibody.

Table 2.5. Primary Antibodies and Dilution Factors

Cytokines	Primary Antibody		Secondary Antibody
	(1° Ab)	1° Ab Dilutions	(2° Ab)
IL-4	Goat anti-human IL-4	1:50	Rabbit anti-goat
IL-10	Goat anti-human IL-10	1:100	Rabbit anti-goat
IL-12	Goat anti-human IL-12	1:50	Rabbit anti-goat
IFN- γ	Goat anti-human IFN- γ	1:100	Rabbit anti-goat
TNF- α	Goat anti-human TNF- α	1:100	Rabbit anti-goat

2.5.4 Detection of Bound Antibody Probes

The tissue sections were incubated with avidin HRP conjugate diluted (1:400) in 1x PBS for 30 minutes at room temperature, then washed three times in 1x PBS for 5 minutes each. The DAB substrate (DAKO, USA) yields a brown-colored reaction product at the site of the target antigen. As described by the manufactures, 2 drops of Buffer Stock Solution, 4 drops of DAB Stock Solution and 2 drops of Hydrogen Peroxide were added to 5 ml dH₂O, and mixed well. The lymph node tissue sections were incubated with 100 μ l freshly prepared DAB substrate and incubated for 5 – 30 minutes at room temperature. The slides were then rinsed in distilled water after the appearance of a brown colour to stop the development of further signal.

To overcome the staining difficulty with the IL-12, the dilution of the primary antibody was decreased to 1:20, and incubated for longer periods, but with the same result.

Counterstaining

The sections were counterstained in haematoxylin (DAKO, USA) for 5 minutes, and then rinsed well in running tap water until a blue colour reaction occurred. Haematoxylin, while not a basic dye like methyl green, has staining properties that closely resemble those of a basic dye. The tissue components stained with this dye also included heterochromatin and nucleoli of the nucleus.

2.6 DUAL LABELING

2.6.1 Brief Description

Dual labeling is the combination of the immunohistochemistry and ISH staining techniques. This allows the staining for both a specific protein (cell receptors) and nucleic acid molecules (*M. tuberculosis* DNA or mRNA) in one tissue section. The CD68 molecule, a macrophage receptor molecule, was the target for the immunohistochemistry staining. The subsequent ISH was applied for the detection of *M. tuberculosis* DNA, as well as for the individual detection of *rpoB*, *narX* and *icl* mRNA in the CD68 stained macrophages.

2.6.2 Immunohistochemistry Staining of CD68 Receptors

2.6.2.1 Pretreatment of Tissue

The tissue was deparafinised, dehydrated and incubated in 3% H₂O₂ in methanol, as described in section 2.5.1. The sections were rinsed in two changes of DEPC dH₂O for 5 minutes each after blocking the endogenous peroxidase, and incubated in 100 µl trypsin (Sigma, USA) for 10 minutes at room temperature. Trypsin digestion, and not heat induced microwaving, was the preferred antigen retrieval method used for the staining of the CD68 molecules. The tissue was again rinsed in DEPC dH₂O for 5 minutes, and incubated with 100 µl sheep serum diluted (1:20) in DEPC 1x PBS for 10 minutes at room temperature.

2.6.2.2 Binding of Primary and Secondary Antibody

One hundred µl of the primary antibody, mouse anti-human CD68, diluted (1:50) in the sheep serum was added to the lymph node sections and incubated in a humidified chamber at 4°C

overnight. The tissues were washed three times in DEPC 1x PBS for 5 minutes each to remove unbound primary antibody. The sections were incubated with the secondary antibody, sheep anti-mouse, diluted with DEPC 1x PBS (1:100) and placed in a humidified chamber at 4°C for one hour. The slides were again washed in DEPC 1x PBS to remove unbound secondary antibody.

The tissue sections were incubated with avidin alkaline phosphatase conjugate diluted (1:400) in DEPC 1x PBS for 30 minutes at room temperature, then washed three times in DEPC 1x PBS for 5 minutes each. The Fuchsin substrate-chromogen (DAKO, USA) yields a fuchsia-colored reaction product at the site of the target antigen. One hundred and twenty µl of Fuchsin chromogen was mixed with 120 µl Activating Agent and incubated at room temperature for 1 minute before the Buffered Substrate (1.76 ml) was added, as described by the manufacturers. The lymph node tissue sections were incubated with 100 µl of prepared Fuchsin substrate-chromogen and incubated for 5 – 30 minutes at room temperature. The slides were then rinsed in two changes of DEPC dH₂O for 5 minutes each.

2.6.2 *In Situ* Hybridisation

The sections were refixed in 0.4% paraformaldehyde at 4°C for 20 minutes, and then rinsed in two changes of DEPC 1x PBS for 5 minutes each. The sections were incubated with Proteinase K for 10 minutes, refixed in 0.4% paraformaldehyde and acetylated as described in section 2.4.1. The tissue was then rinsed in DEPC 1x PBS for 5 minutes after the acetylation, and incubated with 100 µl biotin solution (Vector) for 10 minutes at room temperature, in order to block the biotin activity on the bound avidin conjugates. The sections were rinsed well in DEPC dH₂O for 5 minutes, thereafter dehydrated as described in section 2.4.1.

The technique for the hybridisation and detection of the biotinylated DNA and RNA probes (rpoB, narX and ICL) was followed as described in sections 2.4.2 and 2.4.3, respectively. The slides were incubated in the NBT/BCIP solution until the desired level of signal was achieved (10 – 15 minutes), then rinsed briefly in dH₂O. The slides were then mounted in a compatible permanent mounting medium (Faramount, Dako).

For the dual labeling, it is important that the tissue not be counterstained at all, since the haematoxylin and methyl green dyes will obscure the staining of the CD68 surface molecule.

2.7 PHOTOGRAPHY

The images were captured using a Zeiss microscope (Axioskop 2) fitted with a Sony 3CCV video camera and the images were saved using Axiovision form Zeiss (Germany).

2.8 ASSESSMENT OF SLIDES

In situ hybridisation and immunohistochemistry are empirical staining techniques and cannot be accurately quantitated. For the *in situ* hybridisation analysis, the staining intensity could not be correlated to bacterial load. Staining for the host cytokines was consistent, and granulomas in lymph node tissue were therefore scored either negative or positive for the presence of *M. tuberculosis* DNA or mRNA, and cytokines. It is impossible to accurately determine the number of bacilli present in the lymph node tissue, as one blue spot does not necessarily equate to one bacillus present in the various cells types of the granulomas. The same assessing principle was applied for the immunohistochemistry technique. The granulomas in the lymph node tissue were scored either positive or negative for the various cytokine proteins.

2.9 STATISTICAL EVALUATION OF DATA

The data generated with the *in situ* hybridisation using various riboprobes, as well as the immunohistochemistry staining analysis of host cytokines were statistically evaluated using the EpiInfo 2000 computer program, and P-values ≤ 0.05 were considered as statistically significant. These results were not corrected for multiple testing.

2.10 DNA FINGERPRINTING OF ISOLATED CLINICAL STRAINS FROM LYMPH NODE TISSUE

2.10.1 Brief Description

The single circular *M. tuberculosis* chromosome is digested with a restriction endonuclease, generating fragments of varying size (Figure 2.5). These fragments are separated by electrophoresis through an agarose gel, and then transferred to a nylon membrane. A DNA probe complementary to the 3' region of the IS6110 insertion element was labelled with horse-radish peroxidase. During

hybridisation the probes bind to the fragments of *M.tb* DNA containing the insertion element and excess probe is removed by washing. Positive hybrids are detected when the conjugated enzyme catalyses the oxidation of luminol, which generates light that is detected by exposing photographic film to the membrane in an X-ray cassette to produce an autoradiograph.

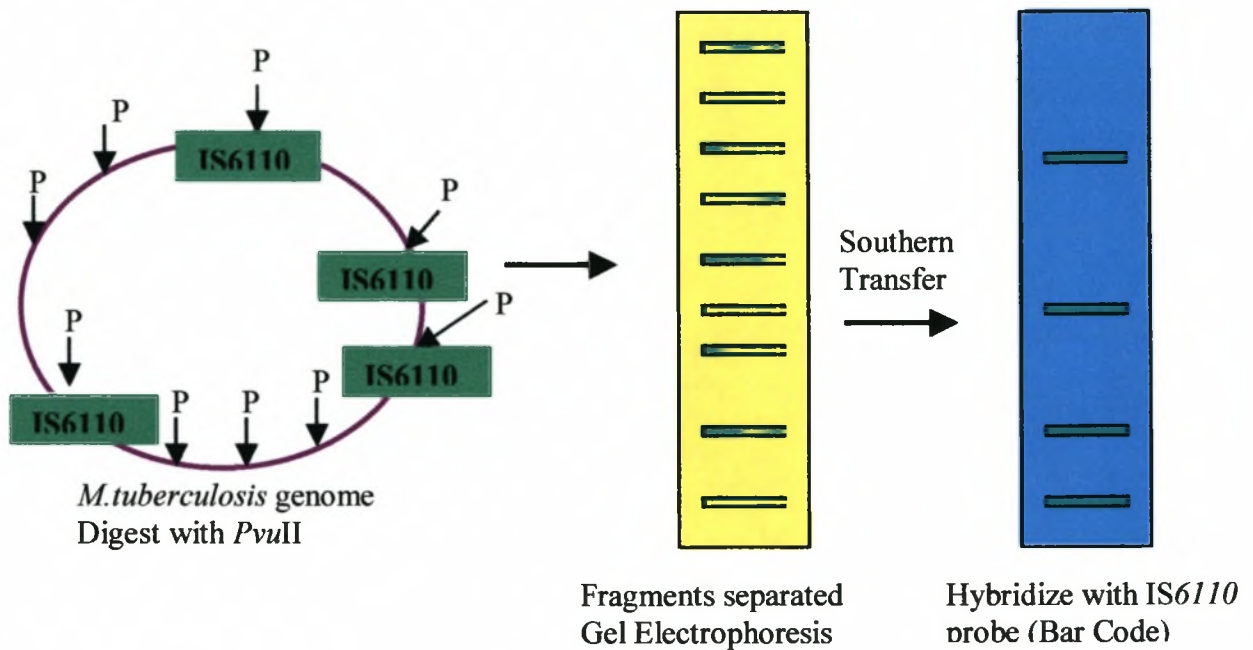


Figure 2.5. *IS6110* Strain Typing of *M. tuberculosis*

2.10.2 Extraction of Mycobacterial DNA

A confluent Lowenstein-Jensen (L-J) slant culture of *Mtb* is required for the DNA isolation.

The L-J slant culture was heat inactivated at 80°C for 1 hour and the DNA extraction was done in a P2 category laminar flow cabinet. Extraction buffer (3 ml) (Appendix 1) was added to the slant and the bacteria were carefully scraped off with a sterile 10 µl loop. The extraction buffer containing the cells was then poured off into a sterile 50 ml polypropylene tube which contained approximately 20 (5 mm) glass balls. A further 3 ml of extraction buffer was poured onto the slant. Any remaining bacterial colonies were scraped off and the buffer was swirled around in the bottle to wash off bacterial matter on the side of the bottle, which was poured into the 50 ml tube. The tube was vigorously shaken and vortexed to break up the clumps of bacteria. Five hundred µl lysozyme (50 mg/ml) and 5 µl RNase A (10 mg/ml) were added to the tube which was then inverted to mix the contents and incubated at 37°C for 2 hours. Proteinase K buffer (Appendix 1) and 150 µl Proteinase

Proteinase K (10 mg/ml) were added, the sample was mixed gently and incubated overnight at 45°C. Five ml of Phenol / Chloroform (Appendix 1) was added to the bacterial preparation and the mixture was shaken gently over a period of approximately 20 minutes. The sample was centrifuged at 3 000 rpm for 30 minutes. The aqueous phase was carefully aspirated, ensuring that none of the inter-phase or phenol phase was taken, and was added to 5 ml chloroform / iso-amylalcohol (Appendix 1). After thorough mixing, the sample was centrifuged at 3 000 rpm for 10 minutes. The aqueous phase was collected and added to 600 µl 3 M Na-acetate (Appendix 1). The contents were mixed and the DNA was precipitated by adding 7 ml cold (-20°C) Isopropanol, after which the tube was gently inverted. The DNA pellet was collected on a glass rod and placed in a 1.5 ml eppendorf tube that contained 1 ml 70% EtOH for approximately 1 minute to remove the salt. The DNA was then transferred to a fresh eppendorf tube and incubated at 65°C for approximately 30 minutes which allowed the DNA to dry. Five hundred µl of TE buffer was added to the dry DNA and the pellet was allowed to rehydrate to release it from the glass rod. The DNA was dissolved in the TE buffer and incubated at 60°C for 1 hour to aid dissolving.

The concentration of the extracted DNA was determined as mentioned before (Section 2.3.1.2). DNA was stored at -20°C.

2.10.3 Restriction Enzyme Digestion of the DNA

Six µg of *M. tuberculosis* DNA was digested with the restriction enzyme *PvuII* (Amersham, UK). The digestion was done in a total volume of 100 µl and the order of addition was as follows: 10 µl 10x Restriction buffer (M for *PvuII*); H₂O to a final volume of 100 µl (according to calculation), 6 µg DNA and 2.5 µl *PvuII* (5 U per µg of DNA). The digestion mixture was then incubated overnight at 37°C, or for a minimum of 4 hours. After digestion, the reaction was incubated at 65°C for 10 minutes to inactivate any remaining enzyme activity.

A mini (5 x 10 cm) 0.8% agarose gel (0.8 g in 1x TBE buffer) was prepared to test for completeness of the restriction digest. Eight µl of the digested sample was mixed with 2 µl 6x loading buffer (Appendix 1) and loaded onto the gel. The test sample was electrophoresed in 1x TBE buffer (Appendix 1) at 100 V for approximately 1 - 2 hours. The gel was stained with Ethidium Bromide (5 µl per 100 ml of 1x TBE running buffer) for 30 minutes. The gel was visualised on a longwave ultraviolet transilluminator (at 245 nm) and a photograph was taken.

2.10.4 Altering Concentrations of the Restricted DNA

The remaining restricted DNA was precipitated with absolute EtOH and redissolved in order to set the digested samples at the same concentration. Ten μl 3 M Na-acetate (pH5.2) and 300 μl cold (-20°C) absolute EtOH was added to the digest to precipitate the restricted DNA. The tube was inverted to mix and incubated at -80°C for 2 hours or overnight at -20°C . The precipitated digested DNA was centrifuged at 4°C in a microfuge at 13 000 rpm for 30 minutes. The supernatant was carefully aspirated and 500 μl 70% EtOH was added to the pellet. Supernatant was carefully removed after centrifugation at 13 000 rpm for 15 minutes and the pellet was dried at 65°C . The optimal digest of 6 μg would have given a lane with an intermediate staining intensity on the photograph. The precipitated digested DNA was redissolved in 20 μl of Loading buffer that contained Marker X (Roche, Germany). For digests with a reduced staining intensity the volume of Loading buffer was reduced (to a minimum of 10 μl), while the volume of Loading buffer was increased for samples with a higher staining intensity on the test gel. The correct volume of Loading buffer with Marker X was added to each sample and the tubes were incubated at 65°C for one hour, with occasional vortexing to ensure that of the digested DNA was dissolved.

2.10.5 Gel Electrophoresis of Restricted DNA

For fingerprinting, 10 μl of the (redissolved) restricted DNA was electrophoresed on a 0.8% agarose gel (2.4 g agarose in 300 ml 1x TBE). The gel was run overnight at 65 V (33 mAmps) in 1x TBE running buffer for a distance of 20 cm. The gel was covered to prevent evaporation and to ensure an even temperature. The restricted DNA samples loaded contained Marker X (Roche, Germany) in the Loading buffer, which acted as an internal marker. The external marker DNA (Marker MTB14323) was loaded in the outside lanes of the gel to enable integral comparison using the software GelCompar 4.1. The gel was transferred to a plastic dish with 1x TBE running buffer, to which Ethidium Bromide (0.5 μl per 100 ml) was added. The gel was stained with gentle shaking for 30 minutes after which it was photographed to establish how evenly the gel had been loaded.

2.10.6 Southern Transfer of the Fingerprinting Gel

DNA from a successful fingerprinting gel was transferred from the agarose onto a charged Nylon membrane (HybondN+, Amersham) by Southern blotting (Sambrook, Fritsch, Miniatis). Briefly after the gel was photographed, the DNA was denatured in the gel by covering it with 0.4 M NaOH (Appendix 1) for 20 minutes with gentle shaking at 42°C . After denaturing, the gel was washed briefly in dH_2O . Three sheets of Whatmann blotting paper and a sheet of Nylon membrane were cut to the size of the fingerprinting gel. The Nylon membrane was marked with a black ballpoint pen to

allow future recognition. Orientation marks (Appendix 1) were positioned in the corner of the membrane to allow future alignment of resultant autoradiographs.

The Southern transfer was set up as described in "Molecular Cloning" (Sambrook, Fritsch, Maniatis). A sheet of Whatmann blotting paper, soaked in 20x SSPE pH 7.4 (Appendix 1), was placed on the blotting apparatus. The gel was placed on top of the paper in an upside down position and the nylon membrane, previously hydrated in H₂O then soaked in 20x SSPE, was placed onto the gel with orientation dots facing toward the gel. To restrict capillary transfer to the gel only, parafilm strips were placed around the gel. The air bubbles were removed and two sheets of Whatmann paper soaked in 20x SSPE was placed onto the membrane. Layers of tissue paper were placed onto the Whatmann paper and covered with a glass plate. An object (± 1 kg) was positioned on the plate and the transfer was done overnight at room temperature. The membrane was removed and rinsed in a 2x SSC solution to remove non-specifically bound DNA. The membrane was placed between 2 sheets of Whatmann paper and baked at 80°C for 2 hours to allow the DNA to be covalently linked to the membrane. After baking the membrane was hydrated in water and sealed in a plastic sleeve until hybridisation.

2.10.7 Labeling of Probes and Hybridisation

Probes used for fingerprinting were labeled using the ECL kit (Amersham, UK) according to the manufacturers instructions.

The membrane was sealed in a plastic bag with 35 ml of the gold buffer (ECL Kit), all the air bubbles removed, and prehybridised at 42°C for a minimum of 1 hour. Prehybridisation and hybridisation was done in a flat-bottomed plastic dish in a shaking waterbath. The hybridisation bag (a sealed plastic bag $\frac{1}{4}$ filled with water) kept the membrane in place and also aided in the even distribution of the buffer over the membrane.

The 200 ng of the IS6110 probe dissolved in H₂O (total volume of 15 μ l) was denatured at 100°C for 5 minutes and was immediately put on ice for a further 5 minutes. Fifteen μ l of the Labeling Mix (Horse Radish Peroxidase) (ECL Kit) was added to and mixed with the denatured probe, after which 15 μ l of the Glutaraldehyde solution (ECL Kit) was added. This mixture was vortexed and incubated at 37°C for 10 minutes. The hybridisation bag was removed from the waterbath and the labeled IS6110 probe was added. A pipette was rolled over the membrane in the bag to mix the labeled probe and the hybridisation buffer. The bag was resealed in such a way that any air bubbles

were excluded. The membrane was placed back in the plastic dish under the weight bag and incubated overnight at 42°C in the shaking waterbath.

After hybridisation, the membrane was removed from the plastic bag and washed twice at 42°C in a plastic dish with 400 ml of the Primary wash buffer (Appendix 1). This was followed by 2 washes of 5 minutes each, at room temperature in 400 ml 2x SSC. The membrane was placed in a new plastic sleeve and all excess fluid was removed. Four ml of the two Detection agents (ECL Kit) were mixed and poured onto the membrane in the bag. The solution was gently spread over the membrane for a period of 90 seconds and then pushed out of the bag. The bag was sealed and exposed to X-ray film for an optimal period of time (varying between 1 minute to 2 hours). The film was initially exposed for a shorter period to assess the strength of the signal. The film was immersed in the developing solution (Appendix 1) for 3 minutes, then transferred to the stopping solution (Appendix 1) for 20 seconds and finally to the fixing solution (Appendix 1) for 1 minute, whereafter it was washed in running tap water for a 5 minutes. The resulting DNA fingerprint consisted of a variable number of bands at varying positions along a "lane" on the autoradiograph.

2.10.8 Data Analysis

Autoradiographs were scanned using a Hewlett Packard Scanjet II cx/T scanner. Scanned samples were normalised using the internal markers and compared using GelCompar 4.1 B (Applied Maths, Kortrijk, Belgium).

CHAPTER THREE

RESULTS

INDEX	PAGE
3.1 PATIENT SELECTION: LYMPH NODE BIOPSIES	64
3.2 PROBES USED FOR <i>IN SITU</i> HYBRIDISATION ANALYSIS	
3.2.1 DNA Probes	66
3.2.2 Riboprobes	66
3.3 REPRODUCIBILITY	68
3.4 CYTOKINE ANALYSIS	68
3.4.1 Cytokine Detection in Granulomas	68
3.4.2 Overall Assessment of Cytokine Expression Patterns	77
3.4.2.1 Type 2 Cytokines	77
3.4.2.2 Type 1 Cytokines	77
3.4.3 Stratification of Host Cytokines	79
3.5 MYCOBACTERIAL DNA DETECTION	
3.5.1 <i>M. tuberculosis</i> DNA Detection in Granulomas	80
3.5.2 Dual Labeling: Co-localisation of CD68 Positive Cells and Mycobacterial DNA	84
3.5.3 Overall Assessment of Mycobacterial DNA Detection In Patients	84
3.6 <i>M. TUBERCULOSIS</i> GENE EXPRESSION	
3.6.1 <i>M. tuberculosis</i> Gene Expression in Granulomas	88
3.6.2 Dual Labeling: Co-localisation of rpoB mRNA to CD68 Positive Cells	95
3.6.3 Overall Assessment of <i>M. tuberculosis</i> Gene Expression	95
3.6.4 Stratification of <i>M. tuberculosis</i> Gene Expression	98
3.7 STRATIFICATION OF MYCOBACTERIAL GENES AND HOST CYTOKINES	100
3.7.1 Passive vs. Active Transcription	100
3.8 STRAIN TYPING <i>M. TUBERCULOSIS</i> CLINICAL ISOLATES	103

3.1 PATIENT SELECTION: LYMPH NODE BIOPSIES

Biopsy samples were collected from 20 patients (8 females; 12 males), between the ages of 3 and 13 years, at Tygerberg Hospital (Table 3.1). Half of each tissue sample was submitted for culture (BACTEC), and the remaining tissue portions were fixed in formalin and embedded in wax. Sections of embedded tissue were used for ZN staining and histological analysis. Only 6 of the tissue samples collected were lymph nodes from children diagnosed with tuberculosis. These samples are listed in Tables 3.1 and 3.2 as patients L1 to L6. One patient was also diagnosed with lymphoma (patient L15). The remaining children presented with cervical swelling caused by abscess formation and no solid lymph nodes were detected. In addition, 3 other samples could not be included as consent from a parent or guardian for performing the study was not given (not listed in Table 3.1).

The 6 confirmed tuberculosis patients comprised 5 males and 1 female. Patient L2 was the only patient that received anti-tuberculosis treatment prior to biopsy. This patient had started his third course of treatment 2 days prior to the biopsy. The diagnosis of patient L4 was made solely on a positive *M. tuberculosis* culture, as no acid-fast bacilli were detected in the biopsy tissue, i.e. ZN staining was negative, and the histological analysis proved inconclusive. The BACTEC culture was only positive after 4 weeks of incubation. Unfortunately, an *M. tuberculosis* culture was not prepared from the biopsy tissue of patient L1, as no tissue sample of this patient was delivered to the Microbiology laboratory, as is standard hospital procedure. Patient L5 was diagnosed with both pulmonary and abdominal tuberculosis.

Table 3.1 Clinical Data of Patients who Donated Biopsy Tissue.

Patient	Age	Sex
L1	6	Male
L2	3	Male
L3	13	Male
L4	12	Female
L5	12	Male
L6	6	Male
L7	3	Female
L8	3	Female
L9	3	Male
L10	4	Female
L11	4	Female
L12	4	Male
L13	4	Male
L14	5	Female
L15	6	Male
L16	7	Male
L17	8	Female
L18	8	Male
L19	10	Female
L20	13	Male

All patient were HIV negative

Table 3.2 Treatment History, ZN and Culture Results of Patients L1 to L6.

Patient	Previous Treatment	Start of Treatment	ZN Staining (Pos / Neg)	Culture (Pos / Neg)
L1	None	After biopsy	Positive	Negative
L2	1997, 1999	2 days prior biopsy	Positive	Positive
L3	None	After biopsy	Positive	Positive
L4	None	After biopsy	Negative	Positive
L5	None	After biopsy	Positive	Positive
L6	None	After biopsy	Positive	Positive

Only these 6 patients who presented with tuberculosis infected lymph node were included in the study

3.2 PROBES USED FOR *IN SITU* HYBRIDISATION ANALYSIS

3.2.1 DNA Probes

The biotinylated MTB484 (Warren *et al*, 1996) probe, used for the detection of *M. tuberculosis* DNA, contains sequences of the highly repetitive element, PGRS, which are specific for members of the *M. tuberculosis* complex (Cole *et al*, 1998). However, as the *M. tuberculosis* sequence PGRS is an expressed sequence (Espitia *et al*, 1999), the likelihood that the biotinylated MTB484 probe would bind to *M. tuberculosis* mRNA existed. In order to resolve whether this was the case, the sections were treated with DNaseI prior to hybridisation. In addition, the probe, but not the tissue section, was denatured, which allowed the single stranded DNA probe to anneal to the mRNA, and not the double stranded (undenatured) DNA molecules. Therefore, sections probed in this manner and which produced a positive signal implied that the biotinylated MTB484 probe was annealing to mycobacterial mRNA. To ensure that the biotinylated MTB484 probe would only bind to *M. tuberculosis* DNA, the sections were treated with RNaseI prior to hybridisation (see Section 2.4.1).

3.2.2 Riboprobes

The SP6 and T7 primers were used for the amplification of various *M. tuberculosis* gene fragments cloned into pGemT-easy plasmids (Promega). All gene fragments were successfully amplified (Figure 3.1), the PCR products were purified and subsequently used as templates for the preparation of biotinylated riboprobes.

The RNA probes do not anneal to bacterial DNA because the denaturation step is omitted, preventing denaturation of the DNA and subsequent annealing of the single stranded RNA probes to double stranded DNA. Therefore, the presence of DNA within the tissue sections did not interfere with the binding of the biotinylated RNA probes. If the antisense probes produce no signal, then either there is no specific mRNA present (i.e. the gene was not transcribed), or the amount of mRNA present is below the sensitivity level of detection for this technique.

To confirm the specificity of hybridisation, the negative controls included hybridisation with the biotinylated RNA sense probe. The synthesised sense probes would consequently have the identical sequence as the target mRNA, and would therefore not hybridise to the target mRNA. The sense probes were synthesised in a similar manner as mRNA, that is by using the antisense DNA strand as template.

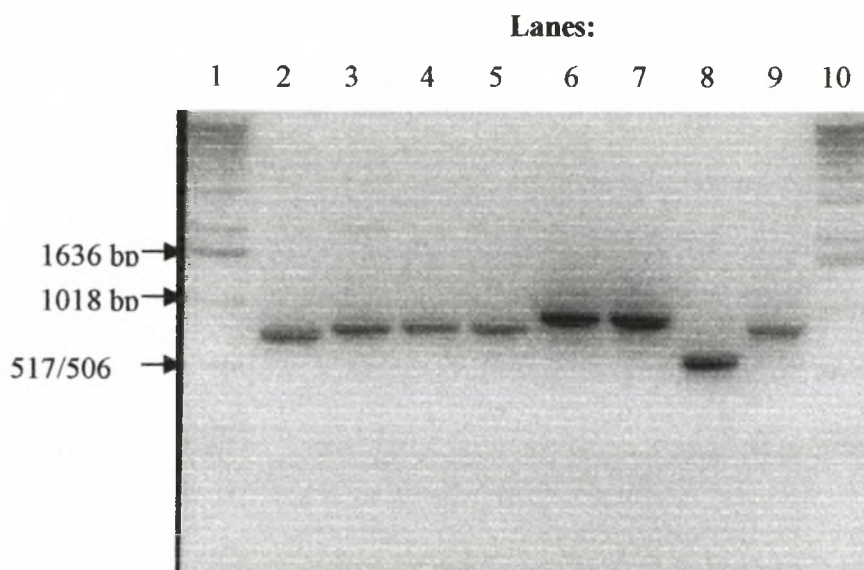


Figure 3.1. Amplification of the various *M. tuberculosis* gene fragments. SP6 and T7 primers specific for the flanking promoter regions of the pGemT-easy plasmids were used to amplify these gene fragments cloned into pGemT-easy vectors. Marker X in lane 1 and 10 served as the standard molecular weight marker. The amplified *M.tuberculosis* gene fragments were loaded on 1% agarose gel in the following order: 2 *rpoB*, 3 *katG*; 4 *narX*; 5 *icl*; 6 *mbtB*; 7 *rel_{MtB}*; 8 *esat-6*; 9 *PPE*

3.3 REPRODUCIBILITY

The *in situ* hybridisation staining for the detection of mycobacterial DNA and mRNA, as well as the immunohistochemistry staining of the host cytokines, were all done in duplicate, producing the same results. That is, the granulomas that were either positive or negative for hybridisation signal were again positive or negative upon duplicate staining. Serial sections, from tissue that had been previously confirmed to contain both DNA and mRNA were used as controls for newly synthesised probes. In each case, the signal pattern was similar to that of the previous hybridisation (Figure 3.2). This demonstrates that the hybridisation conditions as well as the preparation of the sections were consistent. The absence of hybridisation signal for one probe does not indicate the inability of the probe to enter the section as hybridisation with a second probe produced a signal in that region.

3.4 CYTOKINE ANALYSIS

Immunohistochemistry was used to study the host immune response induced by the *M. tuberculosis* infection. This was achieved by analysing the pattern of cytokine production at the site of infection, the human granuloma, using paraffin-embedded lymph node tissue. More specifically, the production of Th1 cytokines IFN- γ , TNF- α and IL-12, as well as Th2 cytokines IL-4 and IL-10 were evaluated. Various goat anti-human (cytokine) antibodies (referred to as the primary antibodies) were used to detect the relevant cytokines, as summarised in Table 2.4. The location of the cytokine-bound antibodies was revealed by the presence of a brown product that resulted from the enzymatic conversion of the DAB substrate by the HRP reporter enzyme. Scanning of the lymph node tissue for each cytokine at low-power magnification allowed an overall assessment of the relative staining of the tissue.

3.4.1 Cytokine Detection in Granulomas

Figures 3.3 to 3.8 are representative sections of patient L6 illustrating cytokine patterns. Figure 3.3 is a compilation of representative sections illustrating IL-4 staining. A high level of IL-4 was detected in the non-necrotic granuloma, with signal mostly localised to the central region of the granuloma (Figure 3.3a). Staining for IL-4 was also detected in the lymphocyte cuff of this non-necrotic granuloma. This cytokine was also associated with the necrotic granuloma (Figure 3.3 c). In these granulomas, the signal was localised predominantly in the lymphocyte cuff.

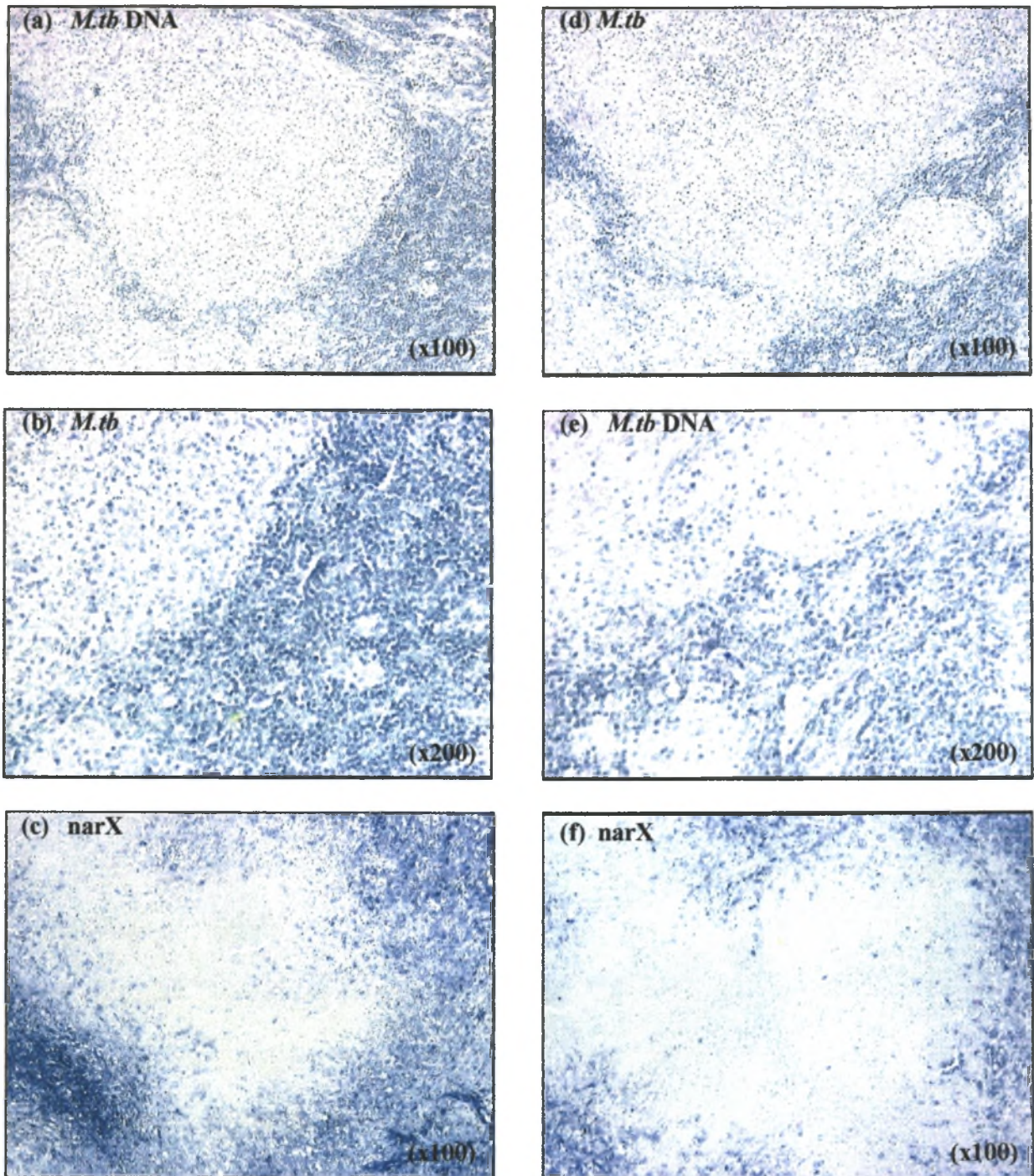


Figure 3.2. *In situ* hybridisation of sections from patient L5. Nuclei stain green, and cells positive for *Mtb* DNA or mRNA stained blue. The *in situ* hybridisation staining for the detection of mycobacterial DNA (a, b) and mRNA (c), were done in duplicate (d-f). Granulomas were repeatedly positive, with similar signal patterns. *M.tb* DNA was detected in the non-necrotic granuloma of consecutive sections, with the signal pattern similar to the previous hybridisation (a, b and duplicates d, e). Signal for *narX* (example of riboprobe reproducible staining) was also similar to the previous hybridisation (c and duplicate f).

Giant cells which were detected at the periphery of both the non-necrotic and necrotic granulomas (Figure 3.3b, d) also stained positive for IL-4. Figure 3.4 shows representative sections of IL-10 staining in non-necrotic and necrotic granulomas. As with IL-4, IL-10 was present at high levels within the central region of the non-necrotic granuloma (Figure 3.4a). The necrotic granuloma also stained positive for this anti-inflammatory cytokine, but with a weaker staining intensity (Figure 3.4c). Signal was mostly localised to the periphery and lymphocyte cuff of the necrotic granuloma. The giant cells present at the periphery of the non-necrotic and necrotic granulomas stained positive for IL-10 (Figure 3.4 b and d, respectively).

The staining intensity for the type 1 cytokine IL-12, in patient L6 was weak, as illustrated in Figure 3.5. In the non-necrotic granuloma, IL-12 was detected mostly at the edges of the granuloma (Figure 3.5a). A limited amount of signal was also detected in the lymphocyte cuff. The giant cells present at the edge of the non-necrotic granuloma were associated with IL-12 (Figure 3.5b). No detectable signal for IL-12 was observed in this particular necrotic granuloma (Figure 3.5c). The giant cells detected at the periphery of the necrotic granuloma were therefore also negative for this cytokine (Figure 3.5d). Figure 3.6 illustrates the high intensity staining for IFN- γ . This cytokine was detected at very high levels within the central region of the non-necrotic granuloma and within the lymphocyte cuff (Figure 3.6a, b). The necrotic granuloma also stained very strongly for IFN- γ (Figure 3.6c, d) Signal in this granuloma was localised predominantly to the periphery and lymphocyte cuff region (Figure 3.6d). Giant cells present in this region also stained positive for IFN- γ . The strongest staining intensity was observed for this cytokine. Staining for TNF- α was similar to that of IFN- γ . Strong signal for TNF- α was detected in the central region, and within the lymphocyte cuff of the non-necrotic granuloma (Figure 3.7a, b). Similar staining intensity was observed in the necrotic granuloma (Figure 3.7c, d). Strong TNF- α staining was localised to the periphery and lymphocyte cuff of the necrotic granuloma, as was also associated with the giant cells present in this region.

Figure 3.8 illustrates the specificity of the immunohistochemical staining. There was no brown signal detected in these sections, which is due to the absence of primary antibody and the specificity of secondary antibodies. Similar results of the cytokine staining were observed for all the patients; data summarised in Appendix VI.

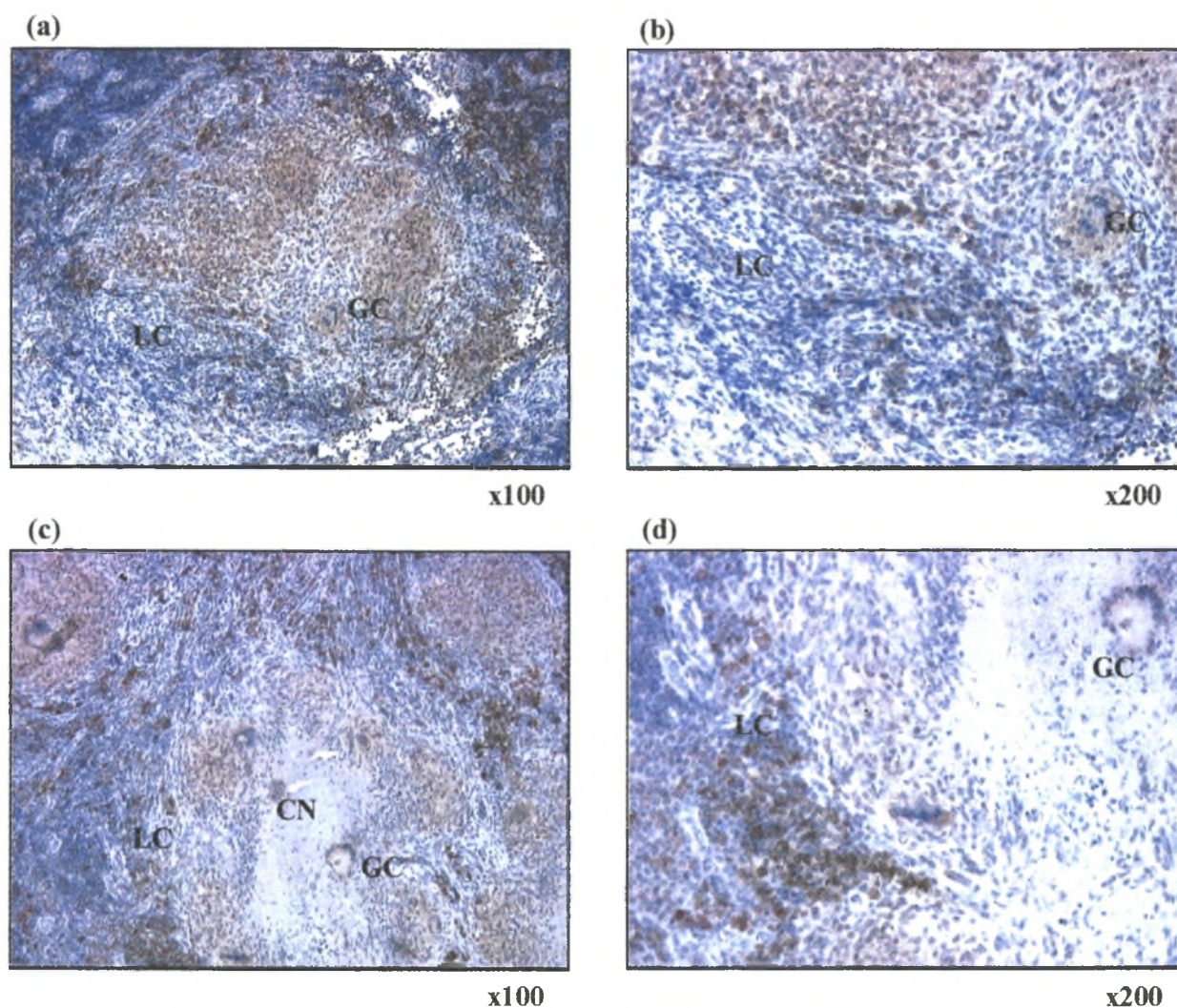


Figure 3.3. Immunohistochemical Staining for IL-4 in a non-necrotic and necrotic granuloma. Nuclei stain blue, and the brown staining illustrates the presence of the IL-4. In the non-necrotic granuloma (a, b), the signal localised to the central region of the granuloma and the lymphocyte cuff (LC). In the necrotic granuloma the staining was localised predominantly in the lymphocyte cuff (c, d). Giant cells (GC) present at the edges of the non-necrotic (b) and necrotic granulomas (d) stained positive for IL-4.

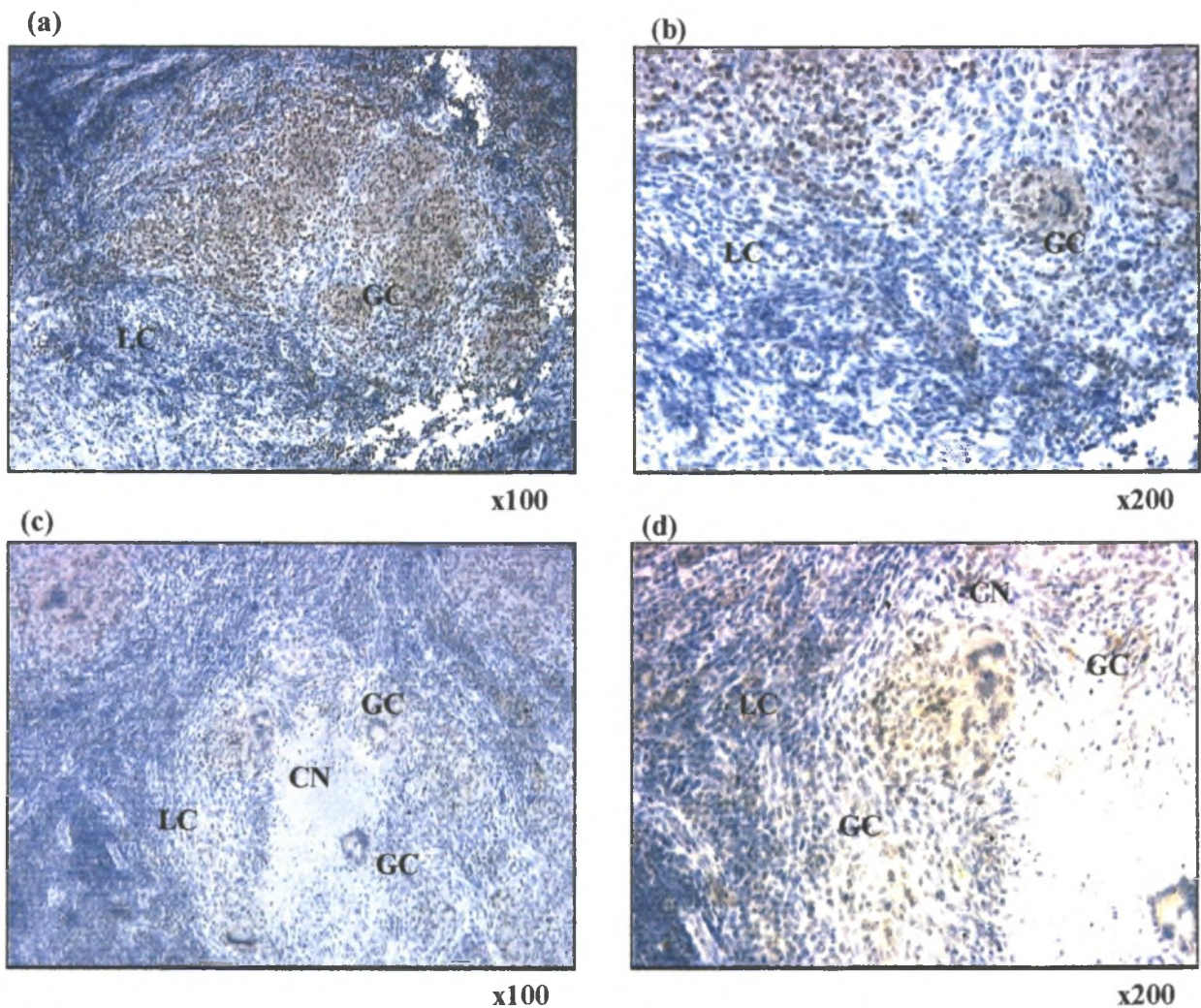


Figure 3.4. Immunohistochemical Staining for IL-10 in a non-necrotic and necrotic granuloma. Nuclei stain blue, and the brown staining illustrates the presence of the IL-10. In the non-necrotic granuloma (a, b), the signal localised to the central region of the granuloma and the lymphocyte cuff (LC). In the necrotic granuloma the staining was localised predominantly in the lymphocyte cuff (c, d). Giant cells (GC) present at the edges of the non-necrotic (b) and necrotic granulomas (d) stained positive for IL-10.

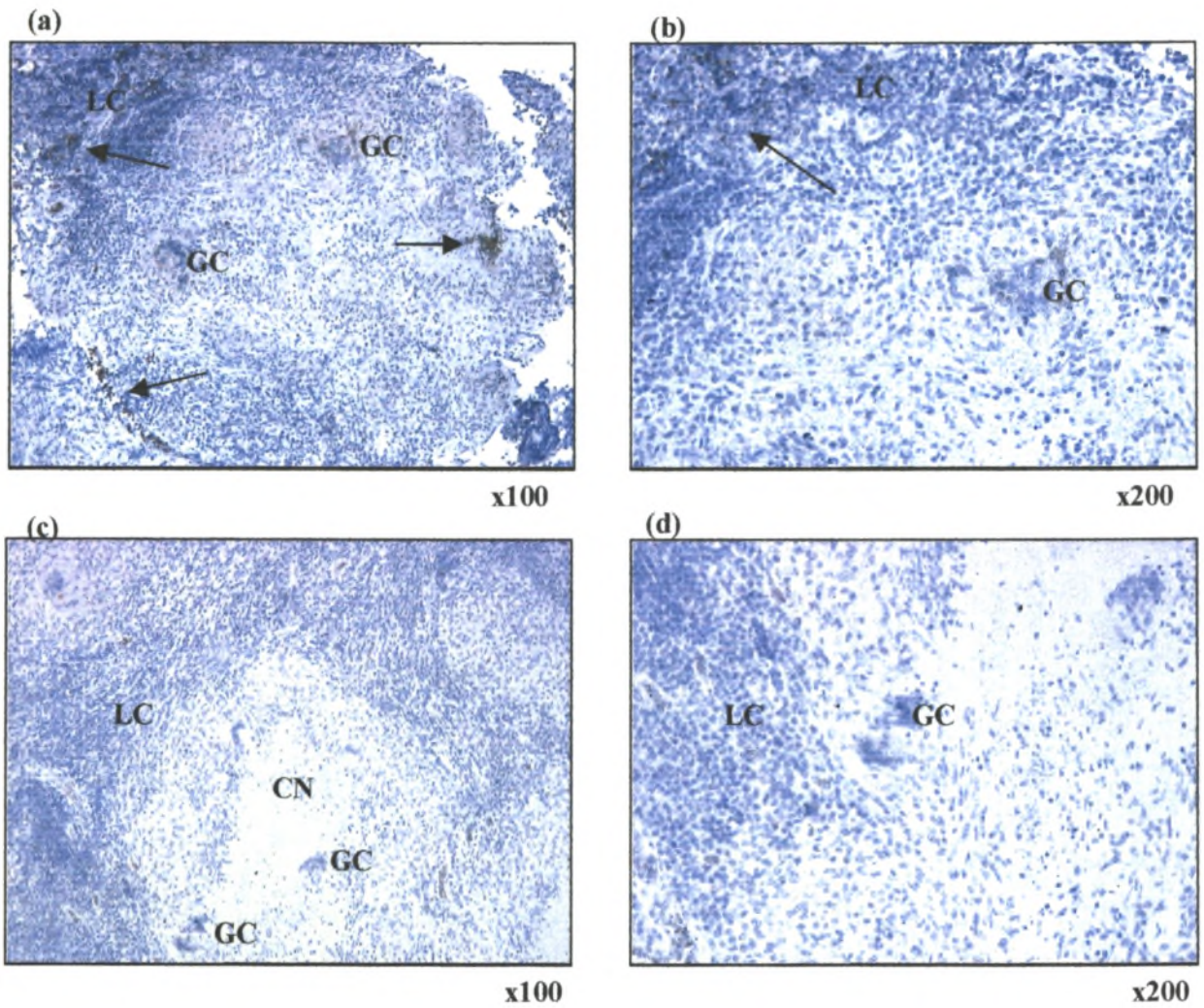


Figure 3.5. Immunohistochemical Staining for IL-12 in a non-necrotic and necrotic granuloma. Nuclei stain blue, and the brown staining illustrates the presence of the IL-12. In the non-necrotic granuloma (a, b), the weak signal localised to the central region of the granuloma and the lymphocyte cuff (LC) (indicated by arrows). There was no staining detected in the necrotic granuloma (c, d). Giant cells (GC) present at the edges of the non-necrotic granuloma (b) stained positive for IL-12, and not the giant cell at the edge of the necrotic granulomas (d)

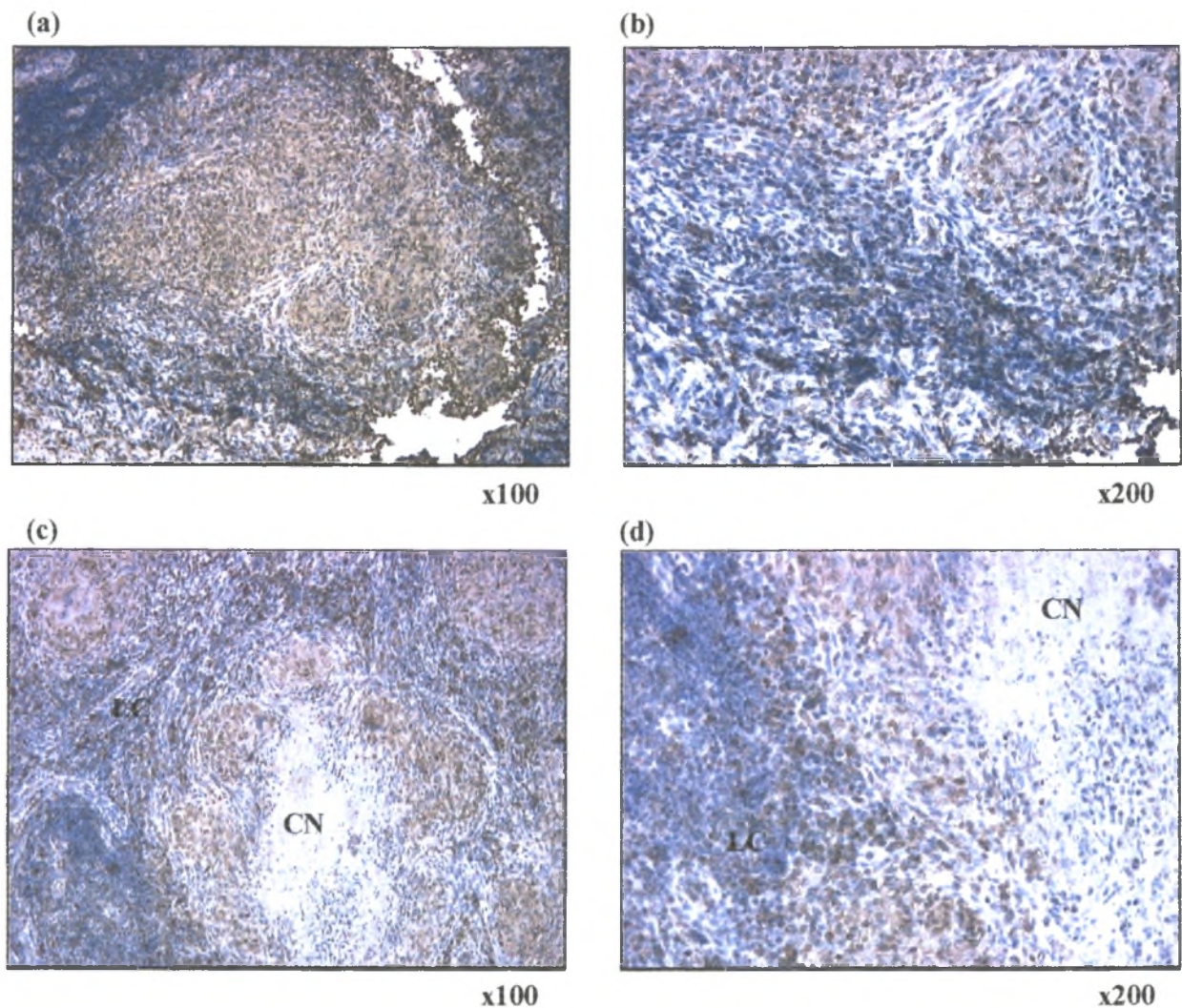


Figure 3.6. Immunohistochemical Staining for IFN- γ in a non-necrotic and necrotic granuloma. Nuclei stain blue, and the brown staining illustrates the presence of the IFN- γ . In the non-necrotic granuloma (a, b), the signal localised to the central region of the granuloma and the lymphocyte cuff (LC). In the necrotic granuloma the staining was localised predominantly in the lymphocyte cuff (c, d). Giant cells (GC) present at the edges of the non-necrotic (b) and necrotic granulomas stained positive for IFN- γ .

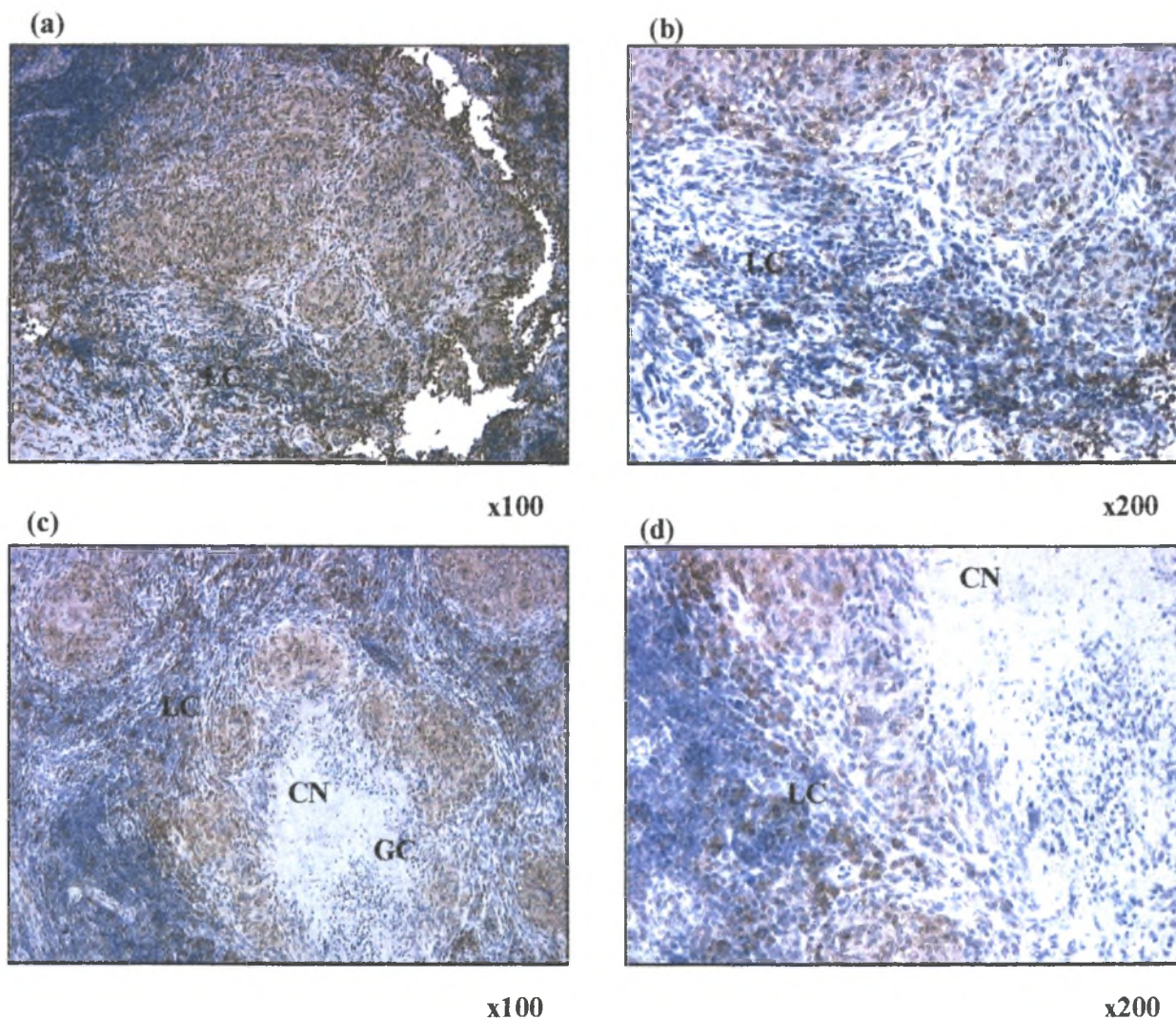


Figure 3.7. Immunohistochemical Staining for TNF- α in a non-necrotic and necrotic granuloma. Nuclei stain blue, and the brown staining illustrates the presence of the TNF- α . In the non-necrotic granuloma (a, b), the signal localised to the central region of the granuloma and the lymphocyte cuff (LC). In the necrotic granuloma the staining was localised predominantly in the lymphocyte cuff (c, d). Giant cells (GC) present at the edges of the necrotic granulomas stained positive for TNF- α (c)

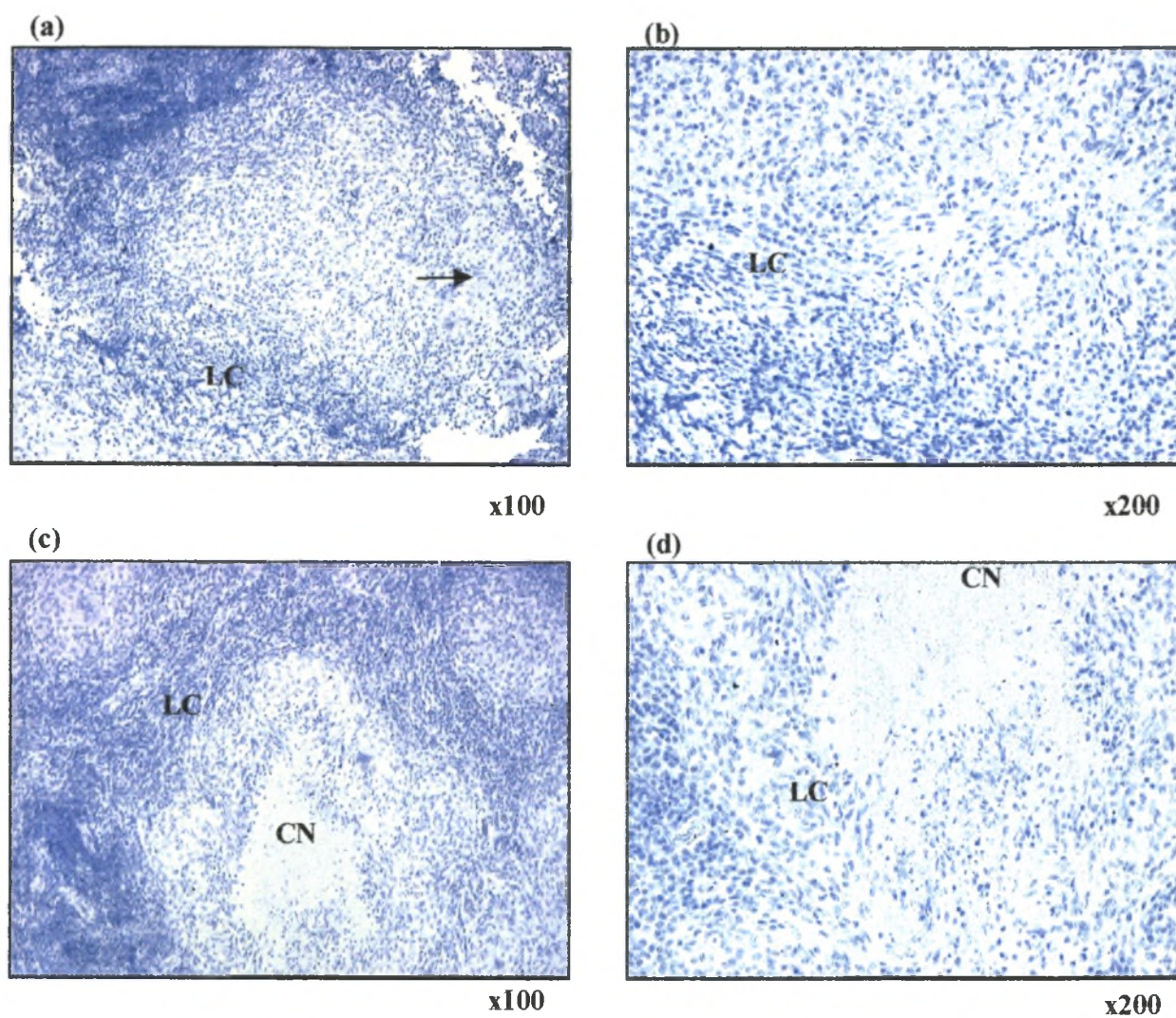


Figure 3.8. Negative control for Immunohistochemical staining. Nuclei stain blue. The absence of brown signal in the non-necrotic and necrotic granulomas is the result of the absence of primary antibody. This negative control illustrates the specificity of the secondary antibody binding.

3.4.2 Overall Assessment of Cytokine Expression Patterns

3.4.2.1 Type 2 Cytokines

IL-4 was detected in all the patients analysed, including patient L2 (treated patient). In contrast to previous reports, a high number of granulomas identified stained positive for IL-4. This cytokine was detected in all the granulomas of patients L6 and L2 (treated patient), and in most of the granulomas for the remaining untreated patients, ranging between 75% in patient L3 to 95.8% in patient L5 (Figure 3.9). IL-10 was also detected in all the patients, but with variable expression between the patients. The number of IL-10 positive granulomas ranged between 38.5% (L4) to 89.5% (L6) (Figure 3.9).

3.4.2.2 Type 1 Cytokines

IFN- γ was detected in all the granulomas of each patient (Figure 3.9). Similarly, TNF- α was detected in all the granulomas of patients L3, L5, L6 and in the treated patient L2, and was also detected in most of the granulomas of patients L4 (76.9%) and L1 (87.5%) (Figure 3.9). There was more variation in the expression of the remaining type 1 cytokine, IL-12. This cytokine was detected in all six patients, and the number of IL-12 positive granulomas ranged from 48.5% for patient L5 to 100% for patient L3 (Figure 3.9).

The overall phenotype for the individual granulomas for each patient demonstrated a predominant Th0 response (Figure 3.10). That is, both Th1 and Th2 cytokines were expressed in the granulomas. Patients L6 and L2 (treated) presented a complete Th0 response, with all the granulomas staining positive for both type 1 and type 2 cytokines. The remaining patients also presented a few Th1 granulomas (i.e. only Th1 cytokines were detected in these microenvironments), ranging between 4.2% for patient L5 to 32.15% for patient L3. None of the granulomas that were identified in the six patients presented with a Th2 phenotype.

It appears there is a balance in the immune response of these TB patients, as both type 1 and type 2 cytokines are expressed. This balance was maintained irrespective of anti-tuberculosis treatment.

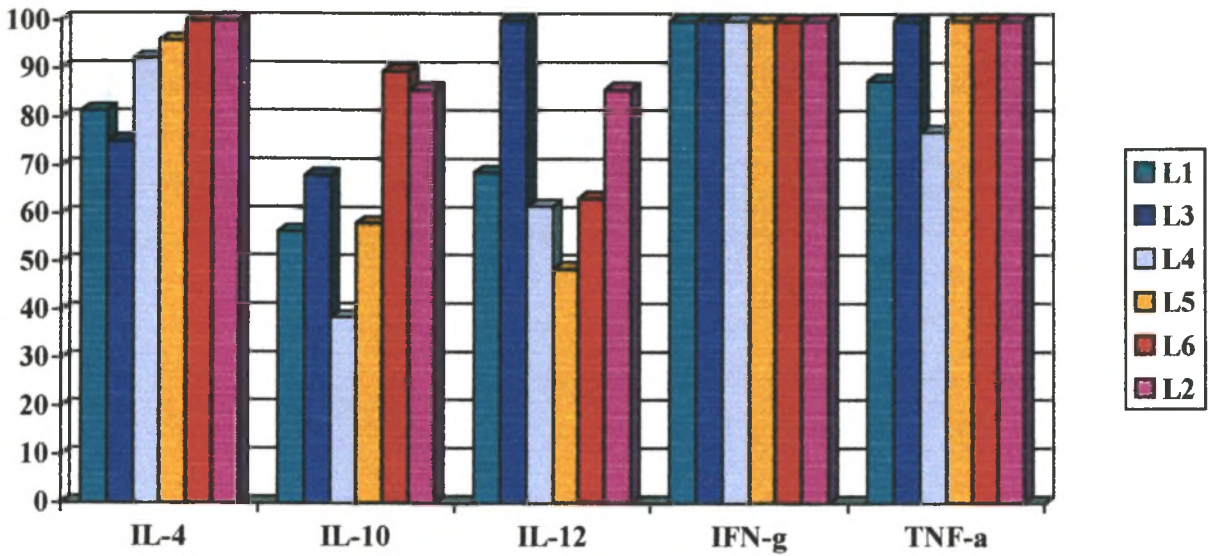


Figure 3.9. Analysis of the Individual Host Cytokine Pattern in each of the Patients. The percentage of positive staining granulomas was determined for each of the cytokines analysed that the (a-b) Th2 cytokines (IL-4, IL-10) and the (c-e) Th1 cytokines (IL-12, IFN-g, TNF-a)

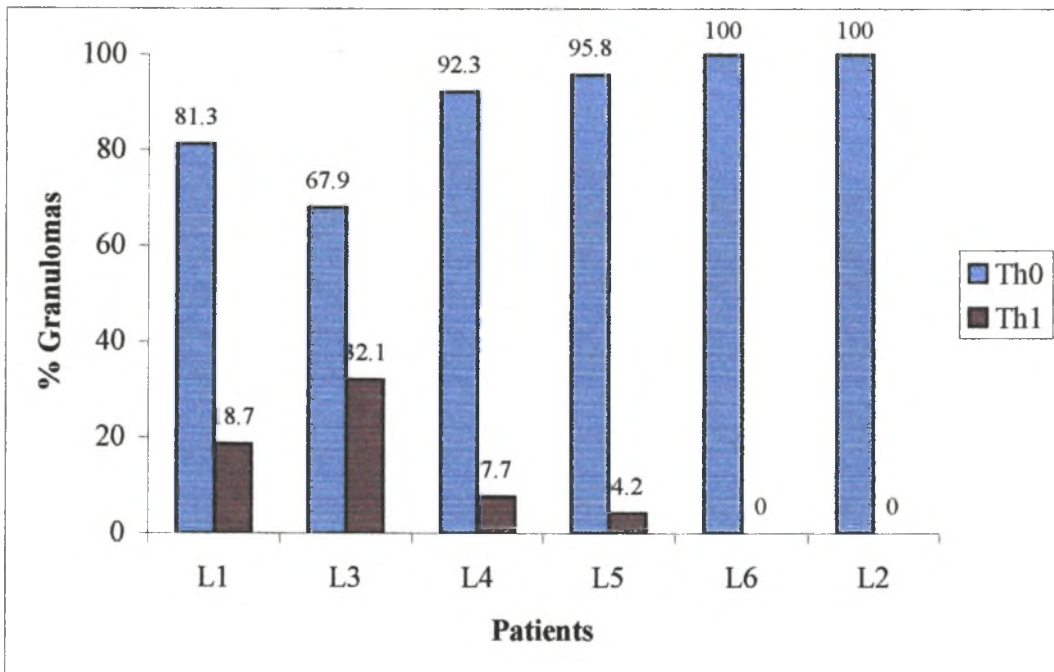


Figure 3.10. Th Phenotypes Detected for the Individual Patients

3.4.3 Stratification of Host Cytokines

The granulomas of the individual patients (Appendix VI) were characterized to generate an overall assessment to allow for stratification of the host cytokine expression.

IFN- γ was present in all the granulomas in each patient and except for the fact that these cytokines were present at elevated levels, no other correlations could be made.

In order to determine whether there were any correlations between IL-4 and other cytokines, the data was sorted into IL-4 negative and IL-4 positive granulomas. IL-10 was significantly absent in the IL-4 negative granulomas (Table 3.3) and was only expressed in those granulomas positive for IL-4 ($p = 0.0000006$). The expression of the type 1 cytokines was approximately constant in both IL-4 subgroups.

The data was also stratified according to the presence or absence of IL-10 in the granulomas, and confirmed the significant correlation between the type-2 cytokines. IL-10 appears to be expressed only in granulomas expressing IL-4. A significant correlation was observed with IL-10 and IL-12 ($p = 0.021$). IL-12 was expressed mostly in granulomas expressing IL-10, and was downregulated in the absence of IL-10.

The data was stratified into subgroups of necrotic and non-necrotic granulomas in order to establish whether there was any correlation between cytokine production and the presence of necrosis. The majority of granulomas containing caseous necrosis stained positive for IL-10, and those lacking this cytokine were mostly non-necrotic granulomas (Table 3.3). Statistical evaluation of these results indicated a significant association between IL-10 and caseous necrosis ($p = 0.000046$). This trend was not observed with IL-4. This cytokine was detected in most granulomas, but with no distinction between the necrotic and non-necrotic granulomas ($p = 2.06$). However, a significant association was also observed between TNF- α and caseous necrosis ($p = 0.0041$). All the granulomas negative for TNF- α also lacked necrosis. In addition, a significant correlation in coordinated expression was also detected between the two cytokines associated with necrosis, viz. IL-10 and TNF- α ($p = 0.0054$).

Table 3.3. Summary of Cytokine Data Stratification

sorting		Cytokines				
		IL-4	IL-10	IL-12	IFN-g	TNF-a
IL-4	Neg	0	0	10	14	14
	%	0.00	0.00	71.43	100.00	100.00
	Pos	93	68	66	93	88
	%	100.00	73.12	70.97	100.00	94.62
	p-value	ns	0.0000006	ns	ns	ns
IL-10	Neg	25	0	22	39	34
	%	64.10	0.00	56.41	100.00	87.18
	Pos	68	68	54	68	68
	%	100.00	100.00	79.41	100.00	100.00
	p-value	0.0000006	ns	0.021	ns	0.0054
IL-12	Neg	27	14	0	31	28
	%	87.10	45.16	0.00	100.00	90.32
	Pos	66	54	76	76	74
	%	86.84	71.05	100.00	100.00	97.37
	p-value	ns	0.021	ns	ns	ns
Necrosis	Non-necr	27	13	20	34	29
	%	79.41	38.24	58.82	100.00	85.29
	Necrotic	66	55	56	73	73
	%	90.41	75.34	76.71	100.00	100.00
	p-value	ns	0.000046	ns	ns	0.0041

* significant correlations are highlighted
 ns = non-significance

3.5 MYCOBACTERIAL DNA DETECTION

3.5.1 *M. tuberculosis* DNA Detection in Granulomas

Consecutive sections of lymph node tissue from six TB patients (Table 3.2) were hybridised with the MTB484 probe to detect the presence of mycobacterial DNA. A total of 107 granulomas were analysed by DNA:DNA *in situ* hybridisation and 88.8% were found to be positive for *M. tuberculosis* DNA. All the granulomas containing caseous necrosis (73), and 22 of the 34 non-necrotic granulomas were positive for *M. tuberculosis* DNA.

Figure 3.11 shows a representative section of a necrotic granuloma from patient L6. Hybridisation signal for the DNA probe occurred mostly in the periphery and in the lymphocyte cuff region of the granuloma (Figure 3.11 a b), where cells with the morphology of macrophages were positive for *M. tuberculosis* DNA (blue signal). Hybridisation signals were also detected in the necrotic region of the granuloma, which was not cell associated (Figure 3.11c). To detect non-specific binding of streptavidin to the sections, hybridisation was also carried out in the absence of the biotinylated probe (Figure 3.11d-e). The results of these controls demonstrate that the appearance of a positive

signal was dependent on specific hybridisation of the biotinylated probes to the target DNA, and was not an artefact of the methodology. Giant cells, located at the periphery of the granuloma, within the lymphocyte cuff, also stained positive for *M. tuberculosis* DNA (Figure 3.11 a, b). Higher magnification of the giant cells (Figure 3.11 f) indicated that the signal was localised to the cytoplasm.

Figure 3.12 (a-c) shows representative sections of a non-necrotic granuloma of patient L5 hybridised with the *M. tuberculosis* DNA probe. This granuloma did not contain caseous necrosis, and was characterised by intact macrophages in the central region. The signal for this granuloma was predominantly localised to the lymphocyte cuff, with less signal detected within the central non-necrotic regions (Figure 3.12a, b). The specificity of the staining was observed by the differential staining observed, particularly at higher magnifications, where both negative (green) and positive cells (blue) for *M. tuberculosis* were detected, especially within the periphery and lymphocyte cuff region (Figure 3.12c). To detect non-specific binding of streptavidin to these sections, hybridisation was also carried out in the absence of the biotinylated probe (Figure 3.12 d-f). Similar results were observed for all the patients; data summarised in Appendix VI.

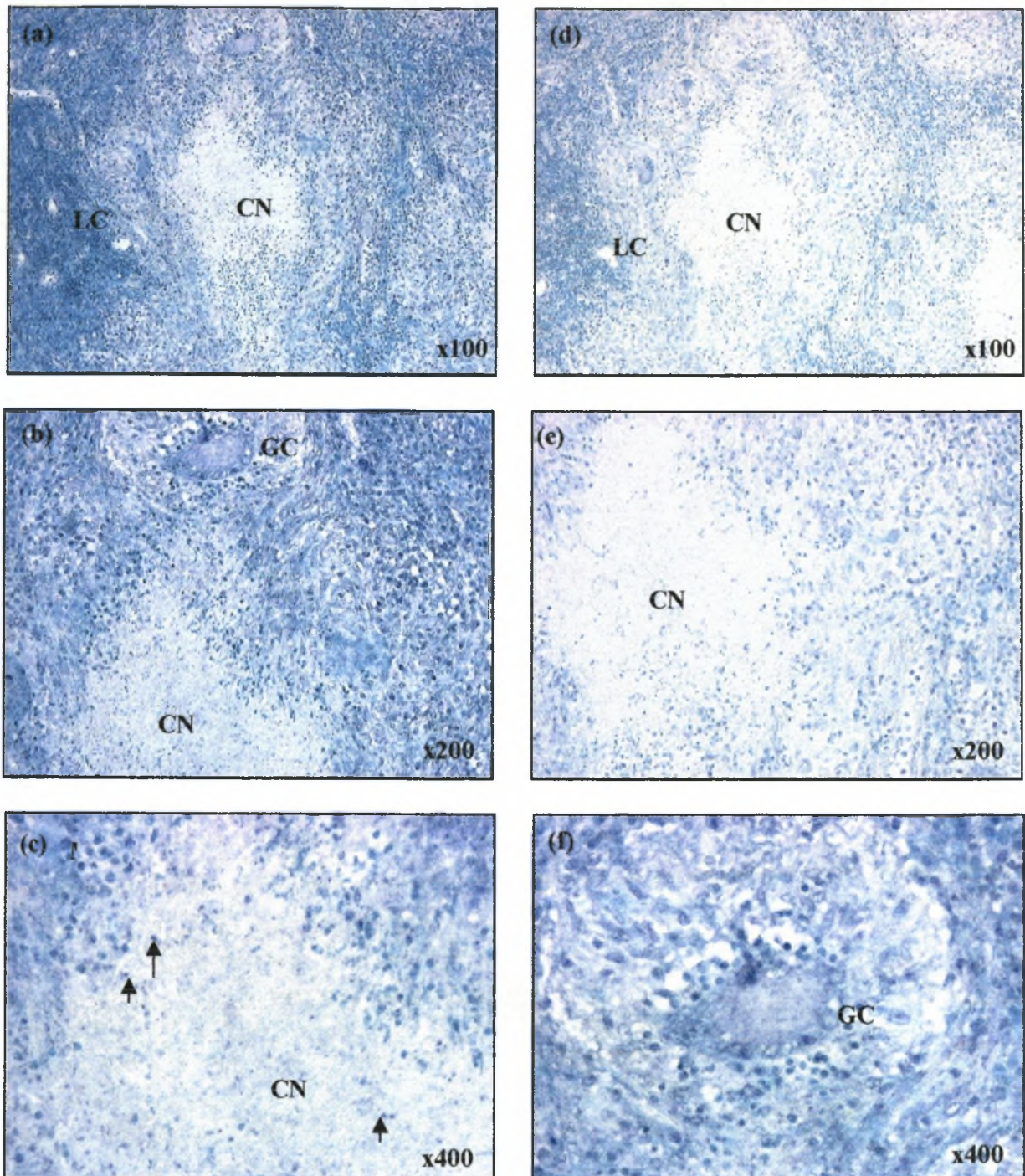


Figure 3.11. *In situ* hybridisation of sections through necrotic granuloma 18 of patient L6. Nuclei stain green, and cells positive for *Mtb* DNA stained blue (a-c, f). Cells with the morphology of macrophages (M) stained positive for *Mtb* DNA, which was more distinguishable at higher magnifications (c, f). *Mtb* DNA also localised within the caseous necrosis (CN), not associated with any cells, as indicated by the arrows (c). The blue signal localised to a giant cell (GC) detected in the lymphocyte cuff (LC). Higher magnification of the giant cell (f) indicated that the signal was localised to the cytoplasm. Negative controls were also included (d-e). Total magnification for each section is indicated below the panel.

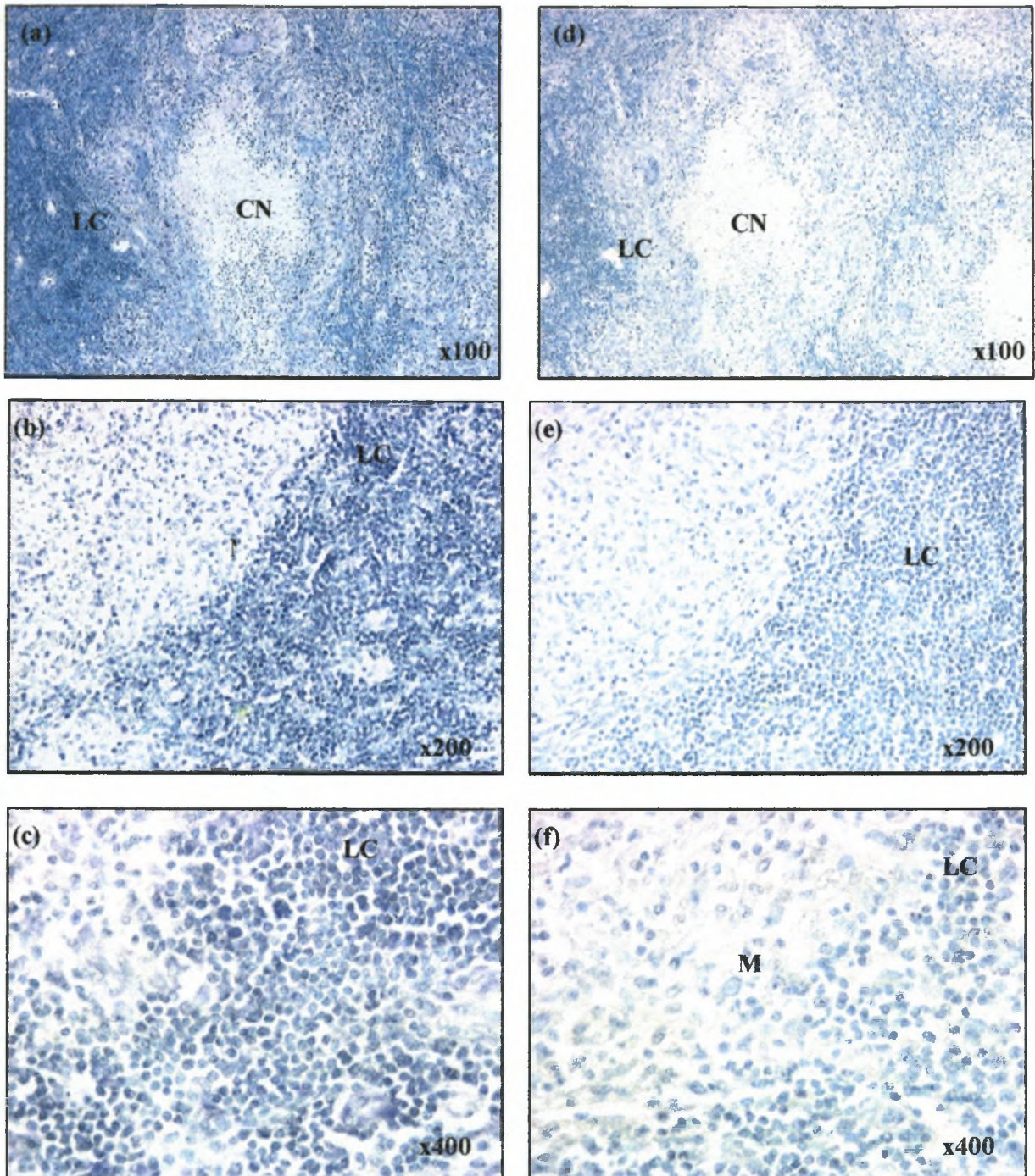


Figure 3.12. *In situ* hybridisation of sections through non-necrotic granuloma 16 from patient L5. Nuclei stain green, and cells positive for *M.tb* DNA stained blue (a-c). Limited signal was detected within the central region of the granuloma, with signal predominantly in the lymphocyte cuff (LC) (b). Cells with the morphology of macrophages (M) stained positive for *M.tb* DNA, which was more distinguishable at higher magnifications (c). Cells negative for *M.tb* DNA were detected within the lymphocyte cuff, along with positive staining cells. Negative controls were also included (d-f). Total magnification of each section is indicated.

3.5.2 Dual Labeling: Co-localisation of CD68 Positive Cells and Mycobacterial DNA

In order to co-localise *M. tuberculosis* DNA to cells with the morphology of macrophages, dual labelling was performed. That is, surface receptor CD68 molecules specific for macrophages were stained to allow co-localisation of the *M. tuberculosis* DNA to these specific cells.

CD68-positive cells (pink) stained positive for *M. tuberculosis* DNA (dark blue) (Figure 3.13). The specificity of the *in situ* hybridisation staining for *M. tuberculosis* DNA is demonstrated by the differential staining observed, particularly at higher magnifications where CD68 stained cells positive and negative for *M. tuberculosis* DNA are easily distinguished (Figure 3.13 b and Figure 3.14 a). *M. tuberculosis* DNA was co-localised with CD68-positive giant cells, which are fused macrophages. CD68-positive giant cells were detected at the periphery of necrotic (Figure 3.13 a, b), and non-necrotic granulomas (Figure 3.13 c, d). The CD68 staining on the giant cell surface is more distinguishable at high magnification (Figure 3.14b).

The results obtained with the hybridisation staining of mycobacterial DNA of the dual labeling, was the same as the “single” *in situ* hybridisation staining.

3.5.3 Overall Assessment of Mycobacterial DNA Detection In Patients

All the patients, with the exception of patient L4, stained positive for acid-fast bacilli by ZN staining (Table 3.2). This patient, however, had a positive (BACTEC) culture, implying that *M. tuberculosis* bacilli were present in the biopsy tissue. Interestingly, *M. tuberculosis* DNA was detected in the granulomas of all six patients (L1 – L6) when using the DNA:DNA *in situ* hybridisation technique. The percentage of granulomas staining positive for each patient is summarised in Figure 3.15. The levels of DNA detected were comparable between all the patients, including the treated patient L2, and the percentage of positive granulomas ranged from 84.6 – 94.7%, with the least number of granulomas identified in patient L4, the ZN negative patient.

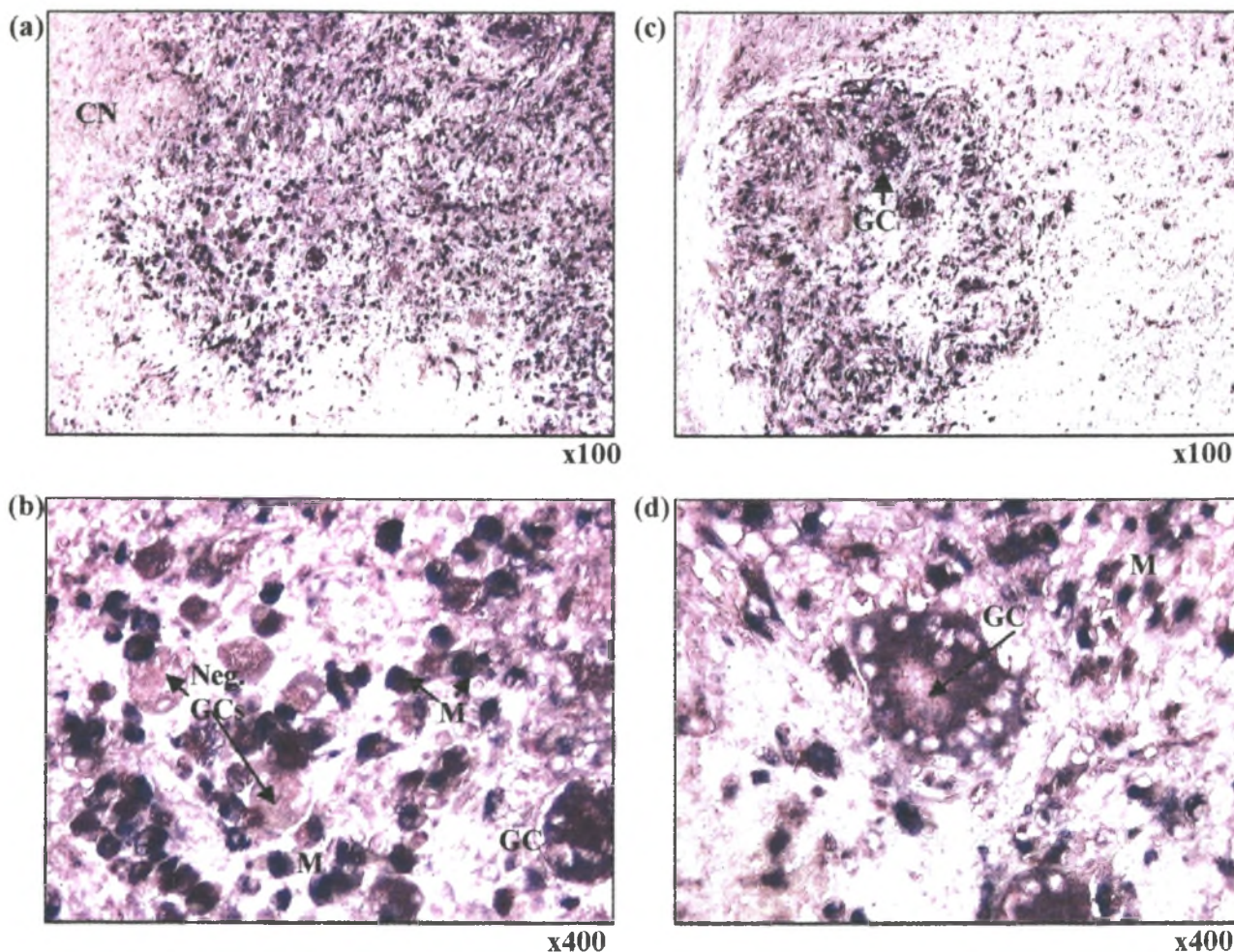


Figure 3.13. Co-localisation of *M. tuberculosis* DNA to CD68 positive cells. Co-localisation of CD68 macrophages (M) with *M. tuberculosis* DNA (a-b) results in dark blue staining within the macrophages (pink). CD68 stained cells not positive for *M. tuberculosis* DNA was detected (Neg GC), as illustrated above (b). Giant cell (GC) was detected in the non-necrotic granuloma (c-d) that stained positive for *M. tuberculosis* DNA

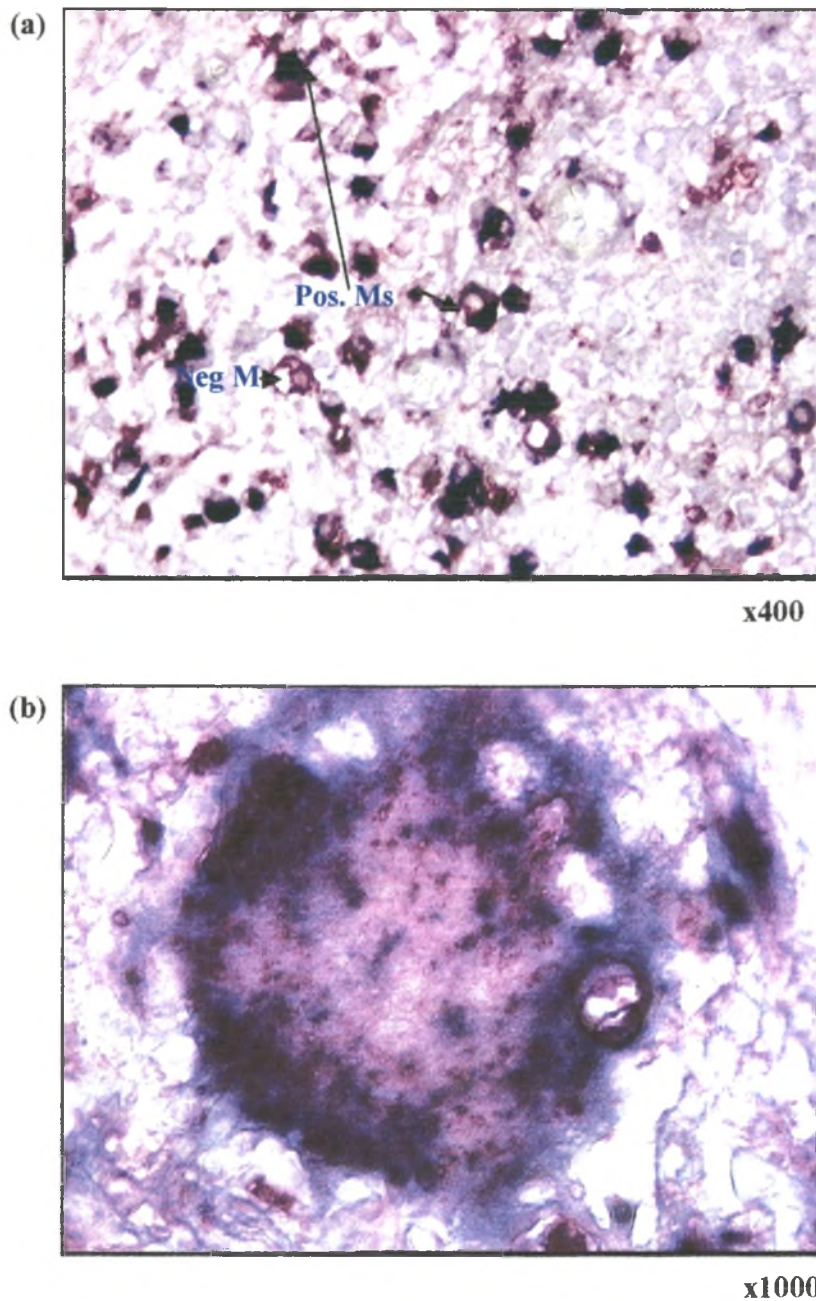


Figure 3.14. High Magnification Illustrating the Co-localisation of *M. tuberculosis* DNA to CD68 positive (a) Macrophages and (b) Giant Cell. (a) CD68 positive macrophages that stained positive for *M. tuberculosis* DNA was detected, as well as CD68 macrophages that did not stain positive for *M. tuberculosis* DNA (Neg M). (b) The high magnification of the giant cell distinguishes between the CD68 staining (pink) and the *M. tuberculosis* DNA ISH staining (dark blue).

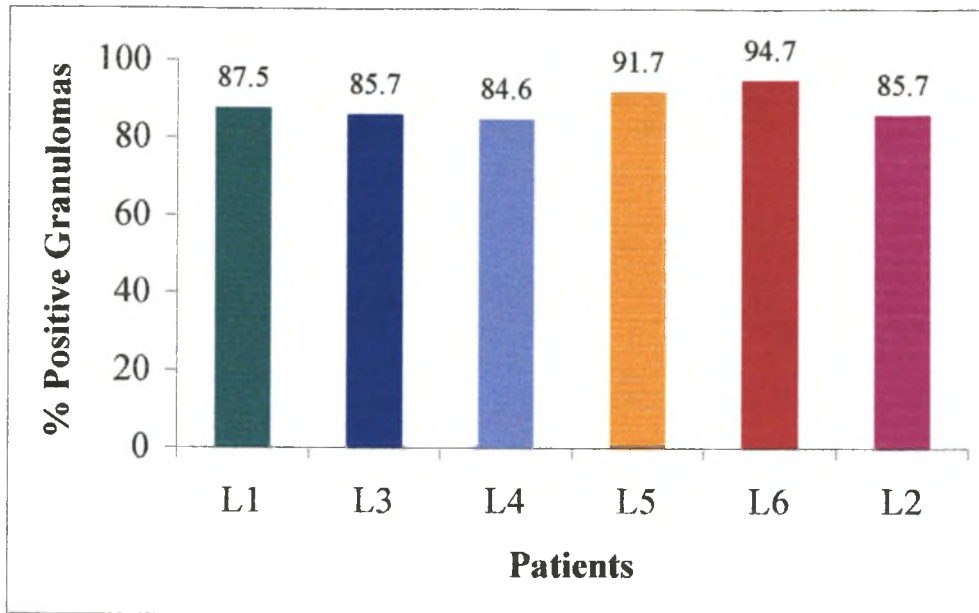


Figure 3.15. Percentage Granulomas Positive for Mycobacterial DNA Detected in Individual Patients. The only treated patient, L2, is represented by the pink bar.

3.6 *M. TUBERCULOSIS* GENE EXPRESSION

3.6.1 *M. tuberculosis* Gene Expression in Granulomas

A series of antisense RNA probes were developed to identify genes required for survival within the hostile environment of the human granuloma. The *in situ* hybridisation experiments revealed that each granuloma within a patient is a microenvironment in which various patterns of *M. tuberculosis* gene expression are observed. Scanning the lymph node sections for each RNA probe at low-power magnification allowed an overall assessment of the relative staining in the granulomas in the tissue. A total of 107 granulomas were analysed from the 6 patients collectively, 73 of which contained caseous necrosis.

Figure 3.16 (a – g) shows representative sections of a necrotic granuloma from patient L5 hybridised with the individual antisense riboprobes viewed under 10x magnification. Positive signal (blue colour) localised predominantly to the periphery and lymphocyte cuff of necrotic granulomas. Signal for certain genes, namely *katG*, *narX*, *icl* and *rel_{Mtb}*, as well as *PPE*, were also detected in the necrotic regions of the granuloma (Figure 3.16 b, c, d, f and g). This illustrates that the bacteria within the restrictive necrotic environment are transcriptionally active. Hybridisation with the riboprobes produced varying staining intensities. The riboprobes producing strong staining intensity were *katG*, *narX*, *icl* and *rel_{Mtb}* (Figure 3.16 b, c, d and f respectively). This necrotic granuloma was weakly positive for *rpoB*, and *mbtB* (Figure 3.16 a, and e, respectively), suggesting that the expression of these genes were not as upregulated as the other genes analysed. No staining was detected for the *esat-6* riboprobe in granulomas of this tissue section, but was detected in other patients (data not shown). The sense probes were used as controls for specificity of the hybridisation, and did not produce any signal, an example of which is illustrated in Figure 3.16h.

Figure 3.17 (a-i) and Figure 3.8 (a-i) shows representative sections of a non-necrotic granuloma of patient L6 hybridised with the individual riboprobes, viewed under 100x magnification. Hybridisation signals (blue) were localised predominantly in the periphery and lymphocyte cuff region of the granuloma. Different staining intensities were detected for the various riboprobes. Cells with the morphology of macrophages stained positive for the various genes and can be detected when viewed under a higher magnification (Figure 3.18 a - i).

Similar results were observed for all patients, as summarised in Appendix VI.

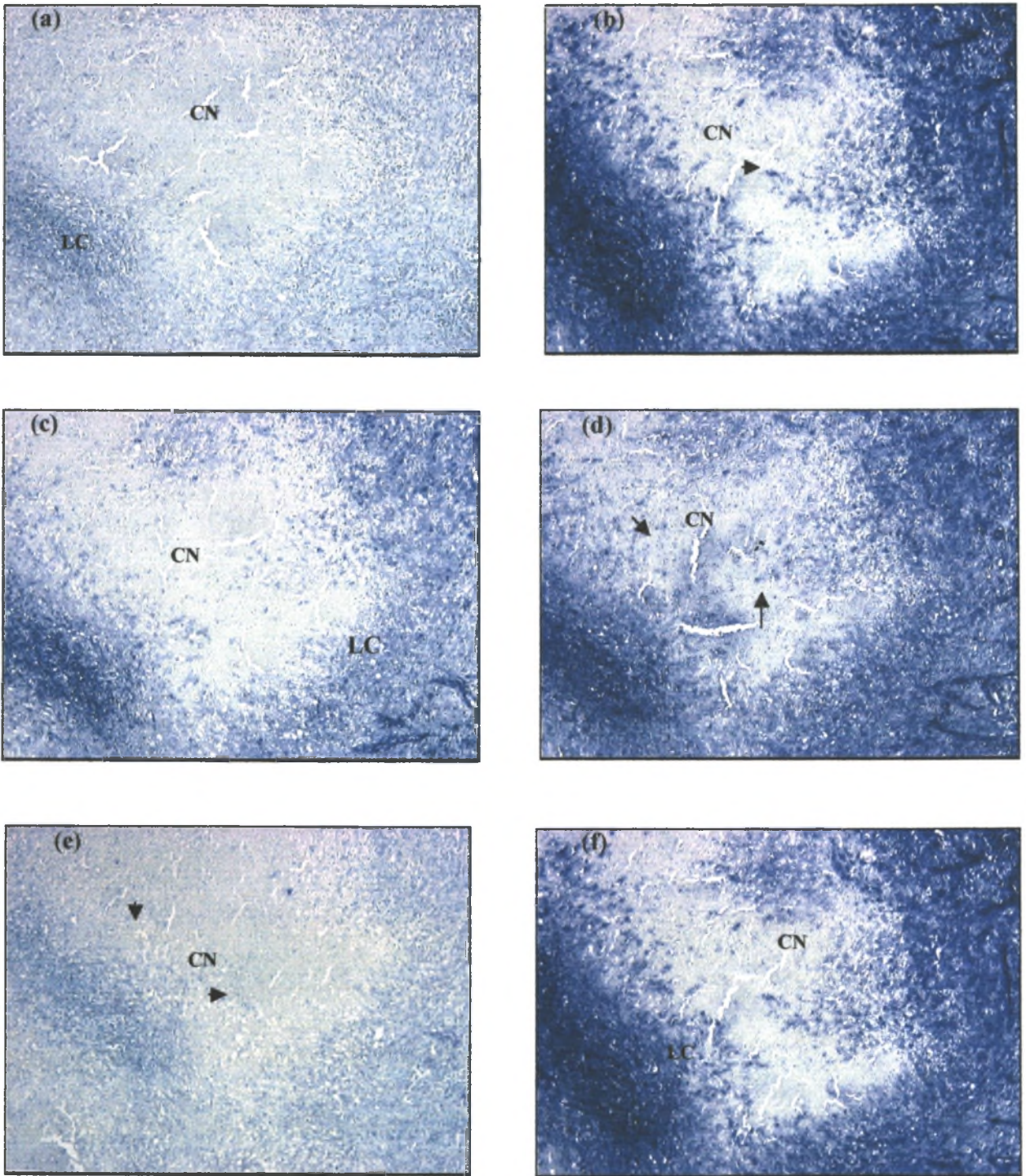


(Figure 3.16. legend on following page (p 90))

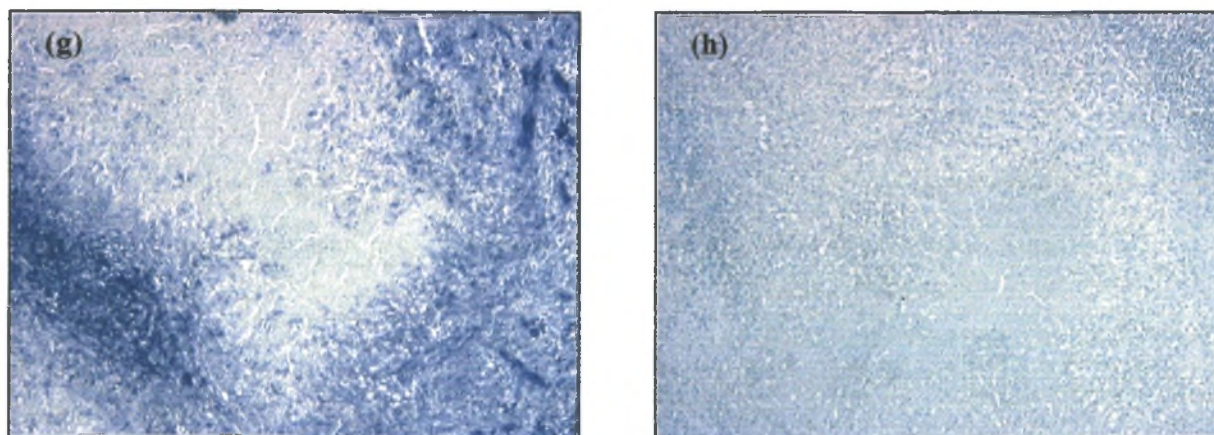
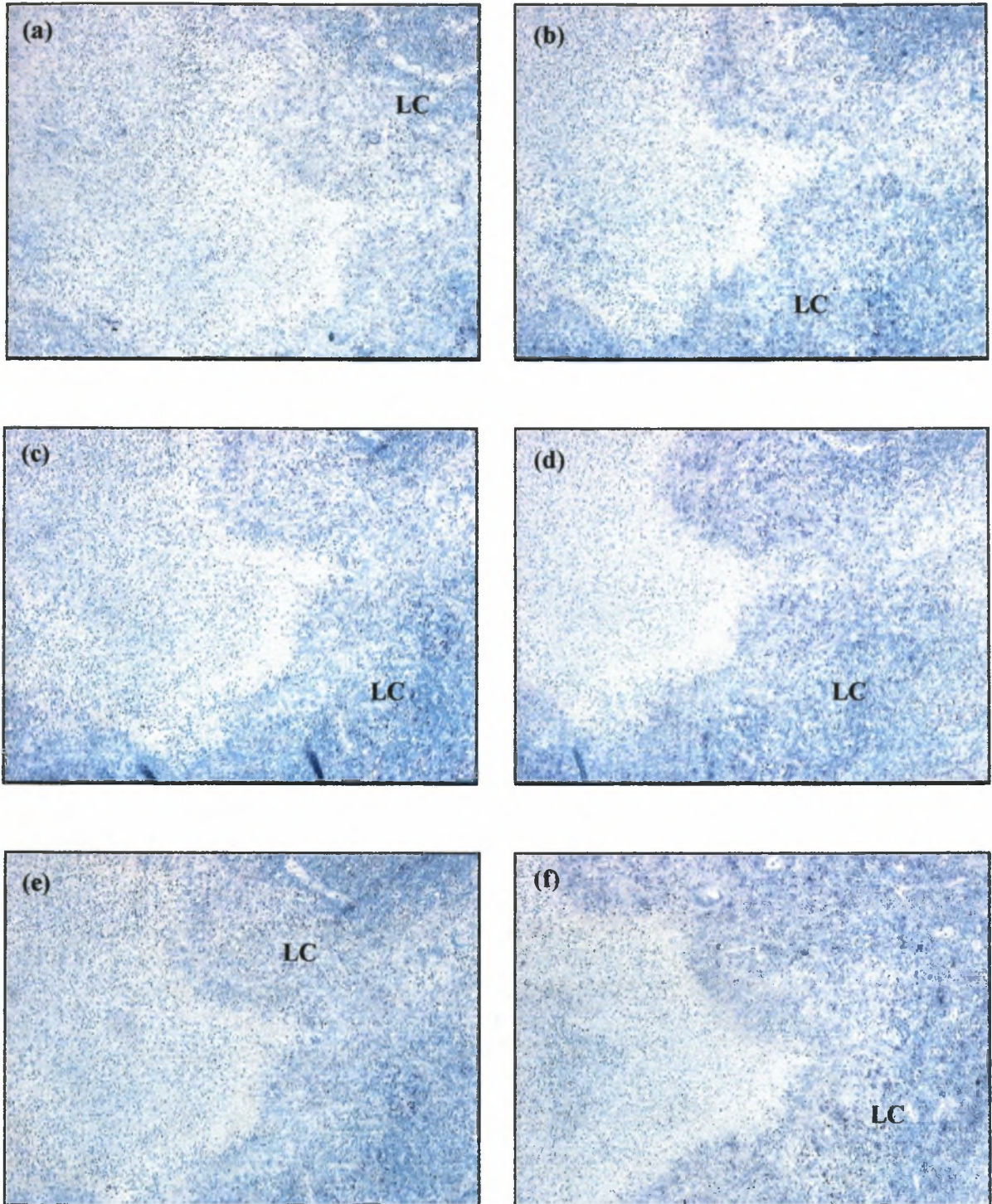


Figure 3.16. In situ hybridisation of necrotic granuloma number 15 from patient L5 at x100 Magnification. Consecutive sections were probed with the following antisense probes: (a) *rpoB*, (b) *katG*, (c) *narX*, (d) *icl*, (e) *mbtB*, (f) *rel_{Mtb}*, (g) *PPE* and (h) sense. The region shown is a representative granuloma across the lymph node biopsy. The remaining probes produced positive (blue) signal, which was localised predominantly to the periphery and lymphocyte cuff (LC) of the granulomas. RNA transcripts of *katG* (b), *narX* (c), *icl* (d), *rel_{Mtb}* (f) and *PPE* (g) also localised to the necrotic region of the granuloma (as indicated by arrows).



(Figure 3.17. legend on following page (p 92))

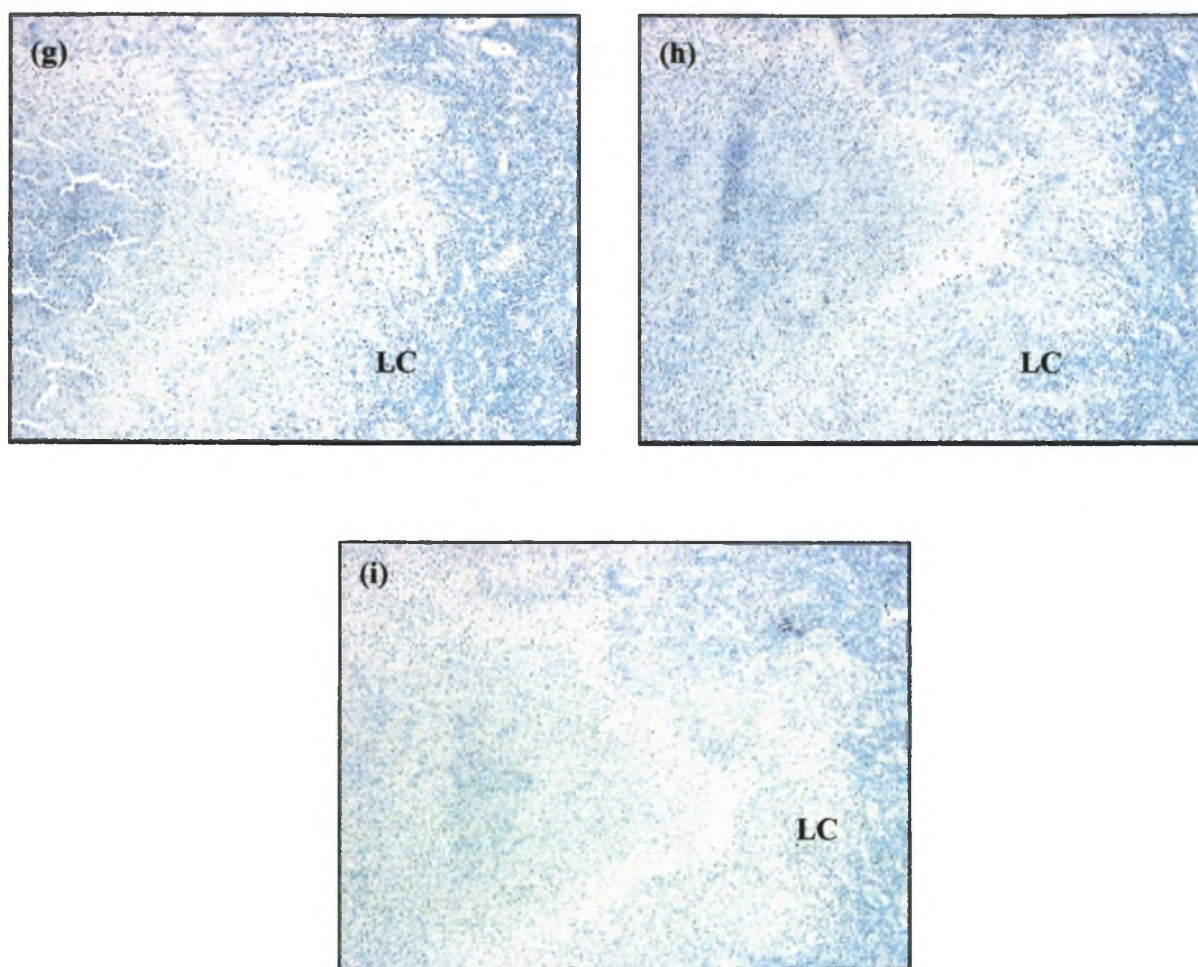
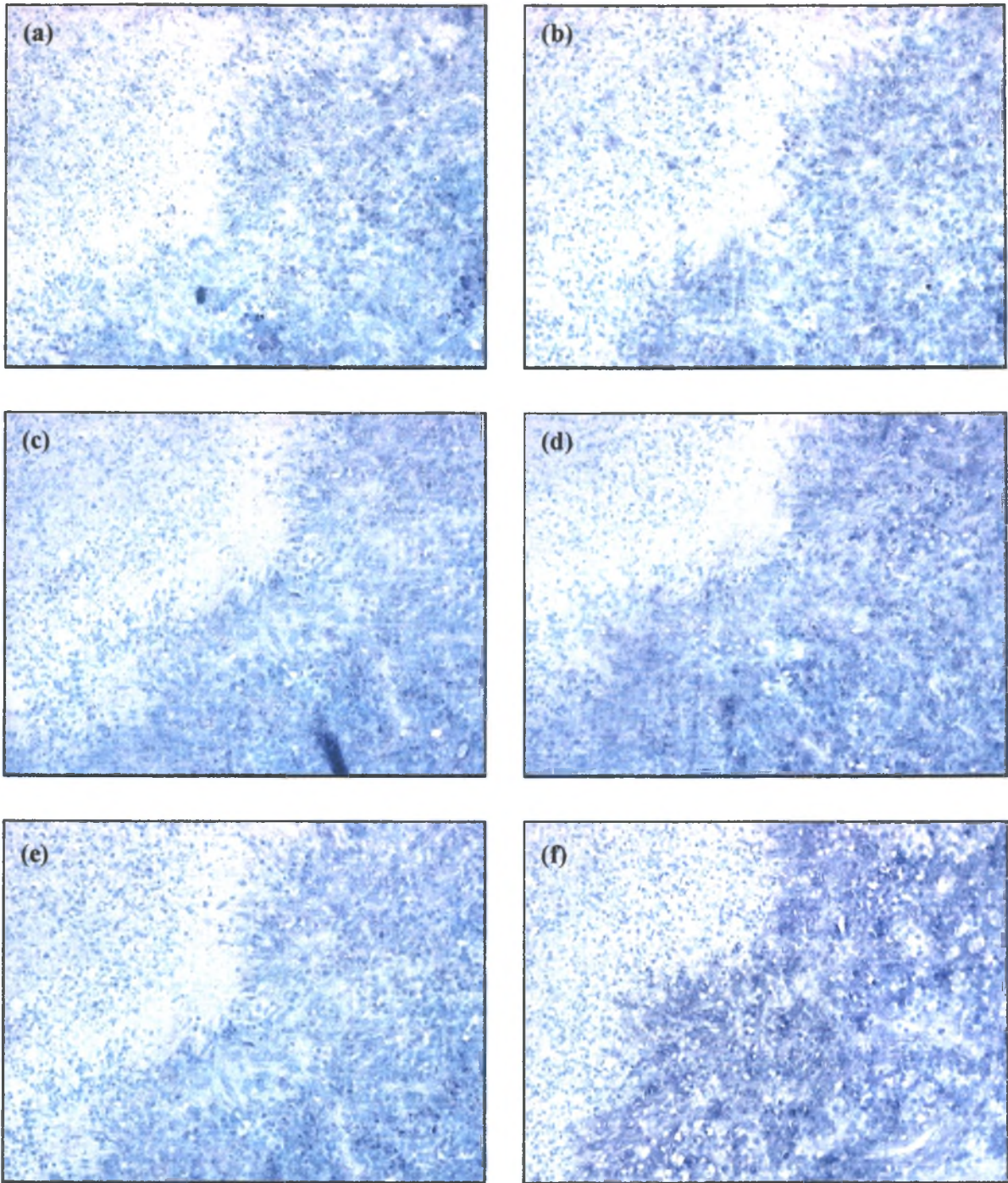


Figure 3.17. In situ hybridisation of non-necrotic granuloma number 15 from patient L6 at x100 Magnification. Consecutive sections were probed with the following antisense probes: (a) *rpoB*, (b) *katG*, (c) *narX*, (d) *icl*, (e) *mbtB*, (f) *rel_{Mtb}*, (g) *esat-6* and (h) *PPE*, as well as sense probes (i). The region shown is a representative granuloma across the lymph node biopsy. The negative controls (i). The hybridised probes produced positive (blue) signal, which was localised predominantly to the periphery and lymphocyte cuff (LC) of the granulomas.



(Figure 3.18. legend on following page (p 94))

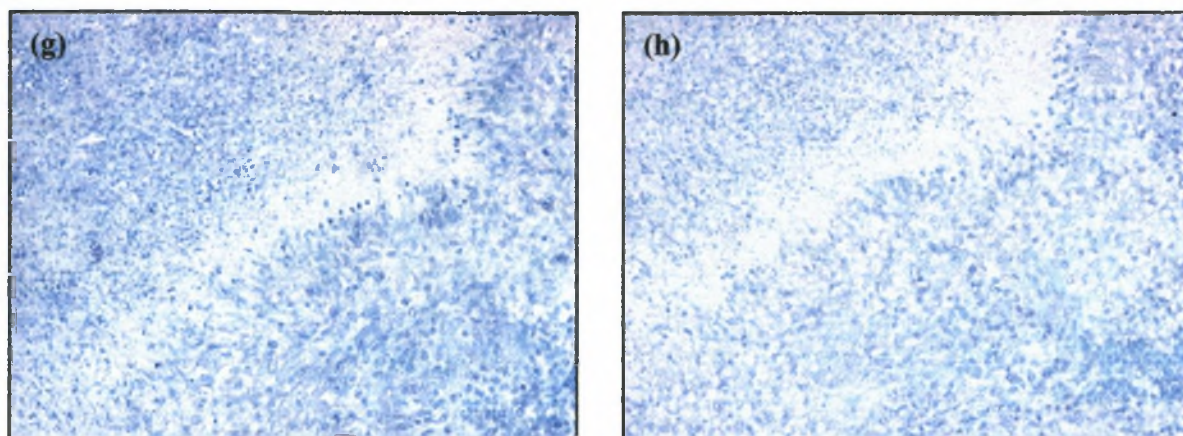


Figure 3.18. In situ hybridisation of sections through granuloma 15 from patient L6 at x200 Magnification. Consecutive sections were probed with (a) *rpoB*, (b) *katG*, (c) *narX*, (d) *icl*, (e) *mbtB*, (f) *rel_{Mtb}*, (g) *esat-6* and (h) *PPE*. Hybridisation signals were localised to cells with the morphology of macrophages (M) at the periphery and lymphocyte cuff region of the granuloma. Limited signal was detected in the central region of the granuloma. Staining for *rel_{Mtb}* (f) was more intense than for the other probes, especially when compared to the weak signal intensity for *PPE*. Hybridisation with *esat-6* riboprobe (g) did not produce any detectable signal.

3.6.2 Dual Labeling: Co-localisation of *rpoB* mRNA to CD68 Positive Cells

M. tuberculosis rpoB mRNA was co-localised to cells with the morphology of macrophages. Surface receptor molecules specific for macrophages were stained to allow co-localisation of the *M. tuberculosis rpoB* mRNA to these specific cells.

Messenger RNA for *rpoB* (dark blue) was co-localised to the CD68-positive cells (pink), as illustrated in Figure 3.19. As with the *M. tuberculosis* DNA, CD68-positive cells that did not contain hybridisation signals for *rpoB* mRNA were also detected among the positive staining *rpoB* CD68 cells at the edge of the necrotic granuloma (Figure 3.19 a, b). *RpoB* mRNA also co-localised to CD68 positive giant cells detected at the edge of the non-necrotic granuloma (Figure 3.19 c, d).

3.7.1 Overall Assessment of *M. tuberculosis* Gene Expression

A consistent level of *rpoB* expression was observed in the untreated patients L1, L3, L4, L5 and L6 (Figure 3.20). However, for patient L2, who was treated with rifampin (for 2 days), no *rpoB* mRNA was detected. Similarly, *katG* mRNA was also not detected in the granulomas of treated patient L2, who was also treated with isoniazid (Figure 3.20). For the untreated patients, there is a clear variability in expression for the *katG* gene. Considerable variability in gene expression of the persistent factors, and those genes of unknown function, was observed between the patients, including the treated patient, L2 (Figure 3.20). The variability in *M. tuberculosis* gene expression between the patients was more evident with *esat-6* staining. Messenger RNA for this gene was detected in most of the granulomas identified for patient L1 and interestingly, was absent in the granulomas of patients L4 and L5 (Figure 3.20).

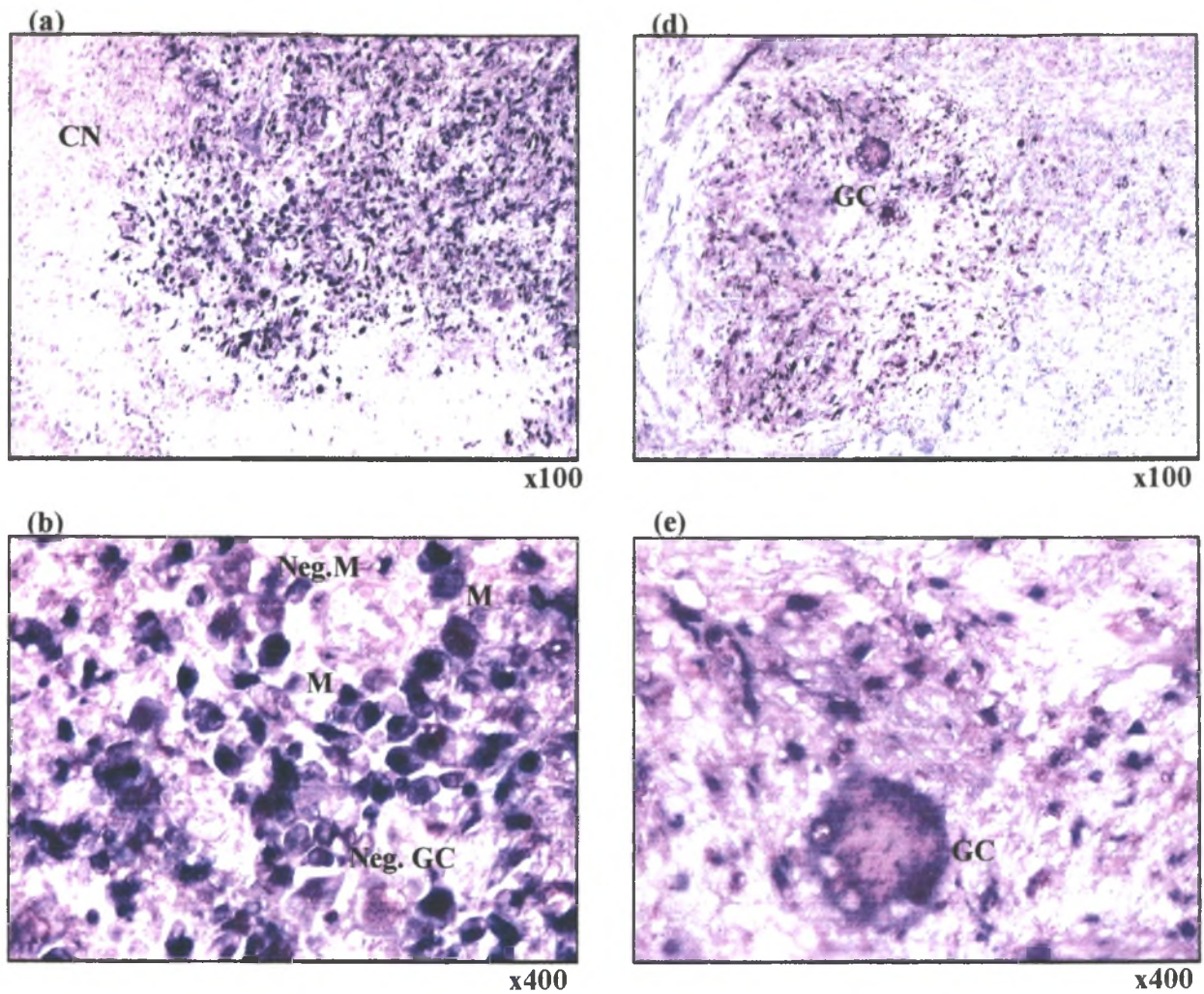


Figure 3.19. Co-localisation of *rpoB* mRNA to CD68 positive cells. Co-localisation of CD68 with *rpoB* mRNA (a, b) results in dark blue staining within the macrophages (M) (pink). CD68 stained cells not positive for *rpoB* mRNA was detected, as illustrated above (b). Giant cell (GC) was detected in the non-necrotic granuoma (c, d) that stained positive for *rpoB* mRNA

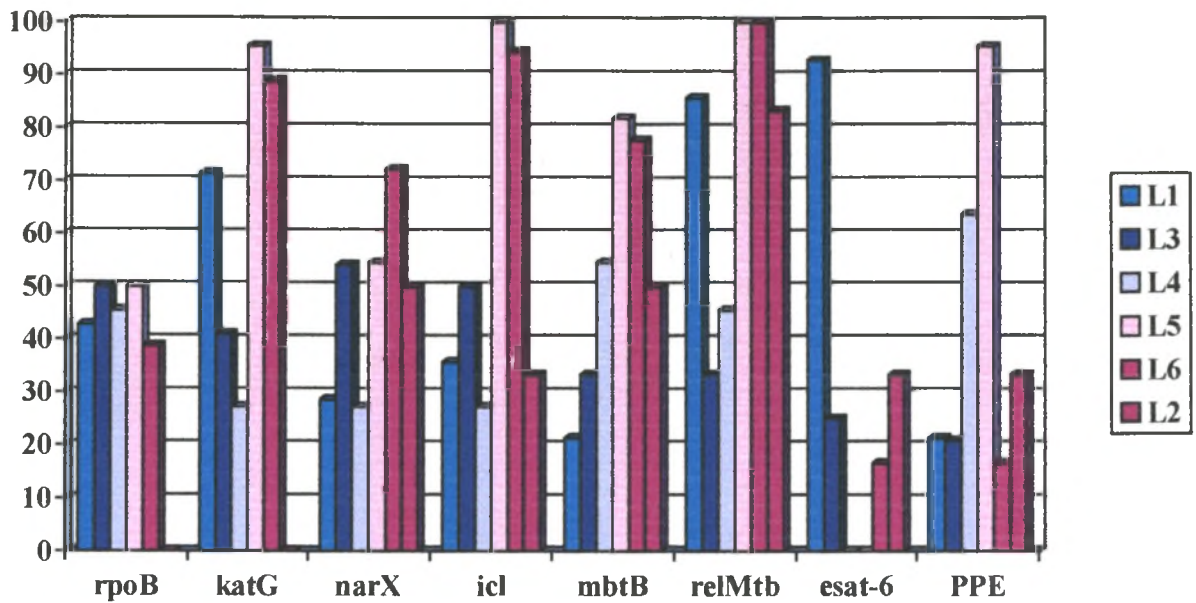


Figure 3.20. Expression Analysis of the Individual *M.tuberculosis* Genes. The percentage of positive staining granulomas was determined for each of the genes in the individual patients. The treated patient, L2, is represented by the pink bar. Messenger RNA for *rpoB* and *katG* was not detected in the granulomas of the treated patient. *RpoB* was present at consistent levels in the untreated patients, but *katG* exhibited more variability in expression between the untreated patients. The remaining genes also displayed variability in expression all the six patients, including the treated patient L2. This variability in gene expression between the patients was more evident with *esat-6*. Messenger RNA for this gene was detected in most of the granulomas identified for patient L1 and interestingly, was absent in the granulomas of patient L4 and L5.

3.6.4 Stratification of *M. tuberculosis* Gene Expression

The granulomas of the individual patients (Appendix IV) were characterized to generate an overall assessment to allow for stratification of gene expression patterns. The presence and absence of signal in the granulomas for all the riboprobes was stratified to determine if any correlations existed in the expression profile of the *M. tuberculosis* genes analysed. The stratification results of all the riboprobes are summarized in Table 3.4.

Review of the data showed that co-expression could not be demonstrated for *rpoB* and any other *M. tuberculosis* gene analysed. The term “co-expression” refers to the detection of mRNA transcripts of two or more mycobacterial genes in the same granuloma. The *M. tuberculosis* genes were expressed at consistent levels with no distinction between *rpoB* negative or positive granulomas.

Stratification of the *katG* expression profile into negative and positive subgroups demonstrated a significant co-expression correlation between *katG* and *icl* ($p = 0.008$). The expression of *katG* occurred mostly in tandem with *icl*. Similarly, a significant correlation in expression between *katG* and rel_{Mtb} ($p = 0.0106$), as well as *katG* and *PPE Rv3018c* ($p = 0.047$) was observed.

A significant co-expression correlation was also observed between *icl* and *narX* ($p = 0.00003$). The regulation of *icl* expression almost mirrored that of *narX*. Similarly, a significant correlation in expression between *icl* and rel_{Mtb} was observed ($p = 0.00003$). This suggests that there is a coordinated expression of *katG*, *icl* and rel_{Mtb} . However, an inverse expression pattern was observed between *icl* and *esat-6* ($p = 0.043$). Most granulomas positive for *icl* were negative for *esat-6*, and conversely, most granulomas negative for *icl* were positive for *esat-6*. It would appear that the expression of the fatty acid metabolising enzyme, isocitrate lyase, and the *ESAT-6* protein occur at different stages of infection.

A significant inverse expression pattern was also observed with *mbtB* and *esat-6* ($p = 0.026$). The downregulation of *mbtB* was coupled with an upregulation of *esat-6* in most granulomas.

The presence or absence of caseous necrosis in the granulomas was stratified in order to determine if any correlations existed between the expression of the mycobacterial genes and tissue damage. All of the genes analysed, with the exception of *narX*, were expressed in approximately the same proportion of non-necrotic and necrotic granulomas (Table 3.4). *NarX* was expressed mostly in granulomas containing caseous necrosis ($p = 0.0062$).

Table 3.4. Summary of *M. tuberculosis* Gene Expression Stratification

		<i>M. tuberculosis</i> Genes								
sorting		DNA	rpoB	katG	narX	icl	mbtB	rel _{Mtb}	esat-6	PPE
RpoB	Neg	54	0	34	25	35	28	41	11	19
	%	100.00	0.00	62.96	46.30	64.81	51.85	75.93	20.37	35.19
	Pos	41	41	26	23	26	24	29	11	22
	%	100.00	100.00	63.41	56.10	63.41	58.54	70.73	26.83	53.66
	p-value	ns	ns	ns	ns	ns	ns	ns	ns	ns
KatG	Neg	35	15	0	16	16	18	20	9	10
	%	100.00	42.86	0.00	45.71	45.71	51.43	57.14	25.71	28.57
	Pos	60	26	60	32	45	34	50	13	31
	%	100.00	43.33	100.00	53.33	75.00	56.67	83.33	21.67	51.67
	p-value	ns	ns	ns	ns	0.008	ns	0.0106	ns	0.047
NarX	Neg	47	18	28	0	20	30	32	12	21
	%	100.00	38.30	59.57	0.00	42.55	63.83	68.09	25.53	44.68
	Pos	48	23	32	48	41	22	38	10	20
	%	100.00	47.92	66.67	100.00	85.42	45.83	79.17	20.83	41.67
	p-value	ns	ns	ns	ns	0.00003	ns	ns	ns	ns
icl	Neg	34	15	15	7	0	15	16	14	15
	%	100.00	44.12	44.12	20.59	0.00	44.12	47.06	41.18	44.12
	Pos	61	26	45	41	61	37	54	8	26
	%	100.00	42.62	73.77	67.21	100.00	60.66	88.52	13.11	42.62
	p-value	ns	ns	0.008	0.00003	ns	ns	0.00003	0.043	ns
MbtB	Neg	43	17	26	26	24	0	29	15	16
	%	100.00	39.53	60.47	60.47	55.81	0.00	67.44	34.88	37.21
	Pos	52	24	34	22	37	52	41	7	25
	%	100.00	46.15	65.38	42.31	71.15	100.00	78.85	13.46	48.08
	p-value	ns	ns	ns	ns	ns	ns	ns	0.026	ns
RelMtb	Neg	25	12	10	10	7	11	0	5	11
	%	100.00	48.00	40.00	40.00	28.00	44.00	0.00	20.00	44.00
	Pos	70	29	50	38	54	41	70	17	30
	%	100.00	41.43	71.43	54.29	77.14	58.57	100.00	24.29	42.86
	p-value	ns	ns	0.0106	ns	0.00003	ns	ns	ns	ns
Esat-6	Neg	73	30	47	38	53	45	53	0	34
	%	100.00	41.10	64.38	52.05	72.60	61.64	72.60	0.00	46.58
	Pos	22	11	13	10	8	7	17	22	7
	%	100.00	50.00	59.09	45.45	36.36	31.82	77.27	100.00	31.82
	p-value	ns	ns	ns	ns	0.043	0.026	ns	ns	ns
PPE	Neg	54	19	29	28	35	27	40	15	0
	%	100.00	35.19	53.70	51.85	64.81	50.00	74.07	27.78	0.00
	Pos	41	22	31	20	26	25	30	7	41
	%	100.00	53.66	75.61	48.78	63.41	60.98	73.17	17.07	100.00
	p-value	ns	ns	0.047	ns	ns	ns	ns	ns	ns
necrosis	Non	22	13	16	5	10	10	17	6	11
	%	100.00	59.09	72.73	22.73	45.45	45.45	77.27	27.27	50.00
	Necr	73	28	44	43	51	42	53	16	30
	%	100.00	38.36	60.27	58.90	69.86	57.53	72.60	21.92	41.10
	p-value	ns	ns	ns	0.0062	ns	ns	ns	ns	ns

* significant correlations are highlighted
 ns = non-significance

3.7 STRATIFICATION OF MYCOBACTERIAL GENES AND HOST CYTOKINES

The expression of the bacterial genes for the various granulomas was stratified along with the cytokine expression also detected in the granulomas (Table 3.5). Stratification was done to determine whether any correlations existed between the *M. tuberculosis* genes and host cytokine expression.

Review of the data showed that a significant correlation existed between the expression of the mycobacterial gene, *mbtB*, and a Th0 cytokine response ($p = 0.0012$). The expression of *mbtB* occurred predominantly in granulomas with an overall Th0 phenotype (Table 3.5). Furthermore, stratification of the granulomas into IL-4 positive and IL-4 negative groups showed that a significant correlation existed between the expression of IL-4 and *mbtB* ($p = 0.005$). The expression of this type 2 cytokine and the mycobacterial gene occurred simultaneously in a number of granulomas (Table 3.5). It is unclear whether the expression of IL-4 is the result of, or conversely, induced the expression of *mbtB* by infecting bacilli.

Associations between IL-10 expression and any of the mycobacterial genes analysed could not be demonstrated. The expression of these genes occurred with no distinction between the absence and presence of IL-10.

An opposite inverse expression pattern for IL-12 and rel_{Mtb} was detected in most granulomas ($p = 0.0037$). This cytokine and mycobacterial gene was hardly expressed in the same granulomas. The stringent response, it would appear, is less active in the presence of IL-12. Conversely, a significant co-expression correlation existed between IL-12 and *esat-6* ($p = 0.043$). The expression of this cytokine and mycobacterial genes occurred in tandem in most granulomas.

3.7.1 Passive vs. Active Transcription

The granulomas were primarily stratified into *rpoB* negative (passive transcription) and *rpoB* positive groups (active transcription), and were followed by further secondary stratification according to the presence and absence of the host cytokines (Table 3.6).

In the granulomas displaying passive transcription, i.e. the *rpoB* negative granulomas, a significant correlation was observed in the Th0 cytokine response and the expression of *mbtB* ($p = 0.020$).

Table 3.5. Summary of Host Cytokine and *M.tuberculosis* Gene Expression Stratification

sorting		<i>M. tuberculosis</i> Genes								
		DNA	rpoB	katG	narX	icl	mbtB	rel _{Mtb}	esat-6	PPE
Th	Th1	13	7	6	6	7	2	9	3	3
	%	100.	53.85	46.15	46.15	53.85	15.38	69.23	23.08	23.08
	Th0	82	34	54	42	54	50	61	19	38
	%	100.	41.46	65.85	51.22	65.85	60.98	74.39	23.17	46.34
	p-value	ns	ns	ns	ns	ns	0.0012	ns	ns	ns
IL-4	Neg.	13	7	6	6	7	2	9	3	3
	%	100.	53.85	46.15	46.15	53.85	15.38	69.23	23.08	23.08
	Pos	82	34	54	42	54	50	61	19	38
	%	100.	41.46	65.85	51.22	65.85	60.98	74.39	23.17	46.34
	p-value	ns	ns	ns	ns	ns	0.005	ns	ns	ns
IL-10	Neg	31	14	19	12	18	13	23	5	16
	%	100.	45.16	61.29	38.71	58.06	41.94	74.19	16.13	51.61
	Pos	64	27	41	36	43	39	47	17	25
	%	100.	42.19	64.06	56.25	67.19	60.94	73.44	26.56	39.06
	p-value	ns	ns	ns	ns	ns	ns	ns	ns	ns
IL-12	Neg	27	14	19	13	21	19	26	2	16
	%	100.	51.85	70.37	48.15	77.78	70.37	96.30	7.41	59.26
	Pos	68	27	41	35	40	33	44	20	25
	%	100.	39.71	60.29	51.47	58.82	48.53	64.71	29.41	36.76
	p-value	ns	ns	ns	ns	ns	ns	0.0037	0.043	ns

* significant correlations are highlighted
 ns = non-significance

MbtB expression occurred predominantly in granulomas with an overall Th0 phenotype. Secondary stratification of data according to IL-4 revealed a co-expression correlation between this cytokine and *mbtB* ($p = 0.020$).

An opposite trend in expression was observed between IL-12 and rel_{Mtb} . This cytokine and mycobacterial gene exhibited a weakly significant opposite expression pattern ($p = 0.05$). That is, they seldom occurred in tandem. All these trends observed between host cytokine and mycobacterial gene expression in the *rpoB* negative granulomas, was also detected by single stratification of data (Table 3.4).

In the granulomas displaying active transcription, i.e. *rpoB* positive granulomas, more significant correlations were detected between host cytokines and mycobacterial genes (Table 3.6). Unlike the *rpoB* negative granulomas, a significant correlation was detected between the Th0 cytokine profile and *katG* ($p = 0.049$). This is presumably as a consequence of the weakly significant co-expression correlation between IL-4 and *katG* ($p = 0.049$). Another correlation detected in the actively transcribing granulomas is that between IL-10 and *narX* ($p = 0.026$). These cytokine and mycobacterial genes appear to be co-expressed in most granulomas (Table 3.6).

A significant inverse expression pattern was observed between IL-12 and *mbtB* ($p = 0.035$), and as with the *rpoB* negative granulomas, between IL-12 and rel_{Mtb} ($p = 0.021$). However, unlike these two mycobacterial persistence factors, a co-expression correlation existed between IL-12 and *esat-6* ($p = 0.021$). This correlation, although not observed in the *rpoB* negative subgroup, was also detected when using single stratification analysis (Table 3.5).

Table 3.6. Stratification of Granuloma into Passive and Active Transcribing Subgroups

RpoB Negative										
Sorting		<i>M. tuberculosis</i> Genes								
		DNA	rpoB	katG	narX	icl	mbtB	rel _{Mtb}	Esat-6	PPE
Th	Th1	6	0	4	4	5	0	6	1	1
	%	100.00	0.00	66.67	66.67	83.33	0.00	100.00	16.67	16.67
	Th0	48	0	30	21	30	28	35	10	18
	%	100.00	0.00	62.50	43.75	62.50	58.33	72.92	20.83	37.50
p-value		ns	ns	ns	ns	ns	0.020	ns	ns	ns
IL-4	Neg.	6	0	4	4	5	0	6	1	1
	%	100.00	0.00	66.67	66.67	83.33	0.00	100.00	16.67	16.67
	Pos	48	0	30	21	30	28	35	10	18
	%	100.00	0.00	62.50	43.75	62.50	58.33	72.92	20.83	37.50
p-value		ns	ns	ns	ns	ns	0.020	ns	ns	ns
IL-10	Neg.	17	0	11	8	12	6	15	3	8
	%	100.00	0.00	64.71	47.06	70.59	35.29	88.24	17.65	47.06
	Pos	37	0	23	17	23	22	26	8	11
	%	100.00	0.00	62.16	45.95	62.16	59.46	70.27	21.62	29.73
p-value		ns	ns	ns	ns	ns	ns	ns	ns	ns
IL-12	Neg.	13	0	9	5	10	7	13	2	6
	%	100.00	0.00	69.23	38.46	76.92	53.85	100.00	15.38	46.15
	Pos	41	0	25	20	25	21	28	9	13
	%	100.00	0.00	60.98	48.78	60.98	51.22	68.29	21.95	31.71
p-value		ns	ns	ns	ns	ns	ns	0.05	ns	ns
RpoB Positive										
Sorting		<i>M. tuberculosis</i> Genes								
		DNA	rpoB	katG	narX	icl	mbtB	Rel _{Mtb}	Esat-6	PPE
Th	Th1	7	7	2	2	2	2	3	2	2
	%	100.00	100.00	28.57	28.57	28.57	28.57	42.86	28.57	28.57
	Th0	34	34	24	21	24	22	26	9	20
	%	100.00	100.00	70.59	61.76	70.59	64.71	76.47	26.47	58.82
p-value		ns	ns	0.049	ns	ns	ns	ns	ns	ns
IL-4	Neg.	7	7	2	2	2	2	3	2	2
	%	100.00	100.00	28.57	28.57	28.57	28.57	42.86	28.57	28.57
	Pos	34	34	24	21	24	22	26	9	20
	%	100.00	100.00	70.59	61.76	70.59	64.71	76.47	26.47	58.82
p-value		ns	ns	0.049	ns	ns	ns	ns	ns	ns
IL-10	Neg.	14	14	8	4	6	7	8	2	8
	%	100.00	100.00	57.14	28.57	42.86	50.00	57.14	14.29	57.14
	Pos	27	27	18	19	20	17	21	9	14
	%	100.00	100.00	66.67	70.37	74.07	62.96	77.78	33.33	51.85
p-value		ns	ns	ns	0.026	ns	ns	ns	ns	ns
IL-12	Neg.	14	14	10	8	11	12	13	0	10
	%	100.00	100.00	71.43	57.14	78.57	85.71	92.86	0.00	71.43
	Pos	26	26	15	14	14	12	15	10	12
	%	100.00	100.00	57.69	53.85	53.85	46.15	57.69	38.46	46.15
p-value		ns	ns	ns	ns	ns	0.035	0.021	0.021	ns

*significant correlations are highlighted

ns = non-significance

3.8 STRAIN TYPING *M. TUBERCULOSIS* CLINICAL ISOLATES

The lymph node tissues of patients L2 to L6 that were cultivated in the BACTEC medium yielded a positive *M. tuberculosis* culture. As stated previously, biopsy tissue of patient L1 was not submitted for culture. The infecting *M. tuberculosis* strain could therefore not be classified, as no culture was available for mycobacterial DNA extraction. The cultivation of the abscess fluid of patient L11 (Table 3.1) also yielded a positive *M. tuberculosis* culture. These 6 clinical isolates were then sub-cultured on LJ-slant agar. The mycobacterial DNA was extracted and the clinical strains were classified using the standardised RFLP protocol (Section 2.9). The extracted *M. tuberculosis* genomic DNA was digested with *PvuII* and fractionated by electrophoresis, along with the marker MTB14323. MTB14323 is a standard molecular weight marker used in the DNA fingerprinting technique for *M. tuberculosis* classification (Kamerbreek *et al*, 1997). The *PvuII* digested *M. tuberculosis* genomic DNA was then transferred to a nylon membrane and hybridised with labeled IS6110 probes.

The banding patterns for the 6 clinical isolates clearly illustrate that these strains are genotypically unrelated (Figure 3.21, Table 3.7). Both low (< 5 bands) and high (\geq 5 bands) copy number strains were identified. Hybridisation with the IS6110 probe resulted in a 4-banding pattern for the clinical isolate L11, and was therefore classified as a low copy number strain. The isolated strains L2 and L6 were effectively classified to family 28 and 11, respectively. The IS6110 typing of the 3 remaining strains proved slightly more complicated. The fingerprint patterns of these strains did not bear any resemblance to banding pattern in our database, and were consequently typed as unique strains. All these patients, incidentally, resided in various regions of the Western Cape. However, the majority of the clinical isolates previously classified by IS6110 typing were obtained from the high tuberculosis incidence community of Ravensmead / Uitsig. Information on strain diversity in other regions of the Western Cape is incomplete; therefore, by classifying these strains as unique simply implies that these clinical isolates have not been identified in the Ravensmead / Uitsig community, and does not suggest that these strains are unique to the communities from which the patients originate.

Table 3.7. Strain Typing of Isolated Clinical Strains. *M. tuberculosis* strains were isolated from lymph node biopsy tissue (L2 – L6) and from the abscess fluid of patient L11

Patient Culture	Strain Family
L2	28
L3	Unique
L4	Unique
L5	Unique
L6	11
L11	*LCN

* LCN: Low Copy Number



Figure 3.21. Strain Typing *M. tuberculosis* Clinical Isolates
Marker MTB14323 (M) in the outside lanes served as the standard molecular weight marker

CHAPTER FOUR

DISCUSSION

INDEX	PAGE
4.1 STUDY SUBJECTS	107
4.2 GRANULOMAS	107
4.3 HOST CYTOKINE ANALYSES	110
4.3.1 Expression of Type 1 Cytokines in Granulomas	110
4.3.2 Expression of Type 2 Cytokines in Granulomas	110
4.3.3 Interplay between Host Cytokines	112
4.4 M. TUBERCULOSIS DETECTION IN HOST TISSUE	113
4.5 M. TUBERCULOSIS GENE EXPRESSION ANALYSES IN THE GRANULOMA	114
4.5.1 Metabolic Factors: Important Factors for Current TB Therapy	
4.5.1.1 <i>RpoB</i>	114
4.5.1.2 <i>KatG</i>	115
4.5.2 Persistence Factors	117
4.5.2.1 <i>NarX</i>	117
4.5.2.2 <i>Icl</i>	118
4.5.2.3 <i>MbtB</i>	118
4.5.2.4 <i>Rel_{Mtb}</i>	119
4.5.3 Mycobacterial Genes of Unknown Function	
4.5.3.1 <i>esat-6</i>	120
4.5.3.2 <i>PPE</i> (Rv3018c)	120
4.5.4 Interplay of Mycobacterial Genes	120
4.6 INTERPLAY OF HOST CYTOKINES AND MYCOBACTERIAL GENES	122
4.6.1 Stratification According to Passive and Active Transcription	122
4.7 SPATIAL ARRANGEMENT OF MYCOBACTERIAL mRNA	123
4.8 SUMMARY OF RESULTS	124
4.9 FUTURE OF THIS RESEARCH	126

4.1 STUDY SUBJECTS

It is likely that anti-tuberculosis drugs could influence not only the *M. tuberculosis* gene expression, but also the host immune response. Therefore the study population included patients with tuberculosis granuloma who had not received any previous treatment. These patients were children with lymph node enlargement. Patient L2, the only patient who had a history of previous tuberculosis and was also currently on therapy when the biopsy was carried out, was eventually included in the study group. The lymph node biopsy tissues used for analysis were obtained from patients between the ages of 3 and 13 years. It is possible that the lymphadenitis of patient L1 was detected relatively early since this patient was examined on a regular basis for a severe asthmatic medical condition. Patient L2 had a history of tuberculosis. It appears that this patient did not respond to previous anti-tuberculosis treatment and started the third course of chemotherapy seven months after completing the second course. The strong granulomatous response seen in patients L3, L5 and L6 could possibly be an indication of a more advanced phase of disease. For patient L6 this notion is supported by the partially disintegrated lymph node tissue, and patient L5 was, as mentioned previously, diagnosed with disseminated tuberculosis (pulmonary and abdominal TB). In the biopsy tissue of patient L4, who presented more non-caseating granulomas, no acid-fast bacilli were detected using the ZN staining technique. Cultivation of the tissue, however, yielded a positive BACTEC *M. tuberculosis* culture. This diagnostic culture technique is at present the most reliable and fastest culture system available, yet for this particular patient, a positive culture was only detected after four weeks. This data implies that a very low number of bacilli were present in the biopsy tissue, which explains both the ZN negative results since this technique will only be successful in detecting AFB present in large numbers (for example, 10 000 per ml in sputum), and the prolonged cultivation period (Allen and Mitchison, 1992; Heifets, 1997).

4.2 ANALYSIS OF TUBERCULOUS GRANULOMAS

The tuberculous granulomas display spatial arrangements involving host cells, cytokines and infecting bacilli. Granulomas are focal mononuclear infiltrations that appear in response to chronic inflammatory stimuli and are therefore a hallmark of mycobacterial infection (Dannenberg, 1991). It was suggested that in *M. tuberculosis* infection, granulomatous lesions form to surround and envelop infected cells within a wall of epithelioid macrophages to contain and prevent bacterial spread (Saunders *et al*, 1999). Granulomas are an essential component of a co-ordinated anti-mycobacterial defence because it is within these structures that T-cell-macrophage co-operation can

take place, allowing macrophages to display effective bactericidal activities (Dannenberg and Rook, 1994).

Previous studies have used various techniques to analyse the cytokine production in response to *M. tuberculosis* infection. However, most of these studies analysed the cytokine response using animal models or *in vitro* systems (Brozna *et al*, 1991; Flesch and Kaufmann, 1991; Juffermans *et al*, 2000; Song *et al*, 2000)). In this study, we employed the immunohistochemistry technique to analyse the cytokine response at the site of disease, that is, in tuberculous lymph node granulomas. It is generally accepted that type-1 cytokines (IFN- γ , TNF- α , IL-12) are expressed during the protective phase of *M. tuberculosis* infection (Modlin, 1994). A switch is then later made to the expression of type-2 cytokines (IL-4, IL-10) during the resolution phase to re-establish homeostasis once infection is under control (Modlin, 1994). The balance between the type-1 and type-2 cytokine responses in tuberculosis may in all probability influence mycobacterial growth, as well as the immunopathology of infection. The immune response to tuberculosis infection is an intricate and complex process, with many studies reporting conflicting results. At present, only a limited number of reports have examined the infection directly at the site of disease. Additionally, the information available concerning the cytokine expression in children with tuberculosis is extremely limited.

Analysing the metabolism of bacilli in their natural host environment is important for design of new drug targets and vaccines. In this study, we used the *in situ* hybridisation staining technique for the analysis of bacterial gene transcription in the lymph node granulomas. Demonstration of a particular mRNA by *in situ* hybridisation is a reflection of the rate of gene transcription (measured by *rpoB* transcription) and the metabolic state of the infecting bacilli in the restrictive granuloma (measured by the transcription of persistent factors). Thus, this technique allows the identification of factors required by the bacilli to adapt to the adverse granuloma environment.

Various studies have focussed on *M. tuberculosis* gene expression in the hope of elucidating which genes are essential for bacterial survival under different growth conditions (Li *et al*, 1998; Camacho *et al*, 1999; Rodriguez *et al*, 1999; Ravn *et al*, 1999). A number of reports have demonstrated that certain genes are upregulated under conditions of stress and oxygen deprivation (Wayne and Hayes, 1996; Ravn *et al*, 1999; Mariani *et al*, 2000). However, as most of these experiments have focussed on genes required for *in vitro* growth or in animal model systems, it was still unknown whether these genes are expressed *in vivo* in the human host. The credibility of the *in vitro* synthetic cultures, especially, is becoming increasingly more questionable. A number of studies have reported

that the nature of *M. tuberculosis* gene expression when analysed in artificial medium culture is proving to be erroneous (Segal and Bosch, 1956). Mariani and colleagues (2000) compared *M. tuberculosis* H37Rv gene-expression in synthetic medium and human macrophage with an interesting outcome. Of the *M. tuberculosis* genes analysed, only a few were found to be expressed in both environments, some genes were expressed only in the *in vitro* culture and others only inside the macrophage. Even synthetic *M. tuberculosis* cultures incubated at different conditions showed differential gene expression. Florczyk and colleagues (2001) identified mycobacterial proteins that were differentially expressed under standing and shaking conditions, thereby demonstrating that subtle differences in bacterial cultivation conditions may have important implications for the study of gene expression in mycobacteria.

Understanding the transcriptional activity of the bacilli within the tuberculous granuloma is still incomplete. We used the *in situ* hybridisation technique to identify mycobacterial mRNA within this restrictive environment. The advantage of using this technique is that it allows for the analysis of gene expression of the infecting bacilli in its natural host. This has become an important aspect in tuberculosis research since *in vitro* conditions do not mimic the human *in vivo* environment; the upregulation of genes *in vitro* may not reflect the regulation *in vivo*. Another advantage of this technique is that the morphology of the cells within the tissue sections is preserved, thus providing additional information concerning the site of gene expression within the tissue.

The rationale for the choice of genes was firstly to analyse *M. tuberculosis* specific sequences already known to be either involved in mycobacterial metabolism and were also key targets for anti-tuberculosis drugs, viz. *rpoB* and *katG*. *RpoB* expression, the encoded protein being an essential component of the RNA polymerase enzyme, was taken as an indication of transcriptional activity of the infecting bacilli (Sheperd *et al*, 1980). The expression of *katG* is a survival mechanism of the bacteria in response to reactive metabolites. The expression of certain potential persistence factors thought to contribute to the survival of bacilli in host cells under conditions of stress (*narX*, *icl*, *mbtB* and *rel_{Mtb}*) was also analysed. Finally, the mycobacterial genes analysed in this study also included two potential immunodominant antigens, viz. *esat-6* and *PPE Rv3018c*. The functions of these proteins have not been fully elucidated.

The immunohistochemistry and *in situ* hybridisation staining techniques allows for the localisation of host cytokines and *M. tuberculosis* mRNA in the lymph node granulomas, thereby enabling the identification of interactions between the host and pathogen within these tuberculous lesions.

4.3 HOST CYTOKINE ANALYSIS

4.3.1 Expression of Type 1 Cytokines in Granulomas

In this study, IFN- γ and TNF- α were detected in the lymph node granulomas of all six paediatric patients, including the treated patient. Our data confirms numerous other studies that reported an increase in IFN- γ and TNF- α production in tuberculosis patients (Ogawa *et al*, 1991; Lin *et al*, 1996; Taha *et al*, 1997; Fenhalls *et al*, 2000). Gamma-interferon in combination with TNF- α enhances the antimycobacterial activity of macrophages and is involved in granuloma formation (Sokal, 1975; Barnes *et al*, 1990; Kindler *et al*, 1989; Pearlman *et al*, 1993). Our data contrasts with the study of Aung and colleagues (2000) who reported an absence of TNF- α and IFN- γ in granulomatous lung lesions of adult tuberculosis patients.

Interleukin-12 was suggested to be a central initiator of the local Th1 response in tuberculosis, with a crucial role in stimulating IFN- γ production by T lymphocytes (Abbas *et al*, 1996; Zhang *et al*, 1994). Previous studies reported that active tuberculosis disease in adults was associated with increased IL-12 production that was generally associated with the cell mediated immunity response (Lin *et al*, 1996; Taha *et al*, 1997). In this study IL-12 was detected in the lymph node granulomas of all six patients. However, the number of IL-12 positive granulomas detected between the patients was inconsistent. In another primary tuberculosis study, Aubert-Pivert and colleagues (2000) observed an increase in IFN- γ and TNF- α production, as well as a reduced expression of IL-12 in active tuberculosis patients. Additionally, mice with disruption of IL-12 cytokine signaling were unable to restrict the growth of *M. tuberculosis* and succumbed to infection (Cooper *et al*, 1997). In humans, deficiencies of the IL-12 receptor were reported to be associated with a predisposition to mycobacterial infection (Altare *et al*, 1998). It was suggested that this cytokine might provide a crucial link between the two cell populations of protective immunity, i.e. mononuclear phagocytes and T lymphocytes (Cooper *et al*, 1995). Therefore, depressed IL-12 production as seen in certain granulomas, could lead to inhibition of macrophage activation, and therefore might be involved in the immunopathogenesis of human active tuberculosis.

4.3.2 Expression of Type 2 Cytokines in Granulomas

Although elevated levels of type-1 cytokines IFN- γ and TNF- α were present in the lymph node granulomas, an overall Th0 cytokine pattern was predominant at this site of infection. Only a limited number of granulomas had an overall Th1 phenotype. The Th0 pattern was the result of elevated levels of type-2 cytokines present in the granulomas, particularly IL-4. This result is consistent with prior reports demonstrating heterogeneity in the pattern of cytokines produced in

response to *M. tuberculosis* (Bergeron *et al*, 1997; Somoskövi *et al*, 1999; Fenhalls *et al*, 2000; Aubert-Pivert *et al*, 2000). Although in our study, much higher levels of IL-4 were detected in the children lymph node granulomas. This data goes against the dogma of type-1 / type-2 cytokine expression where it is believed that type-1 cytokines are expressed during the protective phase, and a switch is later made to the expression of type-2 cytokines during the resolution phase once the infection is under control. Instead of being in a complete protective type-1 phase, or conversely, in a complete type-2 resolution phase, there appears to be a balance in the immune response to *M. tuberculosis* infection. Interestingly, this balance is maintained during the early phase of treatment with anti-tuberculosis drugs.

It is generally accepted that a type-2 cytokine expression relates to unfavourable disease outcomes. Although, it is still unclear whether this association is a cause or consequence of disease, since the functional role for type-2 cytokines in tuberculosis remains speculative. It is possible that high levels of IL-4 and IL-10 are associated with a lower level of resistance to *M. tuberculosis*. The overproduction of the immunosuppressive cytokine IL-10 could reduce the expression of IL-12 and inhibit macrophage activation, thereby limiting the development of a protective Th1 response (Aubert-Pivert *et al*, 2000). Van Crevel and colleagues (2000) investigated the production of IL-4 in patients with tuberculosis in relation to disease severity. Their findings suggested that the type-2 response with increased production in IL-4 might antagonize host defense and lead to tissue necrosis. In an *in vitro* study Hernandez-Pando and colleagues (1994) reported that TNF- α mediated necrosis occurred only in the presence of a mixed Th0 response. In contrast, a Th1 response at the inflammatory site prevented TNF- α mediated damage, whereas a Th2 response promoted tissue damage.

Alternatively, the purpose of type-2 cytokine expression could be to minimize local tissue damage by downregulating production of Th1 cytokines. One possible mechanism of reducing an excessive Th1 response would be to inhibit the production of IL-12 (D'Andrea *et al*, 1993). It has been hypothesised that an excessively high localised production of TNF- α may be responsible for tissue necrosis (Law, 1996). Caseous necrosis results from the killing of macrophages as a result of the tissue damaging delayed-type hypersensitivity response (DTH). Jacobs and colleagues (2000) reported an enhanced DTH response in the absence of IL-10. Also, in a study that analysed the cytokine pattern in tuberculous lung granulomas of haemoptysis patients, a predominant Th1 response was observed (Fenhalls *et al*, 2000). Fenhalls and colleagues reported that a distinction in disease progress could not be established between the haemoptysis patients who presented with a clear Th1 cytokine pattern, to those who also presented with a Th0 pattern of cytokine expression.

This study thus questions the concept of IL-4 expression in tuberculosis patients being indicative of an unfavourable disease outcome. We suggest that the presence of IL-4 might be an integral feature in containing tissue destruction. Therefore, type 2 cytokines might play a vital role in controlling an excessive Th1 response that might otherwise have lead to extensive tissue-damage. It is possible that the excessive levels of type-2 cytokines, particularly IL-4, detected in the lymph node tissue of the six children in this study could be an important element in the rationale as to why cavitation rarely occurs in paediatric tuberculosis. It could help clarify why children with tuberculosis cure spontaneously.

4.3.3 Interplay between Host Cytokines

Comparison of the cytokine patterns enabled us to identify correlations in expression between specific cytokines. The stratification of the granulomas into IL-4 negative and IL-4 positive subgroups allowed for the cytokine expression profiles to be statistically evaluated. Previous studies have shown that IL-4 induces a type-2 response, which includes the production of IL-10 (Swain *et al*, 1988; Kopf *et al*, 1993). It was therefore not surprising to find a significant correlation in the expression of IL-4 and IL-10 ($p = 0.0000006$). IL-10 only occurred in IL-4 positive granulomas. There were no correlations observed between IL4 and any of the type-1 cytokines, since the expression of IFN- γ , TNF- α and IL-12 occurred proportionally in both IL-4 positive and negative granulomas.

The co-ordinated expression pattern observed between IL-10 and IL-12 was however statistically significant ($p = 0.021$). Lin and colleagues (1996) previously reported the production of both IL-12 and IL-10 in lymph node tissue from tuberculosis patients. These investigators found that macrophages rather than Th2 cells produced IL-10. This anti-inflammatory cytokine has a regulatory affect on IL-12, and hereby the type-1 response on a whole (Hseih *et al*, 1993; Fulton *et al*, 1998). D'Andrea and colleagues (1993) showed that IL-10 inhibits lymphocyte IFN- γ production by suppressing IL-12 synthesis in accessory cells. It is possible that IL-10 expression attenuates the type-1 cytokine response, limiting tissue damage (Barnes *et al*, 1990).

Stratification of granulomas also allowed the identification of the significant association between IL-10 and TNF- α ($p = 0.0054$). Interestingly, a correlation was identified between both these cytokines and the presence of caseous necrosis. The majority of the necrotic granulomas stained positive for IL-10 ($p = 0.000046$), a cytokine that had been previously implicated with tissue damage. The exact role of IL-10 in the development of necrosis is still unclear, although numerous

contrasting hypotheses exist about this enigmatic cytokine (Lin *et al*, 1996; Brown *et al*, 2000; Fortsch *et al*, 2000). As with IL-12, it could be argued that the expression of IL-10 prevents an intense, and potentially destructive type-1 response (Barnes *et al*, 1990), thereby preventing further necrosis. Conversely, one could also speculate that IL-10 is in fact, detrimental to the host by augmenting or initiating tissue damage. Hernandez-Pando and colleagues (1994) showed that TNF- α mediated tissue damage only occurred in the presence of type-2 cytokines, including IL-10. The association was also demonstrated between the expression of TNF- α and the presence of caseous necrosis ($p = 0.0041$). Previous studies have also implicated this inflammatory cytokine as an important factor in the development of tissue damage (Barnes *et al*, 1990; Law, 1996).

4.4 *M. TUBERCULOSIS DETECTION IN HOST TISSUE*

The DNA:DNA *in situ* hybridisation technique was used to identify mycobacterial DNA within the restrictive granuloma environment. In this study, mycobacterial DNA was detected in the lymph node biopsy tissue of all six patients. Acid-fast bacilli were detected by ZN staining in only five of the six biopsy specimens, however, since the ZN-negative tissue (L4) yielded a positive BACTEC *M. tuberculosis* culture, it indicated that the hybridisation signal observed was due to bacilli present in the tissue and was not an artefact of methodology. The reproducibility of the *in situ* staining further confirms the validity of the technique. Although this observation was seen in only one patient, it is possible that DNA:DNA *in situ* hybridisation is detecting cell wall deficient forms of *M. tuberculosis* that cannot be ZN stained. The absence of acid-fast bacilli could suggest that these latent bacilli have entered an altered state in which they are no longer acid-fast (Gillespie *et al*, 1986). Alternatively, one could assume that the bacilli remained acid-fast, but were in such low numbers that they were undetectable when using a technique with poor sensitivity such as ZN staining (Heifets, 1997). Both possible rationales suggest that DNA:DNA *in situ* hybridisation is more sensitive than ZN staining for the detection of *M. tuberculosis* in tissue specimens and therefore in future could be an important adjunct in the diagnosis of tuberculosis.

Mycobacterial DNA was detected in ninety-five of the one hundred and seven granulomas identified. The hybridisation signal for the DNA probe was detected in every necrotic granuloma, but absent in twelve of the non-caseating granulomas. It is possible that, in these granulomas, the bacilli was present in such low numbers in the early stage of infection that the *in situ* hybridisation technique, although seemingly more sensitive than the standard ZN staining, was not quite sensitive enough to detect this very low number of bacilli. Alternatively, one could assume that the negative

granulomas are “healed” environments where the bacilli were successfully eliminated by the host immune response. Another possibility could be the result of the intense cytokine milieu observed in all the tissue specimens which caused a cascade event that resulted in granuloma formation in a “bacilli-free” lymph node region.

4.5 *M. TUBERCULOSIS* GENE EXPRESSION ANALYSIS IN THE GRANULOMA

The presence of mycobacterial DNA can be interpreted as either viable bacilli or microbial debris. RNA:RNA *in situ* hybridisation was done, using various antisense riboprobes, to identify transcriptionally active mycobacteria in the lymph node granulomas. Hybridisation signals using the various riboprobes only localised to granulomas associated with mycobacterial DNA. It is generally believed that each granuloma in any given organ represents a unique environment (Dannenberg, 1994). Therefore, the varying conditions in the granulomas would influence the mycobacterial gene expression differently. The data obtained in this study supports this concept.

4.5.1 Metabolic Factors: Important Factors for Current TB Therapy

4.5.1.2 RpoB

An antisense RNA probe was developed to identify bacilli actively expressing the *rpoB* gene as a measure of active growth (Sheperd *et al*, 1980), since this gene encodes RNA polymerase β subunit and is required for gene transcription. The results of the *in situ* hybridisation demonstrated the spatial location of the bacilli in the granuloma as well as differentially identifying bacilli actively expressing *rpoB*.

In this study, *rpoB* mRNA was detected in only five of the six patients with established tuberculosis. In contrast, messenger RNA for *rpoB* was not detected in any of the lymph node granulomas of patient L2, who had been treated with rifampin two days prior the biopsy. The absence of signal in the granulomas of this patient, as well as in the negative (*rpoB*) granulomas in the five untreated patients, could be attributed to very low levels of *rpoB* mRNA in those microenvironments. Since the RNA polymerase β subunit is essential for *M. tuberculosis* transcription, the presence of this protein cannot be excluded, as inhibition of transcription will certainly be bacteriocidal. It is thus possible that the levels of *rpoB* mRNA was below the detection level of the *in situ* hybridisation technique. Interestingly, the two groups of patients (treated and untreated) represent different scenarios; the cause for the reduction of *rpoB* expression in these

patient groups might therefore differ. The downregulation of *rpoB* transcription in the untreated patients could be the bacterial response to the onslaught of the host immune response which could have affected the bacterial growth phase. This notion is supported by a comparative study where Mariani and colleagues (2000) detected a change in the *M. tuberculosis rpoB* gene expression between the infected, non-activated macrophages and those macrophages activated with IFN- γ and LPS. In contrast, in the treated patient (L2), it is possible that combination of host environment and anti-tuberculosis drugs has affected the transcriptional activity of the bacilli. Therefore, the reduction in *rpoB* transcription observed in the granulomas of patient L2 could be a survival response mechanism to the rifampin, where the bacilli downregulated the expression of the target protein. Alternatively, since the transcription of survival genes occurred in these *rpoB* negative granulomas, we may assume that stable forms of the RpoB protein are present and, therefore, the bacilli does not need to transcribe it very often.

Significantly, no *rpoB* expression was detected within the necrotic regions of the positive granulomas, but only occurred in macrophages at the central region and periphery of non-necrotic, and only in the periphery of granulomas containing caseous necrosis. The necrotic regions are presumably very restrictive in nutrients and oxygen, and would therefore have a suppressing effect on the *M. tuberculosis* growth phase and therefore gene expression, more so for the gene involved in active growth transcription. Hu and colleagues (1998) reported that the conditions in the microaerophilic environments had a suppressing effect on bacterial gene expression. Therefore, the fact that *rpoB* mRNA was found in macrophages in the periphery and not within the necrosis could suggest that the bacillus is more transcriptionally active in the macrophages than in other, more restrictive areas of the granuloma.

4.5.1.3 *katG*

The results of the *in situ* hybridisation using the *rpoB* riboprobe provided evidence that this technique could be used to identify genes required for survival within the hostile environment of the human granuloma. The *katG* hybridisation signals, as with *rpoB*, were only detected in the granulomas of the five untreated patients, with patient L2 again being the exception. This suggests that the absence of *katG* signal in the treated patient L2 could be attributed to, as with *rpoB*, the combination of the onslaught of the host response and the anti-tuberculosis drugs. This patient was also treated with isoniazid, a pro-drug that requires oxidative activation of the catalase peroxidase enzyme before exerting a lethal effect. It can therefore be assumed that, as a response to anti-tuberculosis treatment, the bacilli downregulated the *katG* expression to levels too low to be

detected using the *in situ* hybridisation technique. However, unlike *rpoB* protein, the catalase peroxidase enzyme is not essential for survival. It was also suggested that other proteins, such as the AhpC protein, confers protection against hydrogen peroxide mediated damage even in the absence of adequate catalase and peroxidase activities (Sherman *et al*, 1996).

There is a clear variability in expression for *katG* in the untreated patients. In patients L1, L6 and especially L5, the number of *katG* positive granulomas was elevated. It seems that the host immune response did not have much of an inhibiting effect on the transcription of this gene in the granulomas of these three patients. In a comparative gene expression analysis between non-activated and IFN- γ -LPS activated macrophages, *katG* was one of the few genes that was expressed in both these environments (Mariani *et al*, 2000). It does however appear that the host response in patient L3 and L4 was more successful in limiting *katG* expression. Unlike the three former patients, patients L3 and L4 presented fewer *katG* positive granulomas. One could speculate that the low levels of *katG* detected in these patients could be correlated to the specific *M. tuberculosis* strain infecting these patients. The IS6110 typing of the *M. tuberculosis* clinical isolates revealed that these strains were all genotypically unrelated. The objective of DNA fingerprinting the isolates was to show that there are different strains involved that may have different expression profiles. We therefore cannot exclude the possibility that these clinical strains exhibit different levels of *katG* expression. The reduction in catalase peroxidase activity would not necessarily affect the virulence of the infecting strain (Jackett *et al*, 1978a; O'Brien *et al*, 1991). It was reported that low levels of *katG* transcription in certain *M. tuberculosis* strains was compensated by an upregulation of the alkyl hydroperoxide reductase (AhpC) protein, encoded by the *ahpC* gene (Heym *et al*, 1999), which was shown to also mediate resistance to oxidative metabolites. Therefore, *M. tuberculosis* strains with loss of KatG activity could still cause disease.

The *katG* hybridisation signals detected in the granulomas of the untreated patients were detected in the central region and periphery of the non-necrotic granulomas. Also, mRNA for this gene was associated with the necrotic regions of the granulomas. This confirms that these bacilli are indeed viable cells, and not bacterial debris. It also illustrates that these bacteria are able to adapt to the onslaught of reactive oxygen and nitrogen metabolites within the different microenvironments of a granuloma.

4.5.3 Persistence Factors

Numerous studies that have identified genes that are required for persistent tuberculosis infection. These genes may be ideal targets for new drugs against *M. tuberculosis*, since the current anti-tuberculosis drugs are effective only against actively replicating cells.

To understand how certain genes could influence growth, four genes encoding potential persistent factors *narX*, *icl*, *mbtB* and *rel_{Mtb}*, were analysed in the lymph node granulomas. Messenger RNA for all these genes were detected in the six patients, including the treated patient, L2. Unlike the metabolic factors *rpoB* and *katG*, there was no distinction in the expression of these genes between the untreated patients and treated patients with variability in *M. tuberculosis* gene expression observed in the different granulomas of each individual patient.

4.5.2.2 *narX*

The *narX* gene product, a transmembrane protein, has been associated with nitrate reduction during anaerobiosis (Cole *et al*, 1998). In all six patients, *narX* was found to be associated mostly with necrotic granulomas. A significant association was observed between *narX* and the presence of necrosis ($p = 0.0062$), which suggests that the necrotic granulomas are depleted of oxygen and would thus induce the bacteria to adapt by expressing components needed to survive anaerobiosis.

Bacilli expressing *narX* were detected at the periphery and within the necrotic region of the granuloma. The necrotic microenvironment of the granuloma is assumed to be more restrictive, especially regarding oxygen availability. However, the expression of *narX* in the periphery of the granuloma suggests that the bacilli residing in the non-necrotic regions of the granulomas are also experiencing oxygen deprivation. The expression of this gene was reported to be associated with adaptation to the persistent state of the bacilli; one can assume that those granulomas positive and negative for *narX* could be correlated to different growth phases (Hutter and Dick, 2000).

An alternative explanation could be that *narX* is not mandatory for anaerobic respiration. The *M. tuberculosis* genome project revealed the presence of a number of genes, the products of which might be involved in anaerobic respiration and fermentation (Cole *et al*, 1998). Bacteria are able to distinguish the environment in which their replication occurs, and would therefore respond differently in terms of gene expression. Since *narX* expression in mycobacteria has to date only been analysed using *in vitro* systems, it is possible that several other factors might be involved in anaerobiosis adaptation in the human host, and were overlooked using these *in vitro* models. In an

in vitro comparative expression analysis of 23 candidate anaerobic respiratory genes, *narX* was surprisingly the only gene to be upregulated in the anaerobic cultures (Hutter and Dick, 2000). Therefore, it is highly probable that *narX* might not be the ideal solitary marker for monitoring the persistence response in tissue, as was suggested by Hutter and Dick (2000).

4.5.2.3 *icl*

Isocitrate lyase (ICL), an essential enzyme for catabolism of fatty acids, was reported to be required for persistence of the tubercle bacilli during the chronic phase of infection in mice (McKinney *et al*, 2000).

Hybridisation signals for *icl*, as with *narX*, were mostly associated with necrotic granulomas, and were also detected within the caseous necrosis. The necrotic environment is likely to be lipid rich and mycobacteria are well endowed with suitable enzymes for utilizing lipids as a sole carbon source (Cole *et al*, 1998). Therefore, it is likely that lipid metabolism plays an essential role in maintaining mycobacterial viability in the absence of robust growth.

It has been speculated that *icl* expression is induced during the initial phase of infection in response to the immune response, but is then downregulated during the subsequent phase of infection. McKinney and colleagues (2000) also reported that *icl* was dispensable for bacterial growth in the acute phase of infection, but was more important for survival of *M. tuberculosis* in the lungs of mice during the persistent phase. Therefore, the absence of signal in the negative granulomas, especially the non-necrotic granulomas, could be the result of the specific phase of infection. Alternatively, it could be a response to the host environment prior to the immune response. However, the number of *icl* positive granulomas was generally low, with the exception of patient L5, when compared to the expression using the mouse model. The difference between *icl* expression in the human host and animal model systems could be the result of the plasticity of *M. tuberculosis* in sensing the environment (including the host immune response) and consequently adapting different survival strategies.

4.5.2.4 *mbtB*

Many pathogenic bacteria secrete iron-chelating siderophores, mycobactins, in the iron-limiting environments of their vertebrate hosts. Iron is thought to be an essential metal for various bacterial metabolic processes, including growth. *MbtB* transcripts, unlike the other persistent factors

analysed, were not detected within the necrotic region, and was limited to the less restrictive periphery and lymphocyte cuff region of the granulomas. The importance of iron for bacterial metabolism has been demonstrated using an $\Delta mbtB$ mutant defective for synthesis of high affinity siderophores (De Voss *et al*, 2000). These mutant strains were unable to replicate in cultured macrophages. The absence of *mbtB* signal in the granulomas, could be the result of a very low *mbtB* transcription rate which could be an indication of a slow bacillary growth phase in these microenvironments. Alternatively, one could speculate that the negative *mbtB* granulomas are iron-rich environments, which would result in repressed *mbtB* expression. This notion is supported by Gold and colleagues (2001) who showed that mRNA levels of *mbtB* were induced in *M. tuberculosis* cultures starved of iron, but was repressed in iron-rich environment. The transcription of *mbtB* is controlled by IdeR regulator protein that acts as a transcriptional repressor of *mbtB*.

4.5.2.5 *rel_{Mtb}*

Nutrient deprivation, in the form of amino acid and carbohydrate depletion, is likely to coincide with the formation of intact granulomas in a process thought to be essential for curtailing growth of the microorganism (Cunningham and Spreadbury, 1998). Bacteria adapt to nutritional stress for their survival, predominantly through a mechanism termed the stringent response, the hallmark of which is the accumulation of ppGpp (Bremer and Ehrenberg, 1995), also called the stringent factor. *Rel_{Mtb}* ppGpp synthase, encoded by the *rel_{Mtb}* gene, is therefore an essential enzyme in the stringent response.

Rel_{Mtb} mRNA localised in the granuloma periphery and lymphocyte cuff region. Hybridisation signal was also associated with the nutrient restrictive, necrotic region of the granulomas. This environment is assumingly more restrictive in nutrients than the rest of the granuloma and the presence of *rel_{Mtb}* in the necrosis therefore suggests that the bacilli are capable of adapting to the nutrient deprivation. It is possible that the granulomas not staining positive for *rel_{Mtb}* could be negative as a result of very low levels of mRNA transcripts. This reduction of *rel_{Mtb}* expression could be a result of the host environment, i.e. the conditions experienced by bacilli in those particular granulomas have a repressing effect on *rel_{Mtb}* expression.

4.5.4 Mycobacterial Genes of Unknown Function

4.5.4.1 *esat-6*

The ESAT-6 antigen has attracted considerable interest in recent years, as it is recognized early during infection. The function of this protein, however, remains to be elucidated. Similarly to the persistent factors, variability in *esat-6* expression was observed in the lymph node granulomas. Hybridisation signal for this gene was detected in only four of the six patients, including the treated patient (L2). Given that expression of this gene is associated with early infection, the absence of *esat-6* mRNA in the two untreated patients suggest that these granulomas are in an advanced phase of infection. Conversely, the majority of granulomas for patient L1 stained positive for *esat-6* could be indicative of an early infection. Alternatively, the inconsistency in the expression of *esat-6* observed between the individual patients could be correlated to the genotypically unrelated infecting strains. It is possible that the *M. tuberculosis* clinical isolates of patients L4 and L5 simply did not express this protein at all.

The hybridisation signal for *esat-6*, in the four patients, was never detected within the necrotic region of the granulomas. This suggests that *esat-6* is not essential for survival in the restrictive necrotic microenvironment, and therefore not required for persistence.

4.5.4.2 PPE (Rv3018c)

The functions of PPE proteins have not yet been established, although numerous hypotheses exist. The PPE gene Rv3018c was suggested to attribute to bacterial survival in the host macrophage (Camacho *et al*, 1999). Variability in the expression of this gene was also observed in the six patients, and was one of the genes transcribed in the necrotic regions of granulomas. This suggests that the encoded PPE protein might be required for survival in the restrictive necrotic microenvironments, thereby implicating the gene as a potential persistence factor.

4.5.5 Interplay of Mycobacterial Genes

To investigate the interplay between the host environment and the expression of *M. tuberculosis* genes, the granulomas were stratified and submitted for statistical assessment.

In this study no significant correlation could be demonstrated between *rpoB* expression and any other mycobacterial gene. A number of significant correlations were observed with the stratification of granulomas according to *katG* expression. Firstly, *katG* and *icl* were found to be co-expressed in

most of the granulomas ($p = 0.008$). One could speculate that the activated macrophage environment in these granulomas, not only induced *katG* expression, but also the glyoxylate shunt pathway. The expression of *katG* in response to the host onslaught of reactive oxygen and nitrogen species also coincides with the expression of *rel_{Mtb}*, an essential component in generating the stringent response ($p = 0.0106$). A significant correlation was also observed between *katG* and *PPE* RV3018c ($p = 0.008$). It is unclear whether the production of reactive species induced the expression of *PPE*, as it most probably did *katG*, or if any coinciding environment factor(s) induced the expression of this gene.

A significant co-expression correlation was observed between *icl* and *narX* ($p = 0.00003$). This suggests that the depletion of oxygen, indicated by the expression of *narX*, coincides with lipid metabolism in the bacilli, as indicated by the expression of the glyoxylate shunt enzyme *icl*. This confirms the previous study by Wayne and Lin (1982) who noted that glyoxylate shunt enzymes were activated during the metabolic downshift that accompanies oxygen withdrawal. Lipid metabolism in granulomas also coincided with the production of ppGpp, the stringent factor. This is indicated by the significant co-expression correlation observed between *icl* and *rel_{Mtb}* ($p = 0.00003$). It is possible that the stringent response could have induced *icl* expression as part of the bacteria's survival strategy to adapt to nutrient restrictive conditions. One can thus assume that co-ordinated expression of *katG*, *rel_{Mtb}* and *icl* occurred. However, there was no correlation identified in the expression between *katG*, *rel_{Mtb}* and *narX*. We suggest that the varying condition in the individual, unique granulomas lead to subpopulations of bacilli, i.e. the various phases of bacillary growth observed was induced by the environment. The subpopulations of bacilli observed in the granulomas either exhibited a co-ordinated expression pattern of the *katG*, *rel_{Mtb}* and *icl* genes, or alternatively, a co-ordinated expression pattern between *icl* and *narX*.

Icl was also found to have an opposite expression pattern to that of *esat-6* ($p = 0.043$). This suggests that these genes were expressed at different stages of infection. The *esat-6* antigen is apparently expressed primarily during the early phase of infection, whereas *icl* was reported to be required only during the chronic phase of infection.

Esat-6 expression also occurred inversely to that of *mbtB* ($p = 0.026$). This also suggests that these mycobacterial genes are required at different phases of infection. It could be that iron-chelators are required in a later stage of infection when this metal becomes limited.

4.8 INTERPLAY OF HOST CYTOKINES AND MYCOBACTERIAL GENES

In order to determine if any correlations existed between the host response and mycobacterial gene expression the host cytokine data was stratified together with the mycobacterial gene expression data. The knowledge on how the cytokine and mycobacterial gene expression affect each other is very limited. Cappelli and colleagues (2001) found that the activation of macrophages resulted in the upregulation of some mycobacterial genes, and the downregulation of others. However, different results were obtained with the use of different *M. tuberculosis* strains.

In this study we observed a significant association between a Th0 cytokine profile and the expression of *mbtB* ($p = 0.0012$). It is possible that the simultaneous expression of the type 1 and type 2 cytokines could have resulted in the reduction in iron availability. This association was the result of the co-ordinated expression between IL-4 and *mbtB* ($p = 0.005$). Therefore, one could argue that the IL-4 cytokine induced environments lead to the expression of the mycobactin biosynthetic enzyme.

As previously discussed, the bacteria adapts to the adverse host conditions by the stimulation of the stringent response, which results in the production of ppGpp by the *rel_{Mtb}* protein. An opposite expression pattern was detected between *rel_{Mtb}* and IL-12 ($p = 0.0037$). This suggests that the expression of IL-12 results in a more favourable host environment for the infecting bacilli. Conversely, a significant correlation was observed between IL-12 and *esat-6* ($p = 0.043$). This type 1 inducing cytokine and the mycobacterial antigen-encoding gene are presumably both expressed primarily during the early phase of infection.

4.8.1 Stratification According to Passive and Active Transcription

The granulomas were firstly stratified according to transcriptional activity based on the presence or absence of *rpoB* in the granulomas, which was followed by subsequent stratification according to the absence or presence of host cytokines. This was performed in order to assess whether the different transcriptional activity of the bacilli, and presumably the different growth phase, resulted in different correlations between the mycobacterial genes and host cytokines.

As with the single stratification analysis, a significant correlation was identified in the passively transcribing granulomas between *mbtB* and an overall Th0 cytokine profile ($p = 0.020$) and was therefore also detected in expression between IL-4 and *mbtB* ($p = 0.020$). It would appear that the

expression of both type 1 and type 2 cytokines only affected the transcription of *mbtB* in the passively transcribing bacteria.

Unlike IL-4 and *mbtB*, an opposite expression correlation was observed between IL-12 and *rel_{Mtb}*. Furthermore, this trend was observed in both the *rpoB* negative ($p = 0.05$) and *rpoB* positive ($p = 0.021$) granulomas. Therefore, this correlation occurred irrespective of the transcriptional activity, and presumably the growth phase of the bacilli.

In the actively transcribing granuloma subgroup, the *katG* expression was associated with an overall Th0 cytokine profile ($p = 0.049$), and more specifically with IL-4 expression ($p = 0.049$). It would appear that IL-4 expression contributed to the expression of *katG* only in the actively transcribing bacilli.

An interesting correlation observed in the *rpoB* positive granulomas was that between IL-10 and *narX* ($p = 0.026$). This cytokine and mycobacterial gene was co-expressed in most granulomas, but what makes this correlation interesting is the fact that both IL-10 and *narX* displayed an association with caseous necrosis, and were expressed predominantly in necrotic granulomas.

Another unique correlation observed in the *rpoB* positive granulomas was the opposite expression pattern between IL-12 and *mbtB* ($p = 0.035$). Granulomas positive for IL-12 were apparently less restricted in iron, hence the downregulation of *mbtB*, which is required for the synthesis of mycobactins, the iron-scavengers. A correlation observed with the single stratification and also detected in the *rpoB* positive granulomas, was the co-expression pattern between IL-12 and *esat-6*. This suggests that these granulomas are at the initial stages of infection, since this cytokine and mycobacterial gene are presumably expressed predominantly in the early phase of infection, and also the fact that these are actively transcribing bacilli.

4.9 SPATIAL ARRANGEMENT OF MYCOBACTERIAL mRNA

Dannenberg and colleagues (1994) suggested that the development of tuberculosis disease from its onset to its various clinical manifestations be pictured as a series of battles between host and invader. They suggested that in any given organ, each tuberculous granuloma is independent, i.e. each granuloma (or even parts of larger granulomas) may be engaged in any battle in this series, regardless of which battle the other tuberculous granulomas (or parts) are engaged in. The spatial

regardless of which battle the other tuberculous granulomas (or parts) are engaged in. The spatial arrangement of mRNA transcripts for the various genes observed in this study confirms the hypothesis that different microenvironments exist within a single granuloma. In the analysis of signal localization, detailed spatial arrangement of the various gene transcripts in relation to one another in the granulomas was not done. However, generally, variations in the signal pattern of the riboprobes in the granulomas were observed. Figure 4.1 is a schematic illustration of the variation of signaling patterns observed in the granulomas. The expression, or rather, the grouped expression of certain genes did not always occur in the same regions of the granulomas.

Future prospects would therefore include a more detailed analysis of the spatial arrangement of the various genes in the granulomas, and implementing a more sensitive means of scoring the hybridisation signals that would hopefully allow us to measure the varying staining intensities for the individual genes. This then could be correlated to the spatial arrangement of RNA transcripts in the granulomas.

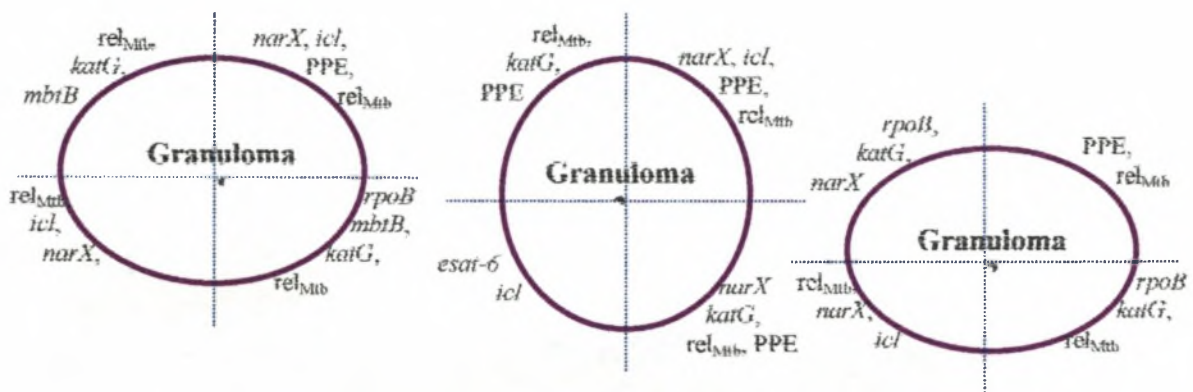


Figure 4.1. Schematic Diagram Illustrating Spatial Arrangements of *M. tuberculosis* Gene Expression in the Lymph Node Granulomas

4.3 SUMMARY OF RESULTS OF THE PRESENT STUDY

Comparing the cytokine profiles for the six patients, we observed a predominant Th0 response in the lymph node granulomas. This implies that there is a balance between type 1 and type 2 cytokines, and therefore goes against the dogma of a type 1 response during the initial protective phase and a type 2 response during the resolution phase. This balance was maintained during the initial phase of treatment (2 days).

Stratification of the cytokine data allowed us to identify various statistically significant associations between the host cytokines. A co-ordinated expression correlation was observed between IL-4 and IL-10 ($p = 0.0000006$), IL-10 and IL-12 ($p = 0.021$) and between IL-10 and TNF- α ($p = 0.0054$). The latter enzymes, viz. IL-10 and TNF- α , were also significantly associated with the presence of caseous necrosis in the granulomas ($p = 0.000046$ and $p = 0.0041$, respectively).

In our study, mycobacterial DNA was detected in 6 patients using *in situ* hybridisation. In contrast, only 5 of the 6 patients were positive for acid-fast bacilli using standard ZN staining. Although this observation was seen in only one patient, it is possible that DNA:DNA *in situ* hybridisation is more sensitive than the ZN staining for the detection of *M. tuberculosis* in tissue sections.

The analysis of mycobacterial gene expression in the lymph node granulomas of the treated patient allowed us to observe a rapid response of bacilli to the anti-tuberculosis drugs, received over a period of only two days. Interestingly, the drug targets of rifampin and isoniazid, i.e. the gene products of *rpoB* and *katG*, respectively, were drastically downregulated to, presumably, elude the lethal effects of these drugs.

The presence of mRNA transcripts of certain genes within the necrosis confirms that the mycobacterial DNA detected in the necrosis is not just bacterial debris, but transcriptionally active cells. It also illustrates that these bacilli are adapting to the anoxic, acidic and nutrient restrictive necrotic microenvironment. However, the absence of *rpoB* mRNA, as well as *mbtB* mRNA in these regions suggests that these bacilli are in a non-replicating phase, since the expression of *rpoB* is a measure of actively growing bacilli, and *mbtB* is involved in iron uptake, a metal required for bacterial growth. This suggests that the development of caseous necrosis was thus successful in inhibiting bacterial growth.

Statistical assessment of the mycobacterial gene expression data allowed co-ordinated expression correlations to be identified between *katG* and *icl* ($p = 0.008$), *katG* and *rel_{Mtb}* ($p = 0.0106$) and between *icl* and *rel_{Mtb}* ($p = 0.00003$). It appears that a co-ordinated expression pattern of these three mycobacterial genes occurred. A co-ordinated expression pattern was also identified between *katG* and *PPE Rv3018c* ($p = 0.008$) and between *icl* and *narX* ($p = 0.00003$). An inverse expression pattern was observed between *esat-6* and *icl* ($p = 0.043$) and between *esat-6* and *mbtB* ($p = 0.026$). A significant association was observed between the expression of *narX* and the presence of caseous necrosis ($p = 0.0062$). This mycobacterial gene was predominantly expressed in granulomas containing necrosis.

The stratification of *M. tuberculosis* gene expression data clearly illustrates the existence of subpopulations of bacilli in the individual granulomas. Specifically, the varying environments induced different phases of bacillary growth and transcriptional adjustment for survival. Furthermore, the spatial arrangement of mRNA transcripts for the various genes observed in this study confirms the hypothesis that different microenvironments, and therefore different subpopulations, exist within a single granuloma.

The stratification of the combined host cytokine and mycobacterial gene expression data revealed a significant association between a Th0 cytokine profile and the expression of *mbtB* ($p = 0.0021$), which was the result of the co-ordinated expression pattern between IL-4 and *mbtB* ($p = 0.005$). A co-ordinated expression correlation was also observed between IL-12 and *esat-6* ($p = 0.043$), and an inverse expression pattern between IL-12 and *rel_{Mtb}* ($p = 0.005$).

Stratifying the data according to mode of transcription (passive vs active), allowed us to identify a significant association between a Th0 cytokine profile and *mbtB* expression ($p = 0.020$), as well as between IL-4 and *mbtB* ($p = 0.020$) in the *rpoB* negative (passive transcription) subgroup. An inverse expression pattern was identified between IL-12 and *rel_{Mtb}* in both the *rpoB* negative ($p = 0.05$) and *rpoB* positive ($p = 0.021$) subgroups. In the *rpoB* positive granulomas, a significant expression pattern was identified between a Th0 cytokine profile and *katG* expression ($p = 0.049$), and a co-ordinated expression correlation between IL-4 and *katG* ($p = 0.049$). A co-ordinated expression pattern was also identified between IL-10 and *narX* ($p = 0.026$), and an inverse expression pattern between IL-12 and *mbtB* ($p = 0.035$).

4.9 THE FUTURE OF THIS RESEARCH

The immediate objective for this project is to recruit more patients. The study subjects would include untreated and treated patients, as well as a series of patients at various phases of treatment in order to analyse and compare the bacterial gene expression in response to the host immune response and chemotherapeutic agents. It will also be interesting to determine the influence of prolonged treatment on the Th1/Th2 balance.

The aim of DNA fingerprinting the isolated *M. tuberculosis* clinical strains was to determine whether a specific gene expression profile, and possibly also the host cytokine response could be correlated to a specific strain type. This was not possible with our limited sample size in which all

the isolates were genotypically unrelated. A larger sample size may provide insights into the relationship between genotype and phenotype.

Future prospects for this research would also include a more detailed analysis of the spatial arrangement of the various mycobacterial genes and host cytokines in the granulomas; also the implementation of a more sensitive means of scoring the signals that would allow the varying staining intensities for the individual genes and cytokines to be accurately quantitated. This then could be correlated to the spatial arrangement of both RNA transcripts and cytokines in the granulomas.

A primary goal in tuberculosis research is the identification and characterisation of *M. tuberculosis* genes thought to be potential candidates in the development of new anti-tuberculosis drugs and vaccines. The techniques used in this study could be used to analyse the expression of these novel genes in the host tissue. Therefore, this type of study has tremendous potential since it allows us to decipher factors controlling gene expression in the human granuloma.

APPENDIX I

BUFFERS AND SOLUTIONS

1.1 Standard Buffers and Solutions

1.1.1 10x Tri-EDTA (TE) Buffer (pH 8.0)

1.21 g Tris base

0.372 g EDTA

dH₂O to 1 l

1.1.2 50x Tris Acetate (TAE) Buffer (pH 8.0)

242 g Tris base

57.1 ml Glacial acetic acid

18.61 g EDTA

dH₂O to 1 l

1.1.3 10x Tris-Borate EDTA (TBE) Buffer (pH 8.0)

108 g Tris base

55 g Boric acid

9.3 g EDTA

dH₂O to 1 l

1.1.4 20x SSC

175 g NaCl

88.2 g Trisodium citrate

dH₂O to 1 l

1.1.5 10x Phosphate Buffered Saline (PBS)

80 g NaCl

2 g KCl

14.4 g Na₂HPO₄

2.4 g KH₂PO₄

dH₂O to 1 l

1.1.6 20x SSPE (pH 7.4)

876.5 g NaCl

138 g NaH₂PO₄

37 g EDTA

44 g NaOH

dH₂O to 5 l

1.1.7 depc dH₂O

100 µl depc to 1 l dH₂O

1.1.8 70% (depc) EtOH

70 ml Absolute EtOH

30 ml (depc) dH₂O

1.1.9 90% (depc) EtOH

90 ml Absolute EtOH

10 ml (depc) dH₂O

1.1.10 0.4 M NaOH

16 g NaOH

dH₂O to 1 l

1.1.11 3 M Na-Acetate (pH 5.5)

408.2 g NaAc-3 H₂O

Adjust pH with glacial acetic acid

dH₂O to 1 l

1.2 1 M Citrate Buffer (pH 6.0)

2.1 g Citrate Hydrate

Adjust pH with NaOH to 6.0

1.3 Chromic Acid

100 g K₂Cr₂O₇

250 ml H₂SO₄

dH₂O to 1 l

1.4 Sputagest

0.1 g DTT

0.78 g NaCl

0.02 g KCl

0.11 g Na₂HPO₄

0.02 g KH₂PO₄

dH₂O to 1 l

1.5 Fixative Solutions: 2x Formaldehyde Fixation Buffer / 4% Paraformaldehyde

72 ml 1 M NaH₂PO₄

28 ml 1 M NaH₂PO₄H₂O

4 g Paraformaldehyde

Adjust pH with 1 M NaOH

1.6 Solutions for preparation of competent *E. coli* cells:

1.6.1 TFB1

100 mM RbCl

50 mM MnCl₂.4H₂O

30 mM Potassium acetate

10 mM CaCl₂

15% glycerol

1.6.2 TFB2

100 mM MOPS, pH 7.0

100 mM RbCl

75 mM CaCl₂

15% glycerol

1.7 Liquid and solid media:

Media were autoclaved at 121°C for 20 minutes

1.7.1 Luria-Bertani (LB) medium

10 g Bacto tryptone

5 g Yeast extract

10 g NaCl

dH₂O to 1 l

1.7.2 LB-Ampicillin-agar plates

10 g Bacto tryptone

5 g Yeast extract

10 g NaCl

12 g Agar

dH₂O to 1 l

1 ml of 50 mg/ml Ampicillin added after autoclaving

1.8 Ampicillin

50 mg/ml in dH₂O, filtered and stored at -20°C

1.9 Buffers used in the ISH probe detection:

1.9.1 Buffer A

100 mM Tris-Cl pH 7.5

150 mM NaCl

1.9.2 Buffer B

100 mM Tris-Cl pH 9.5

50 mM MgCl₂

100 mM NaCl

1.10 Solutions used in the genomic DNA preparation:

1.10.1 Extraction Buffer

50 g Mono Sodium Glutamic Acid

6.06 g Tris base

9.3 g EDTA

1.10.2 Proteinase K Buffer

6.05 g Tris base

9.3 g EDTA

25 g SDS

dH₂O to 500 ml

1.10.3 Phenol / Chloroform

240 ml Chloroform

10 ml Isoamyl alcohol

250 g Phenol crystals

250 mg Hydroxyquinoline

1.11 Solutions used for DNA fingerprinting:

1.11.1 Primary Wash Buffer

720 g Urea

8 g SDS

25 ml 20x SSC

dH₂O to 2 l

1.11.2 Orientation Marker

2 µl Marker X (0.25 µg/µl)

2.5 µg Mtb DNA (H37Rv)

45 µl 0.8 M NaOH

TE to a final volume of 90 µl

1.12 Gel Electrophoresis Loading Dyes:

1.12.1 Bromophenol Blue

50 μ l Bromophenol Blue

3 ml Ficol

TE to a final volume of 20 ml

1.12.2 6x Loading Buffer

30% glycerol

0.25% w/v bromophenol blue

0.6% w/v SDS in TE (pH 8.0)

1.12.3 Loading Buffer with Marker X

6.6 μ l Molecular Weight Marker X (0.25 μ g/ μ l)

8 ml 2x Loading buffer

APPENDIX II**CONSENT FORM: ENGLISH**

Information sheet and consent form for persons participating in the research project: *In Situ Hybridisation Analysis of Mycobacteria tuberculosis Gene Expression and Identification of Host Immune Responses Induced by Various Infecting Strains.*

Project number: 94/107.

Your child has enlarged lymph glands. At the moment the cause of this enlargement is not known and for this reason your child needs to have a biopsy taken of the gland. The surgeon will explain to you exactly how this is done and will get permission for the surgery. One of the causes of big lymph glands in children can be tuberculosis (TB) which is a curable but an infectious disease. The first symptom of TB is usually coughing. TB is spread when a sick adult coughs thereby spreading tiny droplets containing TB germs from his/her lungs into the air. Any person who breathes in the air with these droplets can become infected. TB most often affects the lungs, but can cause big glands in children. We – a team of researchers from the University of Stellenbosch – want to find out the type of *Mycobacterium tuberculosis* strain infecting your child and the type of immune response that he/she exhibits. We would like to examine the lymph glands of children who have TB. We want to ask your permission to include your child in this research project. For our investigations, we would like to culture the infected lymph nodes, extract the bacteria and classify the infecting strains. The type of immune response induced by the infecting strain will also be determined. We also want to do a TB skin test and a chest x-ray. For getting the blood samples, a sterile needle will be used to draw 15 ml of blood (3 teaspoons). One of the tests we need to do is a test for HIV. If you agree to take part in the research project, you will receive counseling before and after the test. If there are signs in the blood that you should be seen by a specialist, we will make an appointment. If the HIV test should be positive we will counsel you and refer you and your child to the HIV-clinic, Department of Paediatrics and Child Health, Tygerberg Hospital. The TB skin test will be done with a small needle, whereby a little amount of fluid will be put into the skin and after 3 days we will read the skin test. The chest x-ray will be done before surgery. There is no danger involved in the taking of blood, doing the skin test or taking the chest radiograph. The only side effect may be a positive skin test, which may itch or ulcerate, but if this happens we will give you a steroid ointment to put on to relieve the itching. If you encounter any problems you can contact Dr Beyers at telephone number 9389114.

You are completely free to choose whether you will give permission for your child to be enrolled in this research project. Refusal to participate will not involve any penalty or change in the standard of medical attention in the hospital or clinic. We will use the blood- and lymph gland samples exclusively for tests on TB and will not do any other research with it. You or your child will not receive any financial reward for participating in this study. All personal information from this study is strictly confidential. The results from the study will be published in medical journals, but without mentioning the names of any person who donated samples.

Patient Details:

Name and Surname: **Date of Birth:**

Address:

I, the undersigned doctor/nursing sister hereby declare that I have informed the patient of the nature, purpose, risks and possible consequences of the research project in his/her own language. I will take full responsibility if the study results of this person need follow-up in terms of treatment and/or counselling

Signature of doctor/nursing sister: **Date:**

Signature of witness: **Date:**

I, the undersigned..... hereby give consent for the inclusion of my

(Name of person giving consent)

child..... in the above research project, in which his/her blood and biopsy

(Name of child)

samples may be used for tuberculosis research and the culturing of bacteria, and that information from his/her medical records may

be used for these research purposes, the nature of which has been explained by

(Name of doctor/nursing sister)

1. The nature of the project has been explained to me
2. I understand the implications of the research and the risks involved
3. The following procedures may be carried out as part of the project:
 - i. Drawing of 15 ml of blood (or 3 teaspoons) for HIV testing and immunological tests related to TB
 - ii. Tuberculin skin testing
 - iii. Chest radiograph
 - iv. Examination and culture of the lymph gland for TB related research.
4. I understand that I can withdraw my child at any stage from the project without influencing my or my child's medical treatment.
5. I understand that there will be no financial rewards

Signature of person giving consent: **Date:**

(i)	(ii).....
Signature of witness	Date	Signature of witness	Date

CONSENT FORM: AFRIKAANS

Informasie blad and toestemmings vorm vir persone wat deelneem in die navorsingsprojek: *In Situ Hybridisation Analysis of Mycobacteria tuberculosis Gene Expression and Identification of Host Immune Responses Induced by Various Infecting Strains.*

Projek nommer: 94/107.

Jou kind het vergrote limf kliere. Op die oomblik is die oorsaak van hierdie vergroting onbekend en vir hierdie rede is dit nodig om 'n biopsie van u kind se klier te neem. Die chirurg sal die prosedure presies aan u verduidelik en sal toestemming kry vir die operasie. Een van die oorsake van groot limf kliere in kinders is tuberkulose (TB) wat 'n aansteeklike maar geneesbare siekte is. Die eerste simptome van TB is gewoonlik hoë en TB word versprei wanneer 'n siek volwassene hoë en sodoende klein druppeltjies met TB kieme van sy / haar longe in die lug versprei. Enige persoon wat die lug met hierdie druppeltjies inasem kan geïnfecteer word. Gewoonlik affekteer TB die longe, maar kan vergrote kliere in kinders veroorsaak. Ons – 'n span navorsers van die Universiteit van Stellenbosch – probeer uitvind die tipe *Mycobacterium tuberculosis* ras wat jou kind infekteer, en die immuun respons hy / sy vertoon. Ons wil graag die limf kliere van kinders wat TB het ondersoek. Om hierdie rede vra ons u toestemming om u kind in hierdie navorsingsprojek in te sluit. Vir ons ondersoek wil ons die geïnfecteerde limf knope kweek, die bakterieë ekstraheer en die infekerende ras klassifiseer. Die tipe immuun respons wat die infekerende ras veroorsaak sal ook bepaal word. Ons wil ook 'n TB vel toets en 'n borskas X-straalfoto neem. Om die bloed te trek, sal 'n steriele naald gebruik word om 15 ml bloed te trek (3 teelepels). Een van die toetse wat ons sal doen is 'n toets vir HIV. Indien u toestem om deel te neem aan die navorsingsprojek, sal die suster vir u voorligting gee oor HIV voor en na die toets. Indien daar tekens in die bloed is dat u deur 'n spesialis gesien moet word, sal ons 'n afspraak reël. Indien die HIV-toets positief is, sal ons vir u berading gee en u en u kind verwys na die HIV-kliniek, Departement van Paediatrie en Kinder Gesondheids, Tygerberg Hospitaal. Die TB vel toets sal gedoen word met 'n klein naald wat 'n klein hoeveelheid vloeistof onder die vel deponer en na 3 dae sal ons die vel toets lees. Die borskas X-straalfoto sal voor die operasie gedoen word. Daar is geen gevaar betrokke by die bloed trek, die vel toets of die borskas X-straalfoto nie. Die enigste newe-effek mag 'n positiewe vel toets wees, wat sal jeuk en ulseer, maar as dit gebeur sal ons u 'n steroïd gee wat die jeuking sal verlos. Indien u enige probleme ondervind kan u Dr Beyers by telefoon nommer 9389114 kontak.

U is volkome vry om te besluit of u toestemming sal gee om u kind te laat deelneem aan hierdie navorsingsprojek. Indien u nie toestemming gee nie, sal u of u kind in geen opsig benadeel word nie en die standaard van mediese sorg wat u by die kliniek of hospitaal ontvang, sal nie verander nie. Die bloed en limf kliere monsters sal slegs vir toetse oor TB gebruik word, en geen ander navorsing nie. U sal geen finansiële vergoeding ontvang vir deelname aan die studie nie. Alle persoonlike informasie verwerf tydens hierdie studie is streng vertroulik. Die resultate van die studie sal in mediese joernale gepubliseer word, maar die name van persone wat monsters geskenk het, sal nie genoem word nie.

Pasiënt Besonderhede:

Naam en Van: Geboorte Datum:

Adres:

Ek, die ondergetekende dokter/verpleegster verklaar hiermee dat ek die pasiënt van die natuur, doel, risiko en moontlike gevolge van die navorsingsprojek in sy / haar taal ingelig. Ek sal volle verantwoordelikheid neem indien die studie resultate van hierdie persoon nabehandeling, in terme van mediese sorg en berading aandui.

Handtekening van dokter/ verpleegster: Datum:

Handtekening van getuies : Datum:

Ek, die ondergetekende....., gee hiermee toestemming vir die insluiting van my
(*Naam van persoon wat toestemming gee*)

kind..... in die bogenoemde navorsingsprojek, waarin sy/ haar bloed en biopsie
(*Naam van kind*)

monsters mag gebruik word vir tuberkulose navorsing en die kweking van bakterieë, en dat informasie van sy/ haar mediese rekords

in sodanige navorsing gebruik mag word, waarvan die natuur aan my verduidelik was deur
(*Naam van dokter/verpleegster*)

1. Die natuur van die projek is aan my verduidelik
2. Ek verstaan die implikasies van die navorsing en die risiko betrokke
3. Die volgende prosedure mag uitgevoer word as deel van die projek:
 - (i) Trekking van 15 ml bloed (of 3 teelepels) vir HIV toetse en immunologiese toetse verwant aan TB
 - (ii) Tuberkulin vel toets
 - (iii) Borskas X-straalfoto
 - (iv) Ondersoek en kweking van die limf klier vir TB verwante navorsing.
4. Ek verstaan dat ek my kind op enige stadium van die projek kan onttrek sonder enige invloed op my of my kind se mediese sorg.
5. Ek verstaan dat daar geen finansieële vergoeding beskikbaar is nie

Handtekening van persoon wat toestemming gee: **Datum:**

(i)	(ii).....
Handtekening van getuies	Datum	Handtekening van getuies	Datum

APPENDIX III:

DIAGNOSTIC TOOLS

Central components of any effective tuberculosis control programme are prompt identification of active cases, institution of therapy and completion of therapy. In patients in whom there is a clinical suspicion of tuberculosis, the first diagnostic step should be a combination of chest radiograph, microscopic examination of clinical material and culture of bacteria. However, the diagnosis of tuberculosis can often be difficult. Some of the problems that occur include (i) low number of organisms for culture, (ii) slow growth of tuberculosis bacilli, (iii) chest radiograph findings absent or misinterpreted, (iv) biopsy material may not be specific, and (v) symptoms and signs of tuberculosis may be attributed to another pre-existing disease.

Clinical Specimens used for Diagnostic Tests:

Any specimen should be collected in a sterile disposable container, with maximum precautions to avoid its contamination with environmental mycobacteria or non-acid-fast bacilli. Specimens from a variety of sites may be appropriate to examine, including sputum, bronchial brushings, gastric lavage, various body fluids as well as biopsy and autopsy tissue specimens.

Sputum

Freshly expectorated sputum is the best sample to confirm a clinical suspicion of *M. tuberculosis*. If a person is not spontaneously producing sputum, induced sputum is the next best specimen for study. This can be obtained by having the patient inhale a warm sterile aerosolised 10% Sodium Chloride solution (Heifets, L., 1997). A series of a minimum of three sputum specimens should be collected preferably on successive days before the start of the antimicrobial therapy (Harvell *et al*, 2000; Heifets, 1997). More than three specimens may be necessary when the smear examination detects only a small number of acid-fast bacilli, or if the acid-fast bacilli are not found in all three initial specimens. Previous studies have demonstrated incrementally higher recovery rates of *M. tuberculosis* with each successive sputum specimen submitted (Levy *et al*, 1989; Lipsky *et al*, 1984).

Before being used in any diagnostic tests, the sputum specimens should foremost be decontaminated and processed. Mycobacteria have an extended generation time (20 – 22 hours)

compared with that of common bacterial flora (40 – 60 minutes). However, the high lipid content of the cell wall makes mycobacteria more resistant to strong acids and alkalis compared with other bacteria. This property has been used to develop the decontamination procedures to eliminate common bacterial flora while keeping the mycobacteria viable. All liquid specimens should also be concentrated by centrifugation prior to culturing (Heifets, 1997).

Although sputum digestion, decontamination and concentration have increased the yield for *M. tuberculosis*, the organism may be killed if the process is improperly performed, resulting in false-negative culture results. Also, in children, tubercle bacilli usually are relatively few and sputum cannot be obtained from children younger than about 10 years of age. Diverse, painstaking methods are then used for the collection of specimens and are essential for the diagnosis of childhood tuberculosis.

Gastric Lavage

Gastric lavage is the specimen of alternative choice when patients cannot expectorate sputum, or if the patient swallows the sputum. To collect gastric washings, sterile water should be passed into the stomach through a plastic tube and the specimen can be collected through the tube with a syringe (Heifets, 1997). As with sputum, gastric washings should also be decontaminated and processed before being used in any experimental procedures. Concentration and culture should be performed as soon as possible after the collection. Previous studies however showed that *M. tuberculosis* could be isolated from gastric aspirate samples of only 30% to 40% from children and 70% from infants with pulmonary tuberculosis (Vallejo *et al*, 1994; Starke and Taylor-Watts, 1989). Gastric lavage is as a consequence not the ideal specimen for the diagnosis of childhood tuberculosis.

Body Fluids

Blood, spinal, pleural, joint and other normally sterile body fluids should be collected aseptically when used for the diagnosis of tuberculosis (Heifets, 1997). Blood specimens are the primary targets for the bacteriologic diagnosis of disseminated mycobacterial infections, primarily in patients with HIV/AIDS. These specimens can be collected in special isolator tubes, or in the preferred inexpensive vacutainers.

An examination of spinal fluid is an essential diagnostic procedure in tuberculous meningitis. A spinal puncture carries some risk of herniation of the medulla, but if meningitis is suspected, the

procedure must be performed regardless of risk. The presence of acid-fast bacilli in cerebrospinal fluid should be diagnostic for the disease. Unfortunately, acid-fast bacilli can be found in this fluid on smear only in a small minority of the patients who have subsequently been shown to have tuberculous meningitis (Kennedy *et al*, 1979). This is not surprising since the number of bacilli usually present in the cerebrospinal fluid in tuberculous meningitis is never large.

Tissue Specimens

Before the availability of antituberculosis chemotherapy, various surgical procedures were used to collapse tuberculosis cavities in the lungs in an attempt to cure the disease. These days, surgical procedures are mainly used in the establishment of definitive diagnosis of tuberculosis after failed attempts with non-invasive or less invasive investigative procedures. Small tissue obtained from biopsy or during autopsy should be transferred aseptically into sterile screw-cap tubes with various specific liquids. Tissue specimens destined for microscopic analysis are usually immersed in fixative solutions, such as paraformaldehyde, while those submitted for culture are transferred to tubes containing saline (Heifets, 1997).

In the event of doubt in the diagnosis of pulmonary abnormality, a tissue biopsy obtainable by surgery is often indicated. Tuberculosis is often represented by single or multiple nodules, which can usually be removed by segmentectomy, a surgical procedure that involves excision of a portion of a lobe of a lung. Sputum and gastric aspirate cultures are usually negative when used to assess lymph node involvement. Consequently, when tuberculous lymphadenitis is suspected, biopsy material must be submitted for culture, staining and histological analysis. Ideally, the solid portion of the node, or of any other tissue specimen, should be cultured and processed for microscopic sections used in staining and histological examinations. Closed-needle biopsy of the pleura has also been accepted as the single most useful procedure for diagnosis of tuberculosis pleuritis, even with a low diagnostic yield range of 50% to 80%. Invasive procedures are often critical to obtain relevant samples for examination for both extrapulmonary and especially paediatric tuberculosis.

Diagnostic Techniques:

Culture

Isolation of mycobacteria from clinical specimens represents a challenge because of the prolonged period of cultivation required for most of them. The yield of sputum culture for detecting *M. tuberculosis* is higher than that of direct sputum examination, but the delay in obtaining results remains a problem. Among 435 positive specimens analysed, Levy and colleagues (1989) reported sensitivity and specificity for sputum culture of 81.5% and 98.4%, respectively.

Cultivation of *M. tuberculosis* and most of the other slowly growing mycobacteria requires special culture media. The most popular are Lowenstein-Jensen (LJ), or other egg-based solid media, Middlebrook 7H10 / 7H11 agar, Middlebrook 7H9 broth, and the radiolabeled BACTEC medium (Heifets, 1997). The egg-based media are the most traditional for isolation of *M. tuberculosis*, although it takes 3 to 8 weeks to achieve visible growth. Well-funded laboratories can detect tuberculosis cases within 7 to 14 days using the sophisticated BACTEC liquid culturing systems (Middlebrook *et al*, 1977). The BACTEC-460 system can be considered the one most frequently in standard use among such systems (Heifets, 1986; Middleton *et al*, 1997). However, some problems inherent to this system have limited its broad use (Heifets, 1997). Among them are (i) the need for disposal of large volumes of low-grade radiolabeled material, (ii) labour time associated with the necessity of loading and unloading of the vials incubated separately, and (iii) manual transfer of the growth index (GI) daily readings to the laboratory worksheet. To elude these drawbacks, Heifets and colleagues (2000) evaluated two manual liquid medium systems, the Mycobacteria Growth Index Tube (MGIT) and MB Redox tube systems, in comparison to the radiometric BACTEC-460 semi automated systems for recovery from sputum specimens. The results illustrated that the BACTEC system was the most reliable for accurate and rapid diagnosis of active disease, which are the central components of any effective tuberculosis control program.

Despite the documented enhanced ability of the BACTEC-460 system, when the clinical material used for diagnostic examinations are respiratory specimens, three sequential samples are still required for a definitive diagnosis of pulmonary tuberculosis (Harvell *et al*, 2000). For the isolation of *M. tuberculosis*, Harvell and colleagues reported a recovery rate of 82% from the first specimens collected ($n = 143$), 10% for the second (92% cumulative rate) and 8% from the third batch of specimens (100% cumulative rate).

Most laboratories in developing countries, if cultures are attempted at all, use solid media such as LJ and Ogawa because of their low cost. This traditional culture method, as stated before, takes an average of 3 weeks under optimal conditions, and the specificity of detection is not as high as with the liquid medium. To circumvent this obstacle, Caviadas and colleagues (2000) developed a new, efficient, reliable and inexpensive method that permits simultaneous *M. tuberculosis* detection as well as drug susceptibility in less than 2 weeks. This assay, unlike other rapid detection systems, does not require either radioactive isotopes or fluorescent indicators, and is particularly well suited for use in developing countries.

Microscopic Analysis:

(i) Staining of Mycobacteria in Clinical Specimens

Mycobacteria are aerobic gram-positive biologically as well as acid-fast bacilli. This term is related to the fact that the mycobacteria cell wall has low permeability to the basic dyes, and it requires a prolonged exposure or heating of the smear to achieve colorisation of the bacteria (Heifets, 1997). Once mycobacteria are stained through these efforts, they retain dyes during the subsequent decolorisation with acids or a mixture of acids and alcohol. One of the most popular acid-fast staining procedure is the Ziehl-Neelsen (ZN) method in which staining with a solution that contains basic fuchsin and phenol is combined with heating. The smear is decolorised with a mixture of hydrochloric acid and ethanol, followed by a counter stain with methylene blue. Microscopic examination under the oil immersion objective reveals slender rods on a blue background.

A provisional diagnosis of tuberculosis can be based on the detection of acid-fast bacilli (AFB) in specimen smears in conjunction with certain clinical symptoms or radiological findings. Smear examination is indeed a rapid method for detection of mycobacteria in clinical specimens. Ease of performance, widespread availability, low cost, and a considerable diagnostic yield makes smear examination an essential component of any diagnostic evaluation. Tuberculosis control programmes in developing countries rely predominantly upon results of stained sputum smears for diagnosis of tuberculosis (De Cock and Wilkinson, 1995). It is much less sensitive than culture isolation (Heifets, 1997; Harvell *et al*, 2000) and it is estimated that the limit of sensitivity is about 10 000 acid-fast bacilli per ml of specimen (Zhoa *et al*, 1997; Wilkinson, 1998). Levy and colleagues (1989) reported sensitivity and specificity for sputum smears of 53.1% and 99.8%, respectively. If AFB are found in the smear, that finding is an indication that the patient is highly infectious, given the aforementioned sensitivity limits of this method.

False-positive results of the smear examinations are the main problems plaguing laboratories using this diagnostic method. Because of the low specificity, using acid-fast bacilli contaminated solutions during the processing or staining manipulations can cause false-positive results, especially with a small number of AFB. Also, the probability of finding acid-fast bacilli in specimens other than sputum is much lower. Negative smear results, however, does not exclude the possibility that the patient may have tuberculosis, which can be confirmed by other methods, such as by culture.

(ii) Histological Analysis of Tissue Specimens

Histological confirmation of disseminated tuberculosis is best sought by biopsy of the lung, liver, bone marrow, or specific tissue that clinically appears involved, such as skin and lymph nodes. The histological features of tuberculosis are characteristic and similar in all sites of infection. Certain foreign agents stimulate a characteristic pattern of reaction in the infected tissue, which allow a diagnosis of disease to be made on biopsy specimens.

Tuberculosis is the most common and important cause of granulomatous inflammation. This is a type of chronic inflammation histologically characterised by the presence of granulomas that are collections of activated macrophages with epithelioid morphology, macrophage derived giant cells (Langerhans giant cells) and surrounding infiltrate of lymphocytes, plasma cells and granulocytes. The histology of mycobacterial adenitis may include non-specific lymphoid infiltrates, small noncaseating granulomas, or typical Langerhans giant cells in areas of extensive necrosis (Huhti *et al*, 1975). However, tuberculous and non-tuberculous mycobacteria-infected lymph nodes cannot be differentiated histologically (Reid *et al*, 1969), and distinction from other granulomatous diseases may be difficult (Huhti *et al*, 1975). In addition, histological examination of transbronchial lung biopsy obtained via the fiberoptic bronchoscope was shown to give a diagnostic yield of smear-negative pulmonary tuberculosis in only 30% to 58% of cases (So *et al*, 1982; Fujii *et al*, 1992). Histological analysis should therefore be combined with culture examination before a definitive diagnosis can be made.

Polymerase Chain Reaction (PCR)

Staining for AFB is known to be the most rapid and economic method for detecting mycobacteria. However, given that half of the new cases of tuberculosis are smear negative (WHO Tuberculosis Report 2001), diagnosis of many patients cannot be confirmed at the time of presentation. This leads to delays in initiating appropriate treatment and / or the use of invasive procedures to firmly establish the diagnosis.

The drawbacks of conventional diagnosis could be solved by application of PCR, which allows *in vitro* amplification of target DNA to a detectable level within a matter of hours (Saiki *et al*, 1988). Various studies have employed this technique for the rapid detection of *M. tuberculosis*, and most have reported a high degree of sensitivity in detecting *M. tuberculosis* in clinical samples by means of DNA amplification (Brisson-Noël *et al*, 1989; Cousins *et al*, 1992; Eisenach *et al*, 1991; Miyazaki *et al*, 1993).

In principle, PCR is a simple test for the detection of microorganism in a clinical sample, however, in practice many problems have been encountered with this method, the most significant being the generation of false positive reactions due to the amplification of contaminating DNA. Clinical materials such as sputum and blood may also contain components that interfere with the amplification of DNA, leading to under estimation of disease. Inter-laboratory comparisons of PCR-based diagnosis have highlighted the difficulty of obtaining reproducibility with such a sensitive technique, and in particular the high rate of false positives which is unacceptable. Noordhoek and colleagues (1994) evaluated the viability of PCR for the detection of mycobacteria in clinical samples, and reported high levels of false-positive PCR results and widely ranged levels of sensitivity. These results again emphasised the requirement of an effective system for monitoring sensitivity and specificity of the PCR technique before it could be used reliably in the diagnosis of tuberculosis.

Sandin (1996) reviewed a number of systems with potential use in the diagnosis of *M. tuberculosis*. They included the Amplified *M. tuberculosis* Direct test (MTD) and the Amplicor *M. tuberculosis* test, which are the only tests approved by the USA Food and Drug Administration. The MTD test uses a transcription-mediated amplification (TMA) system. This method, however, was only approved for use on smear-positive concentrated respiratory specimens obtained from untreated patients.

The Amplicor was evaluated by Bergmann and Woods (1996) using both smear-positive and smear-negative respiratory tract specimens and compared results with those of the culture and medical history. They found that although the specificity was high for all the specimens, the sensitivity was 97.6% and 40% for acid-fast bacilli smear-positive and negative specimens, respectively. This test was approved for use with the same group of clinical specimens as for the MTD test, namely smear-positive respiratory specimens. Nested amplification, compared with conventional single-step PCR, can enhance sensitivity approximately 1 000 fold, but with a high risk of contamination (Liu *et al*, 1994). In order to increase the yield of the amplification reaction, and to improve the sensitivity of

detection of the *M. tuberculosis* complex in smear-negative specimens, Garcia-Quintanilla and colleagues (2000) developed a single tube balanced heminested PCR. This technique showed a higher sensitivity than the standard nested PCR without loss of specificity and with a minimum of cross-contamination.

The nucleic acid amplification methods may provide rapid results, but are not “stand-alone” tests and should still be used in conjunction with conventional cultures. The amplified tests, in general, offer great potential, but the cost of these tests is excessive, and therefore is not an option for laboratories in developing countries, where rapid, inexpensive diagnostic tools are urgently needed.

APPENDIX IV

DETAILED COMPARISON OF *M. TUBERCULOSIS* GENE EXPRESSION AND
CYTOKINE PATTERN OF A SINGLE PATIENT

Untreated Patients:

Patient L1

(i) *M. tuberculosis* Detection and Gene Expression

The diagnosis of this 6 year-old male was based solely on the detection of acid-fast bacilli in the biopsy tissue and was confirmed with histological analysis. Unfortunately, for some unidentified reason, no biopsy tissue of this patient was submitted for culture, as is standard hospital protocol. This patient had no history of previous tuberculosis, and only started anti-tuberculosis therapy when the diagnosis was confirmed, after the biopsy (Table 3.2).

A total of 16 granulomas were identified in the tissue section, as indicated in Figure A1, with 10 of these granulomas containing caseous necrosis. Granulomas were scored on the basis of presence (1) or absence (0) of signal, and not quantitated for amount of signal per granuloma. *M. tuberculosis* DNA was detected in 14 of the 16 (87.5%) granulomas (Table A1). *M. tuberculosis* DNA was associated with all the necrotic granulomas, as well as four of the six non-necrotic granulomas.

Messenger RNA from all the genes analysed was detected in the granulomas of this patient (Table A1; Figure A2). Hybridisation signals for mRNA were always associated with those granulomas positive for *M. tuberculosis* DNA. *RpoB* mRNA was detected in 6 of the 14 (42.8%) granulomas, with granuloma 1 being the only non-necrotic granuloma staining positive for *rpoB* mRNA. The 5 other *rpoB* positive granulomas all contained caseous necrosis. A stronger signal was detected using riboprobes specific for *katG* mRNA, with 10 of the 14 (71.4%) *M. tuberculosis* DNA positive granulomas also stained positive for *katG* riboprobes, including 4 non-necrotic granulomas. Similar hybridisation signals were detected for the persistent factors, *narX* (4/14) and *icl* (5/14). For this patient, *narX* mRNA was detected in all the granulomas positive for *icl*. Messenger RNA of *mbtB* was only detected in the 3 of the 14 (21.4%) *M. tuberculosis* DNA positive granulomas. Unlike the previous 3 persistent factors, the mRNA levels of *rel_{Mtb}* was one of the highest detected for this

patient. *Rel_{Mtb}* mRNA was detected in 12 of the 14 (85.7%) *M. tuberculosis* DNA positive granulomas, including all four, *M. tuberculosis* DNA positive non-necrotic granulomas. *Esat-6* mRNA was restricted to 3 of the 4 non-necrotic (*M. tuberculosis* DNA positive) granulomas, but was on the whole detected in 13 of the 14 (92.8%) granulomas. It was in fact, the highest expressed of the *M. tuberculosis* genes in the tissue of this patient. In contrast, it would seem that *PPE Rv3018c* (3/14), was the one of the weakest expressed.

(ii) Cytokine Analysis

The majority of the 16 granulomas identified in the tissue sections of patient L1 presented an overall Th0 phenotype (81.3%) (Table 3.3). That is, both type 1 and type 2 cytokines were simultaneously released in these granulomas. These included all the necrotic (10/16) and 3 of the 4 non-necrotic granulomas. The granulomas staining positive for Th1 type cytokines and were deficient in Th2 type cytokines, thereby presenting a Th1 phenotype, were the remaining 3 non-necrotic granulomas.

IL-4 and IL-10 were not detected in 3 non-necrotic granulomas that were scored as having an overall Th1 phenotype. IL-4, however, was detected in the remaining 13 granulomas (81.3%), thus including every one of the necrotic granulomas (Table A1, Figure A3). IL-10 staining was observed in only 9 of the 16 (56.3%) granulomas (Figure A3), including 1 non-caseating granuloma (Table A1). IL-12 was detected in 11 of the 16 granulomas identified (68.6%). This included 2 of the 6 non-necrotic, and 9 of the 10 necrotic granulomas (Table A1). IFN- γ was detected in all the granulomas of this patient. The tissue-damaging TNF- α was detected in 14 of the 16 (87.5%) granulomas, including every necrotic granuloma (10/16) (Figure 3.18). Thus, the granulomas not staining positive for this cytokine were 2 non-necrotic granulomas.

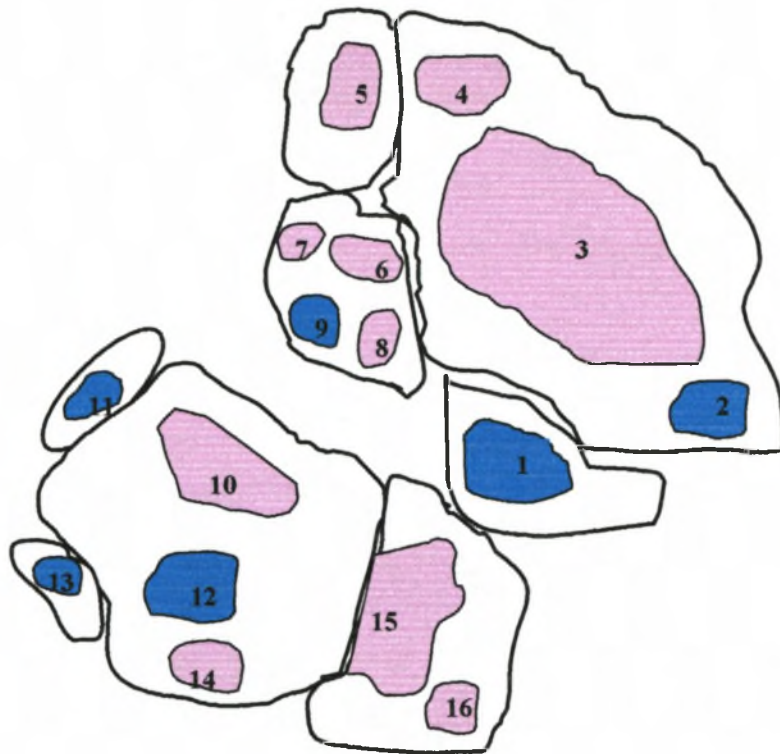


Figure A1 Schematic Representation of the Granulomas within the Lymph Node Tissue of Patient L1. The spatial arrangement of 16 granulomas identified on 2.5x magnification is indicated above. A total of 10 necrotic (●), and 6 non-necrotic (●) granulomas were identified.

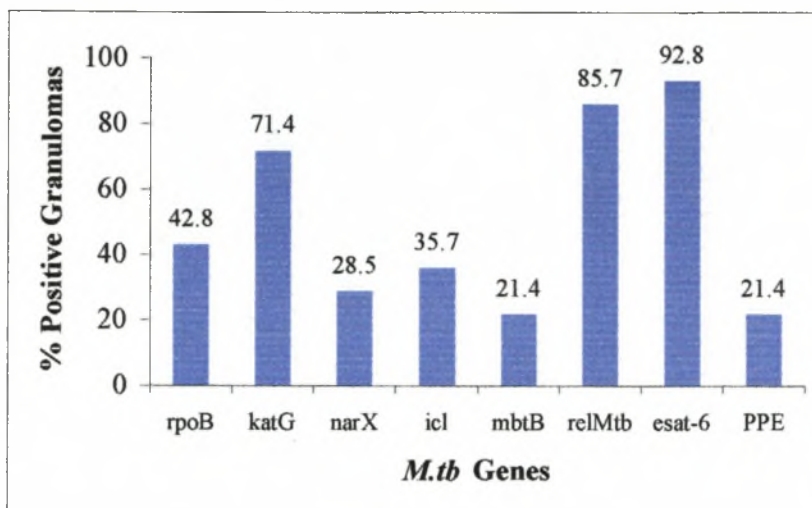


Figure A2. The Expression for the Various *M. tuberculosis* Genes observed in Patient L1. The percentage of hybridisation signal occurring in *M. tuberculosis* DNA associated granulomas were determined for each *M.tb* gene analysed.

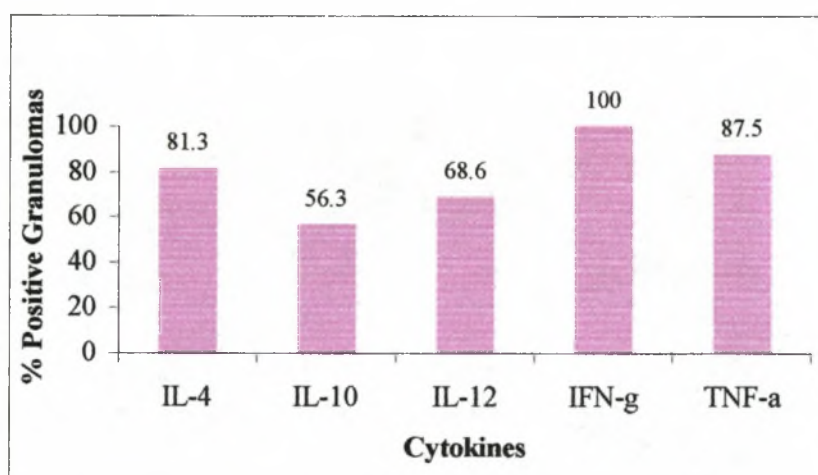


Figure A3. The Pattern of Cytokine Production as observed in Patient L1. The percentage of positive staining granulomas for each cytokine was determined.

Patient L3

(i) *M. tuberculosis* Detection and Gene Expression Analysis

The diagnosis of this 13 year-old male was established with a positive ZN stain and *M. tuberculosis* culture, as well as a positive histological evaluation (Table 3.2). This was one of the five study patients that did not have a history of previous tuberculosis, and only received treatment after biopsy, once diagnosis was confirmed.

This particular patient had a fervent granulomatous response to the *M. tuberculosis* infection. A total of twenty-eight granulomas were identified in the biopsy tissue of which 20 contained caseous necrosis and 8 were non-necrotic (Figure A4). *M. tuberculosis* DNA was associated with all the necrotic granulomas, as well as four of the eight non-necrotic granulomas. Therefore, 24 of the 28 (85.7%) granulomas stained positive for *M. tuberculosis* DNA when using the biotinylated MTB484 DNA probe (Table A2).

RpoB mRNA was detected in all 4 *M. tuberculosis* DNA associated non-necrotic granulomas, as well as 8 necrotic ones (Table A2). Therefore, 12 of the 24 (50%) granulomas identified stained positive with the *rpoB* riboprobe (Figure A5). These granulomas were therefore inefficient in inhibiting bacterial growth. The hybridisation signal for the *katG* specific riboprobe occurred in only 10 of the 24 (43.4%) granulomas, including one non-necrotic granuloma (gran. 19) (Table 3.4). The level of mRNA transcripts for the *narX* gene was seemingly the highest of all the genes analysed for this particular patient. The signal for the *narX* riboprobe was detected in 13 of the 24 (54.1%) granulomas (Table A2), including 1 of the 4 *M. tuberculosis* DNA associated, non-necrotic granulomas (gran. 2) stained. The remaining 12 *narX* positive granulomas all containing caseous necrosis. Similar hybridisation signals were detected for the *icl* riboprobe. Messenger RNA for this gene was detected in 12 of the 24 (52.1%) granulomas identified in the tissue section of this patient. As with *narX*, only 1 non-necrotic granuloma (gran. 1) stained positive for *icl*, though not the same granuloma because *narX* was positive in granuloma 2 (Table A2). *MbtB* mRNA was detected in only 8 of the 24 (33.3%) granulomas, which included the non-necrotic granulomas 1 and 2. The *rel_{Mtb}*, unlike the previous patient, was restricted to only 8 of the 24 (33.3%) granulomas (Table A2). This signal was primarily confined to necrotic granulomas, with granuloma 10 being the single non-necrotic granuloma staining positive when using *rel_{Mtb}* specific riboprobe. The hybridisation signals for both *esat-6* and *PPE Rv3018c* occurred at very low levels. The signal for

esat-6 was observed in 6 of the 24 (25%) granulomas, whilst *PPE* mRNA was only detected in 5 of the 24 (20.5%) granulomas (Table A2).

(ii) Cytokine Analysis

It was estimated that 19 of the 28 (67.9%) granulomas identified in the tissue sections of this patient had an overall Th0 phenotype (Table A2), which included 6 of the 8 non-necrotic, and 13 of the 20 necrotic granulomas. The 9 remaining granulomas only stained positive for Th1 type cytokines, and were therefore scored as Th1 granulomas. These Th1 microenvironments included 2 of the 8 remaining non-necrotic, and 7 of the 20 necrotic granulomas.

Although this study subject presented a rather fervent Th1 cytokine response, the Th2 type cytokines were also detected in the majority of the granulomas (Table A2, Figure A6). Staining for IL-4 was observed in 21 of the 28 (75%) granulomas, which included the 6 of the 8 non-necrotic granulomas. IL-10, as seen with the previous two patients, was detected in the least amount of granulomas (19/28) and like IL-4, was detected in 6 of the 8 non-necrotic granulomas. The Th1 type cytokines analysed (IL-12, IFN- γ and TNF- α) was detected all twenty-eight granulomas identified (Table A2; Figure A6). This particular pattern of cytokine production, where each granuloma stained positive for each of the Th1 type cytokines examined, was unique to this particular patient. This colossal Th1 cytokine milieu contributed to the less than average number of Th0 type granulomas observed in this patient in comparison to the other patients.

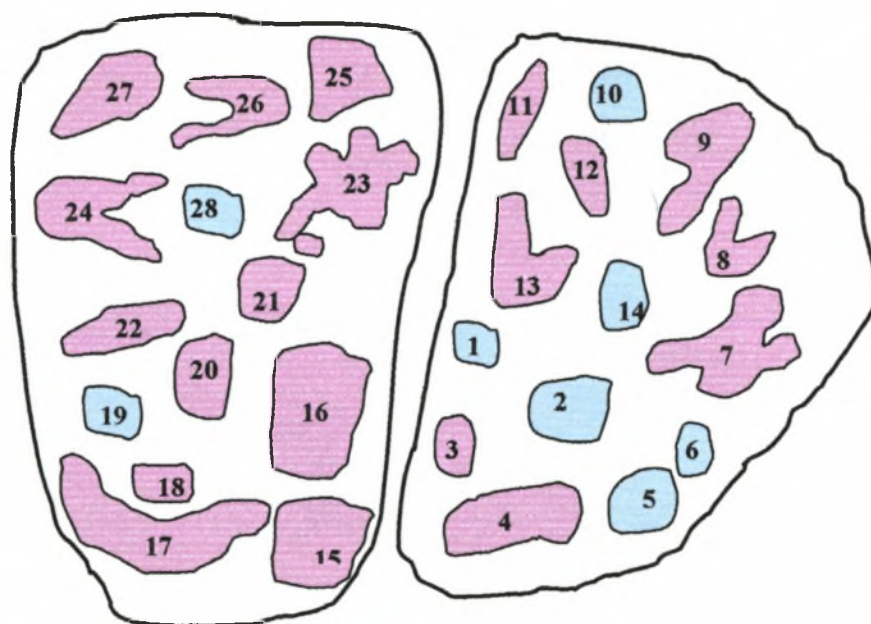


Figure A4. Schematic Representation of the Granulomas within the Lymph Node Tissue of Patient L3. The spatial arrangement of 28 granulomas identified on 2.5x magnification is indicated above. A total of 20 necrotic (●), and 8 non-necrotic (●) granulomas were identified.

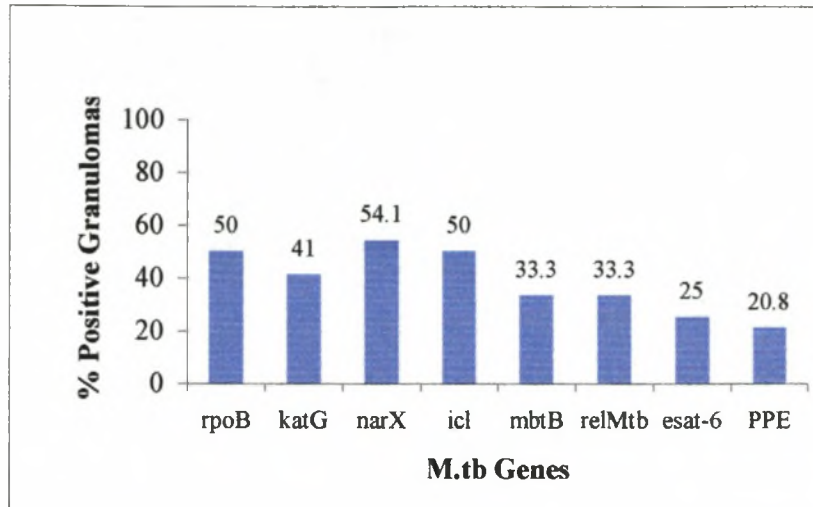


Figure A5. The Expression for the Various *M. tuberculosis* Genes observed in Patient L3. The percentage of hybridisation signal, occurring in *M. tuberculosis* DNA associated granulomas were determined for each *M.tb* gene analysed.

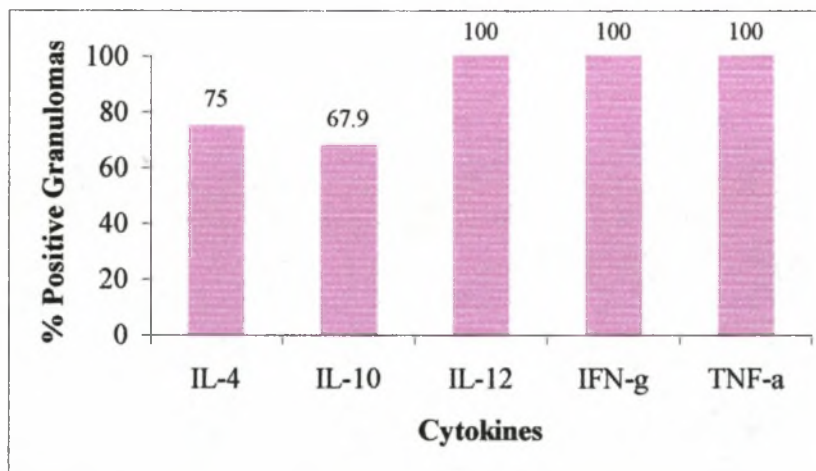


Figure A6. The Pattern of Cytokine Production as observed in Patient L3. The percentage of positive staining granulomas for each cytokine was determined.

Patient L4

(i) *M.tuberculosis* Detection and Gene Expression

Patient L4 was the only female patient included in this study and was one of the five patients that did not have a history of previous tuberculosis. This patient in addition did not receive anti-tuberculosis therapy prior to the biopsy. What were interesting about this particular patient were the undetectable acid-fast bacilli in the biopsy tissue specimen (Table 3.2). Histological analysis of the lymph node tissue was unconvincing, and diagnosis was established exclusively with positive *M. tuberculosis* BACTEC culture. This generally rapid culture system was only positive after four weeks of incubation.

Thirteen granulomas were collectively identified in the lymph node sections of this patient (Figure A7). Unlike any of the other patients, the majority of these granulomas did not contain any caseous necrosis (53.8%), with only 46.2% of the granulomas scored as necrotic. The biotinylated MTB484 DNA probe hybridised to 84.6% (11/13) of the granulomas identified, including five non-necrotic and all of the necrotic granulomas (Table A3).

The hybridisation signal for *rpoB* occurred in 5 of the 11 (45.4%), and included 3 of the 7 non-necrotic, and 2 of the 6 necrotic granulomas. Signal for *katG* was limited to only 3 of the 11 (27.2%) *M.tuberculosis* DNA positive granulomas, which were all non-necrotic granulomas. Hybridisation signals for *narX* and *icl* were also each limited to only 3 of the 11 (27.2%) granulomas, and were detected in only necrotic granulomas. *MbtB* was the highest expressed persistent factor for this patient, with mRNA detected in 6 of the 11 (54.5%) granulomas identified (Figure A8). Messenger RNA for *rel_{Mtb}* was restricted to 5 of the 11 (45.4%) granulomas, of which 3 were non-necrotic and 2 were necrotic. Interestingly, no detectable signal was observed for *esat-6* riboprobes. The highest level of mRNA detected in these granulomas was that of *PPE Rv3018c*, that was detected in 7 of the 11 (63.6%) *M. tuberculosis* DNA positive granulomas (Table A3). Three of the *M. tuberculosis* DNA associated non-necrotic granulomas also stained positive when using the *PPE* specific riboprobe.

(ii) Cytokine Analysis

This patient was unique in having more non-necrotic granulomas than necrotic granulomas in the lymph node sections. A number of these non-necrotic granulomas (6/7) presented with a Th0

phenotype (Table A3). All the necrotic granulomas (6/6) presented with a Th0 phenotype. A total of 92.3% (12/13) granulomas analysed were typed as Th0, concurring with the trend seen in all 6 patients. The remaining granuloma, a non-necrotic granuloma, presented with a Th1 phenotype.

The Th2 cytokine IL-4 was detected in 12 of the 13 (92.3%) granulomas, with the only granuloma not staining positive for this cytokine, obviously being the non-necrotic Th1 granuloma (Figure A9). The IL-10 cytokine staining was limited to only 38.5% (5/13) granulomas. This cytokine was absent in most of the granulomas also lacking necrosis, with the signal detected in 2 of the 7 non-necrotic granulomas. The Th1 cytokine, IL-12, was observed in 8 of the 13 (61.5%) granulomas (Figure A9), which included 4 of the 7 non-necrotic granulomas. IFN- γ , as previously acknowledged, was detected in every granuloma (Figure A9). Staining for TNF- α was observed in 10 of the 13 granulomas (76.9%) (Table A3). Four of the 7 non-necrotic granulomas stained positive for this cytokine.

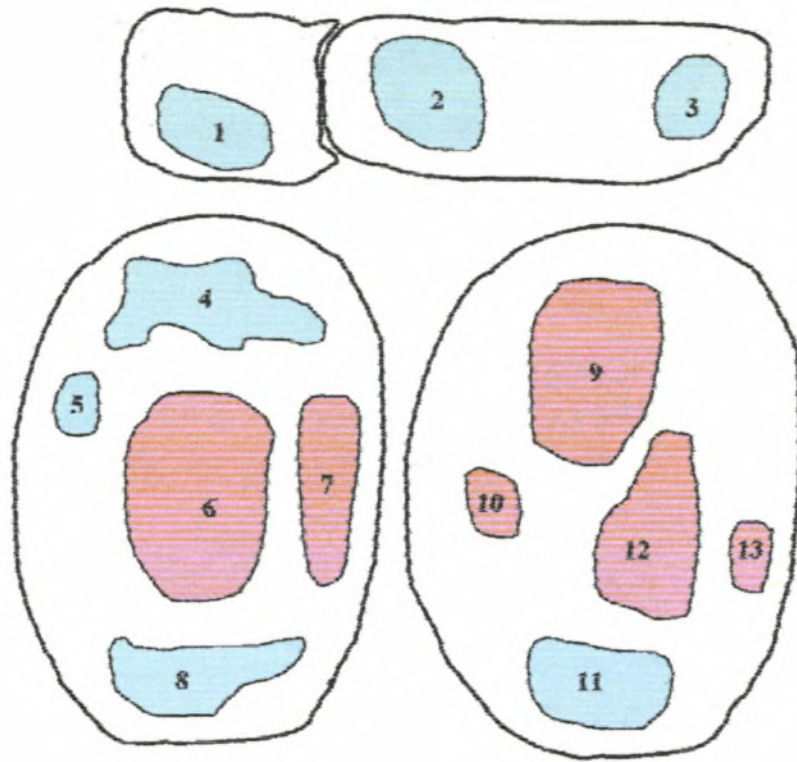


Figure A7. Schematic Representation of the Granulomas within the Lymph Node Tissue of Patient L4. The spatial arrangement of 13 granulomas identified on 2.5x magnification is indicated above. A total of 6 necrotic (●), and 7 non-necrotic (●) granulomas were identified.

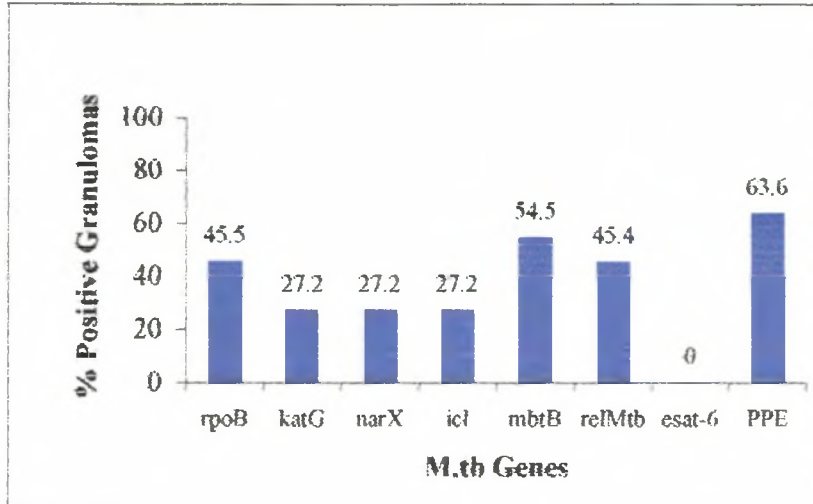


Figure A8. The Expression for the Various *M. tuberculosis* Genes observed in Patient L4. The percentage of hybridisation signal, occurring in *M. tuberculosis* DNA associated granulomas were determined for each *M.tb* gene analysed.

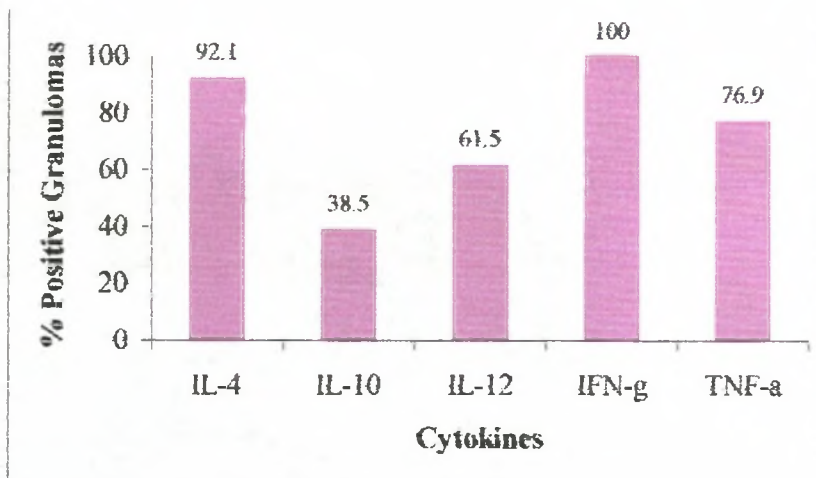


Figure A9. The Pattern of Cytokine Production as observed in Patient L4. The percentage of positive staining granulomas for each cytokine was determined.

Patient L5

(i) *M. tuberculosis* Detection and Gene Expression

Patient L5, a 12 year-old male, had no previous history of tuberculosis. The diagnosis of this patient was based on a positive culture, detection of acid-fast bacilli in the biopsy tissue specimen and was confirmed with conclusive histological analysis. This patient was diagnosed, in addition to the tuberculosis lymphadenopathy, with pulmonary and abdominal tuberculosis.

As with patient L3, this patient had an ardent granulomatous response. A total of 24 granulomas were identified in the fixed tissue section of this patient (Figure A10). Seventy five percent (18/24) of these granulomas contained caseous necrosis. *M. tuberculosis* DNA was detected in 22 of the 24 (91.7%) granulomas (Table A4), which included all the necrotic granulomas and 4 of the 6 non-necrotic granulomas.

The overall *M. tuberculosis* gene expression observed using the *in situ* hybridisation technique was generally high, with the exception of *esat-6*. *RpoB* mRNA was detected in exactly half 50% (11/22) of the granulomas, including 2 of the 4 *M. tuberculosis* DNA positive non-necrotic granulomas (Table A4). The *katG* mRNA was detected in 21 out of 22 (95.4%) granulomas with the necrotic granuloma 22 being the only negative (*M. tuberculosis* DNA positive) granuloma (Figure A11). Hybridisation signals for these genes were detected in all the *M. tuberculosis* DNA associated non-necrotic granulomas. The bacilli are possibly still in log phase growth and adapting to immune response. *NarX* mRNA was detected in 12 of the 22 granulomas (54.5%) identified in the fixed tissue sections (Figure A11). These signals occurred in 11 of the 18 necrotic, and in 1 of the 4 non-necrotic *M. tuberculosis* DNA positive granulomas. mRNA transcripts of *icl* and *rel_{Mtb}* were each detected in 100% of the *M. tuberculosis* DNA positive granulomas (Figure A11). The hybridisation of these riboprobes resulted in a ubiquitous signal in the tissue sections of this patient. *MbtB* was detected in 18 of the 22 *M. tuberculosis* DNA positive granulomas, which included 2 non-necrotic and 16 necrotic granulomas. As with the previous patient (L4) *esat-6* mRNA was not detected in any of the granulomas, whereas the level of *PPE* Rv3018c mRNA was elevated. The hybridisation signal for this gene occurred in 21 of the 22 (95.4%) granulomas (Figure A11). All 4 *M. tuberculosis* DNA positive non-necrotic granulomas stained positive for *PPE*, with only 1 negative necrotic granuloma (gran. 22).

(ii) Cytokine Analysis

Twenty-three of the 24 (95.8%) granulomas identified in the tissue sections of this patient (Table A4) presented with a Th0 phenotype. Granuloma number 10, a non-necrotic granuloma, presented an overall Th1 phenotype.

IL-4 was absent from only 1 non-necrotic granuloma, which was incidentally also the only Th1 granuloma identified. Staining for this cytokine was observed in 23 of the 24 (95.8%) granulomas (Figure A12). IL-10 was detected in 12 of the 24 (50%) granulomas, which included 11 of the 18 necrotic and only 1 of 6 non-necrotic granulomas. The Th1 type cytokine IL-12 was detected in 11 of the 24 (48.5%) granulomas (Figure A12). This included 9 of the 24 necrotic, and only 2 of the 6 non-necrotic granulomas. Along with IFN- γ , staining for TNF- α was detected in all the 24 granulomas (Table A4). In fact, these were the only two cytokines detected in the granuloma.

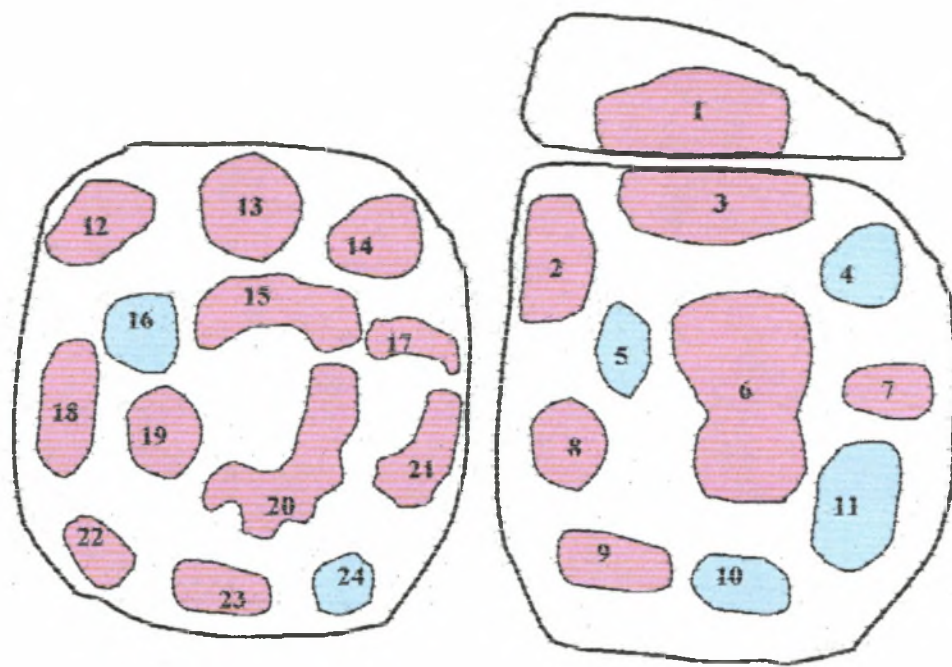


Figure A10. Schematic Representation of the Granulomas within the Lymph Node Tissue of Patient L5. The spatial arrangement of 24 granulomas identified on 2.5x magnification is indicated above. A total of 18 necrotic (●), and 6 non-necrotic (●) granulomas were identified.

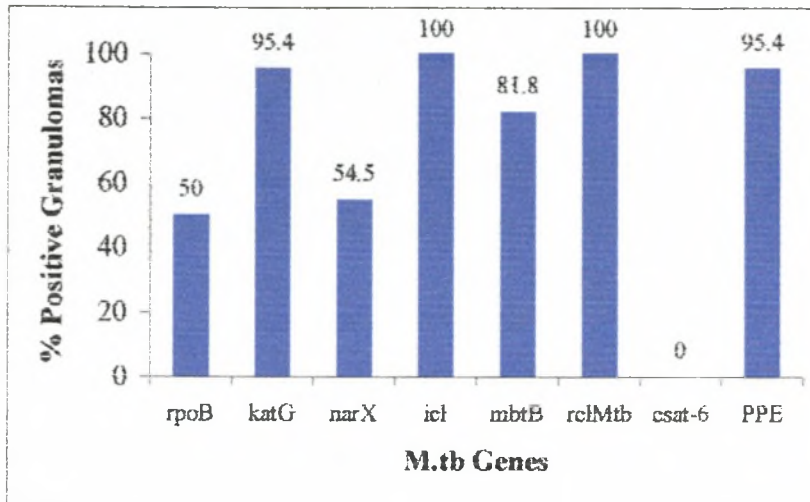


Figure A11. The Expression for the Various *M. tuberculosis* Genes observed in Patient L5. The percentage of hybridisation signal, occurring in *M. tuberculosis* DNA associated granulomas were determined for each *M.tb* gene analysed.

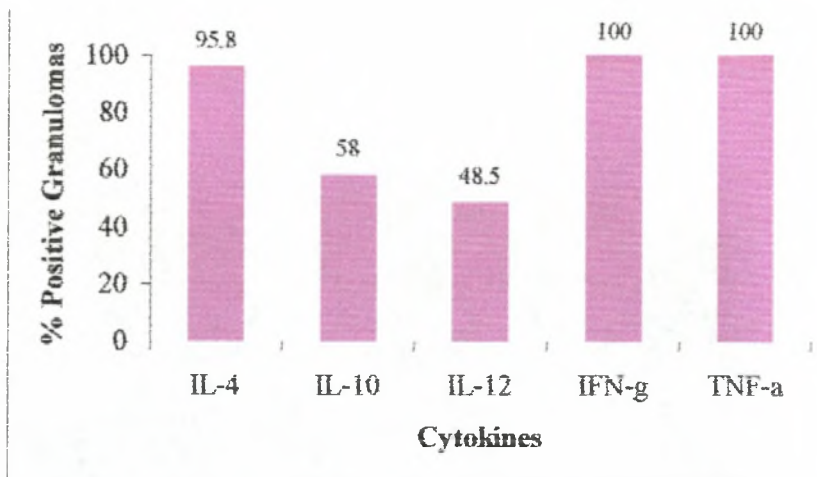


Figure A12. The Pattern of Cytokine Production as observed in Patient L5. The percentage of positive staining granulomas for each cytokine was determined.

Patient L6

(i) *M. tuberculosis* Detection and Gene Expression

The last patient in this study was a 6 year-old male with no previous history of tuberculosis. This patient was not on any anti-tuberculosis medication, and only started treatment once diagnosis was established. Acid-fast bacilli were detected in the biopsy tissue, and cultivation of the infected tissue yielded a positive *M. tuberculosis* culture.

Figure A13 illustrates a schematic representation of the lymph node segments excised from the cervical region from this patient. A total of nineteen granulomas were identified in the 7 tissue fragments (Table A5). Thirteen (68.4%) of these granulomas contained caseous necrosis. *M. tuberculosis* DNA was detected in 18 of the 19 (94.7%) granulomas, with only the non-necrotic granuloma 2 not staining positive for *M. tuberculosis* DNA (Table A5).

Only 7 of the 18 (38.8%) granulomas contained hybridisation signal for the riboprobes specific for *rpoB* mRNA (Figure A14). This included 4 of the 13 necrotic and 3 of the 5 non-necrotic granulomas. Staining for *katG* mRNA was relatively prominent, with signal for hybridised *katG* riboprobes detected in 16 of the 18 (88.8%) granulomas (Table A5). Signal for *katG* was detected in 12 of the 13 necrotic and 4 of the 5 non-necrotic granulomas. *NarX* mRNA was detected in 13 of the 18 (72.2%) granulomas, including 2 non-necrotic and 11 necrotic granulomas also positive for *M. tuberculosis* DNA. Messenger RNA for the glyoxylate shunt enzyme, *icl*, was detected in 17 of the 18 (94.4%) *M. tuberculosis* DNA positive granulomas (Table A5). Signal for *icl* was detected in all the necrotic and in 5 of the 6 non-necrotic granulomas. *MbtB* mRNA, like the rest of the persistent factors, was detected in a number of granulomas (77.7%). As with patient L5, *rel_{Mtb}* mRNA was detected in all the *M. tuberculosis* DNA positive granulomas (100%). The mRNA levels for both *esat-6* and *PPE Rv3018c* were low. The mRNA for these genes were detected in only three various granulomas. Signal for both these riboprobes were detected in 1 necrotic, and in 2 of the 6 non-necrotic granulomas, with granuloma 16 staining positive for both.

(ii) Cytokine Analysis

This patient, as with the previous patient, also exhibited a strong granulomatous response, the majority of granulomas contained caseous necrosis (68.4%). Similarly to patient L2, only

granulomas with an established Th0 phenotype were observed in the fixed tissue sections of this patient (Table A5).

The pattern of cytokine production observed was very similar to patient L2, precisely so for IL-4, IFN- γ and TNF- α . These 3 cytokines were detected in every one of the granulomas identified (Table A5, Figure A15), thus resulting in only Th0 granulomas. IL-10 was detected in 17 of the 19 (89.5%) granulomas (Figure A15). The only granuloma lacking signal for this cytokine were 2 non-necrotic granulomas. As for IL-12, only 12 of the 19 (63.2%) granulomas stained positive for this macrophage secreting cytokine. This included 3 of the 5 non-necrotic and 9 of the 13 necrotic granulomas.

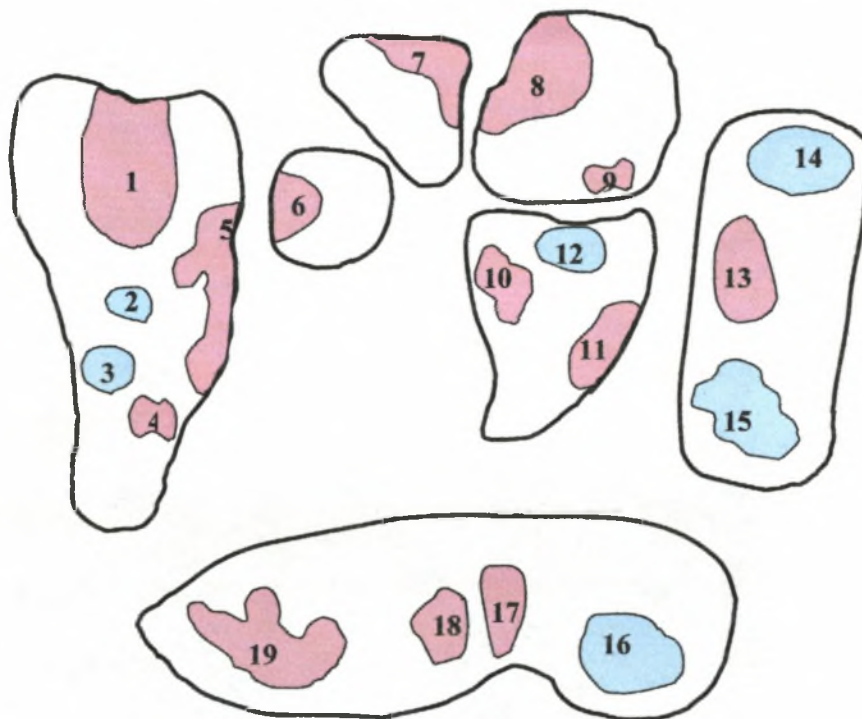


Figure A13 Schematic Representation of the Granulomas within the Lymph Node Tissue of Patient L6. The spatial arrangement of 19 granulomas identified on 2.5x magnification is indicated above. A total of 13 necrotic (●), and 6 non-necrotic (●) granulomas were identified.

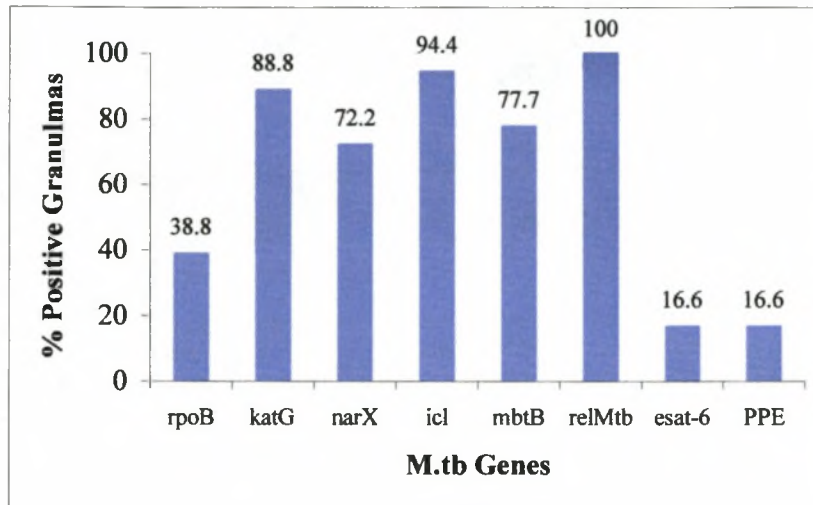


Figure A14. The Expression for the Various *M. tuberculosis* Genes observed in Patient L6. The percentage of hybridisation signal, occurring in *M. tuberculosis* DNA associated granulomas were determined for each *M.tb* gene analysed.

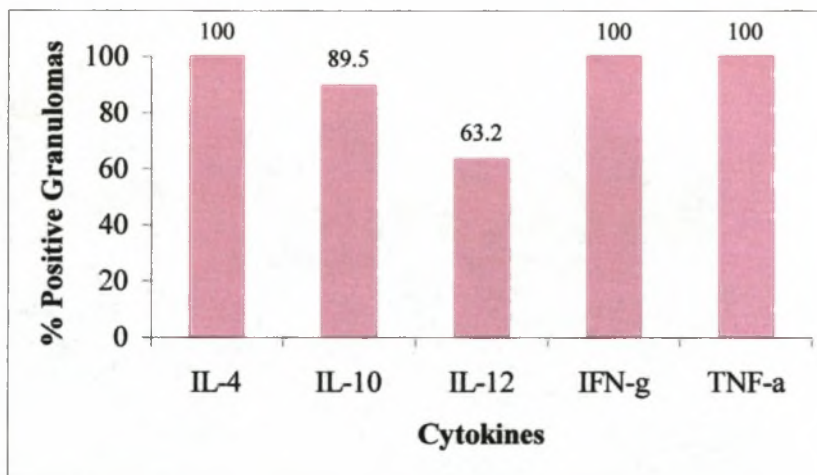


Figure A15. The Pattern of Cytokine Production as observed in Patient L6. The percentage of positive staining granulomas for each cytokine was determined.

Treated Patient:**Patient L2****(i) *M. tuberculosis* Detection and Gene Expression**

The biopsy material of this 3 year-old male was both ZN and culture positive (Table 3.2). This patient, unlike the other 5 patients included in the study, had a history of previous tuberculosis. The patient had first received treatment at the age of 9 months and then again at the age of 2 years. This patient also started his third anti-tuberculosis course of treatment two days prior to the biopsy.

A total of seven granulomas were identified in the fixed tissue section of this patient, as indicated in Figure A16. Six (85.7%) of these granulomas contained caseous necrosis. The *M. tuberculosis* DNA was only associated with these necrotic granulomas (Table A6). No signal was detected in the non-necrotic granuloma.

The *M. tuberculosis* gene expression observed for this patient was different from the 5 untreated patients. No signal was detected for both the *rpoB* and *katG* riboprobes (Table A6, Figure A16). In fact, the level of mRNA transcripts for the remaining *M. tuberculosis* genes analysed in this particular tissue section was generally low, with the exception of *rel_{Mtb}* mRNA (Figure A16). A total of 5 of the 6 (83.3%) granulomas were positive for *rel_{Mtb}* mRNA, with granuloma 5 being the only *M. tuberculosis* DNA positive granuloma not staining positive for this gene (Table A6). As with the previous patient (L1), hybridisation signals for *narX* (3/6) and *icl* (2/6) were very similar, with all the *narX* positive granulomas also staining positive when using the *icl* specific riboprobe (Table A6). *MbtB* mRNA was also detected in 3 of the 6 (50%) granulomas. The remaining genes, namely *esat-6* and *PPE Rv3018c*, were detected in 2 of the (33.3%) granulomas (Figure A17).

(ii) Cytokine Analysis

Every one of the 7 granulomas identified presented a Th0 phenotype (Table A6).

The cytokine milieu was generally quite high. IL-4, IFN- γ and TNF- α were detected in all granulomas identified (Figure A18). The two remaining cytokines, IL-10 and IL-12 were each detected in 6 of the 7 (85.7%) granulomas (Table A6). Staining for IL-10 was absent in the only

non-necrotic granuloma identified for this patient (granuloma 4), whereas IL-12 staining was not detected in granuloma 6, a necrotic granuloma (TableA6).

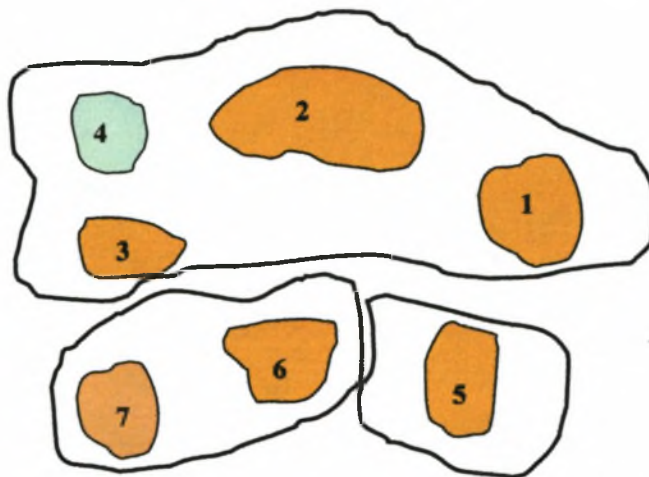


Figure A16 Schematic Representation of the Granulomas within the Lymph Node Tissue of Patient L2. The spatial arrangement of 7 granulomas identified on 2.5x magnification is indicated above. A total of 6 necrotic (●), and 1 non-necrotic (●) granulomas were identified.

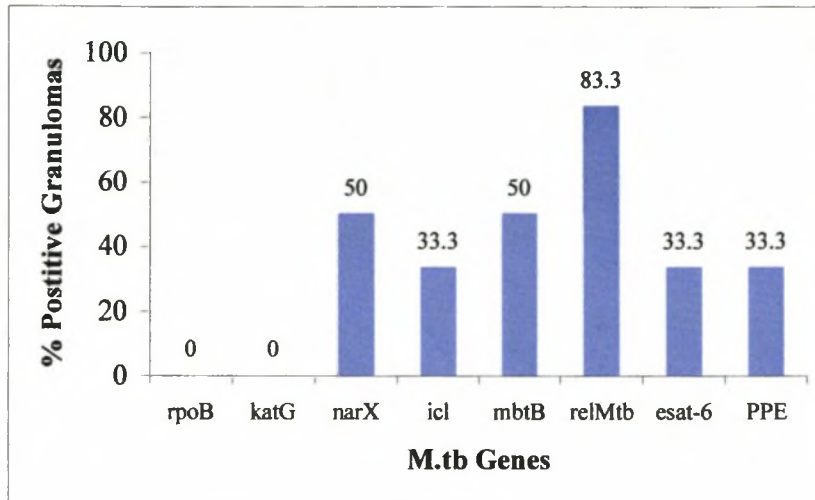


Figure A17. The Expression for the Various *M. tuberculosis* Genes observed in Patient L2. The percentage of hybridisation signal, occurring in *M. tuberculosis* DNA associated granulomas were determined for each *M.tb* gene analysed.

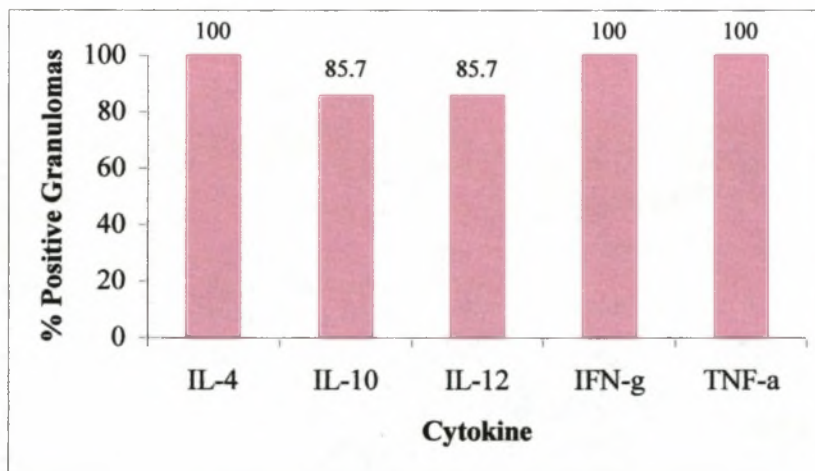


Figure A18. The Pattern of Cytokine Production as observed in Patient L2. The percentage of positive staining granulomas for each cytokine was determined.

Table A8. Stratification of Granulomas According to Expression of *M. tuberculosis* genes (e.g. *rpoB*)

	Necrotic										
	(Y/N)	DNA	rpoB	katG	narX	icl	mbtB	rel _{Mtb}	esat-6	PPE	
Negative RpoB	N	1	0	1	0	0	0	1	1	0	
	N	1	0	1	0	0	0	1	1	1	
	N	1	0	1	0	0	0	1	0	0	
	N	1	0	1	0	0	0	0	0	1	
	N	1	0	0	0	0	0	1	1	0	0
	N	1	0	1	0	1	0	1	0	1	
	N	1	0	1	1	1	1	0	1	0	1
	N	1	0	1	1	1	1	0	1	0	0
	N	1	0	1	0	1	1	1	1	0	0
	Y	1	0	1	0	0	0	0	1	1	0
	Y	1	0	1	0	0	0	0	1	1	0
	Y	1	0	0	1	1	1	0	1	1	0
	Y	1	0	1	0	1	0	1	1	1	0
	Y	1	0	1	0	0	0	1	1	1	0
	Y	1	0	1	0	0	0	0	1	1	0
	Y	1	0	1	0	1	0	1	0	0	0
	Y	1	0	1	0	1	1	1	0	0	0
	Y	1	0	0	0	0	0	1	0	0	1
	Y	1	0	0	0	0	0	1	0	1	0
	Y	1	0	0	0	1	1	0	1	0	0
	Y	1	0	0	1	1	1	0	1	0	0
	Y	1	0	1	1	1	1	0	1	0	0
	Y	1	0	1	1	1	0	0	0	0	1
	Y	1	0	1	1	1	1	0	0	0	0
	Y	1	0	0	1	1	1	0	0	0	0
	Y	1	0	1	1	1	0	0	0	0	0
	Y	1	0	0	0	0	0	0	0	0	0
	Y	1	0	0	0	0	0	1	0	0	1
	Y	1	0	0	1	1	1	0	0	0	1
	Y	1	0	0	1	1	0	0	0	0	1
	Y	1	0	0	0	0	1	1	1	0	0
	Y	1	0	1	0	1	1	1	1	0	1
	Y	1	0	1	0	1	1	1	1	0	1
Y	1	0	1	0	1	1	1	1	0	1	
Y	1	0	1	0	1	1	1	1	0	1	

	Y	1	0	1	0	1	1	1	0	1
	Y	1	0	1	1	1	0	1	0	1
	Y	1	0	1	1	1	1	1	0	1
	Y	1	0	1	1	1	1	1	0	1
	Y	1	0	0	1	1	1	1	0	0
	Y	1	0	1	0	1	1	1	0	0
	Y	1	0	1	1	1	1	1	0	0
	Y	1	0	1	1	1	1	1	0	0
	Y	1	0	1	1	1	1	1	0	0
	Y	1	0	1	0	1	1	1	0	0
	Y	1	0	1	1	1	1	1	0	0
	Y	1	0	1	1	1	1	1	1	0
	Y	1	0	0	0	0	1	0	0	0
	Y	1	0	0	0	0	1	1	0	0
	Y	1	0	0	0	0	0	1	0	0
	Y	1	0	0	1	1	0	1	1	1
	Y	1	0	0	1	1	0	1	0	0
	Y	1	0	0	1	0	1	1	1	1
Positive RpoB	N	1	1	1	1	1	0	1	1	0
	N	1	1	1	0	0	0	0	0	1
	N	1	1	0	0	0	0	1	0	0
	N	1	1	0	0	1	1	0	0	0
	N	1	1	0	1	0	1	0	1	0
	N	1	1	0	0	0	1	1	0	1
	N	1	1	1	0	0	1	1	0	0
	N	1	1	1	0	0	0	0	0	1
	N	1	1	1	0	1	1	1	0	1
	N	1	1	1	0	1	1	1	1	0
	N	1	1	1	1	1	1	1	0	1
	N	1	1	0	0	0	0	1	1	1
	Y	1	1	1	1	1	0	1	1	0
	Y	1	1	0	1	1	0	1	1	0
	Y	1	1	1	0	0	0	1	1	1
	Y	1	1	0	0	0	1	0	0	0
	Y	1	1	0	0	0	1	0	0	1
	Y	1	1	0	0	0	0	0	1	0
	Y	1	1	0	0	0	1	0	0	0
	Y	1	1	1	0	0	1	0	1	1
	Y	1	1	0	1	1	0	0	0	0

	Y	1	1	1	1	0	0	0	1	1
	Y	1	1	1	1	1	0	0	0	0
	Y	1	1	0	1	0	0	1	1	0
	Y	1	1	0	1	1	0	1	0	0
	Y	1	1	0	1	1	1	1	0	0
	Y	1	1	0	0	1	1	1	0	1
	Y	1	1	1	0	1	1	1	0	1
	Y	1	1	1	1	1	0	1	0	1
	Y	1	1	1	1	1	1	1	0	1
	Y	1	1	1	1	1	1	1	0	1
	Y	1	1	1	1	1	1	1	0	1
	Y	1	1	1	1	1	1	1	0	1
	Y	1	1	1	1	1	1	1	0	1
	Y	1	1	1	1	1	1	1	0	1
	Y	1	1	1	1	1	1	1	0	1
	Y	1	1	1	1	1	1	1	0	1
	Y	1	1	1	1	1	0	1	0	1
	Y	1	1	1	1	1	1	1	0	0
	Y	1	1	1	1	1	1	1	0	0
	Y	1	1	1	1	1	0	1	0	0
RpoB Neg.	-	54	0	34	25	35	28	41	11	19
(%)	-	(100)	(0)	(62.9)	(46.3)	(64.8)	(51.8)	(75.9)	(20.3)	(35.19)
RpoB Pos.	-	41	41	26	23	26	24	29	11	22
(%)	-	(100)	(100)	(63.4)	(56.1)	(63.4)	(58.5)	(70.7)	(26.8)	(53.6)

Table A9. Stratification of Granulomas According to Expression of Host Cytokines and *M. tuberculosis* genes (e.g. IL-4)

Granuloma subgroups	DNA	rpoB	katG	narX	icl	mbtB	relMtb	esat-6	PPE
Neg.	1	0	1	0	0	0	1	1	0
IL-4:	1	0	1	1	1	0	1	0	1
	1	0	1	0	1	0	1	0	0
	1	0	0	1	1	0	1	0	0
	1	0	0	1	1	0	1	0	0
	1	0	1	1	1	0	1	0	0
	1	1	1	1	1	0	1	1	0
	1	1	1	0	0	0	0	0	1
	1	1	0	0	0	0	1	0	0
	1	1	0	0	0	1	1	0	1
	1	1	0	0	0	0	0	1	0
	1	1	0	0	0	1	0	0	0
	1	1	0	1	1	0	0	0	0
Pos.	1	0	1	0	0	0	1	1	1
IL-4	1	0	1	0	0	0	1	0	0
	1	0	1	0	0	0	0	0	1
	1	0	0	0	0	1	1	0	0
	1	0	1	0	1	0	1	0	1
	1	0	1	1	1	0	1	0	0
	1	0	1	0	1	1	1	0	0
	1	0	1	0	0	0	1	1	0
	1	0	1	0	0	0	1	1	0
	1	0	0	1	1	0	1	1	0
	1	0	1	0	0	1	1	1	0
	1	0	1	0	1	1	0	0	0
	1	0	0	0	0	1	0	0	1
	1	0	0	0	0	1	0	1	0
	1	0	0	0	1	1	1	0	0
	1	0	1	1	0	0	0	0	1
	1	0	1	1	1	0	0	0	0
	1	0	0	1	1	0	0	0	0
	1	0	1	1	0	0	0	0	0
	1	0	0	0	0	0	0	0	0
	1	0	0	0	0	1	0	0	1
	1	0	0	1	1	0	0	0	1

1	0	0	1	0	0	0	0	1
1	0	0	0	1	1	1	0	0
1	0	1	0	1	1	1	0	1
1	0	1	0	1	1	1	0	1
1	0	1	0	1	1	1	0	1
1	0	1	0	1	1	1	0	1
1	0	1	1	1	0	1	0	1
1	0	1	1	1	1	1	0	1
1	0	1	1	1	1	1	0	1
1	0	0	1	1	1	1	0	0
1	0	1	0	1	1	1	0	0
1	0	1	1	1	1	1	0	0
1	0	1	1	1	1	1	0	0
1	0	1	1	1	1	1	0	0
1	0	1	0	1	1	1	0	0
1	0	1	1	1	1	1	0	0
1	0	1	1	1	1	1	0	0
1	0	1	1	1	1	1	1	0
1	0	0	0	0	1	0	0	0
1	0	0	0	0	1	1	0	0
1	0	0	0	0	0	1	0	0
1	0	0	1	1	0	1	1	1
1	0	0	1	1	0	1	0	0
1	0	0	1	0	1	1	1	1
1	1	0	0	1	1	0	0	0
1	1	0	1	0	1	0	1	0
1	1	1	0	0	1	1	0	0
1	1	1	0	0	0	0	0	1
1	1	1	0	1	1	1	0	1
1	1	1	0	1	1	1	0	1
1	1	1	0	1	1	1	1	0
1	1	1	1	1	1	1	0	1
1	1	0	0	0	0	1	1	1
1	1	1	1	1	0	1	1	0
1	1	0	1	1	0	1	1	0
1	1	1	0	0	0	1	1	1
1	1	0	0	0	1	0	0	0
1	1	0	0	0	1	0	0	1
1	1	1	0	0	1	0	1	1
1	1	1	1	1	0	0	1	1

	1	1	1	1	1	0	0	0	0
	1	1	0	1	0	0	1	1	0
	1	1	0	1	1	0	1	0	0
	1	1	0	1	1	1	1	0	0
	1	1	0	0	1	1	1	0	1
	1	1	1	0	1	1	1	0	1
	1	1	1	1	1	0	1	0	1
	1	1	1	1	1	1	1	0	1
	1	1	1	1	1	1	1	0	1
	1	1	1	1	1	1	1	0	1
	1	1	1	1	1	1	1	0	1
	1	1	1	1	1	1	1	0	1
	1	1	1	1	1	1	1	0	1
	1	1	1	1	1	0	1	0	1
	1	1	1	1	1	1	1	0	0
	1	1	1	1	1	1	1	0	0
	1	1	1	1	1	0	1	0	0
IL-4 Neg	13	7	6	6	7	2	9	3	3
(%)	(100)	(53.8)	(46.1)	(46.1)	(53.8)	(15.4)	(69.2)	(23)	(23)
IL-4 Pos	82	34	54	42	54	50	61	19	38
(%)	(100)	(41.4)	(65.8)	(51.2)	(65.8)	(60.9)	(74.4)	(23.1)	(46.3)

APPENDIX VI**LIST OF SUPPLIERS**

Absolute Ethonal	Merck, UK
Acetic Anhydride	Merck, UK
Acetone	Merck, UK
Agarose	Whitehead Scientific, RSA
3-aminopropyltriethoxysilane	Sigma, USA
Avidin-HRP	DAKO, USA
Axioscope 2 Microscope	Zeiss, Germany
BCIP	GibcoBRL, Switzerland
Bio-11-UTP	GibcoBRL, Switzerland
Biotin-14-CTP	GibcoBRL, Switzerland
3CC Video Camera	Sony, Japan
DAB	Vector, USA
DEPC	Sigma, USA
DnaseI	Roche, Germany
dNTPs	GibcoBRL, Switzerland
dNTPs (PCR Grade)	Roche, Germany
DTT	GibcoBRL, Switzerland
ECL Kit	Amersham, UK
Eppendorf Microtubes	Eppendorf, Germany
Fuchsin-substrate-chromogen	DAKO, USA
Goat anti-human 1° Ab	Roche, Germany
Haemotoxylin	DAKO, USA
Hybond N ⁺ Membranes	Amersham, UK

30% Hydrogen Peroxide	Merck, UK
ISH and Detection Kit	GibcoBRL, Switzerland
Isoproponal	Merck, UK
ITC Camera	Berkenhoff and Drebes, Germany
Levimisole	Vector, USA
Lysozyme	Roche, Germany
Marker X	Roche, Germany
Methyl Green	DAKO, USA
Microfuge	Eppendorf, Germany
Microscope Cover Glasses	Sigma, USA
Microscopic Slides	Sigma, USA
Mineral Oil	Sigma, USA
Mouse anti-human CD86	Roche, Germany
NBT	GibcoBRL, Switzerland
Nucleobond Kit	Amersham, UK
Omnislide Humidity Chamber	Hybaid Ltd, UK
PCR Purification System	GibcoBRL, Switzerland
PGEMT-eazy System	Promega, USA
ProteinaseK	GibcoBRL, Switzerland
<i>PvuII</i> (and Buffer M)	Promega, USA
Rabbit anti-goat (2° Ab)	Roche, Germany
Rabbit Serum	Roche, Germany
Rnase A	Roche, Germany
RNaseOUT Inhibitor	GibcoBRL, Switzerland
Sheep anti-mouse (2° Ab)	Roche, Germany
Sheep Serum	Roche, Germany
SP6 Polymerase (and SP6 Transcript Buffer)	GibcoBRL, Switzerland

Spectrophotometer 120i	Milton Roy, USA
Speed Vac Concentrator	Sorvant, USA
Sorvall CentrifugeRC-5B	Sorvall, Germany
Streptavidin – AP	DAKO, USA
Streptavidin – AP Conjugate	GibcoBRL, Switzerland
T7 Polymerase (and T7 Transcript Buffer)	GibcoBRL, Switzerland
Taq DNA Polymerase (and Buffer)	Roche, Germany
Touchdown Thermal Cycler	Hybaid Ltd, UK
Triethonamine	Merck, UK
Video Graphic Printer	Sony, Japan
Xylene	Merck, UK

APPENDIX VII

COUNTRIES GROUPED ACCORDING TO THE WHO TO ESTIMATE INCIDENCE

Established Market Economies	Eastern Europe	Latin America	Eastern Mediterranean	Africa - low HIV	Africa - high HIV	South East Asia	Western Pacific
Trend Estimated From							
Australia	Albania	Anguilla	Cyprus	Algeria	Botswana	Bhutan	American Samoa
Austria	Armenia	Antigua &	Jordan	Benin	Cent Afr Rep	India	Cambodia
Belgium	Belarus	Barbuda	Lebanon	Comoros	Cote d'Ivoire	Maldives	China, Hong Kong SAR
Canada	Croatia	Argentina	Morocco	Guinea	DR Congo	Sri Lanka	China, Macao SAR
Czech Rep	Esonia	Bahamas	Oman	Madagascar	Kenya	Trend applied to	Cook Is
Denmark	Kazakhstan	Barbados	Qatar	Mali	Lesotho	Bangladesh	Fiji
Finland	Kyrgyzstan	Bermuda	Syria	Mauritania	Malawi	DPR Korea	French Polynesia
France	Latvia	Br Virgin Is	Tunisia	Mauritius	Uganda	Indonesia	Guam
Germany	Lithuania	Cayman Is			UR Tanzania	Myanmar	Kiribati
Greece	Poland	Chile	Trend applied to	Trend applied to	Zambia	Nepal	Lao PDR
Iceland	Romania	Cuba	Afghanistan	Angola	Zimbabwe	Thailand	Malaysia
Japan	Russia	Dominica	Bahrain	Burkina Faso			Marshall Is
Netherlands	Slovakia	Dominican Rep	Djibouti	Cameroon	Trend applied to		Micronesia
New Zealand	Slovenia	Ecuador	Egypt	Cape Verde	Burundi		N Mariana Is
Norway	Tajikistan	El Salvador	Iran	Chad	Congo		Nuara New Caledonia
Portugal	Turky	Grenada	Iraq	Equatorial Guinea	Eritrea		Palau
Singapore	Turkmenistan	Guatemala	Kuwait	Goban	Ethiopia		Rep Korea
Spain	Ukraine	Guyana	Libya	Gambia	Mozambique		Samoa
Sweden	Uzbekistan	Honduras	Pakistan	Ghana	Namibia		Solomon
Switzerland	Yugoslavia	Jamaica	Saudi Arabia	Guinea-Bissau	Rwanda		Tokelau
United Kingdom		Mexico	Somalia	Liberia	South Africa		Tonga
United States	Trend applied to	Montserrat	Sudan	Niger	Swaziland		Tuvalu
	Azerbaijan	Nicaragua	United Arab Emirates	Sao Tome & Principe			Vanuatu
	Bosnia & Herzegovina	Peru	West Bank & Gaza	Senegal			Viet Nam
Trend applied to	Bulgaria	Puerto Rico	Yemen	Seychelles			Wallis & Futuna Is
Andorra	Georgia	St Kitts & Nevis		Sierra Leone			Trend applied to
Israel	Hungary	Tobago		Togo			Brunei Darussalam
Italy	Rep Moldova	Turks & Caicos Is					China
Luxembourg	TFYR	Uruguay					Mongolia
Malta	Macedonia	Venezuela					Papua New Guinea
Monaco							Philippines
San Marino							
		Trend applied to					
		Belize					
		Bolivia					
		Brazil					
		Colombia					
		Costa Rica					
		Haiti					
		Panama					
		Paraguay					
		Suriname					

REFERENCES

- Abbas, A. K., K. M. Murphy, and A. Sher.** 1996. Functional diversity of helper T lymphocytes. *Nature* **383**:787-793.
- Alland, D., G. E. Kalkut, A. R. Moss, R. A. McAdam, J. A. Hahn, W. Bosworth, E. Drucker, and B. R. Bloom.** 1994. Transmission of tuberculosis in New York City. An analysis by DNA fingerprinting and conventional epidemiologic methods. *N.Engl.J Med* **330**:1710-1716.
- Allen, B. W. and D. A. Mitchison.** 1992. Counts of viable tubercle bacilli in sputum related to smear and culture gradings. *Med Lab Sci.* **49**:94-98.
- Altare, F., A. Durandy, D. Lammas, J. F. Emile, S. Lamhamedi, F. Le Deist, P. Drysdale, E. Jouanguy, R. Doffinger, F. Bernaudin, O. Jeppsson, J. A. Gollob, E. Meinel, A. W. Segal, A. Fischer, D. Kumararatne, and J. L. Casanova.** 1998. Impairment of mycobacterial immunity in human interleukin-12 receptor deficiency. *Science* **280**:1432-1435.
- Andersen, P., D. Askgaard, A. Gottschau, J. Bennedsen, S. Nagai, and I. Heron.** 1992. Identification of immunodominant antigens during infection with *Mycobacterium tuberculosis*. *Scand.J Immunol.* **36**:823-831.
- Andersen, P. and I. Heron.** 1993. Specificity of a protective memory immune response against *Mycobacterium tuberculosis*. *Infect.Immun.* **61**:844-851.
- Andersen, P.** 1994. Effective vaccination of mice against *Mycobacterium tuberculosis* infection with a soluble mixture of secreted mycobacterial proteins. *Infect.Immun.* **62**:2536-2544.
- Arend, S. M., P. Andersen, K. E. van Meijgaarden, R. L. Skjot, Y. W. Subronto, J. T. van Dissel, and T. H. Ottenhoff.** 2000. Detection of active tuberculosis infection by T cell responses to early-secreted antigenic target 6-kDa protein and culture filtrate protein 10. *J Infect.Dis.* **181**:1850-1854.
- Arruda, S., G. Bomfim, R. Knights, T. Huima-Byron, and L. W. Riley.** 1993. Cloning of an *M. tuberculosis* DNA fragment associated with entry and survival inside cells. *Science* **261**:1454-1457.
- Aubert-Pivert, E. M., F. M. Chedevergne, G. M. Lopez-Ramirez, J. H. Colle, P. L. Scheinmann, B. M. Gicquel, and J. M. de Blic.** 2000. Cytokine transcripts in pediatric tuberculosis: a study with bronchoalveolar cells. *Tuber.Lung Dis.* **80**:249-258.

- Aung, H., Z. Toossi, S. M. McKenna, P. Gogate, J. Sierra, E. Sada, and E. A. Rich.** 2000. Expression of transforming growth factor-beta but not tumor necrosis factor-alpha, interferon-gamma, and interleukin-4 in granulomatous lung lesions in tuberculosis. *Tuber.Lung Dis.* **80**:61-67.
- Austyn, J. M.** 1996. New insights into the mobilization and phagocytic activity of dendritic cells. *J Exp.Med* **183**:1287-1292.
- Barnes, P. F., S. J. Fong, P. J. Brennan, P. E. Twomey, A. Mazumder, and R. L. Modlin.** 1990. Local production of tumor necrosis factor and IFN-gamma in tuberculous pleuritis. *J Immunol.* **145**:149-154.
- Barnes, P. F., C. L. Grisso, J. S. Abrams, H. Band, T. H. Rea, and R. L. Modlin.** 1992. Gamma delta T lymphocytes in human tuberculosis. *J Infect.Dis.* **165**:506-512.
- Barry, C. E., III.** 1997. New horizons in the treatment of tuberculosis. *Biochem.Pharmacol.* **54**:1165-1172.
- Bean, A. G., D. R. Roach, H. Briscoe, M. P. France, H. Korner, J. D. Sedgwick, and W. J. Britton.** 1999. Structural deficiencies in granuloma formation in TNF gene-targeted mice underlie the heightened susceptibility to aerosol Mycobacterium tuberculosis infection, which is not compensated for by lymphotoxin. *J Immunol.* **162**:3504-3511.
- Behr, M. A., S. A. Warren, H. Salamon, P. C. Hopewell, d. L. Ponce, C. L. Daley, and P. M. Small.** 1999. Transmission of Mycobacterium tuberculosis from patients smear-negative for acid-fast bacilli. *Lancet* **353**:444-449.
- Bendelac, A. and D. T. Fearon.** 1997. Innate pathways that control acquired immunity. *Curr.Opin.Immunol* **9**:1-3.
- Bergeron, A., M. Bonay, M. Kambouchner, D. Lecossier, M. Riquet, P. Soler, A. Hance, and A. Tazi.** 1997. Cytokine patterns in tuberculous and sarcoid granulomas: correlations with histopathologic features of the granulomatous response. *J Immunol.* **159** :3034-3043.
- Bergmann, J. S. and G. L. Woods.** 1996. Clinical evaluation of the Roche AMPLICOR PCR Mycobacterium tuberculosis test for detection of M. tuberculosis in respiratory specimens. *J.Clin.Microbiol.* **34**:1083-1085.

- Berthet, F. X., M. Lagranderie, P. Gounon, C. Laurent-Winter, D. Ensergueix, P. Chavarot, F. Thouron, E. Maranghi, V. Pelicic, D. Portnoi, G. Marchal, and B. Gicquel.** 1998. Attenuation of virulence by disruption of the *Mycobacterium tuberculosis* *erp* gene. *Science* **282**:759-762.
- Bodnar, K. A., N. V. Serbina, and J. L. Flynn.** 2001. Fate of *Mycobacterium tuberculosis* within murine dendritic cells. *Infect.Immun.* **69**:800-809.
- Boesen, H., B. N. Jensen, T. Wilcke, and P. Andersen.** 1995. Human T-cell responses to secreted antigen fractions of *Mycobacterium tuberculosis*. *Infect.Immun.* **63**:1491-1497.
- Boismenu, R. and W. L. Havran.** 1997. An innate view of gamma delta T cells. *Curr.Opin.Immunol* **9**:57-63.
- Boom, W. H., K. A. Chervenak, M. A. Mincek, and J. J. Ellner.** 1992. Role of the mononuclear phagocyte as an antigen-presenting cell for human gamma delta T cells activated by live *Mycobacterium tuberculosis*. *Infect.Immun.* **60**:3480-3488.
- Bremer, H. and M. Ehrenberg.** 1995. Guanosine tetraphosphate as a global regulator of bacterial RNA synthesis: a model involving RNA polymerase pausing and queuing. *Biochim.Biophys.Acta* **1262**:15-36.
- Bridger, W. A. and W. Paranchych.** 1978. *relA* gene control of bacterial glycogen synthesis. *Can.J.Biochem.* **56**:403-406.
- Brisson-Noel, A., B. Gicquel, D. Lecossier, V. Levy-Frebault, X. Nassif, and A. J. Hance.** 1989. Rapid diagnosis of tuberculosis by amplification of mycobacterial DNA in clinical samples. *Lancet* **2**:1069-1071.
- Britton, W. J., N. Meadows, D. A. Rathjen, D. R. Roach, and H. Briscoe.** 1998. A tumor necrosis factor mimetic peptide activates a murine macrophage cell line to inhibit mycobacterial growth in a nitric oxide-dependent fashion. *Infect.Immun.* **66**:2122-2127.
- Brown, D. W., B. S. Baker, J. M. Ovigne, C. Hardman, A. V. Powles, and L. Fry.** 2000. Skin CD4+ T cells produce interferon-gamma in vitro in response to streptococcal antigens in chronic plaque psoriasis. *J Invest Dermatol.* **114**:576-580.

- Brozna, J. P., M. Horan, J. M. Rademacher, K. M. Pabst, and M. J. Pabst.** 1991. Monocyte responses to sulfatide from *Mycobacterium tuberculosis*: inhibition of priming for enhanced release of superoxide, associated with increased secretion of interleukin-1 and tumor necrosis factor alpha, and altered protein phosphorylation. *Infect.Immun.* **59**:2542-2548.
- Byren, I.** 1999. Infectious Diseases with Lymphadenopathy. *In*: Root, R.K. ed: Clinical Infectious Diseases: A Practical Approach. Oxford, Oxford University Press: pp 505 - 512
- Camacho, L. R., D. Ensergueix, E. Perez, B. Gicquel, and C. Guilhot.** 1999. Identification of a virulence gene cluster of *Mycobacterium tuberculosis* by signature-tagged transposon mutagenesis. *Mol.Microbiol* **34**:257-267.
- Cappelli, G., P. Volpe, A. Sanduzzi, A. Sacchi, V. Colizzi, and F. Mariani.** 2001. Human Macrophage Gamma Interferon Decreases Gene Expression but Not Replication of *Mycobacterium tuberculosis*: Analysis of the Host- Pathogen Reciprocal Influence on Transcription in a Comparison of Strains H37Rv and CMT97. *Infect.Immun.* **69**:7262-7270.
- Caviedes, L., T. S. Lee, R. H. Gilman, P. Sheen, E. Spellman, E. H. Lee, D. E. Berg, and S. Montenegro-James.** 2000. Rapid, efficient detection and drug susceptibility testing of *Mycobacterium tuberculosis* in sputum by microscopic observation of broth cultures. The Tuberculosis Working Group in Peru. *J Clin.Microbiol.* **38**:1203-1208.
- Chambers, C. E., D. D. McIntyre, M. Mouck, and P. A. Sokol.** 1996. Physical and structural characterization of yersiniophore, a siderophore produced by clinical isolates of *Yersinia enterocolitica*. *Biometals* **9**:157-167.
- Chang, T. L., C. M. Shea, S. Urioste, R. C. Thompson, W. H. Boom, and A. K. Abbas.** 1990. Heterogeneity of helper/inducer T lymphocytes. III. Responses of IL-2- and IL-4-producing (Th1 and Th2) clones to antigens presented by different accessory cells. *J Immunol.* **145**:2803-2808.
- Chensue, S. W., K. S. Warmington, J. H. Ruth, P. Lincoln, and S. L. Kunkel.** 1995. Cytokine function during mycobacterial and schistosomal antigen-induced pulmonary granuloma formation. Local and regional participation of IFN- gamma, IL-10, and TNF. *J Immunol.* **154**:5969-5976.

- Chevrel-Dellagi, D., A. Abderrahman, R. Haltiti, H. Koubaji, B. Gicquel, and K. Dellagi.** 1993. Large-scale DNA fingerprinting of *Mycobacterium tuberculosis* strains as a tool for epidemiological studies of tuberculosis. *J Clin Microbiol* **31**:2446-2450.
- Chiba, Y. and T. Kurihara.** 1979. Development of pulmonary tuberculosis with special reference to the time interval after tuberculin conversion. *Bull.Int.Union Tuberc* **54**:263-264.
- Chien, Y. H., R. Jores, and M. P. Crowley.** 1996. Recognition by gamma/delta T cells. *Annu.Rev Immunol* **14**:511-532.
- Chouchane, S., I. Lippai, and R. S. Magliozzo.** 2000. Catalase-peroxidase (*Mycobacterium tuberculosis* KatG) catalysis and isoniazid activation. *Biochemistry* **39**:9975-9983.
- Cole, S. T., R. Brosch, J. Parkhill, T. Garnier, C. Churcher, D. Harris, S. V. Gordon, K. Eiglmeier, S. Gas, C. E. Barry, III, F. Tekaiia, K. Badcock, D. Basham, D. Brown, T. Chillingworth, R. Connor, R. Davies, K. Devlin, T. Feltwell, S. Gentles, N. Hamlin, S. Holroyd, T. Hornsby, K. Jagels, B. G. Barrell, and .** 1998. Deciphering the biology of *Mycobacterium tuberculosis* from the complete genome sequence. *Nature* **393**:537-544.
- Constant, S. L. and K. Bottomly.** 1997. Induction of Th1 and Th2 CD4+ T cell responses: the alternative approaches. *Annu.Rev Immunol* **15**:297-322.
- Cooper, A. M., A. D. Roberts, E. R. Rhoades, J. E. Callahan, D. M. Getzy, and I. M. Orme.** 1995. The role of interleukin-12 in acquired immunity to *Mycobacterium tuberculosis* infection. *Immunology* **84**:423-432.
- Cooper, A. M., J. Magram, J. Ferrante, and I. M. Orme.** 1997. Interleukin 12 (IL-12) is crucial to the development of protective immunity in mice intravenously infected with *mycobacterium tuberculosis*. *J Exp.Med* **186**:39-45.
- Cousins, D. V., S. D. Wilton, B. R. Francis, and B. L. Gow.** 1992. Use of polymerase chain reaction for rapid diagnosis of tuberculosis. *J.Clin.Microbiol.* **30**:255-258.
- Cox, J. S., B. Chen, M. McNeil, and W. R. Jacobs, Jr.** 1999. Complex lipid determines tissue-specific replication of *Mycobacterium tuberculosis* in mice. *Nature* **402**:79-83.

- Cunningham, A. F. and C. L. Spreadbury.** 1998. Mycobacterial stationary phase induced by low oxygen tension: cell wall thickening and localization of the 16-kilodalton alpha-crystallin homolog. *J Bacteriol.* **180**:801-808.
- D'Andrea, A., M. Aste-Amezaga, N. M. Valiante, X. Ma, M. Kubin, and G. Trinchieri.** 1993. Interleukin 10 (IL-10) inhibits human lymphocyte interferon gamma- production by suppressing natural killer cell stimulatory factor/IL-12 synthesis in accessory cells. *J Exp.Med* **178**:1041-1048.
- Daley, C. L., P. M. Small, G. F. Schecter, G. K. Schoolnik, R. A. McAdam, W. R. Jacobs, Jr., and P. C. Hopewell.** 1992. An outbreak of tuberculosis with accelerated progression among persons infected with the human immunodeficiency virus. An analysis using restriction-fragment-length polymorphisms. *N.Engl.J Med* **326**:231-235.
- Dannenberg, A. M. Jr.** 1980. Pathogenesis of pulmonary tuberculosis. *In*: Fishman, A.P. ed, *Pulmonary Diseases and Disorders*. New York: McGraw-Hill Book Co.: pp 1264 - 1281
- Dannenberg, A. M., Jr.** 1991. Delayed-type hypersensitivity and cell-mediated immunity in the pathogenesis of tuberculosis. *Immunol.Today* **12**:228-233.
- Dannenberg, A. M., Jr.** 1994. Roles of cytotoxic delayed-type hypersensitivity and macrophage-activating cell-mediated immunity in the pathogenesis of tuberculosis. *Immunobiology* **191**:461-473.
- Dannenberg, A. M. Jr and Rook, G. A. W.** 1994. Pathogenesis of pulmonary tuberculosis: An interplay of tissue-damaging and macrophage-activating immune responses – dual mechanisms that control bacillary multiplication. *In*: Bloom, B. R. ed: *Tuberculosis: Pathogenesis, Protection and Control*. Washington, DC, American Society for Microbiology: pp 459 - 483
- De Cock, K. M. and D. Wilkinson.** 1995. Tuberculosis control in resource-poor countries: alternative approaches in the era of HIV. *Lancet* **346**:675-677.
- de Souza, F. M.** 1999. Modeling the dynamics of HIV-1 and CD4 and CD8 lymphocytes. *IEEE Eng Med Biol.Mag.* **18**:21-24.
- De Voss, J. J., K. Rutter, B. G. Schroeder, and C. E. Barry, III.** 1999. Iron acquisition and metabolism by mycobacteria. *J Bacteriol.* **181**:4443-4451.

- De Voss, J. J., K. Rutter, B. G. Schroeder, H. Su, Y. Zhu, and C. E. Barry, III.** 2000. The salicylate-derived mycobactin siderophores of *Mycobacterium tuberculosis* are essential for growth in macrophages. *Proc.Natl.Acad.Sci.U.S.A* **97**:1252-1257.
- de Waal, M. R., J. S. Abrams, S. M. Zurawski, J. C. Lecron, S. Mohan-Peterson, B. Sanjanwala, B. Bennett, J. Silver, J. E. de Vries, and H. Yssel.** 1995. Differential regulation of IL-13 and IL-4 production by human CD8⁺ and CD4⁺ Th0, Th1 and Th2 T cell clones and EBV-transformed B cells. *Int.Immunol* **7**:1405-1416.
- Del Prete, G., E. Maggi, and S. Romagnani.** 1994. Human Th1 and Th2 cells: functional properties, mechanisms of regulation, and role in disease. *Lab Invest* **70**:299-306.
- Dolin, P. J., M. C. Raviglione, and A. Kochi.** 1994. Global tuberculosis incidence and mortality during 1990-2000. *Bull.World Health Organ* **72**:213-220.
- Draper, J., Scott, R., Armitage, P. and Walden, R.** 1988. *Plant Genetic Transformation and Gene Expression: A Laboratory Manual.* Oxford: Blackwell Scientific Publications.
- Dye, C., G. P. Garnett, K. Sleeman, and B. G. Williams.** 1998. Prospects for worldwide tuberculosis control under the WHO DOTS strategy. Directly observed short-course therapy. *Lancet* **352**:1886-1891.
- Dye, C., S. Scheele, P. Dolin, V. Pathania, and M. C. Raviglione.** 1999. Consensus statement. Global burden of tuberculosis: estimated incidence, prevalence, and mortality by country. WHO Global Surveillance and Monitoring Project. *JAMA* **282**:677-686.
- Dykhhoorn, D. M., R. St Pierre, and T. Linn.** 1996. Synthesis of the beta and beta' subunits of *Escherichia coli* RNA polymerase is autogenously regulated in vivo by both transcriptional and translational mechanisms. *Mol.Microbiol* **19**:483-493.
- Eichel, J., D. Chang, D. Reisenberg, and J. E. J. Cronan.** 1999. Effect of ppGpp on *Escherichia coli* cyclopropane fatty acid synthesis is mediated through, the RpoS sigma factor. *J.Bacteriol.* **181**:572-576.

- Eisenach, K. D., M. D. Sifford, M. D. Cave, J. H. Bates, and J. T. Crawford.** 1991. Detection of *Mycobacterium tuberculosis* in sputum samples using a polymerase chain reaction. *Am.Rev.Respir.Dis.* **144**:1160-1163.
- Enk, A. H., V. L. Angeloni, M. C. Udey, and S. I. Katz.** 1993. Inhibition of Langerhans cell antigen-presenting function by IL-10. A role for IL-10 in induction of tolerance. *J Immunol.* **151**:2390-2398.
- Faith, A., D. M. Schellenberg, A. D. Rees, and D. M. Mitchell.** 1992. Antigenic specificity and subset analysis of T cells isolated from the bronchoalveolar lavage and pleural effusion of patients with lung disease. *Clin Exp.Immunol* **87**:272-278.
- Feng, C. G. and W. J. Britton.** 2000. CD4+ and CD8+ T cells mediate adoptive immunity to aerosol infection of *Mycobacterium bovis* bacillus Calmette-Gu?erin. *J Infect.Dis.* **181**:1846-1849.
- Fenhalls, G., A. Wong, J. Bezuidenhout, P. van Helden, P. Bardin, and P. T. Lukey.** 2000. In situ production of gamma interferon, interleukin-4, and tumor necrosis factor alpha mRNA in human lung tuberculous granulomas. *Infect.Immun.* **68**:2827-2836.
- Fernandez-Botran, R., V. M. Sanders, K. G. Oliver, Y. W. Chen, P. H. Krammer, J. W. Uhr, and E. S. Vitetta.** 1986. Interleukin 4 mediates autocrine growth of helper T cells after antigenic stimulation. *Proc.Natl.Acad.Sci.U.S.A* **83**:9689-9693.
- Fiorentino, D. F., A. Zlotnik, P. Vieira, T. R. Mosmann, M. Howard, K. W. Moore, and A. O'Garra.** 1991. IL-10 acts on the antigen-presenting cell to inhibit cytokine production by Th1 cells. *J Immunol.* **146**:3444-3451.
- Firestein, G. S., W. D. Roeder, J. A. Laxer, K. S. Townsend, C. T. Weaver, J. T. Hom, J. Linton, B. E. Torbett, and A. L. Glasebrook.** 1989. A new murine CD4+ T cell subset with an unrestricted cytokine profile. *J Immunol.* **143**:518-525.
- Flesch, I. E. A. and S. H. E. Kaufmann.** 1991. Mechanisms Involved in Mycobacterial Growth Inhibition by Gamma Interferon-Activated Bone Marrow Macrophages: Role of Reactive Nitrogen Intermediates. *Infect.Immun.* **59**:3213-3218.
- Florczyk, M. A., L. A. McCue, R. F. Stack, C. R. Hauer, and K. A. McDonough.** 2001. Identification and characterization of mycobacterial proteins differentially expressed under standing

and shaking culture conditions, including Rv2623 from a novel class of putative ATP-binding proteins. *Infect.Immun.* 69:5777-5785.

Flynn, J. L., M. M. Goldstein, K. J. Triebold, B. Koller, and B. R. Bloom. 1992. Major histocompatibility complex class I-restricted T cells are required for resistance to *Mycobacterium tuberculosis* infection. *Proc.Natl.Acad.Sci.U.S.A* 89:12013-12017.

Flynn, J. L., M. M. Goldstein, J. Chan, K. J. Triebold, K. Pfeffer, C. J. Lowenstein, R. Schreiber, T. W. Mak, and B. R. Bloom. 1995. Tumor necrosis factor-alpha is required in the protective immune response against *Mycobacterium tuberculosis* in mice. *Immunity.* 2:561-572.

Fortsch, D., M. Rollinghoff, and S. Stenger. 2000. IL-10 converts human dendritic cells into macrophage-like cells with increased antibacterial activity against virulent *Mycobacterium tuberculosis*. *J Immunol* 165:978-987.

Fourie, P. B. and K. Weyer. 2000. Tuberculosis and HIV in South Africa. Medical Research Council Press Release. <http://www.mrc.ac.za/pressrel/20007/7press2000.html> .

Frucht, D. M. and S. M. Holland. 1996. Defective monocyte costimulation for IFN-gamma production in familial disseminated *Mycobacterium avium* complex infection: abnormal IL-12 regulation. *J Immunol* 157:411-416.

Fujii, H., J. Ishihara, A. Fukaura, N. Kashima, H. Tazawa, H. Nakajima, H. Ide, and T. Takahashi. 1992. Early diagnosis of tuberculosis by fiberoptic bronchoscopy. *Tuber.Lung Dis.* 73:167-169.

Fulton, S. A., J. V. Cross, Z. T. Toossi, and W. H. Boom. 1998. Regulation of interleukin-12 by interleukin-10, transforming growth factor-beta, tumor necrosis factor-alpha, and interferon-gamma in human monocytes infected with *Mycobacterium tuberculosis* H37Ra. *J Infect.Dis.* 178:1105-1114.

Gajewski, T. F. and F. W. Fitch. 1988. Anti-proliferative effect of IFN-gamma in immune regulation. I. IFN- gamma inhibits the proliferation of Th2 but not Th1 murine helper T lymphocyte clones. *J Immunol.* 140:4245-4252.

Garcia-Quintanilla, A., L. Garcia, G. Tudo, M. Navarro, J. Gonzalez, and M. T. Jimenez de Anta. 2000. Single-tube balanced heminested PCR for detecting *Mycobacterium tuberculosis* in smear-negative samples. *J.Clin.Microbiol.* **38**:1166-1169.

Gillespie, J., L. L. Barton, and E. W. Rypka. 1986. Phenotypic changes in mycobacteria grown in oxygen-limited conditions. *J Med Microbiol* **21**:251-255.

Glynn, J. R., J. Bauer, A. S. de Boer, M. W. Borgdorff, P. E. Fine, P. Godfrey-Faussett, and E. Vynnycky. 1999. Interpreting DNA fingerprint clusters of *Mycobacterium tuberculosis*. European Concerted Action on Molecular Epidemiology and Control of Tuberculosis. *Int.J Tuberc Lung Dis.* **3**:1055-1060.

Gobin, J., C. H. Moore, J. R. Reeve, Jr., D. K. Wong, B. W. Gibson, and M. A. Horwitz. 1995. Iron acquisition by *Mycobacterium tuberculosis*: isolation and characterization of a family of iron-binding exochelins. *Proc.Natl.Acad.Sci.U.S.A* **92**:5189-5193.

Gobin, J. and M. A. Horwitz. 1996. Exochelins of *Mycobacterium tuberculosis* remove iron from human iron-binding proteins and donate iron to mycobactins in the *M. tuberculosis* cell wall. *J Exp.Med* **183**:1527-1532.

Goebeler, M., T. Yoshimura, A. Toksoy, U. Ritter, E. B. Brocker, and R. Gillitzer. 1997. The chemokine repertoire of human dermal microvascular endothelial cells and its regulation by inflammatory cytokines. *J Invest Dermatol.* **108**:445-451.

Gold, B., G. M. Rodriguez, S. A. Marras, M. Pentecost, and I. Smith. 2001. The *Mycobacterium tuberculosis* IdeR is a dual functional regulator that controls transcription of genes involved in iron acquisition, iron storage and survival in macrophages. *Mol.Microbiol* **42**:851-865.

Gonzalez-Juarrero, M. and I. M. Orme. 2001. Characterization of murine lung dendritic cells infected with *Mycobacterium tuberculosis*. *Infect.Immun.* **69**:1127-1133.

Gordon, A. H., P. D. Hart, and M. R. Young. 1980. Ammonia inhibits phagosome-lysosome fusion in macrophages. *Nature* **286**:79-80.

- Graham, J. E. and J. E. Clark-Curtiss.** 1999. Identification of *Mycobacterium tuberculosis* RNAs synthesized in response to phagocytosis by human macrophages by selective capture of transcribed sequences (SCOTS). *Proc.Natl.Acad.Sci.U.S.A* **96**:11554-11559.
- Harboe, M., T. Oettinger, H. G. Wiker, I. Rosenkrands, and P. Andersen.** 1996. Evidence for occurrence of the ESAT-6 protein in *Mycobacterium tuberculosis* and virulent *Mycobacterium bovis* and for its absence in *Mycobacterium bovis* BCG. *Infect.Immun.* **64**:16-22.
- Harth, G. and M. A. Horwitz.** 1999. An inhibitor of exported *Mycobacterium tuberculosis* glutamine synthetase selectively blocks the growth of pathogenic mycobacteria in axenic culture and in human monocytes: extracellular proteins as potential novel drug targets. *J Exp.Med* **189**:1425-1436.
- Harvell, J. D., W. K. Hadley, and V. L. Ng.** 2000. Increased sensitivity of the BACTEC 460 mycobacterial radiometric broth culture system does not decrease the number of respiratory specimens required for a definitive diagnosis of pulmonary tuberculosis. *J.Clin.Microbiol.* **38**:3608-3611.
- Heath, R. J., S. Jackowski, and C. O. Rock.** 1994. Guanosine tetraphosphate inhibition of fatty acid and phospholipid synthesis in *Escherichia coli* is relieved by overexpression of glycerol-3-phosphate acyltransferase (*plsB*). *J.Biol.Chem.* **269**:26584-26590.
- Heifets, L.** 1986. Rapid automated method (BACTEC system) in clinical mycobacteriology. *Semin.Respir.Med.* **1**:249.
- Heifets, L.** 1997. Mycobacteriology laboratory. *Clin.Chest Med* **18**:35-53.
- Heifets, L., T. Linder, T. Sanchez, D. Spencer, and J. Brennan.** 2000. Two liquid medium systems, mycobacteria growth indicator tube and MB redox tube, for *Mycobacterium tuberculosis* isolation from sputum specimens. *J Clin.Microbiol.* **38**:1227-1230.
- Heinemeyer, E. A., M. Geis, and D. Richter.** 1978. Degradation of guanosine 3'-diphosphate 5'-diphosphate in vitro by the *spoT* gene product of *Escherichia coli*. *Eur.J Biochem.* **89**:125-131.
- Hermans, P. W., D. van Soolingen, E. M. Bik, P. E. de Haas, J. W. Dale, and J. D. van Embden.** 1991. Insertion element IS987 from *Mycobacterium bovis* BCG is located in a hot-spot integration region for insertion elements in *Mycobacterium tuberculosis* complex strains. *Infect.Immun.* **59**:2695-2705.

- Hermans, P. W., D. van Soolingen, and J. D. van Embden.** 1992. Characterization of a major polymorphic tandem repeat in *Mycobacterium tuberculosis* and its potential use in the epidemiology of *Mycobacterium kansasii* and *Mycobacterium goodii*. *J Bacteriol.* **174**:4157-4165.
- Hernandez-Pando, R., H. Orozco, A. Sampieri, L. Pavon, C. Velasquillo, J. Larriva-Sahd, J. M. Alcocer, and M. V. Madrid.** 1996. Correlation between the kinetics of Th1, Th2 cells and pathology in a murine model of experimental pulmonary tuberculosis. *Immunology* **89**:26-33.
- Heym, B., Y. Zhang, S. Poulet, D. Young, and S. T. Cole.** 1993. Characterization of the *katG* gene encoding a catalase-peroxidase required for the isoniazid susceptibility of *Mycobacterium tuberculosis*. *J Bacteriol.* **175**:4255-4259.
- Heym, B., B. Saint-Joanis, and S. T. Cole.** 1999. The molecular basis of isoniazid resistance in *Mycobacterium tuberculosis*. *Tuber.Lung Dis.* **79**:267-271.
- Hoheisel, G. B., L. Tabak, H. Teschler, F. Erkan, C. Kroegel, and U. Costabel.** 1994. Bronchoalveolar lavage cytology and immunocytology in pulmonary tuberculosis. *Am J Respir.Crit Care Med* **149**:460-463.
- Honer zu, B. K., A. Miczak, D. L. Swenson, and D. G. Russell.** 1999. Characterization of activity and expression of isocitrate lyase in *Mycobacterium avium* and *Mycobacterium tuberculosis*. *J.Bacteriol.* **181**:7161-7167.
- Hsieh, C. S., S. E. Macatonia, C. S. Tripp, S. F. Wolf, A. O'Garra, and K. M. Murphy.** 1993. Development of TH1 CD4+ T cells through IL-12 produced by *Listeria*- induced macrophages. *Science* **260**:547-549.
- Hu, Y. M., P. D. Butcher, K. Sole, D. A. Mitchison, and A. R. Coates.** 1998. Protein synthesis is shutdown in dormant *Mycobacterium tuberculosis* and is reversed by oxygen or heat shock. *FEMS Microbiol Lett.* **158**:139-145.
- Huhti, E., E. Brander, S. Paloheimo, and S. Sutinen.** 1975. Tuberculosis of the cervical lymph nodes: a clinical, pathological and bacteriological study. *Tubercle.* **56**:27-36.
- Humphries, M. J., Lam, W. K. and Teah, R.** 1994. Non-Respiratory Tuberculosis. *In: Davies, P. D. O. Clinical Tuberculosis.* London, Chapman and Hall: pp 93 - 122

- Hutter, B. and T. Dick.** 1999. Up-regulation of narX, encoding a putative 'fused nitrate reductase' in anaerobic dormant *Mycobacterium bovis* BCG. *FEMS Microbiol Lett.* **178**:63-69.
- Jackett, P. S., V. R. Aber, and D. B. Lowrie.** 1978. Virulence and resistance to superoxide, low pH and hydrogen peroxide among strains of *Mycobacterium tuberculosis*. *J Gen.Microbiol* **104**:37-45.
- Jackett, P. S., V. R. Aber, and D. B. Lowrie.** 1978(a). Virulence of *Mycobacterium tuberculosis* and susceptibility to peroxidative killing systems. *J Gen.Microbiol* **107**:273-278.
- Jacobs, M., N. Brown, N. Allie, R. Gulert, and B. Ryffel.** 2000. Increased resistance to mycobacterial infection in the absence of interleukin-10. *Immunology* **100**:494-501.
- Johnson, D. R. and J. S. Pober.** 1990. Tumor necrosis factor and immune interferon synergistically increase transcription of HLA class I h. *Proc.Natl.Acad.Sci.U.S.A* **87**:5183-5187.
- Johnsson, K., W. A. Froland, and P. G. Schultz.** 1997. Overexpression, purification, and characterization of the catalase- peroxidase KatG from *Mycobacterium tuberculosis*. *J Biol.Chem.* **272**:2834-2840.
- Johnston, R. B., Jr. and S. Kitagawa.** 1985. Molecular basis for the enhanced respiratory burst of activated macrophages. *Fed.Proc.* **44**:2927-2932.
- Juffermans, N.P., S. Florquin, L. Camoglio, A. Verbou, A.H. Kolk, P. Speedman, S.J.H. van Deventer, and T. van der Poll.** 2000. Interleukin-1 Singaling is Essential for Host Defense during Murine Pulmonary Tuberculosis. *J. Infect. Dis.;* **182**:902-908
- Kashlev, M., J. Lee, K. Zalenskaya, V. Nikiforov, and A. Goldfarb.** 1990. Blocking of the initiation-to-elongation transition by a transdominant RNA polymerase mutation. *Science* **248**:1006-1009.
- Kashlev, M., J. Lee, K. Zalenskaya, V. Nikiforov, and A. Goldfarb.** 1990. Blocking of the initiation-to-elongation transition by a transdominant RNA polymerase mutation. *Science* **248**:1006-1009.
- Kaufmann, S. H.** 1996. gamma/delta and other unconventional T lymphocytes: what do they see and what do they do? *Proc.Natl.Acad.Sci.U.S.A* **93**:2272-2279.

- Kaufmann, S. H. E.** 1993. Immunity to intracellular bacteria. *Annu.Rev.Immunol.* **11**:129-135.
- Keane, J., M. K. Balcewicz-Sablinska, H. G. Remold, G. L. Chupp, B. B. Meek, M. J. Fenton, and H. Kornfeld.** 1997. Infection by *Mycobacterium tuberculosis* promotes human alveolar macrophage apoptosis. *Infect.Immun.* **65**:298-304.
- Keane, J., H. G. Remold, and H. Kornfeld.** 2000. Virulent *Mycobacterium tuberculosis* strains evade apoptosis of infected alveolar macrophages. *J Immunol.* **164**:2016-2020.
- Kennedy, D. H. and R. J. Fallon.** 1979. Tuberculous meningitis. *JAMA* **241**:264-268.
- Kiepiela, P., K. S. Bishop, A. N. Smith, L. Roux, and D. F. York.** 2000. Genomic mutations in the *katG*, *inhA* and *aphC* genes are useful for the prediction of isoniazid resistance in *Mycobacterium tuberculosis* isolates from Kwazulu Natal, South Africa. *Tuber.Lung Dis.* **80**:47-56.
- Kindler, V., A. P. Sappino, G. E. Grau, P. F. Piguet, and P. Vassalli.** 1989. The inducing role of tumor necrosis factor in the development of bactericidal granulomas during BCG infection. *Cell* **56**:731-740.
- Kochi, A.** 1991. The global tuberculosis situation and the new control strategy of the World Health Organization. *Tubercle* **72**:1-6.
- Kontoghiorghes, G. J. and E. D. Weinberg.** 1995. Iron: mammalian defense systems, mechanisms of disease, and chelation therapy approaches. *Blood Rev.* **9**:33-45.
- Kopf, M., G. Le Gros, M. Bachmann, M. C. Lamers, H. Bluethmann, and G. Kohler.** 1993. Disruption of the murine IL-4 gene blocks Th2 cytokine responses. *Nature* **362**:245-248.
- Kornberg, H. L.** 1966. The role and control of the glyoxylate cycle in *Escherichia coli*. *Biochem.J* **99**:1-11.
- Kurt-Jones, E. A., S. Hamberg, J. Ohara, W. E. Paul, and A. K. Abbas.** 1987. Heterogeneity of helper/inducer T lymphocytes. I. Lymphokine production and lymphokine responsiveness. *J Exp.Med* **166**:1774-1787.

- Kvint, K., C. Hosbond, A. Farewell, O. Nybroe, and T. Nystrom.** 2000. Emergency derepression: stringency allows RNA polymerase to override negative control by an active repressor. *Mol.Microbiol* **35**:435-443.
- Laichalk, L. L., J. M. Danforth, and T. J. Standiford.** 1996. Interleukin-10 inhibits neutrophil phagocytic and bactericidal activity. *FEMS Immunol.Med Microbiol* **15**:181-187.
- Lalvani, A., R. Brookes, R. J. Wilkinson, A. S. Malin, A. A. Pathan, P. Andersen, H. Dockrell, G. Pasvol, and A. V. Hill.** 1998. Human cytolytic and interferon gamma-secreting CD8+ T lymphocytes specific for *Mycobacterium tuberculosis*. *Proc.Natl.Acad.Sci.U.S.A* **95**:270-275.
- Lalvani, A., P. Nagvenkar, Z. Udawadia, A. A. Pathan, K. A. Wilkinson, J. S. Shastri, K. Ewer, A. V. Hill, A. Mehta, and C. Rodrigues.** 2001. Enumeration of T cells specific for RD1-encoded antigens suggests a high prevalence of latent *Mycobacterium tuberculosis* infection in healthy urban Indians. *J Infect.Dis.* **183**:469-477.
- Lapierre, L. A., W. Fiers, and J. S. Pober.** 1988. Three distinct classes of regulatory cytokines control endothelial cell MHC antigen expression. Interactions with immune gamma interferon differentiate the effects of tumor necrosis factor and lymphotoxin from those of leukocyte alpha and fibroblast beta interferons. *J Exp.Med* **167**:794-804.
- Law, K., M. Weiden, T. Harkin, K. Tchou-Wong, C. Chi, and W. N. Rom.** 1996. Increased release of interleukin-1 beta, interleukin-6, and tumor necrosis factor-alpha by bronchoalveolar cells lavaged from involved sites in pulmonary tuberculosis. *Am J Respir.Crit Care Med* **153**:799-804.
- Le, T. K., K. H. Bach, M. L. Ho, N. V. Le, T. N. Nguyen, D. Chevrier, and J. L. Guesdon.** 2000. Molecular fingerprinting of *Mycobacterium tuberculosis* strains isolated in Vietnam using IS6110 as probe. *Tuber.Lung Dis.* **80**:75-83.
- Lenzini, L., P. Rottoli, and L. Rottoli.** 1977. The spectrum of human tuberculosis. *Clin Exp.Immunol.* **27**:230-237.
- Levy, H., C. Feldman, H. Sacho, M. H. van der, J. Kallenbach, and H. Koornhof.** 1989. A reevaluation of sputum microscopy and culture in the diagnosis of pulmonary tuberculosis. *Chest* **95**:1193-1197.

- Lewinsohn, D. M., M. R. Alderson, A. L. Briden, S. R. Riddell, S. G. Reed, and K. H. Grabstein.** 1998. Characterization of human CD8⁺ T cells reactive with Mycobacterium tuberculosis-infected antigen-presenting cells. *J Exp.Med* **187**:1633-1640.
- Li, Z., C. Kelley, F. Collins, D. Rouse, and S. Morris.** 1998. Expression of katG in Mycobacterium tuberculosis is associated with its growth and persistence in mice and guinea pigs. *J Infect.Dis.* **177**:1030-1035.
- Liang, S. T., Y. C. Xu, P. Dennis, and H. Bremer.** 2000. mRNA composition and control of bacterial gene expression. *J Bacteriol.* **182**:3037-3044.
- Lichtman, A. H., J. Chin, J. A. Schmidt, and A. K. Abbas.** 1988. Role of interleukin 1 in the activation of T lymphocytes. *Proc.Natl.Acad.Sci.U.S.A* **85**:9699-9703.
- Lin, Y., M. Zhang, F. M. Hofman, J. Gong, and P. F. Barnes.** 1996. Absence of a prominent Th2 cytokine response in human tuberculosis. *Infect.Immun.* **64**:1351-1356.
- Lipsky, B. A., J. Gates, F. C. Tenover, and J. J. Plorde.** 1984. Factors affecting the clinical value of microscopy for acid-fast bacilli. *Rev.Infect.Dis.* **6**:214-222.
- Liu, P. Y. F., Z. Y. Shi, Y. J. Lau, and B. S. Hu.** 1994. Rapid diagnosis of tuberculous meningitis by simplified nested amplification protocol. *Neurology* **44**:1161-1164.
- Livingston, D. H., S. H. Appel, G. Sonnenfeld, and M. A. Malangoni.** 1989. The effect of tumor necrosis factor-alpha and interferon-gamma on neutrophil function. *J Surg.Res* **46**:322-326.
- Loewen, P. C., B. Hu, J. Strutinsky, and R. Sparling.** 1998. Regulation in the rpoS regulon of Escherichia coli. *Can.J Microbiol* **44**:707-717.
- Louden, R. G., J. Williamson, and J. M. Johnson.** 1958. An analysis of 3485 tuberculosis contacts in the city of Edinburgh during 1954 - 1955. *Am Rev Tuberc* **77**:623-643.
- Lundgren, M., U. Persson, P. Larsson, C. Magnusson, C. I. Smith, L. Hammarstrom, and E. Severinson.** 1989. Interleukin 4 induces synthesis of IgE and IgG4 in human B cells. *Eur.J Immunol.* **19**:1311-1315.

- Lurie, M. B.** 1964. Resistance of Tuberculosis: Experimental Studies in Native and Acquired Defence Mechanisms. Cambridge, Mass: Harvard University Press.
- Macatonia, S. E., N. A. Hosken, M. Litton, P. Vieira, C. S. Hsieh, J. A. Culpepper, M. Wysocka, G. Trinchieri, K. M. Murphy, and A. O'Garra.** 1995. Dendritic cells produce IL-12 and direct the development of Th1 cells from naive CD4+ T cells. *J Immunol* **154**:5071-5079.
- Macham, L. P. and C. Ratledge.** 1975. A new group of water-soluble iron-binding compounds from Mycobacteria: the exochelins. *J Gen.Microbiol* **89**:379-382.
- Male, D. K., G. Pryce, and C. C. Hughes.** 1987. Antigen presentation in brain: MHC induction on brain endothelium and astrocytes compared. *Immunology* **60**:453-459.
- Manca, C., S. Paul, C. E. Barry, III, V. H. Freedman, and G. Kaplan.** 1999. Mycobacterium tuberculosis catalase and peroxidase activities and resistance to oxidative killing in human monocytes in vitro. *Infect.Immun.* **67**:74-79.
- Mariani, F., G. Cappelli, G. Riccardi, and V. Colizzi.** 2000. Mycobacterium tuberculosis H37Rv comparative gene-expression analysis in synthetic medium and human macrophage. *Gene* **253**:281-291.
- McClure, W. R. and C. L. Cech.** 1978. On the mechanism of rifampicin inhibition of RNA synthesis. *J Biol.Chem.* **253**:8949-8956.
- McKinney, J. D., B. K. Honer zu, E. J. Munoz-Elias, A. Miczak, B. Chen, W. T. Chan, D. Swenson, J. C. Sacchettini, W. R. Jacobs, Jr., and D. G. Russell.** 2000. Persistence of Mycobacterium tuberculosis in macrophages and mice requires the glyoxylate shunt enzyme isocitrate lyase. *Nature* **406**:735-738.
- McVicar, N.** 1932. The prevalence of certain diseases amongst the natives of the Ciskei. *South African Medical Journal* **6**:721-722.
- Metcalf, C.** A History of Tuberculosis. *In*: Coovadia, H.M. and Benatar, S.R. ed: A Century of Tuberculosis: South African Perspectives. Oxford, Oxford University Press. pp 1 - 31
- Middlebrook, G., Z. Reggiardo, and W. D. Tigertt.** 1977. Automatable radiometric detection of growth of Mycobacterium tuberculosis in selective media. *Am.Rev.Respir.Dis.* **115**:1066-1069.

- Middleton, A. M., M. V. Chadwick, and H. Gaya.** 1997. Evaluation of a commercial radiometric system for primary isolation of mycobacteria over a fifteen-year period. *Eur.J Clin.Microbiol.Infect.Dis.* **16**:166-170.
- Mitchison, D. A.** 1979. Basic mechanisms of chemotherapy. *Chest* **76**:771-781.
- Mitchison, D. A.** 1992. The Garrod Lecture. Understanding the chemotherapy of tuberculosis-- current problems. *J Antimicrob.Chemother.* **29**:477-493.
- Miyazaki, Y., H. Koga, S. Kohno, and M. Kaku.** 1993. Nested polymerase chain reaction for detection of *Mycobacterium tuberculosis* in clinical samples. *J.Clin.Microbiol.* **31**:2228-2232.
- Modlin, R. L., F. M. Hofman, D. A. Horwitz, L. A. Husmann, S. Gillis, C. R. Taylor, and T. H. Rea.** 1984. In situ identification of cells in human leprosy granulomas with monoclonal antibodies to interleukin 2 and its receptor. *J Immunol.* **132**:3085-3090.
- Modlin, R. L.** 1994. Th1-Th2 paradigm: insights from leprosy. *J Invest Dermatol.* **102**:828-832.
- Mohagheghpour, N., D. Gammon, L. M. Kawamura, A. van Vollenhoven, C. J. Benike, and E. G. Engleman.** 1998. CTL response to *Mycobacterium tuberculosis*: identification of an immunogenic epitope in the 19-kDa lipoprotein. *J Immunol* **161**:2400-2406.
- Morse, D., D. R. Brothwell, and P. J. Voko.** 1964. Tuberculosis in Ancient Egypt. *American Review of Respiratory Disease* **90**:524-541.
- Mosmann, T. R., H. Cherwinski, M. W. Bond, M. A. Giedlin, and R. L. Coffman.** 1986. Two types of murine helper T cell clone. I. Definition according to profiles of lymphokine activities and secreted proteins. *J Immunol.* **136**:2348-2357.
- Munk, M. E., A. J. Gatrill, and S. H. Kaufmann.** 1990. Target cell lysis and IL-2 secretion by gamma/delta T lymphocytes after activation with bacteria. *J Immunol* **145**:2434-2439.
- Murray, C. J., K. Styblo, and A. Rouillon.** 1990. Tuberculosis in developing countries: burden, intervention and cost. *Bull.Int.Union Tuberc.Lung Dis.* **65**:6-24.
- Musser, J. M.** 1995. Antimicrobial agent resistance in mycobacteria: molecular genetic insights. *Clin Microbiol Rev.* **8**:496-514.

- Nardell, E. A.** 1993. Beyond four drugs. Public health policy and the treatment of the individual patient with tuberculosis. *Am.Rev.Respir.Dis.* **148**:2-5.
- Nickoloff, B. J. and Y. Naidu.** 1994. Perturbation of epidermal barrier function correlates with initiation of cytokine cascade in human skin. *J Am.Acad.Dermatol.* **30**:535-546.
- Noordhoek, G. T., A. H. Kolk, G. Bjune, D. Catty, J. W. Dale, P. E. Fine, P. Godfrey-Faussett, S. N. Cho, T. Shinnick, S. B. Svenson, and .** 1994. Sensitivity and specificity of PCR for detection of *Mycobacterium tuberculosis*: a blind comparison study among seven laboratories. *J.Clin.Microbiol.* **32**:277-284.
- Nowakowski, M., S. P. Chan, P. Steiner, S. Chice, and H. G. Durkin.** 1992. Different distributions of lung and blood lymphocyte subsets in pediatric AIDS or tuberculosis. *Ann.Clin Lab Sci.* **22**:377-384.
- O'Brien, S., P. S. Jackett, D. B. Lowrie, and P. W. Andrew.** 1991. Guinea-pig alveolar macrophages kill *Mycobacterium tuberculosis* in vitro, but killing is independent of susceptibility to hydrogen peroxide or triggering of the respiratory burst. *Microb.Pathog.* **10**:199-207.
- Ogawa, T., H. Uchida, Y. Kusumoto, Y. Mori, Y. Yamamura, and S. Hamada.** 1991. Increase in tumor necrosis factor α . *Infect.Immun.* **59**:3021-3025.
- Ojha, A. K., T. K. Mukherjee, and D. Chatterji.** 2000. High intracellular level of guanosine tetraphosphate in *Mycobacterium smegmatis* changes the morphology of the bacterium. *Infect.Immun.* **68**:4084-4091.
- Olsen, A. W., P. R. Hansen, A. Holm, and P. Andersen.** 2000. Efficient protection against *Mycobacterium tuberculosis* by vaccination with a single subdominant epitope from the ESAT-6 antigen. *Eur.J Immunol.* **30**:1724-1732.
- Orme, I. M.** 1987. The kinetics of emergence and loss of mediator T lymphocytes acquired in response to infection with *Mycobacterium tuberculosis*. *J Immunol.* **138**:293-298.
- Orme, I. M., A. D. Roberts, J. P. Griffin, and J. S. Abrams.** 1993. Cytokine secretion by CD4 T lymphocytes acquired in response to *Mycobacterium tuberculosis* infection. *J Immunol.* **151**:518-525.

Oswald, I. P., R. T. Gazzinelli, A. Sher, and S. L. James. 1992. IL-10 synergizes with IL-4 and transforming growth factor-beta to inhibit macrophage cytotoxic activity. *J Immunol.* **148**:3578-3582.

Pal, P. G. and M. A. Horwitz. 1992. Immunization with extracellular proteins of *Mycobacterium tuberculosis* induces cell-mediated immune responses and substantial protective immunity in a guinea pig model of pulmonary tuberculosis. *Infect.Immun.* **60**:4781-4792.

Pearlman, E., J.W. Kazura, and F.E. Hazlett, Jr. 1993. Modulation of murine cytokine responses to mycobacterial antigens by helminth-induced T-helper 2 cell responses. *J. Immuno*; **151**: 4857 - 4864

Perez, V. L., J. A. Lederer, A. H. Lichtman, and A. K. Abbas. 1995. Stability of Th1 and Th2 populations. *Int.Immunol.* **7**:869-875.

Primm, T. P., S. J. Andersen, V. Mizrahi, D. Avarbock, H. Rubin, and C. E. Barry, III. 2000. The stringent response of *Mycobacterium tuberculosis* is required for long-term survival. *J.Bacteriol.* **182**:4889-4898.

Punnonen, J. and J. E. de Vries. 1994. IL-13 induces proliferation, Ig isotype switching, and Ig synthesis by immature human fetal B cells. *J Immunol.* **152**:1094-1102.

Quadri, L. E., J. Sello, T. A. Keating, P. H. Weinreb, and C. T. Walsh. 1998. Identification of a *Mycobacterium tuberculosis* gene cluster encoding the biosynthetic enzymes for assembly of the virulence-conferring siderophore mycobactin. *Chem.Biol.* **5**:631-645.

Rao, N. N. and A. Kornberg. 1996. Inorganic polyphosphate supports resistance and survival of stationary- phase *Escherichia coli*. *J Bacteriol.* **178**:1394-1400.

Rathanaswami, P., M. Hachicha, M. Sadick, T. J. Schall, and S. R. McColl. 1993. Expression of the cytokine RANTES in human rheumatoid synovial fibroblasts. Differential regulation of RANTES and interleukin-8 genes by inflammatory cytokines. *J Biol.Chem.* **268**:5834-5839.

Ravn, P., A. Demissie, T. Eguale, H. Wondwosson, D. Lein, H. A. Amoudy, A. S. Mustafa, A. K. Jensen, A. Holm, I. Rosenkrands, F. Oftung, J. Olobo, F. von Reyn, and P. Andersen. 1999. Human T cell responses to the ESAT-6 antigen from *Mycobacterium tuberculosis*. *J Infect.Dis.* **179**:637-645.

- Raynaud, C., G. Etienne, P. Peyron, M. A. Laneelle, and M. Daffe.** 1998. Extracellular enzyme activities potentially involved in the pathogenicity of *Mycobacterium tuberculosis*. *Microbiology* **144** (Pt 2):577-587.
- Reid, J. D. and E. Wolinsky.** 1969. Histopathology of lymphadenitis caused by atypical mycobacteria. *Am.Rev.Respir.Dis.* **99**:8-12.
- Rennick, D., N. Davidson, and D. Berg.** 1995. Interleukin-10 gene knock-out mice: a model of chronic inflammation. *Clin Immunol.Immunopathol.* **76**:S174-S178.
- Riley, D. K., T. J. Babinchak, and E. B. Rotherams, Jr.** 1996. Tuberculosis: yesterday, today, and tomorrow. *Ann.Intern.Med* **124**:455-456.
- Riley, R. L., C. C. Mills, W. Nyka, N. Weinstock, P. B. Storey, L. U. Sultan, M. C. Riley, and W. F. Wells.** 1995. Aerial dissemination of pulmonary tuberculosis. A two-year study of contagion in a tuberculosis ward. 1959. *Am J Epidemiol.* **142**:3-14.
- Rindi, L., N. Lari, and C. Garzelli.** 1999. Search for genes potentially involved in *Mycobacterium tuberculosis* virulence by mRNA differential display. *Biochem.Biophys.Res Commun.* **258**:94-101.
- Rivera, V. M.** 1998. Controlling gene expression using synthetic ligands. *Methods* **14**:421-429.
- Rodriguez, G. M., B. Gold, M. Gomez, O. Dussurget, and I. Smith.** 1999. Identification and characterization of two divergently transcribed iron regulated genes in *Mycobacterium tuberculosis*. *Tuber.Lung Dis.* **79**:287-298.
- Romani, L., P. Puccetti, A. Mencacci, E. Cenci, R. Spaccapelo, L. Tonnetti, U. Grohmann, and F. Bistoni.** 1994. Neutralization of IL-10 up-regulates nitric oxide production and protects susceptible mice from challenge with *Candida albicans*. *J Immunol.* **152**:3514-3521.
- Sad, S. and T. R. Mosmann.** 1994. Single IL-2-secreting precursor CD4 T cell can develop into either Th1 or Th2 cytokine secretion phenotype. *J Immunol* **153**:3514-3522.
- Saiki, R. K., D. H. Gelfand, S. Stoffel, S. J. Scharf, R. Higuchi, G. T. Horn, K. B. Mullis, and H. A. Erlich.** 1988. Primer-directed enzymatic amplification of DNA with a thermostable DNA polymerase. *Science* **239**:487-491.

- Sambrook, J., Fritsch, E. F. and Maniatis, T.** 1989. *Molecular Cloning: A Laboratory Manual*. New York: Cold Spring Harbor Laboratory Press.
- Sanchez, F. O., J. I. Rodriguez, G. Agudelo, and L. F. Garcia.** 1994. Immune responsiveness and lymphokine production in patients with tuberculosis and healthy controls. *Infect.Immun.* **62**:5673-5678.
- Sandin, R. L.** 1996. Polymerase chain reaction and other amplification techniques in mycobacteriology. *Clin.Lab Med* **16**:617-639.
- Saunders, B. M., A. A. Frank, and I. M. Orme.** 1999. Granuloma formation is required to contain bacillus growth and delay mortality in mice chronically infected with *Mycobacterium tuberculosis*. *Immunology* **98**:324-328.
- Schlesinger, L. S., S. R. Hull, and T. M. Kaufman.** 1994. Binding of the terminal mannosyl units of lipoarabinomannan from a virulent strain of *Mycobacterium tuberculosis* to human macrophages. *J Immunol.* **152**:4070-4079.
- Seah, G. T., G. M. Scott, and G. A. Rook.** 2000. Type 2 cytokine gene activation and its relationship to extent of disease in patients with tuberculosis. *J Infect.Dis.* **181**:385-389.
- Seder, R. A., R. Gazzinelli, A. Sher, and W. E. Paul.** 1993. Interleukin 12 acts directly on CD4+ T cells to enhance priming for interferon gamma production and diminishes interleukin 4 inhibition of such priming. *Proc.Natl.Acad.Sci.U.S.A* **90**:10188-10192.
- Seder, R. A. and W. E. Paul.** 1994. Acquisition of lymphokine-producing phenotype by CD4+ T cells. *Annu.Rev Immunol* **12**:635-673.
- Segal, W. and H. Bloch.** 1956. Biochemical differentiation of *Mycobacterium tuberculosis* grown in vivo and in vitro. *J.Bacteriol.* **72**:132-141.
- Selwyn, P. A., D. Hartel, V. A. Lewis, E. E. Schoenbaum, S. H. Vermund, R. S. Klein, A. T. Walker, and G. H. Friedland.** 1989. A prospective study of the risk of tuberculosis among intravenous drug users with human immunodeficiency virus infection. *N.Engl.J Med* **320**:545-550.
- Seyfzadeh, M., J. Keener, and M. Nomura.** 1993. *spoT*-dependent accumulation of guanosine tetraphosphate in response to fatty acid starvation in *Escherichia coli*. *Proc.Natl.Acad.Sci.U.S.A* **90**:11004-11008.

- Sheffield, E. A.** 1994. The Pathology of Tuberculosis. *In*: Davies, P. D. O. Clinical Tuberculosis. London, Chapman and Hall: pp 43 - 54
- Shepherd, N. S., G. Churchward, and H. Bremer.** 1980. Synthesis and activity of ribonucleic acid polymerase in *Escherichia coli*. *J Bacteriol.* **141**:1098-1108.
- Sherman, D. R., K. Mdluli, M. J. Hickey, T. M. Arain, S. L. Morris, C. E. Barry, III, and C. K. Stover.** 1996. Compensatory *ahpC* gene expression in isoniazid-resistant *Mycobacterium tuberculosis*. *Science* **272**:1641-1643.
- Small, P. M., P. C. Hopewell, S. P. Singh, A. Paz, J. Parsonnet, D. C. Ruston, G. F. Schecter, C. L. Daley, and G. K. Schoolnik.** 1994. The epidemiology of tuberculosis in San Francisco. A population-based study using conventional and molecular methods. *N.Engl.J Med* **330**:1703-1709.
- Snow, G. A.** 1970. Mycobactins: iron-chelating growth factors from mycobacteria. *Bacteriol.Rev.* **34**:99-125.
- So, S. Y., W. K. Lam, and D. Y. C. Yu.** 1982. Rapid diagnosis of suspected pulmonary tuberculosis by fiberoptic bronchoscopy. *Tubercle* **63**:195-200.
- Sokal, J. E.** 1975. Editorial: Measurement of delayed skin-test responses. *N.Engl.J Med* **293**:501-502.
- Somoskovi, A., G. Zissel, P. F. Zipfel, M. W. Ziegenhagen, J. Klaucke, H. Haas, M. Schlaak, and J. Muller-Quernheim.** 1999. Different cytokine patterns correlate with the extension of disease in pulmonary tuberculosis. *Eur.Cytokine Netw.* **10**:135-142.
- Song, C. H., H. J. Kim, J. K. Park, J. H. Lim, U. O. Kim, J. S. Kim, T. H. Paik, K. J. Kim, J. W. Suhr, and E. K. Jo.** 2000. Depressed interleukin-12 (IL-12), but not IL-18, production in response to a 30- or 32-kilodalton mycobacterial antigen in patients with active pulmonary tuberculosis. *Infect.Immun.* **68**:4477-4484.
- Sonnenberg, M. G. and J. T. Belisle.** 1997. Definition of *Mycobacterium tuberculosis* culture filtrate proteins by two-dimensional polyacrylamide gel electrophoresis, N-terminal amino acid sequencing, and electrospray mass spectrometry. *Infect.Immun.* **65**:4515-4524.

- Sorensen, A. L., S. Nagai, G. Houen, P. Andersen, and A. B. Andersen.** 1995. Purification and characterization of a low-molecular-mass T-cell antigen secreted by *Mycobacterium tuberculosis*. *Infect.Immun.* **63**:1710-1717.
- Starke, J. K. and K. T. Taylor-Watts.** 1989. Tuberculosis in the pediatric population of Houston, Texa. *Pediatrics* **84**:28-35.
- Swain, S. L., D. T. McKenzie, R. W. Dutton, S. L. Tonkonogy, and M. English.** 1988. The role of IL4 and IL5: characterization of a distinct helper T cell subset that makes IL4 and IL5 (Th2) and requires priming before induction of lymphokine secretion. *Immunol Rev* **102**:77-105.
- Taha, R. A., T. C. Kotsimbos, Y. L. Song, D. Menzies, and Q. Hamid.** 1997. IFN-gamma and IL-12 are increased in active compared with inactive tuberculosis. *Am J Respir.Crit Care Med* **155**:1135-1139.
- Takahashi, M., Y. Kazumi, Y. Fukasawa, K. Hirano, T. Mori, J. W. Dale, and C. Abe.** 1993. Restriction fragment length polymorphism analysis of epidemiologically related *Mycobacterium tuberculosis* isolates. *Microbiol Immunol* **37**:289-294.
- Teran, L. M., M. Mochizuki, J. Bartels, E. L. Valencia, T. Nakajima, K. Hirai, and J. M. Schroder.** 1999. Th1- and Th2-type cytokines regulate the expression and production of eotaxin and RANTES by human lung fibroblasts. *Am.J Respir.Cell Mol.Biol.* **20**:777-786.
- Teunissen, M. B., C. W. Koomen, M. R. de Waal, E. A. Wierenga, and J. D. Bos.** 1998. Interleukin-17 and interferon-gamma synergize in the enhancement of proinflammatory cytokine production by human keratinocytes. *J Invest Dermatol.* **111**:645-649.
- The Medical Research Council Tuberculosis Report.** 1998. Meical Research Council Press Release.
- The South African Tuberculosis Control Programme: Practical Guidelines.** 2000. Department of Health. Cape Town, CTP Book Printers.
- Thierry, D., A. Brisson-Noel, V. Vincent-Levy-Frebault, S. Nguyen, J. L. Guesdon, and B. Gicquel.** 1990. Characterization of a *Mycobacterium tuberculosis* insertion sequence, IS6110, and its application in diagnosis. *J Clin.Microbiol.* **28**:2668-2673.

Ulrichs, T., M. E. Munk, H. Mollenkopf, S. Behr-Perst, R. Colangeli, M. L. Gennaro, and S. H. Kaufmann. 1998. Differential T cell responses to Mycobacterium tuberculosis ESAT6 in tuberculosis patients and healthy donors. *Eur.J Immunol.* **28**:3949-3958.

Ulrichs, T., P. Anding, S. Porcelli, S. H. Kaufmann, and M. E. Munk. 2000. Increased numbers of ESAT-6- and purified protein derivative-specific gamma interferon-producing cells in subclinical and active tuberculosis infection. *Infect.Immun.* **68**:6073-6076.

Umbarger, H. E. and Zubay, G. 1993. The metabolic fate of amino acids. *In: Zubay, G. ed. Biochemistry*, 3rd Edition. Columbia, W. M. C., Brown Publishers: pp 513 - 546

Vallejo, J., L. Ong, and J. K. Starke. 1994. Clinical features, diagnosis and treatment of tuberculosis in infants. *Pediatrics* **94**:1-7.

van Crevel, R., E. Karyadi, F. Preyers, M. Leenders, B. J. Kullberg, R. H. Nelwan, and J. W. van der Meer. 2000. Increased production of interleukin 4 by CD4+ and CD8+ T cells from patients with tuberculosis is related to the presence of pulmonary cavities. *J Infect.Dis.* **181**:1194-1197.

van den Oord, J. J., C. Wolf-Peeters, G. Tricot, and V. J. Desmet. 1984. Distribution of lymphocyte subsets in a case of angiofollicular lymph node hyperplasia. *Am J Clin Pathol.* **82**:491-495.

van Embden, J. D., M. D. Cave, J. T. Crawford, J. W. Dale, K. D. Eisenach, B. Gicquel, P. Hermans, C. Martin, R. McAdam, T. M. Shinnick, and . 1993. Strain identification of Mycobacterium tuberculosis by DNA fingerprinting: recommendations for a standardized methodology. *J Clin.Microbiol.* **31**:406-409.

Vanni, P., E. Giachetti, G. Pinzauti, and B. A. McFadden. 1990. Comparative structure, function and regulation of isocitrate lyase, an important assimilatory enzyme. *Comp Biochem.Physiol B* **95**:431-458.

Vega-Lopez, F., L. A. Brooks, H. M. Dockrell, K. A. De Smet, J. K. Thompson, R. Hussain, and N. G. Stoker. 1993. Sequence and immunological characterization of a serine-rich antigen from Mycobacterium leprae. *Infect.Immun.* **61**:2145-2153.

- Volk, H. D., S. Gruner, P. Falck, and R. Von Baehr.** 1986. The influence of interferon-gamma and various phagocytic stimuli on the expression of MHC-class II antigens on human monocytes--relation to the generation of reactive oxygen intermediates. *Immunol.Lett.* **13**:209-214.
- Warren, R., M. Richardson, S. Sampson, J. H. Hauman, N. Beyers, P. R. Donald, and P. D. van Helden.** 1996. Genotyping of *Mycobacterium tuberculosis* with additional markers enhances accuracy in epidemiological studies. *J Clin.Microbiol.* **34**:2219-2224.
- Warren, R., J. Hauman, N. Beyers, M. Richardson, H. S. Schaaf, P. Donald, and P. van Helden.** 1996(a). Unexpectedly high strain diversity of *Mycobacterium tuberculosis* in a high-incidence community. *S.Afr.Med J* **86**:45-49.
- Wayne, L. G. and K. Y. Lin.** 1982. Glyoxylate metabolism and adaptation of *Mycobacterium tuberculosis* to survival under anaerobic conditions. *Infect.Immun.* **37**:1042-1049.
- Wayne, L. G.** 1994. Dormancy of *Mycobacterium tuberculosis* and latency of disease. *Eur.J Clin Microbiol Infect.Dis.* **13**:908-914.
- Wayne, L. G. and L. G. Hayes.** 1996. An in vitro model for sequential study of shutdown of *Mycobacterium tuberculosis* through two stages of nonreplicating persistence. *Infect.Immun.* **64**:2062-2069.
- Wayne, L. G. and L. G. Hayes.** 1998. Nitrate reduction as a marker for hypoxic shutdown of *Mycobacterium tuberculosis*. *Tuber.Lung Dis.* **79**:127-132.
- Wei, J., J. L. Dahl, J. W. Moulder, E. A. Roberts, P. O'Gaora, D. B. Young, and R. L. Friedman.** 2000. Identification of a *Mycobacterium tuberculosis* gene that enhances mycobacterial survival in macrophages. *J Bacteriol.* **182**:377-384.
- Wengenack, N. L., M. P. Jensen, F. Rusnak, and M. K. Stern.** 1999. *Mycobacterium tuberculosis* KatG is a peroxynitritase. *Biochem.Biophys.Res Commun.* **256**:485-487.
- WHO Report on the Tuberculosis Epidemic: Global Tuberculosis Programme.** 2001. Geneva, Switzerland.

- Wiid, I. J. F., C. Werely, N. Beyers, P. Donald, and P. D. van Helden.** 1994. Oligonucleotide (GTG)₅ as a marker for *Mycobacterium tuberculosis* strain identification. *J Clin Microbiol* **32**:1318-1321.
- Wilkinson, D., S. Bechan, C. Connolly, E. Standing, and G. M. Short.** 1998. Should we take a history of prior treatment, and check sputum status at 2-3 months when treating patients for tuberculosis? *Int.J Tuberc.Lung Dis.* **2**:52-55.
- Wilson, T., B. J. Wards, S. J. White, B. Skou, G. W. de Lisle, and D. M. Collins.** 1997. Production of avirulent *Mycobacterium bovis* strains by illegitimate recombination with deoxyribonucleic acid fragments containing an interrupted *ahpC* gene. *Tuber.Lung Dis.* **78**:229-235.
- Wilson, T., G. W. de Lisle, J. A. Marcinkeviciene, J. S. Blanchard, and D. M. Collins.** 1998. Antisense RNA to *ahpC*, an oxidative stress defence gene involved in isoniazid resistance, indicates that *AhpC* of *Mycobacterium bovis* has virulence properties. *Microbiology* **144 (Pt 10)**:2687-2695.
- Wilson, T. M., G. W. de Lisle, and D. M. Collins.** 1995. Effect of *inhA* and *katG* on isoniazid resistance and virulence of *Mycobacterium bovis*. *Mol.Microbiol* **15**:1009-1015.
- Yang, Z. H., K. Ijaz, J. H. Bates, K. D. Eisenach, and M. D. Cave.** 2000. Spoligotyping and polymorphic GC-rich repetitive sequence fingerprinting of *mycobacterium tuberculosis* strains having few copies of IS6110. *J Clin Microbiol* **38**:3572-3576.
- Yssel, H., M. R. de Waal, M. G. Roncarolo, J. S. Abrams, R. Lahesmaa, H. Spits, and J. E. de Vries.** 1992. IL-10 is produced by subsets of human CD4⁺ T cell clones and peripheral blood T cells. *J Immunol* **149**:2378-2384.
- Yu, K., C. Mitchell, Y. Xing, R. S. Magliozzo, B. R. Bloom, and J. Chan.** 1999. Toxicity of nitrogen oxides and related oxidants on mycobacteria: *M. tuberculosis* is resistant to peroxyxynitrite anion. *Tuber.Lung Dis.* **79**:191-198.
- Zhang, M., M. K. Gately, E. Wang, J. Gong, S. F. Wolf, S. Lu, R. L. Modlin, and P. F. Barnes.** 1994. Interleukin 12 at the site of disease in tuberculosis. *J Clin Invest* **93**:1733-1739.
- Zhao, F. Z., M. H. Levy, and S. Wen.** 1997. Sputum microscopy results at two and three months predict outcome of tuberculosis treatment. *Int.J Tuberc.Lung Dis.* **1**:570-572.

Zhu, X., H. J. Stauss, J. Ivanyi, and H. M. Vordermeier. 1997. Specificity of CD8+ T cells from subunit-vaccinated and infected H-2b mice recognizing the 38 kDa antigen of *Mycobacterium tuberculosis*. *Int.Immunol* **9**:1669-1676.

Zimmerman, M.R. 1979. Pulmonary and osseous tuberculosis in an Egyptian mummy. *Bulletin of the New York Academy of Medicine*; **55**: 604-608

Zubay, G. 1993. Regulation of Gene Expression in Prokaryotes. *In*: Zubay, G. ed. *Biochemistry*, 3rd Edition. Columbia, W. M. C., Brown Publishers: pp 864 – 894.

Table A1. Individual Granuloma Assessment of Patient L1. Granulomas are numbered according to Figure A1, and were scored as necrotic (Y) or non-necrotic (N), and as negative (0) or positive (1) for signal (ISH and Immunohistochemistry)

Gran.	Necrotic (Y/N)	DNA	rpoB	katG	narX	icl	mbtB	rel _{Mtb}	esat-6	PPE	IL-4	IL-10	IL-12	IFN-g	TNF-a	Th gran.
1	N	1	1	1	1	1	0	1	1	0	0	0	1	1	1	Th-1
2	N	0	0	0	0	0	0	0	0	0	0	0	0	1	1	Th-1
3	Y	1	1	1	1	1	0	1	1	0	1	1	1	1	1	Th-0
4	Y	1	0	1	0	0	0	1	1	0	1	1	1	1	1	Th-0
5	Y	1	0	1	0	0	0	1	1	0	1	0	1	1	1	Th-0
6	Y	1	0	0	1	1	0	1	1	0	1	1	1	1	1	Th-0
7	Y	1	0	1	0	1	0	1	1	0	1	1	1	1	1	Th-0
8	Y	1	1	0	1	1	0	1	1	0	1	1	1	1	1	Th-0
9	N	1	0	1	0	0	0	1	1	0	0	0	0	1	1	Th-1
10	Y	1	0	1	0	0	1	1	1	0	1	1	1	1	1	Th-0
11	N	1	0	1	0	0	0	1	1	1	1	0	0	1	0	Th-0
12	N	1	0	1	0	0	0	1	0	0	1	1	1	1	1	Th-0
13	N	0	0	0	0	0	0	0	0	0	1	0	0	1	0	Th-0
14	Y	1	1	1	0	0	0	1	1	1	1	1	1	1	1	Th-0
15	Y	1	1	0	0	0	1	0	0	0	1	1	1	1	1	Th-0
16	Y	1	1	0	0	0	1	0	0	1	1	0	0	1	1	Th-0
Total	10	14	6	10	4	5	3	12	13	3	13	9	11	16	14	Th0 = 13
(%)	(62.5)	(87.5)	(42.8)	(71.4)	(28.5)	(35.7)	(21.4)	(85.7)	(92.8)	(21.4)	(81.3)	(56.3)	(68.6)	(100)	(87.5)	Th1 = 3

Table A2. Individual Granuloma Assessment of Patient L3. Granulomas are numbered according to Figure A4, and were scored as necrotic (Y) or non-necrotic (N), and as negative (0) or positive (1) for signal (ISH and Immunohistochemistry)

Gran.	Necrotic (Y/N)	DNA	rpoB	katG	narX	icl	mbtB	rel _{Mtb}	esat-6	PPE	IL-4	IL-10	IL-12	IFN-g	TNF-a	Th gran.
1	N	1	1	0	0	1	1	0	0	0	1	1	1	1	1	Th-0
2	N	1	1	0	1	0	1	0	1	0	1	1	1	1	1	Th-0
3	Y	1	1	1	1	0	0	0	1	1	1	1	1	1	1	Th-0
4	Y	1	1	0	1	0	0	1	1	0	1	1	1	1	1	Th-0
5	N	0	0	0	0	0	0	0	0	0	1	1	1	1	1	Th-0
6	N	0	0	0	0	0	0	0	0	0	1	1	1	1	1	Th-0
7	Y	1	0	1	1	0	0	0	0	1	1	1	1	1	1	Th-0
8	Y	1	0	0	0	1	1	1	0	0	1	1	1	1	1	Th-0
9	Y	1	1	1	0	0	1	0	1	1	1	1	1	1	1	Th-0
10	N	1	1	0	0	0	0	1	0	0	0	0	1	1	1	Th-1
11	Y	1	1	0	0	0	0	0	1	0	0	0	1	1	1	Th-1
12	Y	1	0	1	1	1	0	0	0	0	1	1	1	1	1	Th-0
13	Y	1	0	1	0	1	1	0	0	0	1	1	1	1	1	Th-0
14	N	0	0	0	0	0	0	0	0	0	1	1	1	1	1	Th-0
15	Y	1	0	0	1	1	0	1	0	0	0	0	1	1	1	Th-1
16	Y	1	0	1	0	1	0	1	0	0	0	0	1	1	1	Th-1
17	Y	1	1	0	1	1	0	0	0	0	0	0	1	1	1	Th-1
18	Y	1	0	0	1	1	0	1	0	0	0	0	1	1	1	Th-1
19	N	1	1	1	0	0	0	0	0	1	0	0	1	1	1	Th-1
20	Y	1	1	0	1	1	0	1	0	0	1	1	1	1	1	Th-0
21	Y	1	0	0	1	1	0	0	0	0	1	1	1	1	1	Th-0
22	Y	1	1	1	1	1	0	0	0	0	1	1	1	1	1	Th-0
23	Y	1	0	0	0	0	1	0	0	1	1	1	1	1	1	Th-0
24	Y	1	0	1	1	0	0	0	0	0	1	1	1	1	1	Th-0
25	Y	1	1	0	0	0	1	0	0	0	0	0	1	1	1	Th-1
26	Y	1	0	0	0	0	1	0	1	0	1	1	1	1	1	Th-0
27	Y	1	0	1	1	1	0	1	0	0	0	0	1	1	1	Th-1
28	N	0	0	0	0	0	0	0	0	0	1	1	1	1	1	Th-0
Total	20	24	12	10	13	12	8	8	6	5	21	19	28	28	28	Th0 = 19
(%)	(71.4)	(85.7)	(50)	(41.6)	(54.1)	(50)	(33.3)	(33.3)	(25)	(20.8)	(75)	(67.9)	(100)	(100)	(100)	Th1 = 9

Table A3. Individual Granuloma Assessment of Patient L4. Granulomas are numbered according to Figure A7, and were scored as necrotic (Y) or non-necrotic (N), and as negative (0) or positive (1) for signal (ISH and Immunohistochemistry)

Gran.	Necrotic (Y/N)	DNA	rpoB	katG	narX	icl	mbtB	rel _{Mtb}	esat-6	PPE	IL-4	IL-10	IL-12	IFN-g	TNF-a	Th gran.
1	N	0	0	0	0	0	0	0	0	0	1	0	1	1	0	Th-0
2	N	1	0	1	0	0	0	0	0	1	1	1	1	1	1	Th-0
3	N	0	0	0	0	0	0	0	0	0	1	0	1	1	0	Th-0
4	N	1	1	1	0	0	1	1	0	0	1	0	0	1	1	Th-0
5	N	1	0	0	0	0	1	1	0	0	1	0	0	1	0	Th-0
6	Y	1	1	0	1	1	1	1	0	0	1	1	0	1	1	Th-0
7	Y	1	1	0	0	1	1	1	0	1	1	1	0	1	1	Th-0
8	N	1	1	0	0	0	1	1	0	1	0	0	0	1	1	Th-1
9	Y	1	0	0	0	0	0	0	0	0	1	1	1	1	1	Th-0
10	Y	1	0	0	1	1	0	0	0	1	1	0	1	1	1	Th-0
11	N	1	1	1	0	0	0	0	0	1	1	0	1	1	1	Th-0
12	Y	1	0	0	1	0	0	0	0	1	1	1	1	1	1	Th-0
13	Y	1	0	0	0	0	1	0	0	1	1	0	1	1	1	Th-0
Total	6	11	5	3	3	3	6	5	0	7	12	5	8	13	10	Th0 = 12
(%)	(46.2)	(84.6)	(45.4)	(27.2)	(27.2)	(27.2)	(54.5)	(45.4)	(0)	(63.6)	(92.13)	(38.5)	(61.5)	(100)	(76.9)	Th1 = 1

Table A4. Individual Granuloma Assessment of Patient L5. Granulomas are numbered according to Figure A10, and were scored as necrotic (Y) or non-necrotic (N), and as negative (0) or positive (1) for signal (ISH and Immunohistochemistry)

Gran.	Necrotic (Y/N)	DNA	rpoB	katG	narX	icl	mbtB	rel _{Mtb}	esat-6	PPE	IL-4	IL-10	IL-12	IFN-g	TNF-a	Th gran.
1	Y	1	1	1	1	1	1	1	0	1	1	1	0	1	1	Th-0
2	Y	1	0	1	1	1	1	1	0	1	1	1	1	1	1	Th-0
3	Y	1	1	1	1	1	1	1	0	1	1	1	1	1	1	Th-0
4	N	0	0	0	0	0	0	0	0	0	1	0	1	1	1	Th-0
5	N	1	1	1	0	1	1	1	0	1	1	0	1	1	1	Th-0
6	Y	1	1	1	1	1	1	1	0	1	1	1	0	1	1	Th-0
7	Y	1	0	1	0	1	1	1	0	1	1	1	0	1	1	Th-0
8	Y	1	1	1	1	1	0	1	0	1	1	0	0	1	1	Th-0
9	Y	1	0	1	1	1	0	1	0	1	1	0	1	1	1	Th-0
10	N	1	0	1	1	1	0	1	0	1	0	0	0	1	1	Th-1
11	N	1	0	1	0	1	0	1	0	1	1	1	0	1	1	Th-0
12	Y	1	0	1	0	1	1	1	0	1	1	1	0	1	1	Th-0
13	Y	1	1	1	0	1	1	1	0	1	1	1	0	1	1	Th-0
14	Y	1	1	1	1	1	1	1	0	1	1	1	1	1	1	Th-0
15	Y	1	0	1	0	1	1	1	0	1	1	0	1	1	1	Th-0
16	N	1	1	1	0	1	1	1	0	1	1	0	0	1	1	Th-0
17	Y	1	0	1	0	1	1	1	0	1	1	0	1	1	1	Th-0
18	Y	1	0	1	0	1	1	1	0	1	1	1	1	1	1	Th-0
19	Y	1	1	1	1	1	1	1	0	1	1	1	1	1	1	Th-0
20	Y	1	1	1	1	1	1	1	0	1	1	1	1	1	1	Th-0
21	Y	1	1	1	1	1	1	1	0	1	1	0	0	1	1	Th-0
22	Y	1	0	0	0	1	1	1	0	0	1	0	0	1	1	Th-0
23	Y	1	0	1	1	1	1	1	0	1	1	0	0	1	1	Th-0
24	N	0	0	0	0	0	0	0	0	0	1	0	0	1	1	Th-0
Total	18	22	11	21	12	22	18	22	0	21	23	12	11	24	24	Th0 = 23
(%)	(75)	(91.7)	(50)	(95.4)	(54.5)	(100)	(81.8)	(100)	(0)	(95.4)	(95.8%)	(58%)	(48.5%)	(100%)	(100%)	Th1 = 1

Table A5. Individual Granuloma Assessment of Patient L6. Granulomas are numbered according to Figure A13, and were scored as necrotic (Y) or non-necrotic (N), and as negative (0) or positive (1) for signal (ISH and Immunohistochemistry)

Gran.	Necrotic (Y/N)	DNA	rpoB	katG	narX	icl	mbtB	rel _{Mtb}	esat-6	PPE	IL-4	IL-10	IL-12	IFN-g	TNF-a	Th gran.
1	Y	1	0	1	1	1	1	1	0	0	1	1	1	1	1	Th-0
2	N	0	0	0	0	0	0	0	0	0	1	0	0	1	1	Th-0
3	N	1	0	1	1	1	0	1	0	0	1	0	0	1	1	Th-0
4	Y	1	1	1	1	1	0	1	0	1	1	1	1	1	1	Th-0
5	Y	1	1	1	1	1	1	1	0	0	1	1	1	1	1	Th-0
6	Y	1	0	1	1	1	1	1	0	0	1	1	1	1	1	Th-0
7	Y	1	0	1	1	1	1	1	0	0	1	1	1	1	1	Th-0
8	Y	1	0	1	0	1	1	1	0	0	1	1	1	1	1	Th-0
9	Y	1	0	1	1	1	1	1	0	0	1	1	1	1	1	Th-0
10	Y	1	0	1	1	1	1	1	0	0	1	1	1	1	1	Th-0
11	Y	1	0	0	1	1	1	1	0	0	1	1	0	1	1	Th-0
12	N	1	1	1	0	1	1	1	1	0	1	1	1	1	1	Th-0
13	Y	1	0	1	1	1	1	1	1	0	1	1	1	1	1	Th-0
14	N	1	0	1	0	1	1	1	0	0	1	1	1	1	1	Th-0
15	N	1	1	1	1	1	1	1	0	1	1	1	0	1	1	Th-0
16	N	1	1	0	0	0	0	1	1	1	1	1	1	1	1	Th-0
17	Y	1	0	1	0	1	1	1	0	0	1	1	0	1	1	Th-0
18	Y	1	1	1	1	1	1	1	0	0	1	1	0	1	1	Th-0
19	Y	1	1	1	1	1	0	1	0	0	1	1	0	1	1	Th-0
Total	13	18	7	16	13	17	14	18	3	3	19	17	12	19	19	Th0 = 19
(%)	(68.4)	(94.7)	(38.8)	(88.8)	(72.2)	(94.4)	(77.7)	(100)	(16.6)	(16.6)	(100)	(89.5)	(63.2)	(100)	(100)	

Table A6. Individual Granuloma Assessment of Patient L2. Granulomas are numbered according to Figure A16, and were scored as necrotic (Y) or non-necrotic (N), and as negative (0) or positive (1) for signal (ISH and Immunohistochemistry)

Gran.	Necrotic (Y/N)	DNA	rpoB	katG	narX	icl	mbtB	rel _{Mtb}	esat-6	PPE	IL-4	IL-10	IL-12	IFN-g	TNF-a	Th gran.
1	Y	1	0	0	0	0	1	1	0	0	1	1	1	1	1	Th-0
2	Y	1	0	0	0	0	0	1	0	0	1	1	1	1	1	Th-0
3	Y	1	0	0	1	1	0	1	1	1	1	1	1	1	1	Th-0
4	N	0	0	0	0	0	0	0	0	0	1	0	1	1	1	Th-0
5	Y	1	0	0	0	0	1	0	0	0	1	1	1	1	1	Th-0
6	Y	1	0	0	1	1	0	1	0	0	1	1	0	1	1	Th-0
7	Y	1	0	0	1	0	1	1	1	1	1	1	1	1	1	Th-0
Total	6	6	0	0	3	2	3	5	2	2	7	6	6	7	7	Th0 = 7
(%)	(85.7)	(85.7)	(0)	(0)	(50)	(33.3)	(50)	(83.3)	(33.3)	(33.3)	(100)	(85.7)	(85.7)	(100)	(100)	